U.S. Department
of Commerce

Volume 108
Number 1
January 2010

# Fishery Bulletin

**U.S. Department of Commerce**
Gary Locke
Secretary of Commerce

**National Oceanic and Atmospheric Administration**
Jane Lubchenco, Ph.D.
Administrator of NOAA

**National Marine Fisheries Service**
James W. Balsiger, Ph.D.
Acting Assistant Administrator for Fisheries

# Fishery Bulletin

**Scientific Editor**
Richard D. Brodeur, Ph.D.

**Associate Editor**
Julie Scheurer

National Marine Fisheries Service
Northwest Fisheries Science Center
2030 S. Marine Science Dr.
Newport, Oregon 97365-5296

**Managing Editor**
Sharyn Matriotti

National Marine Fisheries Service
Scientific Publications Office
7600 Sand Point Way NE
Seattle, Washington 98115-0070

**Editorial Committee**

| | |
|---|---|
| John Carlson | National Marine Fisheries Service, Panama City, Florida |
| Kevin Craig | Florida State University, Tallahassee, Florida |
| Jeff Leis | Australian Museum, Sydney, New South Wales, Australia |
| Rich McBride | National Marine Fisheries Service, Woods Hole, Massachusetts |
| Rick Methot | National Marine Fisheries Service, Seattle, Washington |
| Adam Moles | National Marine Fisheries Service, Auke Bay, Alaska |
| Frank Parrish | National Marine Fisheries Service, Honolulu, Hawaii |
| Dave Somerton | National Marine Fisheries Service, Seattle, Washington |
| Ed Trippel | Department of Fisheries and Oceans, St. Andrews, New Brunswick, Canada |
| Mary Yoklavich | National Marine Fisheries Service, Santa Cruz, California |

***Fishery Bulletin* web site: www.fishbull.noaa.gov**

The *Fishery Bulletin* (ISSN 0090-0656) is published quarterly by the Scientific Publications Office, National Marine Fisheries Service, NOAA, 7600 Sand Point Way NE, BIN C15700, Seattle, WA 98115-0070. Periodicals postage is paid at Seattle, WA. POSTMASTER: Send address changes for subscriptions to Fishery Bulletin, Superintendent of Documents, Attn.: Chief, Mail List Branch, Mail Stop SSOM, Washington, DC 20402-9373.

Although the contents of this publication have not been copyrighted and may be reprinted entirely, reference to source is appreciated.

The Secretary of Commerce has determined that the publication of this periodical is necessary according to law for the transaction of public business of this Department. Use of funds for printing of this periodical has been approved by the Director of the Office of Management and Budget.

**For sale** by the Superintendent of Documents, U.S. Government Printing Office, Washington, DC 20402. Subscription price per year: $36.00 domestic and $50.40 foreign. Cost per single issue: $21.00 domestic and $29.40 foreign. **See back for order form.**

The *Fishery Bulletin* carries original research reports and technical notes on investigations in fishery science, engineering, and economics. It began as the Bulletin of the United States Fish Commission in 1881; it became the Bulletin of the Bureau of Fisheries in 1904 and the *Fishery Bulletin* of the Fish and Wildlife Service in 1941. Separates were issued as documents through volume 46; the last document was No. 1103. Beginning with volume 47 in 1931 and continuing through volume 62 in 1963, each separate appeared as a numbered bulletin. A new system began in 1963 with volume 63 in which papers are bound together in a single issue of the bulletin. Beginning with volume 70, number 1, January 1972, the *Fishery Bulletin* became a periodical, issued quarterly. In this form, it is available by subscription from the Superintendent of Documents, U.S. Government Printing Office, Washington, DC 20402. It is also available free in limited numbers to libraries, research institutions, State and Federal agencies, and in exchange for other scientific publications.

U.S. Department
of Commerce
Seattle, Washington

Volume 108
Number 1
January 2010

# Fishery Bulletin

## Contents

### *Articles*

1–14 **Chen, Xinjun, Siquan Tian, Yong Chen, and Bilin Liu**
A modeling approach to identify optimal habitat and suitable fishing grounds for neon flying squid (*Ommastrephes bartramii*) in the Northwest Pacific Ocean

15–29 **Cadigan, Noel G., and Jeff J. Dowden**
Statistical inference about the relative efficiency of a new survey protocol, based on paired-tow survey calibration data

30–38 **Hannah, Robert W., Stephen A. Jones, William Miller, and Jayme S. Knight**
Effects of trawling for ocean shrimp (*Pandalus jordani*) on macroinvertebrate abundance and diversity at four sites near Nehalem Bank, Oregon

39–44 **Barry, Patrick D., Sherry L. Tamone, and David A. Tallmon**
Evaluation of the capture efficiency and size selectivity of four pot types in the prospective fishery for North Pacific giant octopus (*Enteroctopus dofleini*)

45–55 **Saldierna-Martínez, Ricardo J., Gerardo Aceves-Medina, and Enrique A. González-Navarro**
Larval development of the spotfin tonguefish (*Symphurus oligomerus* Mahadeva and Munroe, 1990) (Pleuronectiformes: Cynoglossidae) from the Gulf of California, Mexico

56–69 **Butler, Christopher M., Paul J. Rudershausen, and Jeffrey A. Buckel**
Feeding ecology of Atlantic bluefin tuna (*Thunnus thynnus*) in North Carolina: diet, daily ration, and consumption of Atlantic menhaden (*Brevoortia tyrannus*)

The National Marine Fisheries Service (NMFS) does not approve, recommend, or endorse any proprietary product or proprietary material mentioned in this publication. No reference shall be made to NMFS, or to this publication furnished by NMFS, in any advertising or sales promotion which would indicate or imply that NMFS approves, recommends, or endorses any proprietary product or proprietary material mentioned herein, or which has as its purpose an intent to cause directly or indirectly the advertised product to be used or purchased because of this NMFS publication.

The NMFS Scientific Publications Office is not responsible for the contents of the articles or for the standard of English used in them.

70–78 **Elizabeth A. Chilton**
Maturity and growth of female dusky rockfish (*Sebastes variabilis*) in the central Gulf of Alaska

79–86 **Miller, Cara E., and Donald M. Baltz**
Environmental characterization of seasonal trends and foraging habitat of bottlenose dolphins (*Tursiops truncatus*) in northern Gulf of Mexico bays

87–97 **Lynch, Abigail J., Jan R. McDowell, and John E. Graves**
A molecular genetic investigation of the population structure of Atlantic menhaden (*Brevoortia tyrannus*)

98–105 **Gerard, Trika, and Barbara Muhling**
Variation in the isotopic signatures of juvenile gray snapper (*Lutjanus griseus*) from five southern Florida regions

106–116 **Gannon, Damon P., and Janet G. Gannon**
Assessing trends in the density of Atlantic croaker (*Micropogonias undulatus*): a comparison of passive acoustic and trawl methods

117 **Guidelines for authors**

**Subscription form** (Inside cover page)

# A modeling approach to identify optimal habitat and suitable fishing grounds for neon flying squid (*Ommastrephes bartramii*) in the Northwest Pacific Ocean

**Xinjun Chen (contact author)**[1,2,3]
**Siquan Tian**[1,2,3]
**Yong Chen**[3,4]
**Bilin Liu**[1,2,3]

Email address for contact author: xjchen@shou.edu.cn

[1] College of Marine Sciences
Shanghai Ocean University
999 Hucheng Ring Road
Shanghai 201306, China

[2] The Key Laboratory of Shanghai Education Commission
for Oceanic Fisheries Resources Exploitation
999 Hucheng Ring Road
Shanghai 201306, China

[3] The Key Laboratory of Sustainable Exploitation of Oceanic Fisheries Resources
(Shanghai Ocean University)
Ministry of Education
999 Hucheng Ring Road
Shanghai 201306, China;

[4] School of Marine Sciences
University of Maine
Orono, Maine 04469

**Abstract**—We developed a habitat suitability index (HSI) model to understand and identify the optimal habitat and potential fishing grounds for neon flying squid (*Ommastrephes bartramii*) in the Northwest Pacific Ocean. Remote sensing data, including sea surface temperature, sea surface salinity, sea surface height, and chlorophyll-*a* concentrations, as well as fishery data from Chinese mainland squid fleets in the main fishing ground (150–165°E longitude) from August to October, from 1999 to 2004, were used. The HSI model was validated by using fishery data from 2005. The arithmetic mean modeling with three of the environmental variables—sea surface temperature, sea surface height anomaly, and chlorophyll-*a* concentrations—was defined as the most parsimonious HSI model. In 2005, monthly HSI values >0.6 coincided with productive fishing grounds and high fishing effort from August to October. This result implies that the model can reliably predict potential fishing grounds for *O. bartramii*. Because spatially explicit fisheries and environmental data are becoming readily available, it is feasible to develop a dynamic, near real-time habitat model for improving the process of identifying potential fishing areas for and optimal habitats of neon flying squid.

Manuscript submitted 1 December 2008.
Manuscript accepted 28 August 2009.
Fish. Bull. 108:1–14 (2010).

The views and opinions expressed or implied in this article are those of the author (or authors) and do not necessarily reflect the position of the National Marine Fisheries Service, NOAA.

Two predominant currents, the warm Kuroshio Current and the cold Oyashio Current, meet in the Northwest Pacific Ocean. The interaction of these two currents between the subtropical and subarctic fronts forms a transition region (Roden, 1991). The dynamic of the physical oceanographic structures in this region, including meandering eddies and frontal zones, results in a highly productive habitat, which serves as a favorable feeding ground for various commercially important species, such as neon flying squid (*Ommastrephes bartramii*), Pacific saury (*Cololabis saira*), anchovy (*Engraulis japonicus*), and albacore (*Thunnus alalunga*) (Pearcy, 1991; Zainuddin et al., 2006).

The neon flying squid (*O. bartramii*) is an important oceanic squid, which has been commercially harvested by the Japanese since 1974, and later by South Koreans and the Chinese (including Taiwanese) (Wang and Chen, 2005). There are four stocks of *O. bartramii* (Bower and Ichii, 2005). Of the four stocks, the western winter-spring cohort of neon flying squid is a traditional fishing target for the Chinese mainland squid jigging fleet in the area of 39–46°N latitude and 150–165°E longitude from August to November (Chen and Tian, 2005), with Chinese mainland jigging representing from 75% to 84% of the total catch (Chen et al., 2008a).

The biology and distribution of *O. bartramii* have been the subject of several studies in recent decades (Yatsu and Watanabe, 1996; Yatsu and Mori, 2000; Watanabe et al., 2004; Wang and Chen, 2005). The western winter-spring cohort of neon flying squid can be found from subtropical waters to the subarctic boundary during the first half of the summer and then migrates northward into the subarctic domain from August to November. *Ommastrephes bartramii* gradually mature in fall and are thought to begin their spawning

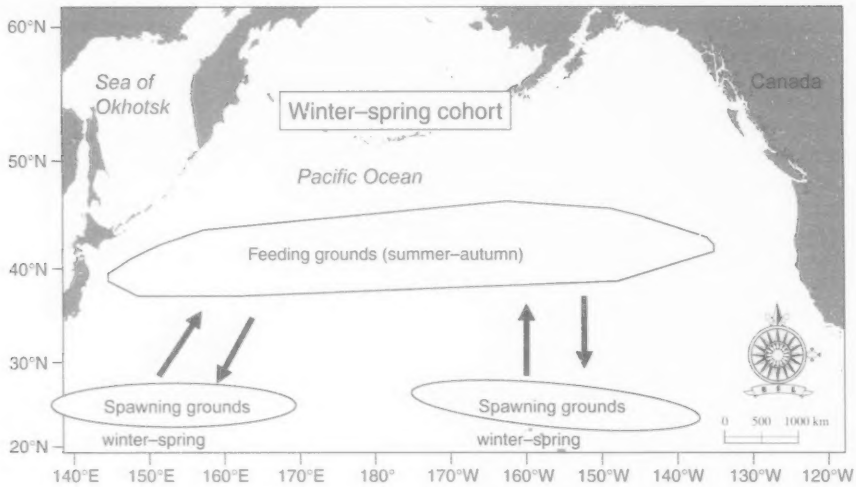


**Figure 1**

Migration pattern of the winter–spring cohort of neon flying squid (*Ommastrephes bartramii*) in the North Pacific Ocean (Ichii et al., 2006).

migration in October and November (Fig. 1; Ichii et al., 2006). For a short-lived, single year-class population and opportunist species, the biophysical environment plays an important role in controlling the distribution and abundance of *O. bartramii* (Chen, 2004; Wang and Chen, 2005).

Many studies have shown that environmental variables such as sea surface temperature (SST), sea surface salinity (SSS), sea surface height anomaly (SSHA), chlorophyll-*a* (chl-*a*) concentrations, and current can strongly influence the distribution and availability of neon flying squid to fisheries (Chen, 1997; Chen and Chiu, 1999; Wang et al., 2003; Chen and Tian, 2005; Tian, 2006; Chen et al., 2007). Chen (1997) reported that monthly preferred SSTs for this squid species varied with seasons and areas, and the monthly preferred SST tended to decrease gradually from west to east. In the waters between 150°–165°E longitude, the monthly favorable SSTs were 12–14°C, 14–17°C, 15–19°C, 14–18°C, 10–13°C, and 12–15°C, respectively, for the months of June to November (Chen, 1997; Chen and Tian, 2005; Tian, 2006). While in the waters of 165–180°E longitude, the favorable SST in June and July ranged from 11–15°C (Chen and Tian, 2005; Tian, 2006). Yatsu and Watanabe (1996) reported that catch per unit of effort (CPUE) for the driftnet fishery near the Subarctic boundary in July was highest during years with a strong gradient between the 11 and 15°C SST isotherms. Chen and Chiu (1999) found that the distribution and abundance of *O. bartramii* in the central North Pacific Ocean were strongly influenced by water temperature and salinity, with temperature having a higher predictive power for estimating stock abundance. Tian (2006) reported that the monthly favorable SSSs for squid were 33.8–34.3, 33.3–34.4, 33.0–34.2, 33.0–33.7, 33.0–33.8 and 33.3–33.8 from June to November, respectively, in the north Pacific. Chen et al. (2007) discussed the influence of large-scale oceanic phenomena such as the Kuroshio Extension and El Niño Southern Oscillation (ENSO) events on squid distribution and recruitment. They concluded that these phenomena influence squid by affecting the SST and SSS of the spawning and feeding grounds.

From July to November, *O. bartramii* migrate north to feed. The presence of plankton also is a basic necessity for the presence of this squid (Chen, 2004). Wang et al. (2003) reported that a skewed distribution function could be used to describe the relationship between chlorophyll-*a* concentration and *O. bartramii* catch in the waters of 150–165°E longitude and 41–45°N latitude from August to October, and that the area with chlorophyll-*a* content ranging from 0.15 to 3 mg/m$^3$ produced 95% of the total catch. Xu et al. (2004) found that in the waters of 152°E–171°W longitude and 39°–42°N latitude during June and July, *O. bartramii* tended to aggregate near areas with the highest abundance (50–100 ind/m$^3$) of crustaceans (mainly Copepoda and Thaliacea).

Sea surface height anomaly (SSHA) is an important marine environmental variable that is closely related to the distributions of some fish species (Zhang et al., 2001) and is also considered an important environmental indicator for finding fishing grounds (Chen, 2004). Tian (2006) reported that *O. bartramii* is mainly distributed in the areas where the value of SSHA is below or near zero from August to November. Lu and Chen (2008) found that the squid *Illex argentinus* preferred habitats with zero or negative values of SSHA in the southwest Atlantic Ocean. This phenomenon also existed in the study of habitat suitability for chub

mackerel (*Scomber japonicus*) in the East China Sea (Chen et al., 2009) and in the study of the distribution of fishing grounds for purpleback flying squid (*Symlectoteuthis oualaniensis*) in the northwest Indian Ocean (Chen and Shao, 2006).

Based on the previous results, it was found that *O. bartramii*, as a short-lived (1-year) species, is usually aggregated in the waters with favorable ranges of SST, SSS, SSHA, and chl *a*. Although the favorable ranges of these environmental variables for *O. bartramii* are known, a robust method to predict where *O. bartramii* will aggregate in the traditional fishing grounds from these variables is not yet available. It is important to develop a model to predict the occurrence of aggregations of *O. bartramii* to reduce bycatch of untargeted species, reduce fuel costs, and improve efficiency of the fishery.

Habitat suitability index (HSI) modeling can be used in combination with the geographic information system (GIS) technology to create maps important to fisheries management (Eastwood et al., 2001). HSI models are based on suitability indices that reflect habitat quality as a function of one or more environmental variables. Recently, HSI modeling methods have been successfully used to identify and forecast potential fishing grounds for bigeye tuna (*Thunnus obesus*) (Feng et al., 2007; Chen et al., 2008b) and chub mackerel (Chen et al., 2009). Because near real-time environmental variables such as SST, chl *a*, and SSHA can be easily measured by remote sensing, an HSI modeling approach has great potential for estimating abundance (which will be used for resource management), and for forecasting fishing grounds.

The objectives of this study were to develop an HSI model to detect the potential fishing grounds for neon flying squid by using remote sensing data in combination with fisheries data, and to find the optimal habitat for *O. bartramii* on their feeding grounds to provide a scientific basis for the management of this species. The environmental variables considered in this study included SST, SSS, SSHA, and chl *a*, all of which have been identified as critical to the distribution and abundance of *O. bartramii* in previous studies (e.g., Chen, 1997; Wang et al., 2003; Xu et al., 2004; Tian, 2006).

## Methods and materials

### Fishery data

The area of 39–46°N latitude and 150–165°E longitude is an important traditional fishing ground for *O. bartramii* from August to November (Chen and Tian, 2005). Between 75% and 84% of the total catch has been landed in this area by Chinese mainland squid jigging fleets during the last decade (Chen et al., 2008a). Fishery data from 1999 to 2005 from this area were compiled monthly (Chinese Mainland Squid Technical Group, Shanghai Ocean University, Shanghai, China). These data, including squid catch per fishing day and fishing position, were georeferenced and grouped into a unit of 0.5°×0.5° latitude and longitude.

We assumed no bycatch in the squid fishery (Wang and Chen, 2005) and that catch per unit of effort (CPUE) (tons [t]/day [d]) of the squid jigging vessels is a good indicator of stock abundance on the fishing grounds (Chen et al., 2008c). The nominal CPUE in one fishing unit of 0.5°×0.5° was calculated as follows:

$$CPUE_{ymi} = \frac{C_{ymi}}{F_{ymi}}, \quad (1)$$

where $CPUE_{ym}$ = monthly nominal CPUE(t/d) at $i$ fishing units in month $m$ and year $y$;
$C_{ymi}$ = monthly catch (t) at $i$ fishing units in month $m$ and year $y$; and
$F_{ymi}$ = number of fishing days at $i$ fishing unit in month $m$ and year $y$.

### Satellite remote sensing data

Physical and biological environmental data used to describe oceanographic conditions in our survey area included SST, SSS, SSHA, and chl *a*. Monthly SST data with a spatial resolution of 0.5°×0.5° were obtained from the Physical Oceanography Distributed Active Archive Center (PODAAC) of the National Aeronautics and Space Administration (NASA) website (http://podaac.jpl.nasa.gov/DATA_CATALOG/index.html, accessed October 2008). Monthly SSS and SSHA data sets, both with a spatial resolution of 0.5°×0.5°, were downloaded from the IRI/LDEO Climate Data Library (http://iridl.ldeo.columbia.edu, accessed October 2008). Monthly chl-*a* level-3 standard map images with a spatial resolution of 9 km, from the "sea viewing wide field of view sensor (SeaWiFS), were obtained from the Goddard Space Flight Center on the NASA website (http://oceancolor.gsfc.nasa.gov/SeaWiFS/, accessed October 2008).

### Establishment of the HSI model

The potential fishing grounds could be estimated through a habitat model combined with satellite-derived environmental factors. Fishing effort has been considered an index of fish occurrence or fish availability (Andrade and Garcia, 1999), and also successfully used in developing HSI models (Gillis et al., 1993; Swain and Wade, 2003; Zainuddin, et al., 2006; Tian et al., 2009). Therefore, we first analyzed fishing effort in relation to the above four environmental variables to identify the probability of *O. bartramii* availability. The probability, expressed as a suitability index (SI), was defined from the relationships between fishing effort and environmental variables. The highest probability value (SI=1) is associated with the fishing effort in a given interval of the environmental variables, which represents the most favorable environmental condition (Brown et al., 2000). The lowest probability value (SI=0) indicates the lowest fishing

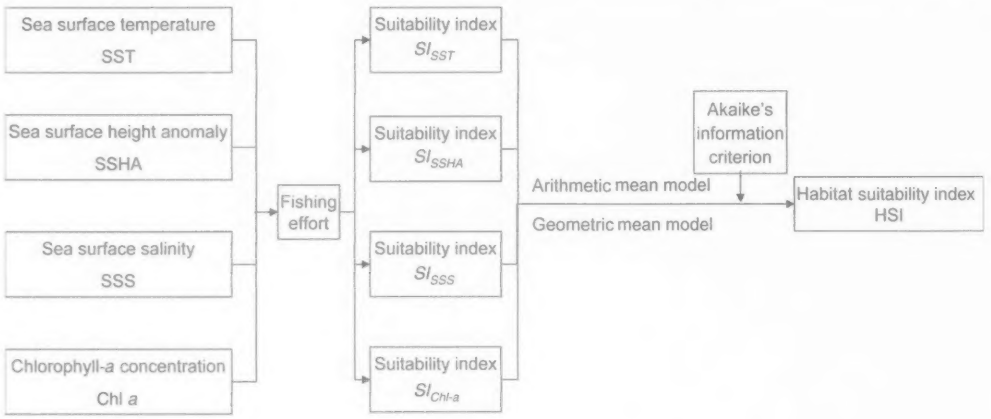


**Figure 2**

Procedure for estimating the habitat suitability index (HSI) for neon flying squid (*Ommastrephes bartramii*) in the Northwest Pacific Ocean and the procedure for selecting the HSI model based on Akaike's information criterion.

effort (i.e., equal to 0) in the presence of fishing. The SI values between 0 and 1 were assigned to the ranges of the corresponding environmental variable (Table 1; Brown et al., 2000).

The SI values derived from each variable were then combined into the empirical HSI model (Fig. 2). Two empirical HSI models, the arithmetic mean model (AMM) and the geometric mean model (GMM) are commonly used to estimate habitat availability (U.S. Fish and Wildlife Service, 1980a, 1980b; Hess and Bay, 2000; Lauver et al., 2002; Chen et al., 2009). The HSI is a univariate variable also having a value between 0 and 1 (Brooks, 1997). The two empirical HSI models were described as follows:

**Table 1**

Definitions of suitability index values for *Ommastrephes bartramii* based on the fishing effort of Chinese squid jigging fleets in one fishing unit of 0.5° latitude × 0.5° longitude in the Northwest Pacific Ocean.

| Suitability index value | Description of habitat use |
|---|---|
| 1 | The highest fishing effort in the Chinese squid jigging fishery |
| 0.5 | Common occurrence or average fishing effort in the Chinese squid jigging fishery (between 2000 fishing days and the highest fishing effort) |
| 0.1 | Rare occurrence or low fishing effort in the Chinese squid jigging fishery (fewer than 2000 fishing days) |
| 0 | Fishing effort is zero in the Chinese squid jigging fishery (0 fishing days) |

AMM (Hess and Bay, 2000; Chen et al., 2009):

$$HSI_{AMM} = \frac{1}{n}\sum_{i=1}^{n} SI_i; \quad (2)$$

and GMM (Lauver et al., 2002; Chen et al., 2009):

$$HSI_{GMM} = (\prod_{i=1}^{n} SI_i)^{1/n}; \quad (3)$$

where $SI_i$ = the SI for $i^{th}$ environmental variable;
$n$ = the number of environmental variables used in the model;
$i$ = 1, 2, ..., and $n$.

On the basis of previous studies on the relationship between environmental variables and squid catch, we considered SST as the primary variable for identifying habitat for *O. bartramii* and used different combinations of one (SST), two (SST and one other variable), three (SST and two other variables), and four (SST, SSS, SSHA, and chl *a*) variables as habitat data. The SI values derived from different combinations of habitat variables were then combined into the HSI model (Fig. 2).

### Selection of HSI model and validation

The monthly HSI values from August to October of 1999–2004 were estimated by the approach described above. The percentages of total fishing effort from 1999

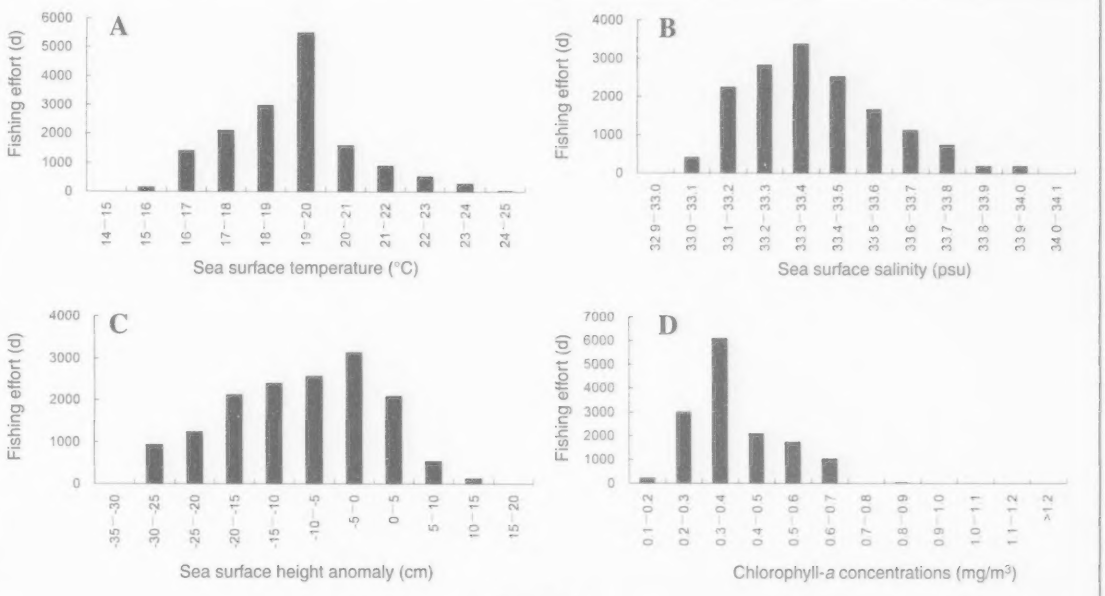


**Figure 3**

The total fishing effort measured in days (d) for *Ommastrephes bartramii* in the Northwest Pacific Ocean by the Chinese squid jigging fleets in relation to (**A**) sea surface temperature, (**B**) sea surface salinity, (**C**) sea surface height anomaly, and (**D**) chlorophyll-*a* concentrations during August 1999–2004.

to 2004 were also produced according to ranges of calculated HSI values (i.e., HSI = [0–0.2]; [0.2–0.4]; [0.4–0.6]; [0.6–0.8]; and [0.8–1.0]). Therefore, we assumed that a positive linear relationship exists between the value of HSI and fishing effort. The model can be written as

$$Y = a + bX,$$

where $Y$ = the percentage of the fishing effort corresponding to different HSI values calculated for the same time;
$X$ = the HSI value; and
$a$ and $b$ are the two parameters to be estimated.

The performance of different HSI models with one, two, three, and four environmental variables were evaluated and compared to identify the most suitable HSI model based on the Akaike's information criterion (AIC; Akaike, 1981).

The model that yielded the minimum AIC value was selected as the best model. This model was then used for model testing and validation. The spatial distributions of HSI values derived from the above selected HSI model in 2005 were mapped with Marine Explorer, vers. 4.0 (Environmental Simulation Laboratory Co, Ltd, Saitama, Japan) for forecasting potential fishing grounds and were compared with the actual fishery data from the Chinese squid jigging fleets in 2005.

## Results

### Squid catch in relation to environmental variables

During August, fishing effort was highest in waters with SSTs ranging from 17° to 20°C (Fig. 3A), and the preferred SST tended to be centered at 19–20°C. High fishing effort (>2000 days) with respect to SSS occurred in areas where sea surface salinity (SSS) varied from 33.1 to 33.5 (Fig. 3B), and where the preferred SSS was between 33.3 and 33.4. We also found that high fishing effort (>2000 days) related to SSHA and chl *a* occurred in waters with SSHA ranging from –20 cm to 5 cm and with chl-*a* values between 0.2 to 0.4 mg/m$^3$. The optimum SSHA and SSS tended to be between –5 and 0 cm and between 0.3 and 0.4 mg/m$^3$ (Fig. 3, C and D). Similar results were shown for September and October (Figs. 4 and 5).

The spatial distribution of fishing effort for *O. bartramii* from August of 2004 is presented in Figure 6 to show its relationship with environmental variables SST, SSS, SSHA, and chl *a*. The center of fishing areas with a high aggregation of squid occurred in the waters of 42°–44° N latitude and 154°–157°E longitude (Fig. 6). The environmental ma; s of four variables indicated that squid were aggregated mostly in warm water near the 19°C SST isotherm (Fig. 6A) and 33.3 psu SSS isohaline (Fig. 6B), in the edge of a cold ring near the –5 cm SSHA (Fig. 6C), and in relatively high

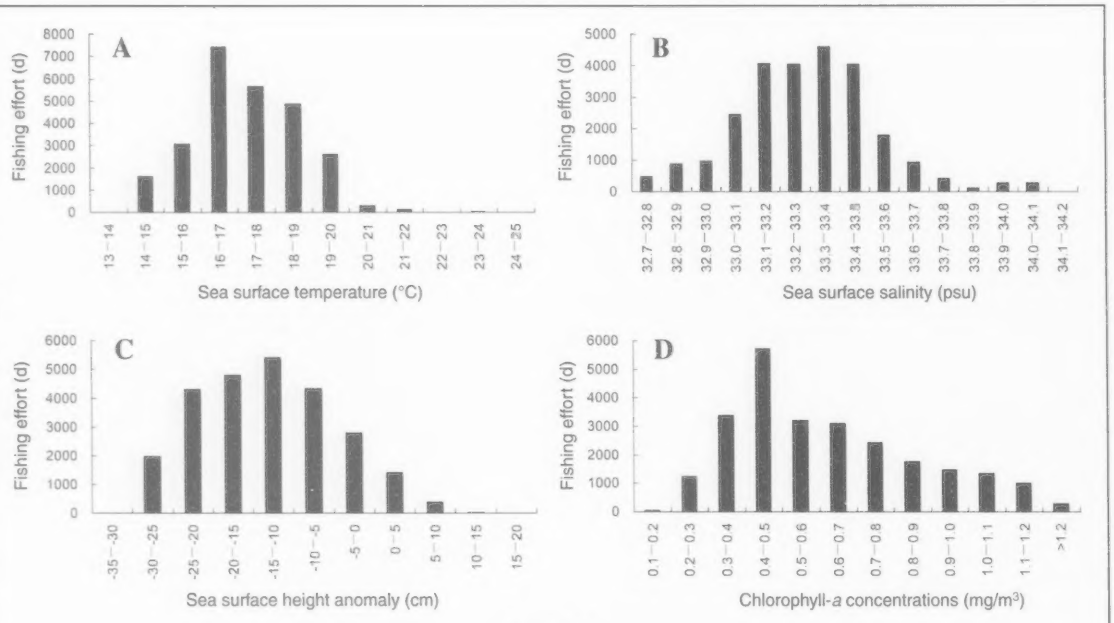


**Figure 4**

The total fishing effort measured in days (d) for *Ommastrephes bartramii* in the Northwest Pacific Ocean by the Chinese squid jigging fleets in relation to (**A**) sea surface temperature, (**B**) sea surface salinity, (**C**) sea surface height anomaly, and (**D**) chlorophyll-*a* concentrations during September 1999–2004.

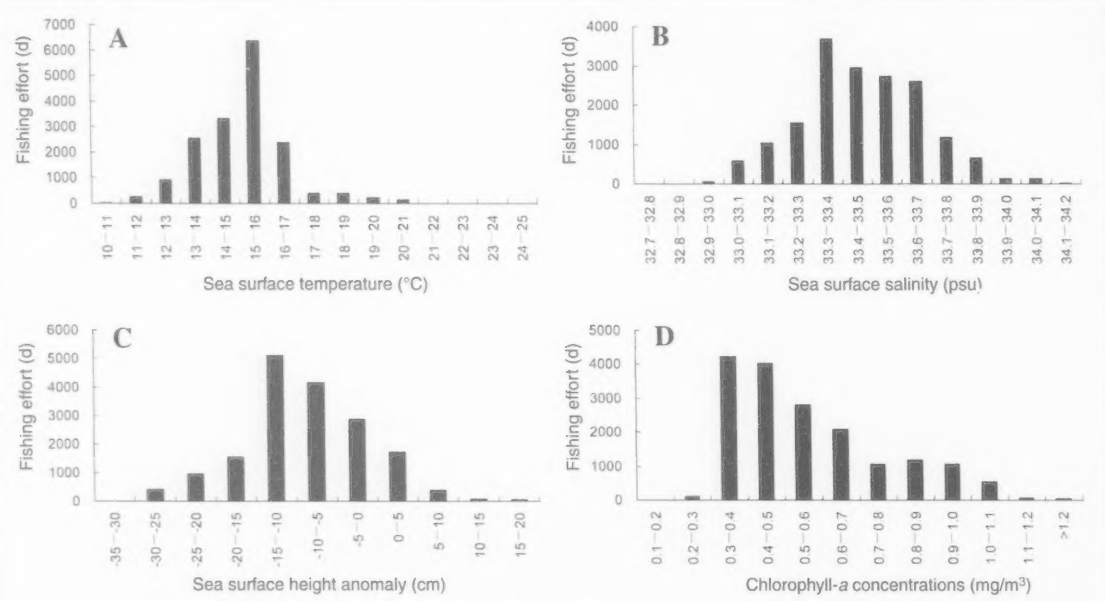


**Figure 5**

The total fishing effort measured in days for *Ommastrephes bartramii* in the Northwest Pacific Ocean by the Chinese squid jigging fleets in relation to (**A**) sea surface temperature, (**B**) sea surface salinity, (**C**) sea surface height anomaly, and (**D**) chlorophyll-*a* concentrations during October 1999–2004.

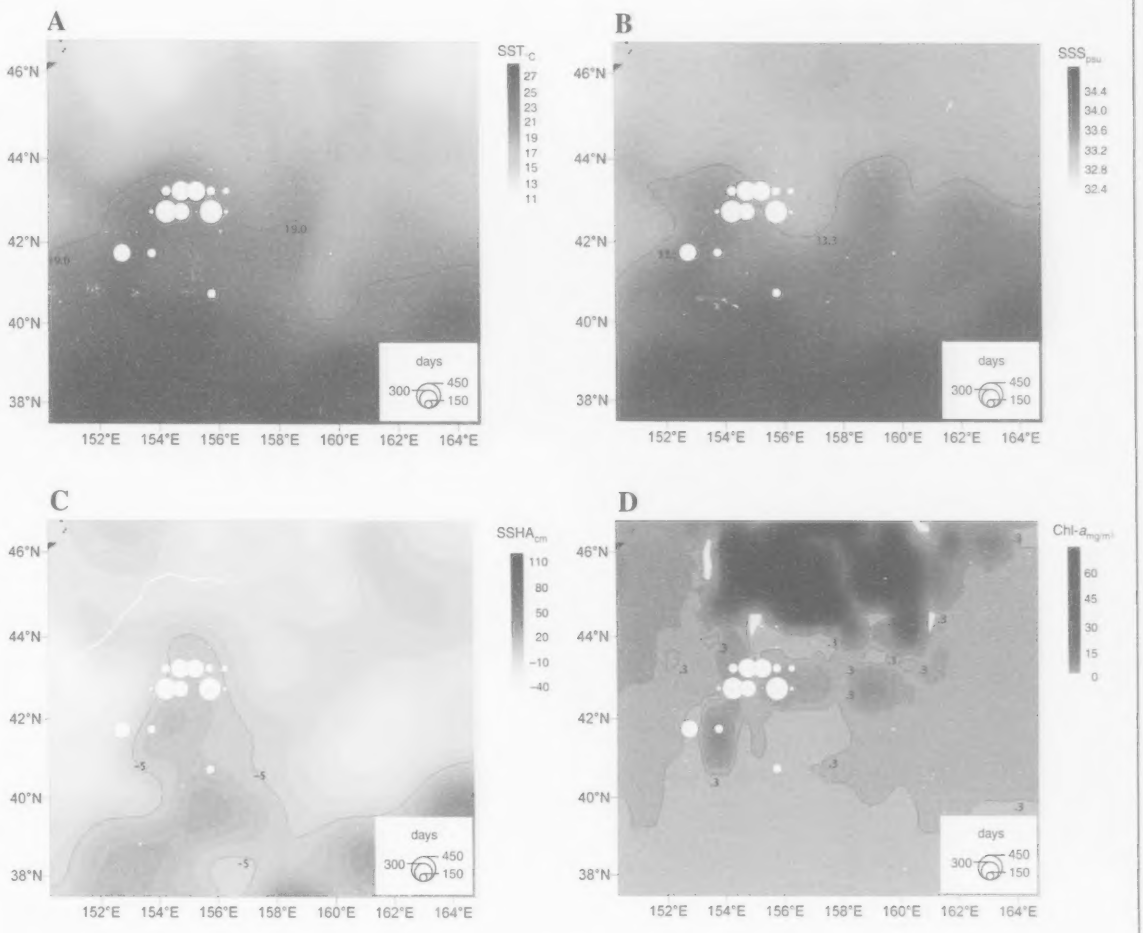


**Figure 6**

The spatial distribution of fishing effort for *Ommastrephes bartramii* in the Northwest Pacific Ocean from the Chinese squid jigging fleets during August 2004 overlaid on (**A**) sea surface temperature (SST), (**B**) sea surface salinity (SSS), (**C**) sea surface height anomaly (SSHA), and (**D**) chlorophyll-*a* (chl-*a*) images. The numbers 19.0, 33.3, −5, and 0.3 in the maps represent 19.0 SST isotherm, 33.3 SSS isohaline, −5 cm SSHA and 0.3 mg/m$^3$ chl *a*, respectively.

chl-*a* concentration of about 0.3 mg/m$^3$ (Fig. 6D) during August in 2004.

Because these four environmental variables are closely related with *O. bartramii* distribution, we rescaled them with SI values (ranging from 0 to 1) based on histogram distributions (Figs. 3, 4, and 5). On the basis of the SI definition (Brown et al., 2000; Table 1), the highest fishing effort was given an SI value of 1, the total fishing effort below 2000 days was given an SI value of 0.1, and the total fishing effort between the highest fishing effort and 2000 days was given an SI value of 0.5. The definitions of SI values for the four environmental variables are shown in Table 2.

### HSI model selection

The different HSI models with one, two, three, and four environmental variables were evaluated for the most parsimonious HSI model. The HSI model with one variable (SST) was the best for predicting the percentage of fishing effort in an area when the GMM was applied (Table 3), whereas the HSI model with three variables (SST, SSHA, and chl *a*) was the best when the AMM was applied (Table 3). When the same sets of environmental variables were used for the two empirical HSI models, respectively, the AMM model yielded better results in predicting the fishing effort because its AIC value was less than that of the GMM model.

Therefore, we determined that the AMM model with three variables, SST, SSHA, and chl *a*, was the most parsimonious HSI model (Table 3).

To further compare the performances of AMM and GMM, we estimated the average actual percentage of fishing catch, average actual percentage of fishing effort, and average CPUE of *O. bartramii* according to the grouped HSI values from AMM and GMM with three variables, SST, SSHA, and chl *a*, from August to October, 1999–2004. From August to October, the area with the HSI value >0.6 had 58.8% of the total catch, 56.63% of the total fishing effort for the AMM model (Fig. 7, A and B), but 51.46% of the total catch and 46.56% of the total fishing effort based on the GMM model (Fig. 7, A and B). The area with the HSI value of less than 0.4 yielded 15.48% and 38.58% of the total catch according

**Table 2**

Definition of suitability index (SI) values for the four environmental variables—sea surface temperature (SST), sea surface salinity (SSS), sea surface height anomaly (SSHA), and chlorophyll-*a* (chl-*a*) concentrations—used to develop a model to predict occurrences of *Ommastrephes bartramii* aggregations from August to October in the Northwest Pacific Ocean.

| Month | SI | SST (°C) | Chl *a* (mg/m3) | SSHA (cm) | SSS (psu) |
|---|---|---|---|---|---|
| August | 1 | ≥19 and <20 | ≥0.3 and <0.4 | ≥–5 and <0 | ≥33.3 and <33.4 |
| | 0.5 | ≥17 and <19 | ≥0.2 and <0.3 | ≥–20 and <–5 | ≥33.1 and <33.3 |
| | | ≥20 and <21 | ≥0.4 and <0.6 | ≥0 and <5 | ≥33.4 and <33.6 |
| | 0.1 | ≥15 and <17 | ≥0.1 and <0.2 | ≥–30 and <–20 | ≥33.0 and <33.1 |
| | | ≥21 and <25 | ≥0.6 and <0.9 | ≥5 and <15 | ≥33.6 and <34.0 |
| | 0 | <15 and ≥25 | <0.1 and ≥0.9 | <–30 and ≥15 | <33.0 and ≥34.0 |
| September | 1 | ≥16 and <17 | ≥0.4 and <0.5 | ≥–15 and <–10 | ≥33.3 and <33.4 |
| | 0.5 | ≥15 and 16 | ≥0.3 and <0.4 | ≥–25 and <–15 | ≥33.0 and <33.3 |
| | | ≥19 and <20 | ≥0.5 and <0.8 | ≥–10 and <0 | ≥33.4 and <33.5 |
| | 0.1 | ≥14 and <15 | ≥0.1 and <0.3 | ≥–30 and <–25 | ≥32.7 and <33.0 |
| | | ≥20 and <23 | ≥0.8 and <1.3 | ≥0 and <15 | ≥33.5 and <34.1 |
| | 0 | <14 and ≥23 | <0.1 and ≥1.3 | <–30 and ≥15 | <32.7 and ≥34.1 |
| October | 1 | ≥15 and <16 | ≥0.3 and <0.4 | ≥–15 and <–10 | ≥33.3 and <33.4 |
| | 0.5 | ≥13 and <15 | ≥0.4 and <0.7 | ≥–10 and <5 | ≥33.4 and <33.7 |
| | | ≥16 and <17 | | | |
| | 0.1 | ≥10 and <13 | ≥0.2 and <0.3 | ≥–30 and <–15 | ≥32.9 and <33.3 |
| | | ≥17 and <21 | ≥0.7 and <1.3 | ≥5 and <20 | ≥33.7 and <34.1 |
| | 0 | <10 and ≥21 | <0.2 and ≥1.3 | <–30 and ≥20 | <32.9 and ≥34.1 |

**Table 3**

Parameters of linear regression model between the percentage of fishing effort and habitat suitability index (HSI) and AIC value for the two HSI models, geometric mean model (GMM) and arithmetic mean model (AMM), under different combinations of environmental variables, sea surface temperature (SST), sea surface salinity (SSS), sea surface height anomaly (SSHA), and chlorophyll-*a* (chl-*a*) concentrations. The linear regression model can be written as $Y=a+bX$, where $Y$ and $X$ represent the percentage of fishing effort and HSI, respectively. ΔAIC is the difference in Akaike's information criterion (AIC) values between that model and the best model.

| | GMM | | | | AMM | | | |
|---|---|---|---|---|---|---|---|---|
| Environmental variables | *a* | *b* | AIC | ΔAIC | *a* | *b* | AIC | ΔAIC |
| SST | 7.01 | 44.97 | 64.78 | 0 | 7.01 | 44.97 | 64.78 | 3.81 |
| SST, SSS | 13.05 | 13.47 | 71.06 | 6.28 | 8.64 | 15.68 | 76.65 | 15.68 |
| SST, SSHA | 6.19 | 27.62 | 76.54 | 11.76 | 4.26 | 31.47 | 75.77 | 14.8 |
| SST, chl *a* | 17.42 | 5.17 | 75.99 | 11.21 | 11.80 | 16.41 | 68.61 | 7.64 |
| SST, SSHA, chl *a* | 19.57 | 0.87 | 80.03 | 15.25 | 6.53 | 26.94 | 60.97 | 0 |
| SST, SSS, SSHA | 11.18 | 17.64 | 84.64 | 19.86 | –2.01 | 44.03 | 77.24 | 16.27 |
| SST, SSS, chl *a* | 19.08 | 1.84 | 77.16 | 12.38 | 2.58 | 34.85 | 62.26 | 1.29 |
| SST, SSS, SSHA, chl *a* | 18.39 | 3.23 | 71.60 | 6.82 | 1.11 | 37.78 | 70.00 | 9.03 |

to the AMM and GMM models, respectively (Fig. 7A), and produced 16.02% and 41.39% of the total fishing effort according to the AMM and GMM models accordingly (Fig. 7B).

Moreover, the monthly CPUEs from 1999 to 2004 were compiled and calculated according to the grouping of AMM-based and GMM-based HSI values estimated from the three environmental variables (SST, SSHA, and chl *a*). The CPUE values were found to increase with the AMM-based HSI value, but the CPUE was not the same for the GMM-based HSI value (Fig. 7C). When the AMM-based HSI values for an area ranged from 0 to 0.2, the average CPUE was only equal to 1.44 ±0.34 t/d (mean ±standard deviation). For the areas with HSI values ranging between 0.6 and 0.8 and higher than 0.8, the average CPUEs were 2.50 ±0.26 t/d and 3.01 ±0.59 t/d, respectively (Fig. 7C). All the results from the fishery data from 1999 to 2004 indicated that the AMM model was more suitable than the GMM model for estimating the HSI for *O. bartramii*, as we assumed.

### HSI model validation

With the HSI value estimated from the AMM model in 2005, we mapped the spatial distribution of monthly HSI values, fishing locations, and CPUEs (Fig. 8). The HSI values >0.6 were mainly found in the areas of 152°30′–156°30′E longitude and 42°30′–44°00′N latitude, and 156–159°E longitude and 40°30′–42°30′N latitude (Fig. 8A), in which the catch and fishing effort occupied 78.17% and 65.17% of the total catch and total effort, respectively (Fig. 9, A and B) and the average CPUE was 3.51 t/d in August (Fig. 9C). In September, the HSI values >0.6 were widely distributed in the waters of 150°30′–151°30′E longitude and 40°30′–41°30′N latitude, and 152–165°E longitude and 40°30′–43°30′N latitude (Fig. 8B), in which the catch and fishing effort were 96.36% and 93.19% of the total catch and effort, respectively (Fig. 9, A and B) and the average CPUE was 3.77 t/d (Fig. 9C). However, there was no fishing activity in the area between 156–160°E longitude and 40°30′–42°N latitude, and 160–165°E longitude and 40°30′–43°30′N latitude (Fig. 8B). In October, the HSI values >0.6 were located in the areas of 152°30′–156°E longitude and 42°30′–44°30′N latitude, 156–157°45E longitude and 42°–43°N latitude, 158°–160°E longitude and 41°–43°N latitude, and 162°–163°30′E longitude and 43–44°30′N latitude (Fig. 8C), where the catch and fishing effort were 68.90% and 68.16% of the total catch and efforts (Fig. 9, A and B), respectively, and the average CPUE was 3.10 t/d (Fig. 9C). These results indicate that AMM can yield a reliable prediction of the potential fishing ground for *O. bartramii*.

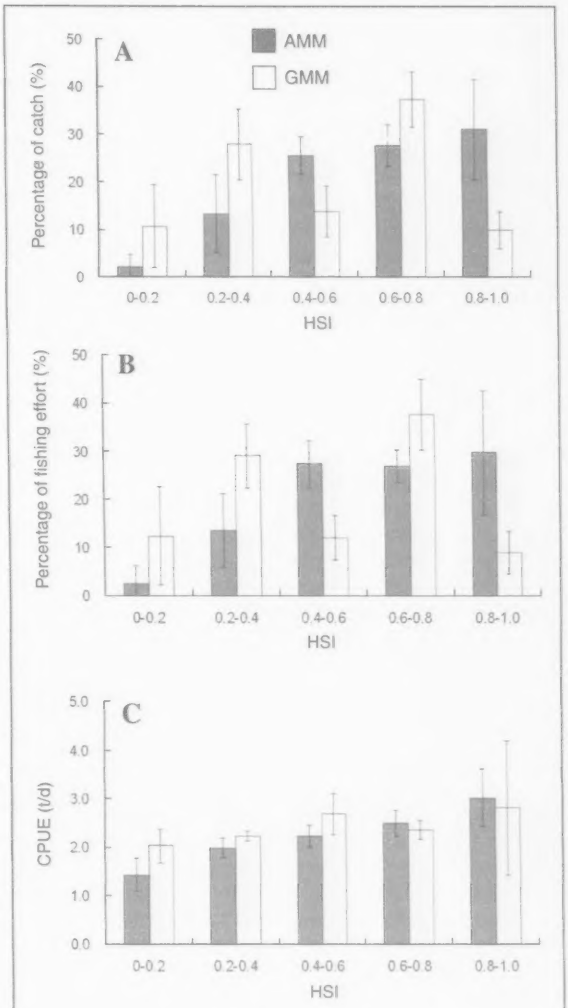


**Figure 7**

The relationship between the habitat suitability index (HSI) values estimated from the arithmetic mean model (AMM) and the geometric mean model (GMM), and (**A**) actual percentage of catch, (**B**) actual percentage of fishing effort, and (**C**) catch per unit of effort (CPUE) for *Ommastrephes bartramii* from 1999 to 2004 in the Northwest Pacific Ocean.

## Discussion

The biophysical environments in the transition zone region of North Pacific Ocean have been hypothesized to influence the migration, distribution, and abundance of *O. bartramii* (Tian, 2006; Ichii et al., 2009). Within more specific ranges, the highest density of *O. bartramii* was found in waters with favorable ranges of SST, SSS, SSHA, and chl *a* (Table 2). These ranges can be considered indicators of areas with the highest probability of finding *O. bartramii*. The highest squid abundance or optimum habitat were concentrated around the 19–20°C SST isotherm, the 33.3–33.4 psu SSS isohaline, and the 0.3mg/m$^3$ chl-*a* isopleth in August; 16–17°C SST, 33.3–33.4 psu SSS, and 0.4–0.5 mg/m$^3$ chl *a* in September;

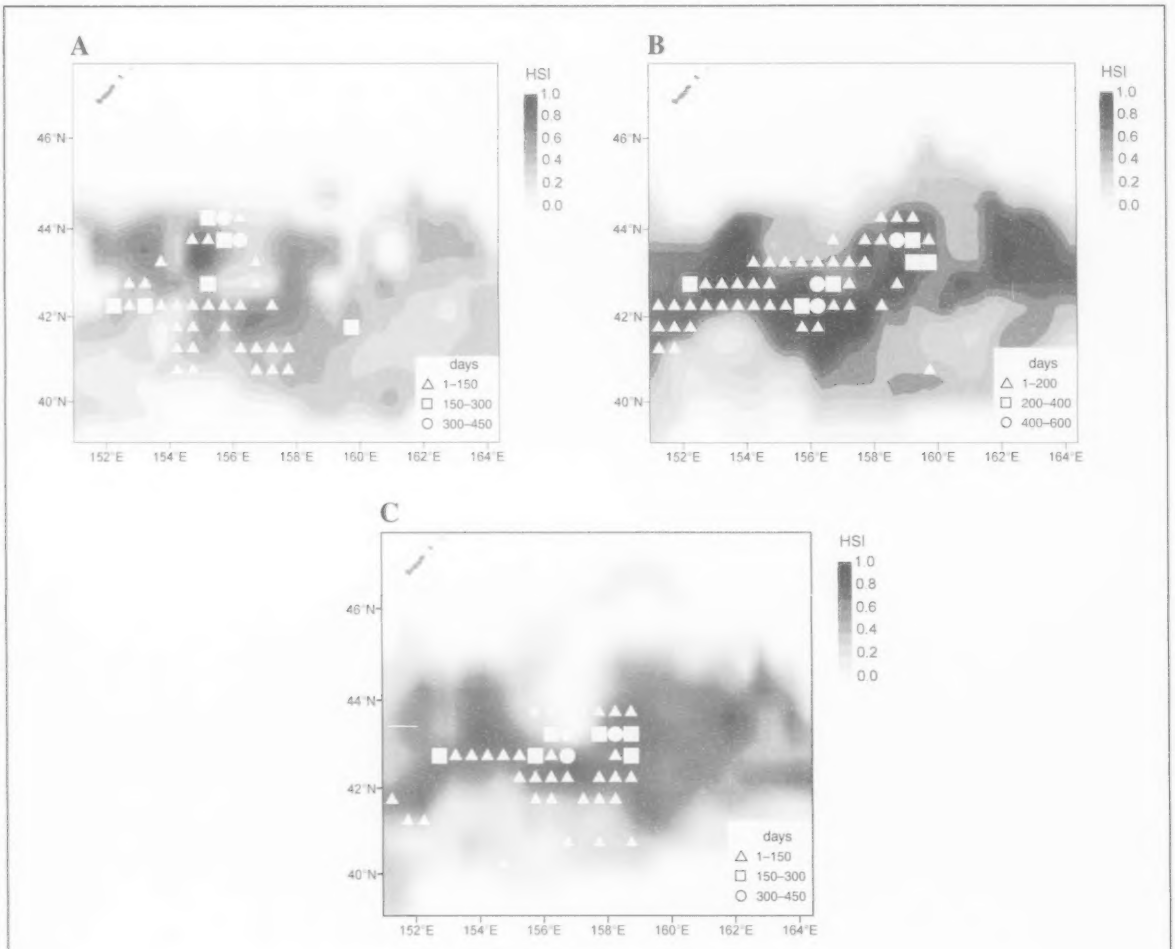


**Figure 8**

The spatial distribution of fishing effort for *Ommastrephes bartramii* from the Chinese squid jigging fleets in (**A**) August, (**B**) September, and (**C**) October 2005 overlaid on the habitat suitability index (HSI) map generated from the arithmetic mean model with three environmental variables (sea surface temperature, sea surface height anomaly, and chlorophyll-*a* concentrations).

and 15–16°C SST, 33.3–33.4 psu SSS, and 0.3–0.4 mg/m$^3$ chl *a* in October. The results are the same as those in previous findings (Chen and Chiu, 1999; Chen, 1997; Tian, 2006) and indicate that the dynamics of high *O. bartramii* aggregations were influenced by the progression of seasonal cooling (thermal and SSS front), and that the movement of the chl-*a* front can be predicted by using the specific levels of the proxy variables. These proxy indicators appear to play a critical role in formulating and patterning potential *O. bartramii* habitat and migration routes.

The SSHA field is coupled with the dynamics (currents) and thermodynamics (heat balance) of the upper ocean. Convergences and divergences of the water mass transport in the surface layer of the ocean result in positive and negative sea level anomalies, respectively (Zagaglia et al., 2004). Variations in water density, which are dominantly controlled by changes in temperature or in heat storage (changes in the mixed layer depth or its temperature), also give rise to sea level anomalies (Polito et al., 2000). It is natural, therefore, to expect that changes in SSHA can be related to variations in the CPUE and *O. bartramii* distribution. Each species has a salinity preference and congregates at vertical salinity breaks, as at horizontal salinity "fronts" (Chen, 2004). We found that *O. bartramii* distribution is closely related to the environmental variables, SST, SSS, SSHA, and chl *a*. Of the four environmental variables considered in this study, SST, SSHA, and chl *a* can be easily obtained in near real-time from remote

sensing, and they are more important than SSS in forecasting *O. bartramii* habitat. Although the chl *a* and SST data obtained from remote sensing have limitations (Arrigo et al., 1998; Santos, 2000) and errors may occur in areas where the cloudy weather is frequent, these environmental data are commonly used in marine fisheries (Santos, 2000; Wang et al., 2003; Zagaglia et al., 2004; Zainuddin et al., 2006; Chen et al., 2008b). Moreover, because *O. bartramii* undertake vertical diel movements, inhabiting water depths of 0–40 m during night and 150–350 m during the day (Wang and Chen, 2005), other environmental variables, such as water temperature at the different depths and the vertical structure of water temperature, need to be considered in future analyses.

Fishing effort is a good indicator in estimating SI values when commercial fishery data are used. In the squid jigging fishery of North Pacific Ocean, Chinese mainland fisherman first determine the fishing area with the help of near real-time SST and SSHA data from remote sensing and then locate the fishing position by using an echo-sounder (Chen, 2004; Wang and Chen, 2005). Therefore, fishing effort can be considered an index of squid occurrence. Although the nominal CPUE is affected by fishing boats, fishing technology, light power, and other environmental factors in the commercial fishery, CPUE is not suitable for estimating SI values. Tian et al. (2009) also reported that a fishing effort-based HSI model performed better than the CPUE-based HSI model in defining optimal habitats for neon flying squid, whereas the CPUE-based HSI model tended to overestimate the range of optimal habitats and underestimate monthly variations in the spatial distribution of optimal habitats.

Clearly, we found that *O. bartramii* are not randomly distributed in relation to environmental conditions. Outputs produced from HSI modeling can indicate the spatiotemporal variation of squid habitat conditions. Many fish habitat models have been developed by using combined empirical and GIS-based spatial modeling techniques (Rubec et al., 1999; Brown et al., 2000; Feng et al., 2007; Chen et al., 2008b). These approaches differ in their assumptions, inputs, and outputs. This study indicates that the HSI modeling approach, which is relatively simple and straightforward, may be an appropriate method for pinpointing optimal habitats and potential fishing grounds of squid. Because nearly every commercially important marine species is sensitive to SST and has a seasonal optimum SST range, and because the near real-time SST can be obtained from remote sensing, SST is usually considered a basic input variable in developing an HSI model (Eastwood et al., 2001; Le Pape et al., 2003; Zagaglia et al., 2004; Zainuddin et al., 2006).

Different HSI models with one to four variables tended to yield varying results. For the same set of environmental variables, the AMM model performed better than the GMM model because its AIC value was smaller (Table 3). The AMM model with three variables, SST, SSHA, and chl *a*, had the lowest AIC value for fishing effort. To further evaluate the performance of the AMM models, we compared their outputs with corresponding abundance density (CPUE). We found that the average

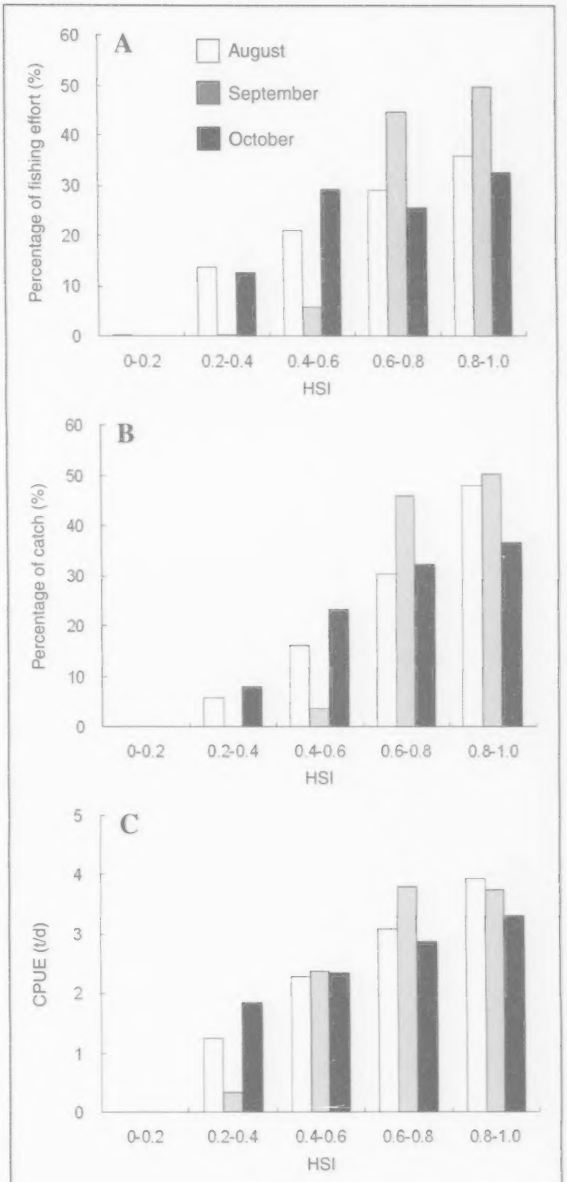


**Figure 9**

The relationship between the habitat suitability index (HSI) values estimated from the arithmetic mean model with three environmental variables (sea surface temperature, sea surface height anomaly, and chlorophyll-*a* concentrations), and (**A**) actual percentage of the total catch, (**B**) percentage of fishing effort, and (**C**) catch per unit of effort (CPUE) for *Ommastrephes bartramii* from August to October 2005.

CPUE of *O. bartramii* increased from 1.44 t/d (0–0.2 of HSI) to 3.01 t/d (0.8–1.0 of HSI) and that the improvement in HSI occurred from August to October, 1999–2004. This approach, however, is not equivalent to testing the accuracy of the HSI model for predicting the quality of habitat for a species (Wakeley, 1988). In the evaluation of habitat quality, it is important to capture both the habitat characteristics and habitat selection in the linkage between physical environments and habitat preference of target species because only a precise HSI model can yield a reliable assessment (Chen, et al., 2008b). However, the uncertainty associated with the HSI model predictions usually results from the degree of reliability of the SI curve, input data, and the HSI model structure (Chen et al., 2009).

The AMM-based HSI modeling approach used in the present study was generally successful for its intended use in mapping habitat and forecasting fishing grounds when the three environmental variables (SST, SSHA, and chl *a*) were used, whereas GMM may be appropriate for determining potential fishing grounds when only one environmental variable (SST) is used. This result shows that SST is the most important environmental variable in the HSI modeling for neon flying squid. Different structures of HSI models would lead to different results, and the optimum HSI is different when different combinations of environmental variables are considered. Chen et al. (2009) also selected the AMM model as the optimum HSI model combined with four environmental variables (SST, SSHA, SSS, and chl *a*) in studying habitat suitability for chub mackerel in the East China Sea. Other different approaches are also used in addressing fish-habitat modeling. Norcross et al. (1997) modeled habitat suitability for flatfish by using a regression tree analysis in Alaska, and Swartzman et al. (1992) and Stoner et al. (2001) used generalized additive models for modeling flatfish distribution in the Bering Sea and for winter flounder (*Pseudopleuronectes americanus*) in New Jersey, respectively. Le Pape et al. (2003) characterized the distribution of common sole (*Solea solea*), using a general linear model. Eastwood et al. (2001) applied regression quantiles and GIS procedures to model the spatial variations in spawning habitat suitability for *S. solea*. The model output better reflects theoretical findings on the spatiotemporal nature of the species' response to preferred environmental conditions. The AMM model with three environmental variables (SST, SSHA, and chl *a*) was considered to be the most parsimonious model in this study. However, we may need to conduct more studies for estimating HSI using other methods. Some of these methods may include allocating different weights for different environment variables in developing HSI models and considering more environmental variables that may influence *O. bartramii* distributions, such as water temperatures at different depths, vertical structure of water temperature, and currents.

HSI models can be applied to identify potential fishing grounds, but an optimal strategy for the squid fishermen in searching for fishing grounds would be to target an area with high habitat-suitability indices (>0.6) yielded from the AMM model. A dynamic near real-time habitat model incorporating more environmental variables, such as currents, fronts, winds, and other environmental variables, may further improve the process of identifying potential fishing areas.

## Acknowledgments

We thank the Shanghai Ocean University for providing the catch data, and NASA and The International Research Institute for Climate Prediction (IRI/LDEO) Climate Data Library of Columbia University for providing the environmental data. This study is supported by National 863 project (2007AA092201), National Nature Science Foundation (NSFC40876090), the Program for New Century Excellent Talents in University (NCET-06-0437), and Shanghai Leading Academic Discipline Project (Project S30702).

## Literature cited

Akaike, H.
1981. Likelihood of a model and information criteria. J. Econometrics 16:3–14.

Andrade, H. A., and A. E. Garcia.
1999. Skipjack tuna in relation to sea surface temperature off the southern Brazilian coast. Fish. Oceanogr. 8:245–254.

Arrigo, K. R., D. Worthen, A. Schnell, and M. P. Lizotte.
1998. Primary production in Southern Ocean waters. J. Geophys. Res. 103 (C8):15587–15600.

Bower, J. R., and T. Ichii.
2005. The red flying squid (*Ommastrephes bartramii*): A review of recent research and the fishery in Japan. Fish. Res. 76:39–55.

Brooks, R. P.
1997. Improving habitat suitability index models. Wildl. Soc. Bull. 25:163–167.

Brown, S. K., K. R. Buja, S. H. Jury, M. E. Monaco, and A. Banner.
2000. Habitat suitability index models for eight fish and invertebrate species in Casco and Sheepscot Bays, Maine. N. Am. J. Fish. Manag. 20:408–435.

Chen, C. S., and T. S. Chiu.
1999. Abundance and spatial variation of *Ommastrephes bartramii* (Mollusca: Cephalopoda) in the eastern North Pacific observed from an exploratory survey. Acta Zool. Taiwanica 10(2):135–144.

Chen, X. J.
1997. An analysis on marine environment factors of fishing ground of *Ommastrephes bartramii* in northwest Pacific. J. Shanghai Fish. Univ. 6:285–287.
2004. Fisheries resources and oceanography, 141–160 p. Ocean Press, Beijing.

Chen X. J., Y. Chen, S. Q. Tian, B. L. Liu, and W. G. Qian.
2008c. An assessment of the west winter-spring cohort of neon flying squid (*Ommastrephes bartramii*) in the Northwest Pacific Ocean. Fish. Res. 92:221–230.

Chen, X. J., B. Feng, and L. X. Xu.
2008b. A comparative study on habitat suitability index of bigeye tuna in the Indian Ocean. J. Fish. Sci. China 15(2):269–278.

Chen, X. J., G. Li, B. Feng, and S. Q. Tian.
2009. Habitat suitability of chub mackerel (*Scomber japonicus*) in the East China Sea. J. Oceanogr. 65(1):93–102

Chen, X. J., B. L. Liu, and Y. Chen.
2008a. A review of the development of Chinese distant-water squid jigging fisheries. Fish. Res. 89:211–221.

Chen, X. J., and F. Shao.
2006. Study on the resource characteristics of *Symlectoteuthis oualaniensis* and their relationships with the sea conditions in the highsea of the northwestern Indian Ocean. Periodical of Ocean University of China 36(4):611–616.

Chen, X. J. and S. Q. Tian.
2005. Study on the catch distribution and relationship between fishing ground and surface temperature for *Ommastrephes bartramii* in the northwest Pacific Ocean. J. Ocean Univ. Qingdao 35:101–107.

Chen, X. J., X. H. Zhao, and Y. Chen.
2007. El Niño/La Niña influence on the western winter-spring cohort of neon flying squid (*Ommastrephes bartramii*) in the northwestern Pacific Ocean. ICES J. Mar. Sci. 64:1152–1160.

Eastwood, P. D., G. J. Meaden, and A. Grioche.
2001. Modelling spatial variations in spawning habitat suitability for the sole *Solea solea* using regression quantiles and GIS procedures. Mar. Ecol. Progr. 224:251–266.

Feng, B., X. J. Chen, and L. X. Xu.
2007. Study on distribution of *Thunnus obesus* habitat in the Indian Ocean based on ecological suitability. J. Fish. China 31(6):805–812.

Gillis, D.M., R.M. Peterman, and A.V. Tyler.
1993. Movement dynamics in a fishery: application of the ideal free distribution to spatial allocation of effort. Can. J. Fish. Aquat. Sci. 50:323–333.

Hess, G. R., and J. M. Bay.
2000. A regional assessment of windbreak habitat suitability. Environ. Monit. Assess. 61(2):237–254.

Ichii, T., K. Mahapatra, H. Okamura, and Y. Okada.
2006. Stock assessment of the autumn cohort of neon flying squid (*Ommastrephes bartramii*) in the North Pacific based on past large-scale high seas driftnet fishery data. Fish. Res. 78:286–297.

Ichii, T., K. Mahapatra, M. Sakai, and Y. Okada.
2009. Life history of the neon flying squid: effect of the oceanographic regime in the North Pacific Ocean. Mar. Ecol. Progr. 378:1–11.

Lauver, C. L., W. H. Busby, and Whistler J. L.
2002. Testing a GIS model of habitat suitability for a declining grassland bird. Environ. Manag. 30(1):88–97.

Le Pape, O., F. Chauvet, S. Mahevas, P. Lazure, D. Guerault, and Y. Desaunay.
2003. Quantitative description of habitat suitability for the juvenile common sole (*Solea solea*, L.) in the Bay of Biscay (France) and the contribution of different habitats to the adult population. J. Sea Res. 50:139–149.

Lu, H. J., and X. J. Chen.
2008. Catch distribution of *Ommastrephes bartramii* and its relationship with sea surface temperature in the North Pacific Ocean in 2006. J. Guangdong Ocean Univ. 3:230–234.

Norcross, B. L., F. Mutter, and B. A. Holladay.
1997. Habitat models for juvenile pleuronectids around Kodiak Island, Alaska. Fish. Bull. 95:504–520.

Pearcy, W. G.
1991. Biology of the transition region. *In* Biology, oceanography, and fisheries of the North Pacific transition zone and Subarctic frontal zone (J. A. Wetherall, ed.), p. 39–55. NOAA Tech. Rep. NMFS 105.

Polito, P. S., O. T. Sato, and W. T. Liu.
2000. Characterization and validation of the heat storage variability from TOPEX/Poseidon at four oceanographic sites. J. Geophys. Res. 105:16911–16921.

Roden, G. I.
1991. Subarctic-subtropical transition zone of the North Pacific: large- scale aspects and mesoscale structure. *In* Biology, oceanography and fisheries of the North Pacific transition zone and Subarctic frontal zone (J. A. Wetherall, ed.), vol. 105, p. 1–38. NOAA Tech. Rep. NMFS 105.

Rubec, P. J., J. C. W. Bexley, H. Norris, M. S. Coyne, M. E. Monaco, S. G. Smith, and J. S. Ault.
1999. Suitability modeling to delineate habitat essential to sustainable fisheries. *In* Fish habitat: essential fish habitat and rehabilitation (L. Benaka, ed.), p. 108–133. Am. Fisheries Soc., Symp. 22, Bethesda, MD.

Santos, A. M. P.
2000. Fisheries oceanography using satellite and airborne remote sensing methods: a review. Fish. Res. 49:1–20.

Stoner, A. W., J. P. Manderson, and J. P. Pessuti.
2001. Spatially explicit analysis of estuarine habitat for juvenile winter flounder: combining generalized additive models and geographic information systems. Mar. Ecol. Progr. 213:253–271.

Swain, D. P., and E. J. Wade.
2003. Spatial distribution of catch and effort in a fishery for snow crab (*Chionoecetes opilio*): tests of predictions of the ideal free distribution. Can. J. Fish. Aquat. Sci. 60: 897–909.

Swartzman, G. L., C. Huang, and S. Kaluzny.
1992. Analysis of Bering Sea groundfish survey data using generalized additive models. Can. J. Fish. Aquat. Sci. 49(7):1366–1378.

Tian, S. Q.
2006. Evaluation on neon flying squid *Ommastrephes bartramii* stock in the Northwest Pacific Ocean and its relationship with marine environmental factors. Ph. D. diss., 132 p. College of Marine Sciences, Shanghai Fisheries University (renamed as Shanghai Ocean University in 2008), Shanghai, China.

Tian, S. Q., X. J. Chen, Y. Chen, L. X. Xu, and X. J. Dai.
2009. Evaluating habitat suitability indices derived from CPUE and fishing effort data for *Ommastrephes bartramii* in the northwestern Pacific Ocean. Fish. Res. 95:181–188.

U.S. Fish and Wildlife Service.
1980a. Habitat evaluation procedures (HEP). Ecological Service Manual 102. GPO, Washington, D.C.
1980b. Standards for the development of habitat suitability index models. Ecological Service Manual 103. GPO, Washington, D.C.

Wakeley, J. S.
1988. A method to create simplified versions of existing habitat suitability index (HSI) models. Environ. Manag. 1:79–83.

Wang, W. Y., C. H. Zhou, Q. Q. Shao, Y. C. Xue, T. Y. Zhang, and T. Z. Rong.
2003. An application of RS/GIS on study on the migration dynamics of *Ommastrephes bartramii*. High Tech. Lett. 11:90–93.

Wang, Y. G., and X. J. Chen.
2005. The resource and biology of economic oceanic squid in the world. Ocean Press, Beijing, China.
Watanabe, H., T. Kubodera, T. Ichii and S. Kawahara.
2004. Feeding habits of neon flying squid *Ommastrephes bartramii* in the transitional region of the central North Pacific. Mar. Ecol. Progr. 266:173–184.
Xu, Z. L., X. S. Cui, and H. L. Huang.
2004. Distribution of zooplankton in *Ommastrephes bartramii* fishing ground of the north Pacific Ocean and its relationship with the fishing ground. J. Fish. China. 5:515–521.
Yatsu, A., and J. Mori.
2000. Early growth of the autumn cohort of neon flying squid, *Ommastrephes bartramii*, in the North Pacific Ocean. Fish. Res. 45:189–194.
Yatsu, A., and T. Watanabe.
1996. Interannual variability in neon flying squid abundance and oceanographic conditions in the central North Pacific, 1982–1992. Bull. Nat. Res. Inst. Far Seas Fish. 33:123–138.
Zagaglia, C. R., J. A. Lorenzzetti, and J. L. Stech.
2004. Remote sensing data and longline catches of yellowfin (*Thunnus albacares*) in the equatorial Atlantic. Rem. Sens. Environ. 93:267–281.
Zainuddin, M., H. Kiyofuji, K. Saitoh, and S. Saitoh.
2006. Using multi-sensor satellite remote sensing and catch data to detect ocean hot spots for albacore (*Thunnus alalunga*) in the northwestern North Pacific. Deep-Sea Res. Part II Top. Stud. Oceanogr. 53:419–431.
Zhang, T. Y., Q. Q. Shao, and C. H. Zhou.
2001. Application of satellite altimeter data in fishery stock assessment. Fish. Sci. 20(6):4–8.

# Statistical inference about the relative efficiency of a new survey protocol, based on paired-tow survey calibration data

**Noel G. Cadigan (contact author)**[1]

**Jeff J. Dowden**[2]

Email address for contact author: noel.cadigan@dfo-mpo.gc.ca

[1] Fisheries and Oceans Canada
Northwest Atlantic Fisheries Center
80 East White Hills Road
St. John's, NL, Canada A1C 5X1

[2] Research and Evaluation Department
Newfoundland and Labrador Centre for Health Information
28 Pippy Place
St. John's, NL, Canada A1B 3X4

**Abstract**—Paired-tow calibration studies provide information on changes in survey catchability that may occur because of some necessary change in protocols (e.g., change in vessel or vessel gear) in a fish stock survey. This information is important to ensure the continuity of annual time-series of survey indices of stock size that provide the basis for fish stock assessments. There are several statistical models used to analyze the paired-catch data from calibration studies. Our main contributions are results from simulation experiments designed to measure the accuracy of statistical inferences derived from some of these models. Our results show that a model commonly used to analyze calibration data can provide unreliable statistical results when there is between-tow spatial variation in the stock densities at each paired-tow site. However, a generalized linear mixed-effects model gave very reliable results over a wide range of spatial variations in densities and we recommend it for the analysis of paired-tow survey calibration data. This conclusion also applies if there is between-tow variation in catchability.

Manuscript submitted 20 April 2009.
Manuscript accepted 14 September 2009.
Fish. Bull. 108:15–29 (2010).

The views and opinions expressed or implied in this article are those of the author (or authors) and do not necessarily reflect the position of the National Marine Fisheries Service, NOAA.

Surveys are an important source of information for most fish stock assessments. They provide indices of abundance often used in mathematical models of the population to estimate absolute stock size and to provide future catch advice or to evaluate catch options for fishery managers (Kimura and Somerton, 2006). Survey indices are measures that we expect to be proportional to, or to indicate, stock size. The expected value of a random index $R_y$ available for year $y$ is related to stock size ($S_y$) by the model $E(R_y)=qS_y$. The constant of proportionality, $q$, is usually referred to as the catchability of the index. Although we cannot directly infer stock size from a time series of indices $R_1, \ldots, R_Y$ we can infer trends in stock size when $q$ is the same each year. The survey observation is commonly referred to as a *set* (as in *set* the gear), or a *tow* when a trawl is used. The average survey catch for all sets provides an index of stock size. If the same survey protocols are used from year to year then the catchability of the index should remain relatively constant. The catchability may depend on length or age of fish, and we consider such extensions later in this article.

There are many stock assessment models that are based on survey indices (e.g., see Quinn and Deriso, 1999) and information on fishing and natural mortality, to estimate absolute stock size. For most models it is necessary to have a fairly long time-series of survey indices, often 10 years or more. Over such time frames it may be necessary to change survey protocols. This could be due to a need to replace the survey vessel, or to change gears for new priority species, etc. When such changes occur, it is useful to have information about how the catchability of the new survey protocol compares to the old protocol.

Performing simultaneous paired-tow surveys using both protocols (e.g., old and new vessels, old and new fishing gears) provides direct data on how the catchabilities compare (e.g., Kimura and Zenger, 1997) Another approach is to simply fish side by side using both protocols and use the paired-catch data to estimate the ratio of catchabilities. We refer to this ratio as the relative efficiency,

$$\rho = \frac{q_c}{q_t}, \qquad (1)$$

where $q_c$ and $q_t$ = the catchabilities of the old (control, $c$) and new (test, $t$) survey protocols.

Notations are given in Table 1. If the fish densities entering both trawls are the same, or similar, and densities at different tow sites vary considerably, then for the same number of tows a paired-tow calibration study should produce better results than the

**Table 1**

Definitions of variables and acronyms for models used to estimate relative efficiency from comparative fishing data.

| | |
|---|---|
| $R_{ij}$ | Random variable for catches obtained at the $i$'th paired-tow station by survey protocol $j$=$c$ (control) or $j$=$t$ (test) |
| $r_{ij}$ | Observation of $R_{ij}$ |
| $R_i$ | $R_{ic}+R_{it}$ |
| $R_{ijk}$ | Catches at the $i$'th tow station and $k$'th length class by survey protocol $j$ |
| $R_{ik}$ | Total catch (from both vessels) at length class $k$ from set $i$, $R_{ick}+R_{itk}$ |
| $n$ | Total number of paired-tow stations |
| $n_i$ | Number of length classes caught in the i'th pair of tows |
| $n^*$ | Total number of sets and length classes, $n^* = \sum_i n_i$ |
| $\lambda_{ij}$ | Fish densities encountered at station $i$ and tow $j$ |
| $\delta_i$ | $\log(\lambda_{ic}/\lambda_{it})$ |
| $q_j$ | Probability an encountered fish is captured, $j$=$c$, $t$ |
| $\rho$ | Relative efficiency, $\rho=q_c/q_t$ |
| $\beta$ | $\log(\rho)$ |
| $p$ | Probability a captured fish was caught by the control protocol |
| $D_{ij}$ | Tow duration at the $i$'th paired-tow station by vessel $j$ |
| $F_{ijl}$ | Subsampling fraction for length $l$ fish |
| $Z_{il}$ | Logit offset, $Z_{il}=\log(D_{ic}F_{icl}/D_{it}F_{itl})$ |
| $\phi$ | Binomial over-dispersion |
| $\sigma^2$ | Random effect variance |
| CIs | Confidence intervals |
| GLIM | Generalized linear model |
| MLE | Maximum likelihood estimation |
| GLMM | Generalized linear mixed model |
| PQLE | Penalized quasi-likelihood estimation |
| CV | Coefficient of variation |
| VO | Vessel-effect over-dispersed binomial model estimation |
| VM | Vessel-effect binomial model with random intercept for each set; marginal MLE |
| VP | Vessel-effect binomial model with random intercept for each set; PQLE |
| VLO | Vessel- and length-effects over-dispersed binomial model estimation |
| $VLM_i$ | Vessel- and length-effects binomial model with random intercept for each set; marginal MLE |
| $VLP_i$ | Vessel- and length-effects binomial model with random intercept for each set; PQLE |
| $VLM_{is}$ | Vessel- and length-effects binomial model with random intercept and slope for each set; marginal MLE |
| $VLP_{is}$ | Vessel- and length-effects binomial model with random intercept and slope for each set; PQLE |

simultaneous survey approach. This is analogous to the common paired versus unpaired experiment situation (e.g., Devore, 1991). Pelletier (1998) reviewed estimation methods used in many vessel calibration experiments.

The basic data obtained from paired-tow calibration studies are the catches $R_{ij}$ obtained at the $i$th paired-tow station ($i$=1, ... ,$n$) by survey protocols $j$=$c$ (control) or $j$=$t$ (test). Let $\lambda_{ij}$ denote the fish densities encountered at station $i$ and tow $j$. These densities may be different because of small-scale spatial heterogeneity in stock densities. We assume that each tow catches fish with probabilities $q_c$ and $q_t$ which are the same from site to site (i.e., $i$), and that catches are Poisson random variables with means

$$E(R_{it}) = q_t\lambda_{it} = \mu_i, \text{and } E(R_{ic}) = q_c\lambda_{ic} = \rho\mu_i \exp(\delta_i), \quad (2)$$

where $\delta_i = \log(\lambda_{ic}/\lambda_{it})$.

If both vessels encounter exactly the same stock densities at each tow station, then $\delta_i$=0, $i$=1, ... , $n$.

When there is no spatial heterogeneity in stock densities, $\rho$ can be estimated by using a Poisson generalized linear model (GLIM; e.g., McCullagh and Nelder, 1989). This is essentially the approach used by Benoît and Swain (2003), although they adjusted for extra-Poisson variability in the catches. There are $2n$ observations that can be used to estimate the $n$ density parameters ($\mu$) and $\rho$. Pelletier (1998) used a similar approach, with a negative binomial mean-variance assumption, which is a type of Poisson over-dispersion. These approaches are complicated because the number of $\mu$ parameters can be large if many tow stations are sampled, and the situation is worse if there are length effects.

A better approach for inferences about $\rho$ (see section 4.5 in Cox and Snell, 1989, and example 3.1 in Reid, 1995) when catches are Poisson random variables is to use the conditional distribution of $R_{i,c}$, given $R_i = R_{ic}+R_{it}$. Let $r_i$ be the observed value of $R_i$. The conditional distribution is binomial with a probability mass function

$$prob(R_{ic} = x \mid R_i = r_i) = \binom{r_i}{x} p^x (1-p)^{r_i - x}, \quad (3)$$

where $p = \rho/(1+\rho)$ is the probability a captured fish is taken by the control vessel.

The only unknown parameter in this distribution is $\rho$. The $n$ nuisance $\mu$ parameters are eliminated in Equation 3. There are $n$ conditional observations that can be used to estimate $\rho$. For the binomial distribution $E(R_{ic})=r_i p$ and $\mathrm{Var}(R_{ic})=r_i p(1-p)$. This approach is commonly used in commercial fishing gear size-selectivity studies (e.g., Millar 1992).

Paired-tow experiments do not eliminate spatial heterogeneity between the stock densities fished by each vessel. This heterogeneity leads to Poisson over-dispersion which has to be properly accounted for to provide reliable statistical inferences. Similarly, the relative efficiency may vary somewhat from site to site and this must also be accounted for. It is well-known in fishing gear selectivity studies that not accounting for over-dispersion and correlation leads to confidence intervals that are too narrow and spurious statistical significance (Fryer, 1991; Millar et al., 2004).

An approach to deal with over-dispersion is to use quasi-likelihood (e.g., McCullagh and Nelder, 1989) with a Poisson over-dispersion parameter $\phi$, $\mathrm{Var}(R_{ij})= \phi\, E(R_{ij})$, or a binomial over-dispersion parameter, $\mathrm{Var}(R_{ic} \mid R_i=r_i)= \phi\, r_i p(1-p)$. Confidence intervals (CIs) are adjusted based on an estimate of $\phi$. This was the approach used by Benoît and Swain (2003) to account for extra-Poisson variation, and Lewy et. al. (2004) to account for extra-binomial variation. Benoît[1] observed that using an over-dispersion parameter did not completely account for the true variability in the data and too often led to the false statistical conclusion that $\rho \neq 1$. Benoît used randomization approaches to test for statistical significance of vessel effects. We consider this approach further in the *Discussion* section.

A reasonable assumption for spatial heterogeneity in stock densities is that $\lambda_{ic}$ and $\lambda_{it}$ in Equation 2 are independent and identically distributed gamma random variables with means $\lambda_i$ and variances $\tau\lambda_i^2$. If $R_{ic} \mid \lambda_{ic}$ and $R_{it} \mid \lambda_{it}$ are Poisson distributed, then the marginal distributions of $R_{ic}$ and $R_{it}$ are negative binomials (e.g., see Cameron and Trivedi, 1998). This distribution is often suggested to be appropriate for modeling the variability of measurement error in trawl survey catches (e.g., Gunderson, 1993). This implicitly provides a rationale for assuming stock densities are gamma distributed. Dowden[2] showed that $\tau$=0.049, 0.223, 0.372 corresponds to $\mathrm{Var}(\delta_i)$=0.1, 0.5, and 0.9, and that the distribution of $\delta$ (see Eq. 2) is well approximated by a normal distribution with $\sigma^2=\mathrm{Var}(\delta_i)$. In this case a generalized linear mixed-effects model (GLMM; e.g., McCulloch and Searle, 2001) can be used to estimate $\rho$ and account for spatial heterogeneity in stock densities. GLMMs contain both fixed and random effects, and usually the random effects are assumed to have normal distributions. We refer to models with no random effects as fixed effects models (e.g., GLIMs).

GLMMs are frequently used to account for heterogeneity in fishing gear size-selectivity data (e.g., Fryer, 1991; Fryer et al., 2003; Millar et al., 2004). Fryer et al. (2003), Cadigan et al.[3] and Holst and Revill (2008) used GLMMs with paired-tow calibration data. Cadigan et al.[3] compared models with and without random effects for vessel calibration data for seven species, and suggested that GLMMs provided results that were more reliable. Cadigan et al.[3] concluded that vessel effects were not significantly different from zero; however, different conclusions could be drawn from some of their GLIM results.

There are a variety of approaches available for fitting GLMMs. A common approach is marginal maximum-likelihood estimation (MLE), which is limited in the complexity of random effects that can be accommodated. A more flexible approach is penalized quasi-likelihood estimation (PQLE). Bolker et al. (2009) provided some advantages and disadvantages of these methods. They also provided many references, including some for software packages. In some situations, PQLE is known to produce biased estimates of fixed-effect parameters like $\rho$.

In this article we extend the analyses for one of the stocks considered by Cadigan et al.[3]. By means of simulation studies we examine which of the approaches—the GLIM, GLMM with marginal MLE, or GLMM with PQLE—provides more reliable statistical inferences about $\rho$. We focus on the bias in estimates of $\rho$, on the accuracy of CIs, and on the power to detect if $\rho \neq 1$ (i.e., a true difference in catchabilities between vessels). Our purpose is to recommend the most reliable approach, at least for paired-tow survey calibration studies similar to those in Cadigan et al.[3]. We focus on methods to accommodate within-pair variations in stock densities, but our methods are also applicable when there is between-set variations in relative efficiency.

[1] Benoît, H. P. 2006. Standardizing the southern Gulf of St. Lawrence bottom trawl survey time series: Results of the 2004–2005 comparative fishing experiments and other recommendations for the analysis of the survey data. DFO Can. Sci. Advisory Secretariat Res. Doc. 2006/008. [Available from http://www.dfo-mpo.gc.ca/csas/csas/publications/resdocs-docrech/2006/2006_008_e.htm, accessed April 2009.]

[2] Dowden, J. J. Generalized linear mixed effects models with application to fishery data. M.A.S. practicum report, 128 p. Memorial Univ. Newfoundland. St. John's, Newfoundland and Labrador, Canada.

[3] Cadigan, N. G., S. J. Walsh, and W. Brodie. Relative efficiency of the Wilfred Templeman and Alfred Needler research vessels using a Campelen 1800 shrimp trawl in NAFO Subdivision 3Ps and Divisions 3LN. DFO Can. Sci. Advisory Secretariat Res. Doc. 2006/085. [Available from http://www.dfo-mpo.gc.ca/csas/Csas/Publications/ResDocs-DocRech/2006/2006_085_e.htm, accessed April 2009.]

## Materials and methods

We focus on statistical inferences for $\rho$ (i.e., Eq. 1) based on data obtained from paired-tow vessel calibration studies like those described in Cadigan et al.[3]. Briefly, in their study, data from paired-tows were collected to quantify potential differences in the catchabilities of two research survey vessels fishing with the same trawl and other protocols. Ranges of catch sizes, fish sizes in the catch, and tow depths were sought for the distributions of the species likely to be encountered. Tow stations were selected randomly as part of research surveys. High density aggregations were not specifically targeted because information was required on differences in catchability when stock densities were both high and low—a variability in densities that typically occurs in research surveys. The full details of this calibration study are given in Cadigan et al.[3]. We use their data on witch flounder (*Glyptocephalus cynoglossus*) as a case study to illustrate methods.

The focus in Cadigan et al.[3] was on the relative efficiency of two vessels fishing with otherwise identical protocols (gears, speed, tow duration, etc.). Hence, in this article we refer to vessel effects, but more generally the effects relate to differences in fishing protocols.

The first step in analyzing calibration data is to examine whether there is an effect on total catch per set. In the next section we describe a model for this purpose. Effects on the length compositions of the catches are considered later in this article.

### Vessel effect

A common approach used for analyzing comparative fishing data is binomial regression with an adjustment for over-dispersion. This is one of the options we considered. In the conditional binomial model defined by Equation 3, the logit function of the binomial probability ($p$) is

$$\log\left(\frac{p}{1-p}\right)=\log(\rho)=\beta, \tag{4}$$

and $\beta$ can be estimated as the intercept with a logit link function by using software for binomial regression. The range of $\beta$ is $(-\infty, \infty)$. We derived CIs for $\rho$ by exponentiating intervals for $\beta$ and therefore CIs for $\rho$ should have better coverage properties, and they at least would never include infeasible values. We used version 9.1.3 of SAS/STAT (SAS, Cary, NC.) PROC GENMOD software to estimate this model, and we used the option (dscale) that estimates $\phi$ as the deviance divided by the degrees of freedom. We also selected the option (lrci) that provides two-sided CIs based on the profile likelihood function. We refer to this GLIM model and estimation approach as the VO (vessel-effect binomial model with over-dispersion) approach.

If there is spatial heterogeneity in stock densities, then the model for the logit proportion of catch taken by the control vessel at station $i$ is

$$\log\left(\frac{p_i}{1-p_i}\right)=\beta+\delta_i, \tag{5}$$

Usually it is reasonable to assume that the ratio of stock densities varies randomly from site to site. Earlier we claimed it was reasonable to assume $\delta_i \sim N(0, \sigma^2)$, $i=1, \ldots n$. In this case equation 5 defines a standard GLMM and there are many approaches and software packages available to estimate $\beta$ and $\sigma^2$ (e.g., Bolker et al., 2009). We examined the robustness of statistical inferences about $\rho$ to the normal approximation for $\delta$ (see *Simulations* section) when $\delta$ is actually a log ratio of gamma random variables.

We used two different packages to estimate the GLMMs. The first was SAS/STAT PROC NLMIXED, which fits nonlinear mixed models, including binomial logistic regression, using marginal MLE. We refer to this model and estimation procedure as the VM (vessel effect and random set-effects binomial model with marginal MLE) approach. The second was the more flexible SAS/STAT PROC GLIMMIX, which fits GLMMs using PQLE. We refer to this as the VP (vessel effect and random set-effects binomial model with PQL estimation) approach. We used the default estimation method in PROC GLIMMIX, which is a restricted pseudolikelihood estimation with an expansion around the current estimate of the best linear unbiased predictors of the random effects. Both packages provide Wald-type CIs for fixed-effect parameters such as $\beta$.

### Vessel and fish-length effects

Length effects are expected if there is a change in the survey trawl, but they could also occur with only a change in the survey vessel. Length-based models for paired-tow comparative fishing data are straightforward extensions of the models in the previous section. The data are extended to include the paired catches at length, $R_{ijk}$, $i=1, \ldots, n$; $j=1,2$; $k=1, \ldots n_i$, where $n_i$ is the number of length classes caught in the $i$'th pair of tows.

If it is reasonable to assume that there are no between-pair differences in the length distributions of fish encountered by both vessels, then binomial logistic regression models are appropriate. Usually the effect of length will be such that relative efficiency changes monotonically with length, $l$. If the change is linear in $\beta=\log(\rho)$, then a binomial GLIM with a logistic link can be used to estimate the intercept and slope; that is, $\beta \equiv \beta(l) = \beta_0+\beta_1 l$ in Equation 4, where $\beta$ is taken to be a function of length, $\beta(l)$. If the length effect is more complicated, then alternative models may be required (see Fryer et al., 2003; Holst and Revill, 2008); however, in this article we focus only on linear models.

If there is spatial heterogeneity in stock densities, then the situation is more complicated. If the heterogeneity is such that one vessel encounters more fish than the other, but otherwise the length distributions are the same, then the use of a random intercept binomial GLMM is appropriate:

$$\log\left(\frac{p_{ik}}{1-p_{ik}}\right)=\beta_0+\delta_i+\beta_1 l_{ik}, \tag{6}$$

$$\delta_i \overset{iid}{\sim} N(0,\sigma^2),\ i=1,\ldots,n;\ k=1,\ldots,n_i,$$

where $p_{ik}$ = the probability that at site $i$ a length $l_{ik}$ captured fish came from the control vessel.

Holst and Revill (2008) used a random intercepts model, although their models for fixed lengths effects were more complicated than what we consider. However, if there are differences in the length distributions encountered by both vessels then Equation 6 will not be appropriate. The differences will usually be such that $\delta=\log(\lambda_c/\lambda_t)$ varies smoothly with length. Several hypothetical examples are also shown in Figure 1. This type of spatial heterogeneity can be approximated by linear functions, whose slopes ($\delta_1$) and intercepts ($\delta_0$) vary randomly from set to set. A GLMM for this model is

$$\log\left(\frac{p_{ik}}{1-p_{ik}}\right)=\beta_0+\delta_{i0}+(\beta_1+\delta_{i1})l_{ik},$$
$$\delta_{ij} \overset{iid}{\sim} N(0,\sigma_j^{\,2}),\ i=1,\ldots,n; \tag{7}$$
$$j=0,1;\ k=1,\ldots,n_i.$$

This is a common GLMM used in fishing gear selectivity studies. If the means of the densities are the same and the only difference is the height of the distributions, then the $\delta$ log ratio would be a horizontal line in Figure 1, which is the type of effect accounted for in Equation 6.

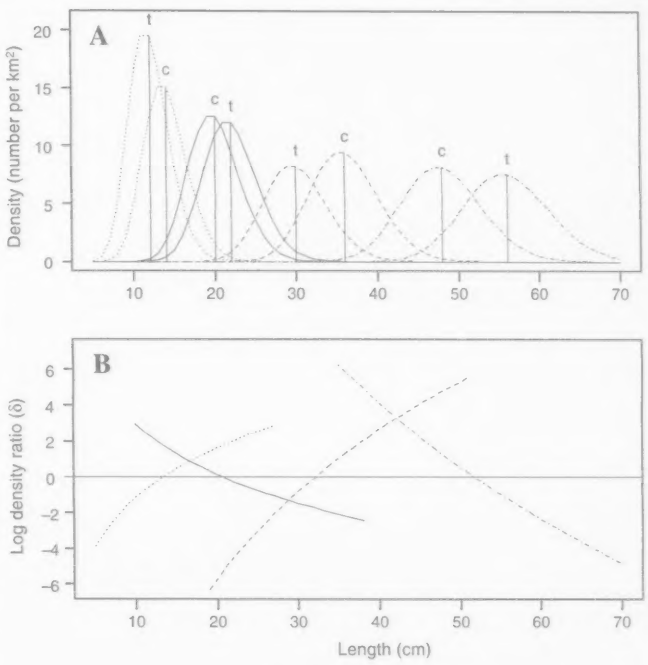


**Figure 1**

(**A**) Hypothetical length distributions of fish encountered by the control (c) and test (t) fishing protocols from paired-tow fishing experiments, to illustrate the impact of within-pair variations in stock densities on the relative efficiency of the test compared to the control protocol. Line types correspond to pairs of tows. Thin vertical lines indicate mean length per tow and coefficients of variation equal to 0.5. (**B**) Corresponding log density ratios (i.e., $\delta$'s) are shown for ranges of lengths where the average density (in A) was greater than 0.01.

We used the same SAS software to estimate the length-based GLIMs and GLMMs. We denote the length-based model with no random effects as VLO. Mixed-effects random intercept models are denoted as $VL_i$, (i.e., Eq. 6), and models with random intercepts and slopes are denoted as $VL_{is}$. Models and estimation methods are denoted as $VLM_i$, $VLP_i$, $VLM_{is}$, and $VLP_{is}$ (see Table 1) depending on whether marginal MLE or PQLE is used.

Standard errors for $\beta(l)=\beta_0+\beta_1 l=\log\{\rho(l)\}$ can be constructed from the estimates of $\beta_0$ and $\beta_1$, and their estimated covariances:

$$SE\left\{\hat{\beta}(l)\right\}=\left\{\mathrm{var}(\hat{\beta}_0)+2\mathrm{cov}(\hat{\beta}_0,\hat{\beta}_1)l+\mathrm{var}(\hat{\beta}_1)l^2\right\}^{1/2}. \tag{8}$$

These standard errors can be used to produce approximate 95% pointwise CIs for $\rho(l)$:

$$CI=\exp\left[\hat{\beta}(l)\pm 1.96\times SE\left\{\hat{\beta}(l)\right\}\right]. \tag{9}$$

Occasionally in comparative fishing the duration ($D_{ij}$) of the tows may differ somewhat between vessels. Also, because of operational time constraints the catches may have to be subsampled for some species. The subsampling fraction ($F_{ijl}$) may depend on size as well. To account for these effects we added an offset ($Z$) to Equations 6 and 7, $Z_{il}=\log(D_{ic}F_{icl}/D_{it}F_{itl})$. For length-pooled analyses of vessel effects we added the offset $Z_i=\log(D_{ic}F_{ic}/D_{it}F_{it})$ to Equation 5, where $F_{ij}$ is the total subsampling fraction.

## Simulations

**Vessel effects** The design of the simulation experiments mimicked the design for the data analyzed by Cadigan et al.[3], that is, we simulated data for the seven species that they considered, and for the same number of tows and total catches for both paired-tows ($R$). This design is summarized in Table 2. Therefore, for example, in

**Table 2**

Paired-tow fishing simulation parameters based on the species in Cadigan et al.[3] $n$ is the total number of paired-sets, $n^*$ is the total number of sets and length classes, $R=R_t+R_c$ is the total catch by the test (t) and control (c) vessels, and $R_t/R_c$ is the ratio of catches from each vessel. The mean, median and coefficient of variation (CV) are for total catch (R). R25 and R75 are the lower and upper 25th percentiles of $R$. See Table 1 for definitions of notations.

| Species | $n$ | $n^*$ | $R$ | $R_t/R_c$ | mean | median | R25 | R75 | CV |
|---|---|---|---|---|---|---|---|---|---|
| American plaice (*Hippoglossoides platessoides*) | 105 | 2035 | 11,494 | 1.051 | 109.5 | 40.0 | 9 | 169 | 126 |
| Atlantic cod (*Gadus morhua*) | 91 | 1132 | 3926 | 1.067 | 43.1 | 4.0 | 2 | 31 | 217 |
| Deepwater redfish (*Sebastes mentella*) | 63 | 1030 | 12,069 | 1.207 | 191.6 | 88.0 | 14 | 379 | 104 |
| Greenland halibut (*Reinhardtius hippoglossoides*) | 56 | 585 | 1359 | 1.243 | 24.3 | 13.5 | 4 | 36 | 120 |
| Thorny skate (*Raja radiata*) | 79 | 990 | 2394 | 1.124 | 30.3 | 9.0 | 3 | 20 | 226 |
| Witch flounder (*Glyptocephalus cynoglossus*) | 57 | 970 | 5046 | 1.334 | 88.5 | 52.0 | 6 | 151 | 108 |
| Yellowtail flounder (*Limanda ferruginea*) | 24 | 536 | 5795 | 1.250 | 241.5 | 159.0 | 5 | 503 | 102 |

the simulation based on American plaice (*Hippoglossoides platessoides*), data were generated for 105 paired-tows with an average $R$ of 109.5. Twenty-five percent of the sets had $R \leq 9$, and 25% of sets had $R \geq 169$. The number of paired-tows in the seven sets of simulations varied from 25 to 105 which is a practical range consistent with many comparative fishing studies (e.g., Table 2 in Pelletier, 1998). The catches ranged from low (Atlantic cod, *Gadus morhua*) to high (yellowtail flounder, *Limanda ferruginea*). Some of the stocks had very skewed catches; for example, Atlantic cod and thorny skate (*Raja radiata*) had mean catches that exceeded their 75th percentiles.

The simulations were similar to a parametric bootstrap procedure; however we varied $\beta$ and $\sigma^2$ to examine how the accuracy of statistical inferences varied with changes in these parameters. The values of $\beta$ ranged from 0 to 2 by increments of 0.25, with $\beta=0$, or $\rho=1$, representing no vessel effect, and $\beta=2$, or $\rho=7.4$, representing a test vessel catchability that was 14% of the control vessel. Note that this range in $\beta$ is much larger than the results in Cadigan et al. (Table 7 in Cadigan et al.[3]). Their largest absolute estimate was 0.08; however, these simulations were designed to examine the accuracy of statistical inferences for small and large vessel effects. The levels of $\sigma^2=0$, 0.1, 0.5, and 0.9 represented no to high spatial heterogeneity and broadly reflected the range of estimates in Cadigan et al. (Table 7 in Cadigan et al.[3]). The lowest estimate of $\sigma^2$ in Cadigan et al.[3] was 0.10 for Greenland halibut (*Reinhardtius hippoglossoides*), and the highest estimate was 0.99 for Atlantic cod.

Simulated catches for the control vessel ($R_c$) were generated as binomial random numbers; the number of trials was equal to the observed $R$ in Cadigan et al.[3] and probability was based on Equation 5. The $\delta$s were generated randomly from a normal distribution with mean zero and variance $\sigma^2$. The simulated test vessel catch was $R_t=R-R_c$. Note that the total catches for each paired-tow, $R_1, \ldots, R_n$, were the same in each simulation; hence, our simulation results were conditioned on these values.

We examined the robustness of the GLMM results to the assumption of a normal distribution for the random effects, $\delta$, when in fact $\delta$ was the log of a ratio of two independent and identically distributed gamma random variables with $\mathrm{Var}(\delta)=\sigma^2$.

Estimates and 95% CIs for $\beta$ were obtained from 2000 simulations. We approximated the estimation bias as the median $\beta$ from the simulations minus the true simulation value. Bias results based on means were very similar. The coverage accuracy of the CIs was measured as the proportion of simulations in which the CI contained the true value of $\beta$. If the 95% CIs are accurate, then the simulation proportion should be close to 0.95. We also computed the proportion of simulations in which $\beta$ was less than the lower CI, and the proportion in which $\beta$ was greater than the upper CI. If the CIs are two-sided accurate, then these proportions should both equal 0.025.

We performed other simulations using a much finer scale for $\beta$ to examine the power of detecting a vessel effect based on the proportion of simulations whose CIs did not cover zero when the true $\beta$ was greater than zero.

**Vessel and fish-length effects** These simulations were similar to those described in the last section. We simulated data for the seven species and with the same number of tows and total catches-at-length for both

paired-tows ($R_l$). However, there was an additional simulation factor for the slope of the length effect. We standardized lengths in the data from Cadigan et al.[3]:

$$l_{std} = \frac{l - l_{50}}{l_{75} - l_{25}}, \tag{10}$$

where $l_\alpha$ = the $\alpha$th percentile of the lengths from all sets, weighted by total catch, for each species.

This standardization allowed us to use the same slopes in simulations for different species; we considered $\beta_1$=0, 0.5, 1.0 to represent no, medium, and large length effects. This scale increased the number of simulations three-fold. The length-based models were also slower to estimate because of the larger size of the data sets (see $n^*$ in Table 2), and to save time we reduced the number of simulations to 1000.

We simulated data from Equation 7. We set $\sigma_1^2=\sigma_2^2=\sigma^2$ and used the same values as before, $\sigma^2$=0, 0.1, 0.5, and 0.9. However, we fitted both Equation 6 and Equation 7 to the simulated data. This procedure allowed us to examine the accuracy of statistical inferences from the random intercept model, which is a common mixed effects model, when slopes were random as well. We summarized the simulations for $\beta(l_{std})=\beta_0+\beta_1 l_{std}$ at three points, $l_{std}$=0, 0.5, and 1.0, which reflects relative efficiency at median to large lengths.

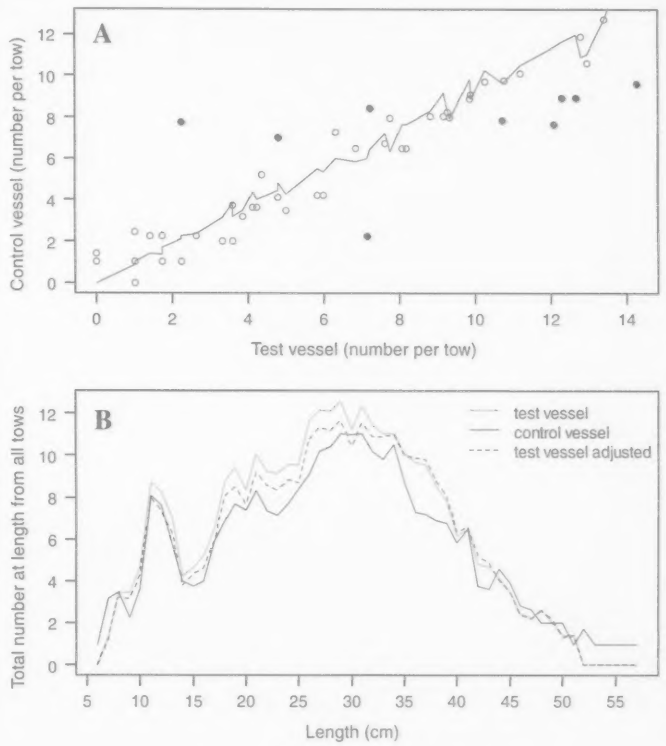


**Figure 2**

Comparative fishing survey results for witch flounder (*Glyptocephalus cynoglossus*). (**A**) Catches from the test and control vessels with 57 paired-tows. Thick line segments connect the offset adjustments for differences in tow duration and subsampling of catches (see text for further detail) and indicate equal catchability (i.e., $\rho$=1); that is, if $\rho$=1, the scatter of points should be centered around the offset adjustments. Solid circles indicate paired-sets with substantially different catches. (**B**) Total catch per 1-cm length classes over all sets, for the test vessel, the test vessel adjusted for tow duration and subsampling, and the control vessel.

## Results

### Case study

We illustrate methods using data for witch flounder from Cadigan et al.[3]. There is some evidence that the catchability of the control vessel was less than the test vessel. For example, there were five sets (solid circles in Fig. 2 where the test vessel caught more than 100 fish but the control vessel caught fewer than 100 fish. Rarely were catches by the control vessel much larger than the test vessel. However, in most paired-tows the catches by both vessels, when adjusted for tow distance and subsampling, were similar. The length distributions over all sets (Fig. 2, bottom panel) did not indicate that potential differences in catchabilities were length dependent because catch differences were approximately equally distributed over a broad range of sizes.

The GLIM estimate of $\beta$=log($\rho$) (Table 3; VO model) was significantly less than zero indicating that the control vessel had a catchability that was significantly less than the test vessel. However, both GLMM estimates (VM, VP) were somewhat larger and not significant, indicating that the test and control vessels catchabilities were not significantly different. The VM and VP estimates of $\beta$ and $\sigma^2$ were very similar. The PQL software (PROC GLIMMIX) we used did not provide standard errors for the estimate of $\sigma^2$, but the marginal MLE software (PROC NLMIXED) did.

The length-based models provided similar results, with the GLIM model (VLO) producing significant differences whereas the mixed models did not. Note that the length-based estimates are very different from those in Cadigan et al.[3] because we standardized lengths (i.e.,

**Table 3**

Parameter estimates, standard errors (SE), and lower and upper 95% confidence interval limits from various models for paired-tow comparative fishing data. See Table 1 for definitions of model acronyms and parameters. The $v$ and $l$ parameter subscripts indicate a vessel or fish-length effect.

| Model | Parameter | Estimate | SE | Lower | Upper |
|---|---|---|---|---|---|
| VO | $\beta_v$ | −0.153 | 0.069 | −0.290 | −0.018 |
| | $\phi$ | 5.888 | — | — | — |
| VP | $\beta_v$ | −0.094 | 0.093 | −0.279 | 0.091 |
| | $\sigma_v^2$ | 0.301 | 0.088 | — | — |
| VM | $\beta_v$ | −0.097 | 0.093 | −0.283 | 0.089 |
| | $\sigma_v^2$ | 0.302 | 0.089 | 0.124 | 0.480 |
| VLO | $\beta_v$ | −0.166 | 0.037 | −0.239 | −0.094 |
| | $\beta_l$ | −0.053 | 0.052 | −0.154 | 0.048 |
| | $\phi$ | 1.628 | — | — | — |
| $VLP_i$ | $\beta_v$ | −0.102 | 0.092 | −0.286 | 0.082 |
| | $\beta_l$ | 0.058 | 0.052 | −0.045 | 0.160 |
| | $\sigma_v^2$ | 0.296 | 0.086 | — | — |
| $VLM_i$ | $\beta_v$ | −0.105 | 0.092 | −0.290 | 0.079 |
| | $\beta_l$ | 0.058 | 0.052 | −0.047 | 0.164 |
| | $\sigma_v^2$ | 0.295 | 0.086 | 0.121 | 0.468 |
| $VLP_{is}$ | $\beta_v$ | −0.099 | 0.094 | −0.288 | 0.090 |
| | $\beta_l$ | 0.059 | 0.080 | −0.098 | 0.215 |
| | $\sigma_w^2$ | 0.299 | 0.088 | — | — |
| | $\sigma_l^2$ | 0.119 | 0.061 | — | — |
| $VLM_{is}$ | $\beta_v$ | −0.103 | 0.095 | −0.294 | 0.088 |
| | $\beta_l$ | 0.061 | 0.081 | −0.101 | 0.224 |
| | $\sigma_w^2$ | 0.303 | 0.091 | 0.121 | 0.484 |
| | $\sigma_l^2$ | 0.122 | 0.065 | −0.008 | 0.252 |

Eq. 10) but Cadigan et al.[3] did not. The 25th, 50th, and 75th length percentiles were 22, 29, and 34 cm. CIs for $\rho(l)$ based on Equation 9 were derived for $l_{std}=0, \ldots, 2$ (Fig. 3). The VLO model suggested $\rho(l)$ decreased with $l$ and was significantly different from one over the range of lengths. The four mixed models all indicated a slight increase in $\rho(l)$ with $l$ but were not significantly different from one for any length. The CIs for the random intercept model (Eq. 6) were shorter than those for the random intercept and slope models, especially when $l_{std}>1$. The marginal MLE CIs ($VLM_i$, $VLM_{is}$) were slightly wider than PQLE CIs ($VLP_i$, $VLP_{is}$).

## Simulations

**Vessel effect** Simulation results were very similar for the seven species. We present the best and worst cases in Figures 4 and 5. The VO model performed poorly even when there was small spatial heterogeneity in stock densities (i.e., $\sigma^2=0.1$). The likelihood ratio CIs had poor coverage properties and the probability that they contained the true value of the vessel effect ($\beta$) was much less than the 95% nominal value. When $\sigma^2$ and $\beta$ were large this method produced biased estimates of $\beta$ and very inaccurate CIs. Note that to facilitate comparison of the methods the $y$-axis was fixed to be less than the range of some of the GLIM results, particularly in Figure 5. The VP CIs were more accurate, except when $\sigma^2\geq 0.5$ for the thorny skate simulation (Fig. 5). For larger values of $\beta$ the CIs from this method covered less than 95%, about 80% for $\sigma^2=0.9$ and $\beta=2$. The bias was negative which meant that the lower and upper bounds were too small. The VM CIs were quite reliable across the range of values for $\sigma^2$ and $\beta$, and for all seven simulation scenarios (i.e., species). The log gamma ratio simulation results were almost identical to the normal simulations results and are not presented.

We performed simulations at a finer scale of $\beta$ to determine the size of a vessel effect that could be detected with a power of 0.8 or 0.95, based on the VM model. The power was computed from the proportion of CIs that did not cover zero. The results are shown in Table 4, expressed in terms of percent change, $100\times(\rho-1)$. For example, when $\sigma^2=0.5$ there was a 95% chance of detecting a 44% increase in catchability with data like that for American plaice.

**Vessel and length effects** The VLO model performed poorly compared to the mixed models and those results are not presented. We examined statistical inferences for $\beta(l_{std})$ based on the $VLM_i$, $VLP_i$, $VLM_{is}$, and $VLP_{is}$ models. Note that simulated data were generated by using Equation 7 but fitted with both Equation 6 and Equation 7; hence, the results based on Equation 6, i.e. $VLM_i$ and $VLP_i$, will reflect model mis-specification biases. Results were similar for each simulation scenario (i.e., species). We present results for $\beta(l_{std})$ only for the Atlantic cod scenario, small and medium spatial variability ($\sigma=0.1, 0.5$), no or large lengths effects ($\beta_1=0, 1$), and at the center of the length distribution ($l_{std}=0$; Fig. 6 or at a larger value ($l_{std}=1$; Fig. 7).

The random intercept models gave unreliable results especially when $l_{std}=1$. The total random effect variance based on Equation 7 increased with length and this was not accounted for by the $VLM_i$ or $VLP_i$ models. The poor performance of CIs for $\beta(l_{std})$ derived from the $VLM_i$ and $VLP_i$ models was caused by both bias in estimates of $\beta(l_{std})$ and bias in estimates of the variance of the estimator for $\beta(l_{std})$. These biases are a complicated function of $\beta_0$, $\beta_1$, $\sigma^2$ and $l_{std}$.

The PQL estimation bias was similar to the results of the vessel effects only simulation (not shown for Atlantic cod) when $l_{std}=0$, which is not surprising because the conditional distributions based on Equation 5 and Equation 7 are essentially the same in this case. However, when $l_{std}=1$ the $VLP_{is}$ model gave less accurate results compared to those when $l_{std}=0$. The $VLM_{is}$ model gave reliable results in all simulation settings.

The worst case $VLM_{is}$ result for the lower 95% CI coverage was for the deepwater redfish (*Sebastes mentella*) scenario in which the simulation coverage was 0.057 (nominal value is 0.025) when $\beta_0=0.5$, $\beta_1=1$, $\sigma^2=0.5$, and $l_{std}=0$. The worst case result for the upper interval

**Table 4**

The size of a vessel effect (i.e., change in relative efficiency, $\rho$–1, in %) that can be detected with power=0.8 or 0.95. Columns are for values of $\sigma^2$ (i.e., the random effect variance) and rows are for species simulation scenarios.

| | Power=0.8 /$\sigma^2$ | | | | Power=0.95 /$\sigma^2$ | | | |
|---|---|---|---|---|---|---|---|---|
| Species | 0.0 | 0.1 | 0.5 | 0.9 | 0.0 | 0.1 | 0.5 | 0.9 |
| American plaice (*Hippoglossoides platessoides*) | 5 | 13 | 23 | 32 | 9 | 24 | 44 | 64 |
| Atlantic cod (*Gadus morhua*) | 10 | 18 | 33 | 42 | 17 | 33 | 68 | 92 |
| deepwater redfish (*Sebastes mentella*) | 5 | 15 | 30 | 43 | 7 | 27 | 60 | 99 |
| Greenland halibut (*Reinhardtius hippoglossoides*) | 16 | 23 | 39 | 54 | 28 | 44 | 86 | 134 |
| thorny skate (*Raja radiata*) | 13 | 20 | 34 | 45 | 23 | 38 | 71 | 101 |
| witch flounder (*Glyptocephalus cynoglossus*) | 8 | 17 | 34 | 49 | 13 | 31 | 72 | 113 |
| yellowtail flounder (*Limanda ferruginea*) | 8 | 25 | 62 | 101 | 13 | 50 | 164 | 372 |

was 0.055 when $\beta_0$=2, $\beta_1$=0, $\sigma^2$=0.9, and $l_{std}$=0 for Atlantic cod. In 95% of the simulations for all species the absolute error for the lower CI was less than 0.013, and for the upper interval it was less than 0.016. This demonstrates that CIs from the $VLM_{is}$ model were almost always very accurate.

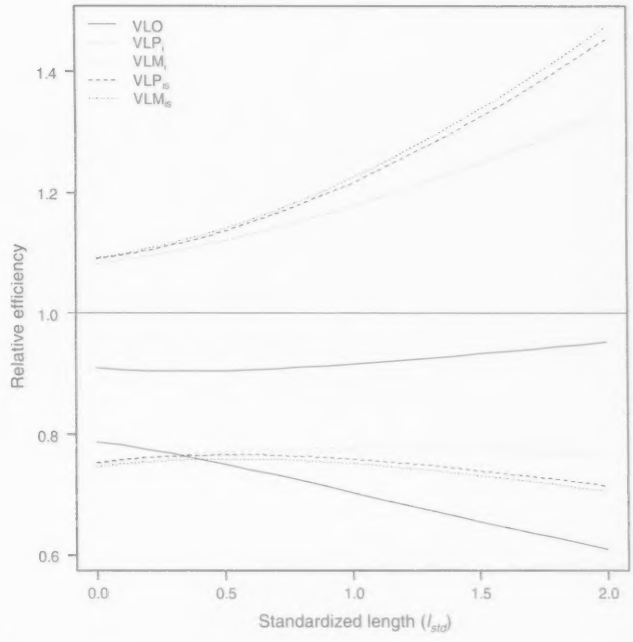


**Figure 3**

95% confidence intervals for the relative efficiency of the test vessel compared to the control vessel for catches (in numbers) of witch flounder (*Glyptocephalus cynoglossus*). Relative efficiency was modeled as a function of length $l$, $\rho(l)=\exp(\beta_0+\beta_1 l)$, and length was standardized, $l_{std}=(l-l_{50})/(l_{75}-l_{25})$, where $l_\alpha$ was the $\alpha\times100$% percentile of the lengths caught in all sets. The five models indicated by different line patterns and shading are described in Table 1. Two lines of the same pattern and shading are plotted for the lower and upper confidence interval endpoints. The thin horizontal line represents equal catchability, $\rho(l)=1$.

## Discussion

Our simulation results demonstrated that the commonly used over-dispersed binomial logistic regression model did not provide accurate statistical inferences for paired-trawl calibration data when there was spatial variation in stock densities. In practice, such variations will occur and therefore this approach is not recommended. Fortunately, our simulations showed that a binomial logistic regression model that included random site effects in addition to fixed vessel effects did provide accurate inferences for a wide range of spatial variations in stock densities. This conclusion also applied to pooled or length-based analyses. We recommend this binomial generalized linear mixed-effects model (GLMM) for analyzing comparative fishing data. When assessing for length effects, we recommend using a binomial GLMM with between-site random variation in both the vessel and length effects.

Between-set variability in catchability is commonly observed in covered-codend experiments (e.g., Fryer 1991, Millar et. al. 2004) that directly measure catchability. This will also produce between-site variability in $\rho$. Trenkel and Skaug (2005) assumed that the Poisson density for fish abundance was spatially constant on a small scale (~1000 km$^2$), and that between-haul variation in catchability caused all additional Poisson over-dispersion in bottom-trawl survey catches. Cadigan et al.[2] demonstrated that this type of

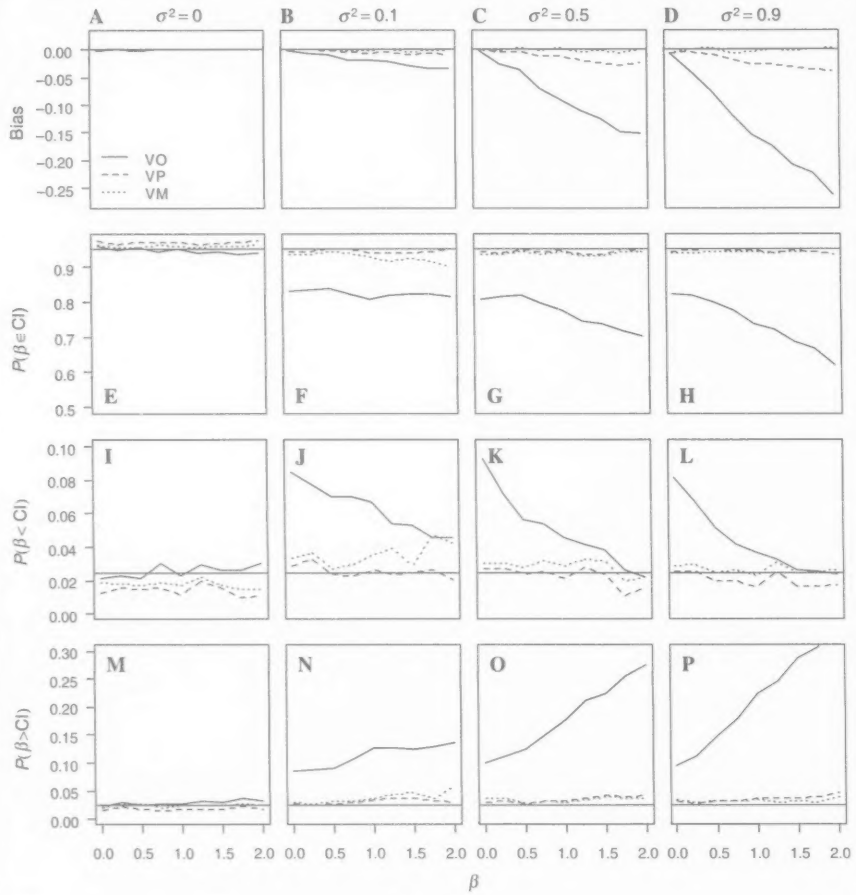


**Figure 4**

Paired-tow comparative fishing simulation results for log relative efficiency ($\beta$) of the test vessel compared to the control vessel. Simulations were based on the yellowtail flounder (*Limanda ferruginea*) scenario and data were generated for different assumed values of $\beta$ (i.e., $\beta_0$) and spatial heterogeneity ($\sigma^2$) in fish densities encountered in each tow. Three models of spatial heterogeneity, described in Table 1, were used to estimate $\beta$, and three line patterns are used to show the results from each model. Panel columns are for levels of $\sigma^2$ (i.e., $\sigma^2$=0 in **A**, **E**, **I**, and **M**, etc.) and the $x$-axis of each panel are for levels of $\beta$. Bias (**A–D**) is the simulation median estimate of $\beta$ minus $\beta_0$. CI indicates confidence interval, and P($\beta \in$ CI) indicates the probability the CI contains $\beta$, etc. References lines (solid) are shown in each panel, at zero (**A–D**), 0.95 (**E–H**), and 0.025 (**I–P**).

variability has a similar effect to that of spatial heterogeneity in stock densities encountered by both vessels at a trawl station. Hence, these two sources of variability are confounded in paired-trawl experiments and the random effects represent the cumulative impacts of both types of variability. For reasons outlined in the previous paragraph, we recommend the GLMM approach when there is between-set variability in catchability.

Our power analyses indicated that 50% changes in catchability could not be detected with high probability (i.e., 0.95) for some species. For example, with data like that obtained for Atlantic cod (see Table 2, and Cadigan et al.[3]) the power was fairly low. For this stock, the estimate of $\sigma^2$ was 0.99 and our power analysis indicated that we could detect only large changes in catchability (>90%) in this situation. Estimates of $\sigma^2$ were closer to 0.5 for most other species, in which case the power to detect a 50% change in catchability would be between 0.8 and 0.95. The exception was for yellowtail flounder which would have even lower power when $\sigma^2$=0.5 because of the smaller number of positive sets ($n$=24) for this species. Changes in catchability between 20%

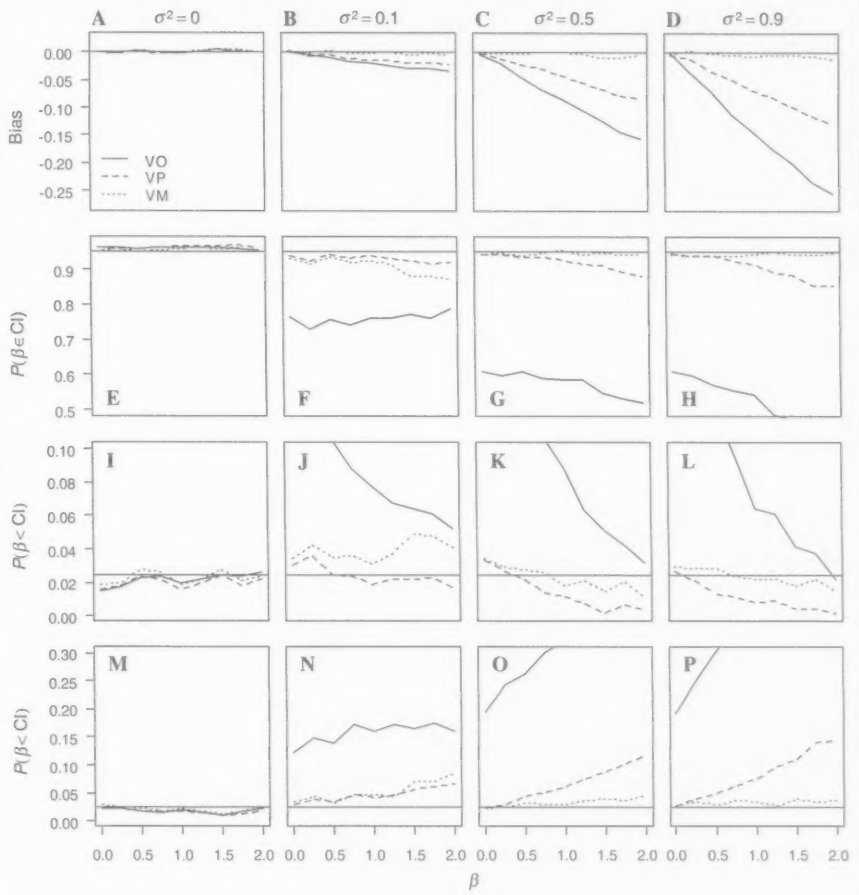


**Figure 5**

Paired-tow comparative fishing simulation results for log relative efficiency ($\beta$) of the test vessel compared to the control vessel. Simulations were based on the thorny skate (*Raja radiata*) scenario and data were generated for different assumed values of $\beta$ (i.e., $\beta_0$) and spatial heterogeneity ($\sigma^2$) in fish densities encountered in each tow. Three models of spatial heterogeneity, described in Table 1, were used to estimate $\beta$, and three line patterns are used to show the results from each model. Panel columns are for levels of $\sigma^2$ (i.e., $\sigma^2$=0 in **A**, **E**, **I**, and **M**, etc.) and the $x$-axis of each panel are for levels of $\beta$. Bias (**A–D**) is the simulation median estimate of $\beta$ minus $\beta_0$. CI indicates confidence interval, and P($\beta \in$CI) indicates the probability the CI contains $\beta$, etc. References lines (solid) are shown in each panel, at zero (**A–D**), 0.95 (**E–H**), and 0.025 (**I–P**).

and 50% would be important in stock assessment, and our simulation results indicated that more sets would be necessary to detect such changes in a comparison of paired-tow fishing data when the amount of spatial heterogeneity is similar to the levels in Cadigan et al.[3]. If spatial heterogeneity could somehow be removed or kept low, then 50% changes in catchability could be detected with high power.

Another common approach to analyze comparative fishing data is to log transform catches and use normal linear models for analysis; however, this approach does not often adequately account for the stochastic nature of the data (e.g., counts) and involves arbitrary choices to deal with zero catches. However, the lognormal approach may be reasonable and appropriate in some situations, or when the focus is on catch weights (e.g., Kingsley et al., 2008).

We studied two methods to estimate GLMMs. One was based on maximizing the marginal likelihood, integrated over the random effects. The other approach was penalized quasi-likelihood estimation based on a linearization of the model and a double optimization

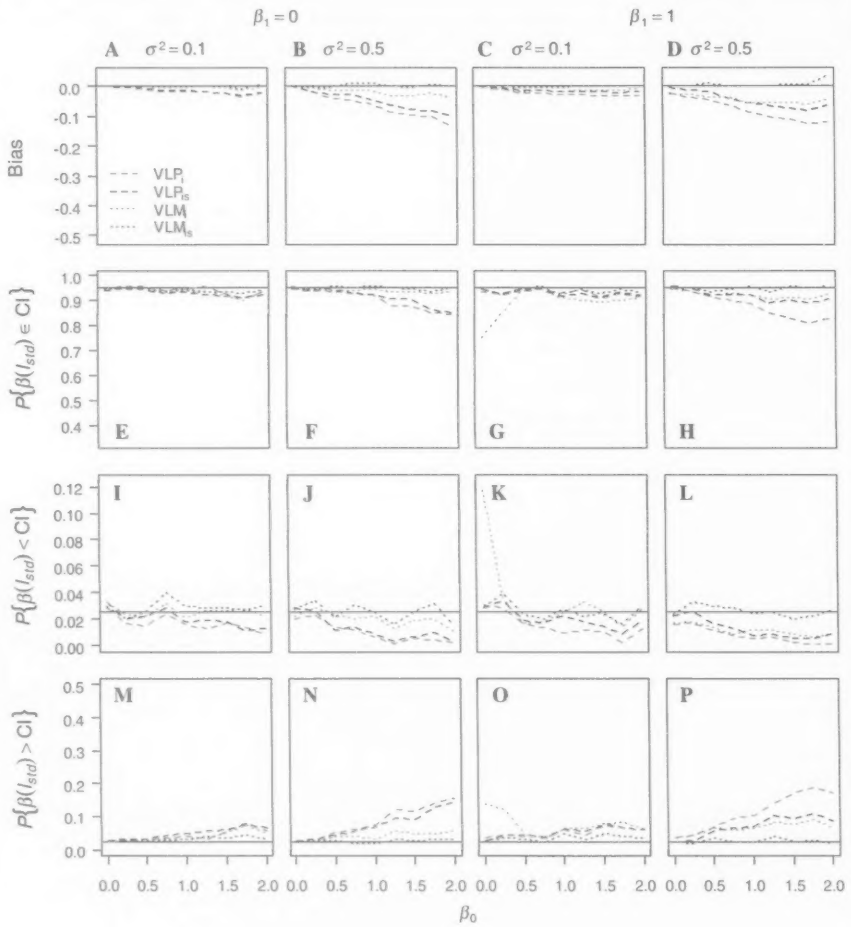


**Figure 6**

Paired-tow fishing simulation results for log relative efficiency ($\beta$) of the test vessel compared to the control vessel. Simulations were based on the Atlantic cod (*Gadus morhua*) scenario and fish-length–based data were generated for different assumed values of $\beta(l)=\beta_0+\beta_1 l$ and spatial heterogeneity ($\sigma^2$) in fish densities encountered in each tow. Lengths were standardized, $l_{std}=(l-l_{50})/(l_{75}-l_{25})$, where $l_\alpha$ was the $\alpha$×100% percentile of the lengths caught in all sets. Four models of spatial heterogeneity, described in Table 1, were used to estimate $\beta(l)$, and four line patterns and shadings are used to show the results from each model at $l_{std}=0$. Panel columns are for levels of $\sigma^2$ and $\beta_1$ (i.e., $\sigma^2=0$ and $\beta_1=0$ in **A**, **E**, **I**, and **M**, etc.) and the *x*-axis of each panel are for levels of $\beta_0$. Bias (**A–D**) is the simulation median estimate of $\beta$ minus $\beta_0$. CI indicates confidence interval, and $P\{\beta(l_{std})\in CI\}$ indicates the probability the CI contains $\beta(l_{std})$, etc. References lines (solid) are shown in each panel, at zero (**A–D**), 0.95 (**E–H**), and 0.025 (**I–P**).

procedure. The advantage of the latter approach was its ability to accommodate more complicated types of random effects like those with autocorrelation. However, our simulations results indicated that estimates and CIs from the linearization method were less reliable than those from the marginal likelihood approach. We recommend the marginal approach to estimate GLMMs for comparative fishing data.

We demonstrated that statistical inferences from GLMMs based on normal distribution random effects were equally as accurate when the random effects were actually the log of a ratio of two independent and identically distributed gamma random variables, which we hypothesize is a real and important source of overdispersion in vessel calibration studies. This is good because otherwise we could not recommend the stan-

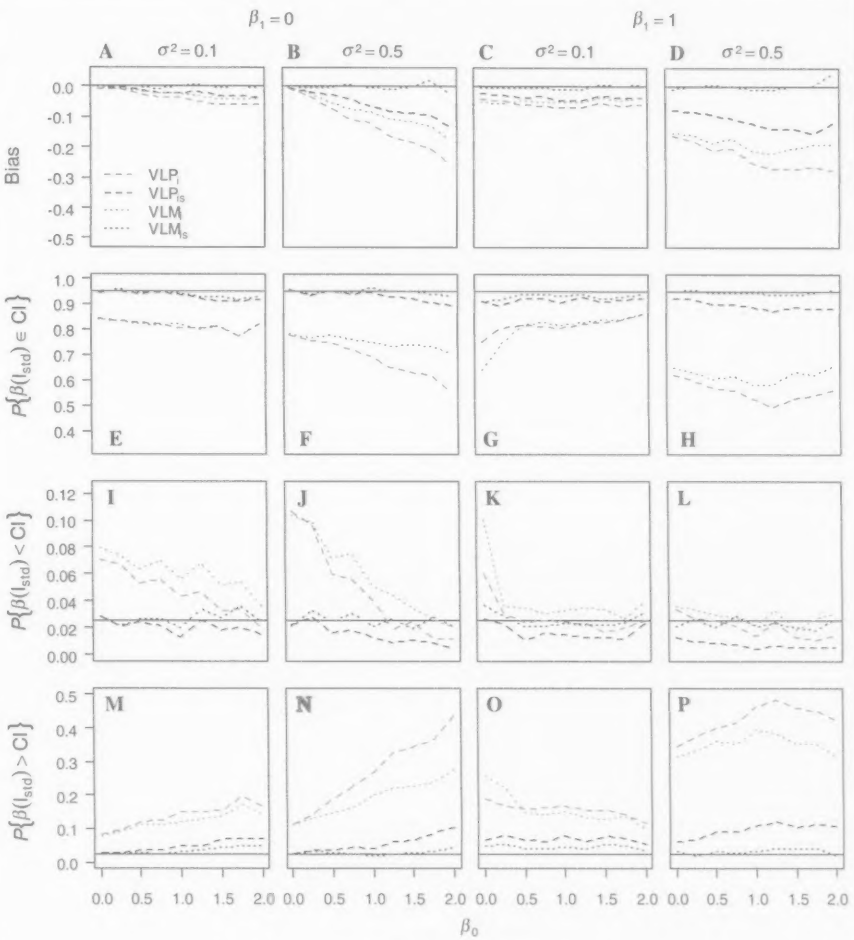


**Figure 7**

Paired-tow fishing simulation results for log relative efficiency ($\beta$) of the test vessel compared to the control vessel. Simulations were based on the Atlantic cod (*Gadus morhua*) scenario and length based data were generated for different assumed values of $\beta(l)=\beta_0+\beta_1 l$ and spatial heterogeneity ($\sigma^2$) in fish densities encountered in each tow. Lengths were standardized, $l_{std}=(l-l_{50})/(l_{75}-l_{25})$, where $l_\alpha$ was the $\alpha\times100\%$ percentile of the lengths caught in all sets. Four models of spatial heterogeneity, described in Table 1, were used to estimate $\beta(l)$, and four line patterns and shadings are used to show the results from each model at $l_{std}=1$. Panel columns are for levels of $\sigma^2$ and $\beta_1$ (i.e., $\sigma^2=0$ and $\beta_1=0$ in **A**, **E**, **I**, and **M**, etc.) and the $x$-axis of each panel are for levels of $\beta_0$. Bias (**A–D**) is the simulation median estimate of $\beta$ minus $\beta_0+\beta_1$. CI indicates confidence interval, and $P\{\beta(l_{std})\in CI\}$ indicates the probability the CI contains $\beta(l_{std})$, etc. References lines (solid) are shown in each panel, at zero (**A–D**), 0.95 (**E–H**), and 0.025 (**I–P**).

dard GLMM approach. However, this does not mean that GLMMs are always robust to mis-specifications of random effects (e.g., Heagerty and Kurland, 2001). We demonstrated this in our length-based simulations.

We demonstrated that the random intercept model gave inaccurate statistical inferences (bias and CIs) if there was between-set random variations in length effects. This is a type of model mis-specification. However, we did not fully examine the other side of this result, which is bias caused by assuming between-set random variation in length effects when in fact none exists. Results from simulations with $\sigma^2=0$ for both vessel and length effects showed that the random intercept and slope model (i.e., $VLM_{is}$) provided reliable statistical

inferences when no random effects exist, and we speculate that the same result will hold when only random intercept effects exist. Hence, we recommend the $VLM_{is}$ approach when there is either within-pair variation in the density of fish or in their length compositions.

A type of model we did not consider involves large-scale within-pair random variations in the densities of fish encountered by both vessels, and smaller-scale length-specific random variations in length compositions. When plotted like Figure 1, log density ratios would appear as a scatter of points about horizontal lines. The intercepts of the horizontal lines would depend on the large-scale random variation in the fish densities, and the variation in the scatter about these horizontal lines would depend on the smaller-scale length-specific random variations in length compositions. These types of effects can be modeled with hierarchical random effects (i.e., set, and length within set). This procedure would be fairly straightforward with a PQL approach but more difficult with marginal MLE. The reliability of estimates (relative efficiency and variance parameters) is uncertain. Even more complicated hierarchical random-effect models for both vessel and catch length-composition effects could be considered. This was beyond our scope but important to understand for reliable statistical inference. In reality, random effects in log density ratios may also have non-normal and skewed distributions, and it would be helpful to understand the robustness of $VLM_{is}$ to these types of model mis-specifications.

Another sensible simulation procedure is to specify the stock densities fished by both vessels from site to site, and generate random catches for both vessels. The stock densities could be specified by using a variety of spatial models, as long as the within-pair and between-pair variations in densities are reasonably consistent with what one might expect in practice. However, this would not be a conditional simulation because the total catches by both vessels (and for all sets) would vary from simulation to simulation. It would still be useful to examine if the conditional CIs are accurate in this more general setting. However, the results from our conditional simulations were very similar for each of the seven species scenarios we considered and we anticipate they would also be accurate in the more general setting.

Cadigan et al. (2006) used a random effect for $\delta \equiv \delta(l)$ that was autocorrelated in length $l$, $\text{corr}\{\delta(l),\delta(l')\}=\gamma^{|l-l'|}$. This is a strategy to model smooth functions (e.g., Brown and de Jong, 2001). We used a simpler approach based on the assumption that $\delta(l)$ varied linearly with $l$. A GLMM in which $\delta(l)$ is autocorrelated can be fitted by using PQL software, but is time consuming to simulate and therefore we decided to focus on Equation 7 which is much easier to estimate.

Another approach to estimate relative efficiency (i.e., Pelletier, 1998) is maximum likelihood based on the negative binomial (NB) distribution. We have pursued this approach; however, there are complications in estimating the NB over-dispersion parameter based on the joint likelihood of both trawl catches and this problem affects the accuracy of CIs. The conditional approach is also more complicated for the NB distribution. We will report on this elsewhere.

Fryer et al. (2003) showed how to use spline methods for smooth, but otherwise nonparametric, estimates of relative efficiency. This is a useful estimation approach, especially to check the adequacy of a parametric model. The simple logistic-linear model we considered may be sufficient to test whether there is a significant length-dependent vessel effect but the logistic-linear model may not be sufficiently flexible for reliable estimation of relative efficiency over all lengths.

Lewy et. al. (2004) advocated paired-trawls along the same trawl track-line to avoid complications due to spatial variations in stock densities. However, such trawling introduces a different complication which involves disturbance of the fish densities encountered by the second vessel because of the fishing activity of the first vessel.

Another potential advantage of GLMMs is less sensitivity to outliers. Figures 14 and 15 of Cadigan et al.[2] indicated that GLMM estimates of $\beta$ were less sensitive to outliers than GLIM estimates. This lack of sensitivity is a considerable advantage because identifying outliers is time consuming in practice when conversion factors are estimated for many species. In addition, standard errors may be too small when observations are incorrectly deemed to be outliers and removed from the analysis. Atlantic cod and thorny skate had mean total catches (for both vessels) that exceeded the 75th percentile (Table 2), indicating that there were a few large catches that may have undue influence on estimates. The GLMMs seem better suited for this type of data. It would be useful to test these methods through simulation to assess robustness to outliers. The randomization approach used by Benoît[1] is another appropriate and robust procedure (e.g., Cox and Hinkley, 1974, p. 180–181) to test for the statistical significance of vessel effects, and we recommend this approach in addition to the use of GLMMs. However, it does not provide robust estimates of vessel effects and the approach cannot replace a GLMM.

## Acknowledgments

The authors are grateful for the expertise, assistance, and many discussions with S. Walsh and B. Brodie, of the Northwest Atlantic Fisheries Center, Fisheries and Oceans Canada (DFO). M. Koen-Alonso of DFO also provided comments on earlier draft.

## Literature cited

Benoît, H.P., and D. P. Swain.
2003. Accounting for length- and depth-dependent diel variation in catchability of fish and invertebrates in an annual bottom-trawl survey. ICES J. Mar. Sci. 60:1298–1317.

Bolker, B. M., M. E. Brooks, C. J. Clark, S. W. Geange, J. R. Poulsen, M. H. H. Stevens and J.-S. S. White.
2009. Generalized linear mixed models: a practical guide for ecology and evolution. Trends Ecol. Evol. 24:127–135.

Brown, P. E., and P. de Jong.
2001. Nonparametric smoothing using state space techniques. Can. J. Stat. 29:37–50.

Cameron, A. C., and P. K. Trivedi.
1998. Regression analysis of count data, 411 p. Cambridge Univ. Press, Cambridge.

Cox, D. R., and D. V. Hinkley.
1974. Theoretical statistics, 511 p. Chapman and Hall, London.

Cox, D. R., and E. J. Snell.
1989. Analysis of binary data, 2nd ed., 236 p. Chapman and Hall, London.

Devore, J. L.
1991. Probability and statistics for engineering and sciences, 3rd ed., 716 p. Brooks/Cole Publ. Co., Pacific Grove, CA.

Fryer, R.J.
1991. A model of between-haul variability in selectivity. ICES J. Mar. Sci. 48:281–290.

Fryer, R.J., A.F. Zuur, and N. Graham.
2003. Using mixed models to combine smooth size-selection and catch-comparison curves over hauls. Can. J. Fish. Aquat. Sci. 60:448–459.

Gunderson, D. R.
1993. Surveys of fisheries resources, 248 p. John Wiley, New York.

Heagerty, P. J., and B. F. Kurland.
2001. Misspecified maximum likelihood estimates and generalised linear mixed models. Biometrika 88:973–985.

Holst, R., and A. Revill.
1997. A simple statistical method for catch comparison studies. Fish. Res. 95:254–259.

Kimura, D. K., and D. A. Somerton.
2008. Review of statistical aspects of survey sampling for marine fisheries. Rev. Fish. Sci. 14:245–283.

Kimura, D. K., and H. H. Zenger.
2006. Standardizing sablefish (*Anoplopoma fimbria*) long-line survey abundance indices by modeling the log-ratio of paired comparative fishing CPUES. ICES J. Mar. Sci. 54:48–59.

Kingsley, M. C. S., K. Wieland, B. Bergström, and M. Rosing.
2008. Calibration of bottom trawls for northern shrimp. ICES J. Mar. Sci. 65: 873–881.

Lewy, P., J. R. Nielsen, and H. Hovgård.
2004. Survey gear calibration independent of spatial fish distribution. Can. J. Fish. Aquat. Sci. 61:636–647.

McCullagh, P., and J. A. Nelder.
1989. Generalized linear models, 2nd ed., 511 p. Chapman and Hall, London.

McCulloch, C. E., and S. R. Searle.
2001. Generalized, linear, and mixed models, 325 p. John Wiley & Sons, New York.

Millar, R. B.
1992. Estimating the size-selectivity of fishing gear by conditioning on the total catch. J. Am. Stat. Assoc. 87:962–968.

Millar, R. B, M. K. Broadhurst, and W. G. Macbeth.
2994. Modelling between-haul variability in the size-selectivity of trawls. Fish. Res. 67:171–181.

Pelletier, D.
1998. Intercalibration of research survey vessels in fisheries: a review and an application. Can. J. Fish. Aquat. Sci. 55:2672–2690.

Quinn, T. J., and R. B. Deriso.
1999. Quantitative fish dynamics, 542 p. Oxford Univ. Press, New York.

Reid, N.
1995. The roles of conditioning in inference. Stat. Sci. 10:138–199.

Trenkel, V. M., and H. J. Skaug.
2005. Disentangling the effects of capture efficiency and population abundance on catch data using random effects models. ICES J. Mar. Sci. 62:1543–1555.

# Effects of trawling for ocean shrimp (*Pandalus jordani*) on macroinvertebrate abundance and diversity at four sites near Nehalem Bank, Oregon

**Robert W. Hannah (contact author)**[1]
**Stephen A. Jones**[1]
**William Miller**[1]
**Jayme S. Knight**[2]

Email address for contact author: bob.w.hannah@state.or.us

[1] Oregon Department of Fish and Wildlife
Hatfield Marine Science Center
2040 SE Marine Science Drive
Newport, Oregon 97365

[2] Alaskan Observers, Inc.
130 Nickerson, #206
Seattle, Washington 98109

**Abstract**—Surveys with a remotely operated vehicle (ROV) at four mud-habitat sites with different histories of ocean shrimp (*Pandalus jordani*) trawling showed measurable effects of trawling on macroinvertebrate abundance and diversity. Densities of the sea whip (*Halipteris* spp., $P<0.01$), the flat mud star (*Luidia foliolata*, $P<0.001$), unidentified Asteroidea ($P<0.05$), and squat lobsters (unidentified Galathoidea, $P<0.001$) were lower at heavily trawled (HT) sites, as was invertebrate diversity based on the Shannon-Wiener index. Sea cucumbers (unidentified Holothuroidea) and unidentified corals (Hydrocoralia) were observed at lightly trawled (LT) sites but not at HT sites. Hagfish (*Eptatretus* spp.) burrows were the dominant structural feature of the sediment surface at all sites and were more abundant at the HT sites ($P<0.05$), a result potentially related to effects from fishery discards. Substantial heterogeneity was found between the northern and southern site pairs, indicating high site-to-site variability in macroinvertebrate densities in these deep (146–156 m) mud habitats. Two of the study sites were closed to trawling in June 2006. The data from this study can be used in combination with future surveys to measure recovery rates of deep, mud, seafloor habitats from the effects of trawling, thus providing a critical piece of information for ecosystem-based management.

Manuscript submitted 24 April 2009.
Manuscript accepted 17 September 2009.
Fish. Bull. 108:30–38 (2010).

The views and opinions expressed or implied in this article are those of the author (or authors) and do not necessarily reflect the position of the National Marine Fisheries Service, NOAA.

Intensive fishing with bottom trawls and dredges can have significant effects on some types of seafloor habitats (Auster et al., 1996; Collie et al., 1997). The reduction in habitat complexity that can result from trawling is of particular concern because of the potential for reductions in fish production at impacted sites (Lindholm et al., 1999). In continental shelf waters off the United States west coast (excluding Alaska), the effect of mobile fishing gears on seafloor habitats has received very little study. The research that has been conducted has focused on effects from otter trawls used to harvest groundfish (Engel and Kvitek, 1998; Hixon and Tissot, 2007). However, the principal trawl fishery currently operating on soft-bottom habitats on the outer continental shelf in these waters is the fishery for ocean shrimp (*Pandalus jordani*). Habitat impacts from ocean shrimp trawls are likely to be different from those from groundfish trawls (Gibbs et al., 1980; Kaiser et al., 2002). Ocean shrimp trawls are considered to be semipelagic gear: they comprise a footrope system that incorporates a chain or cable groundline partially covered with 6.4-cm diameter rubber discs, but are configured to elevate the fishing line of the net about 35–70 cm above the bottom (Hannah and Jones, 2000, 2003). No studies of the physical effects of ocean shrimp trawling on the seafloor ecosystem have been conducted. We report here on the first such study examining the condition of mud-seafloor habitats in the areas primarily impacted by ocean shrimp trawling.

The lack of research on the effects of trawling on some U.S. west coast seafloor habitats has been caused, in part, by a lack of suitable control sites that have not been previously trawled (Engel and Kvitek, 1998). However, some of the areas of rocky habitat that have been recently closed to trawling also contain limited sections of soft-bottom habitat that have been historically trawled, but that are now closed to trawling. The closure of these areas creates an opportunity to study habitat impacts from chronic trawling by examining how these areas recover after closure, in comparison to nearby areas of similar habitat that continue to be trawled. One such area is a section of mud habitat that has historically been trawled for ocean shrimp but is now enclosed within the Nehalem Bank Essential Fish Habitat no-trawl zone (Fig. 1) that was closed to trawling in June 2006. One objective of this study was to conduct an

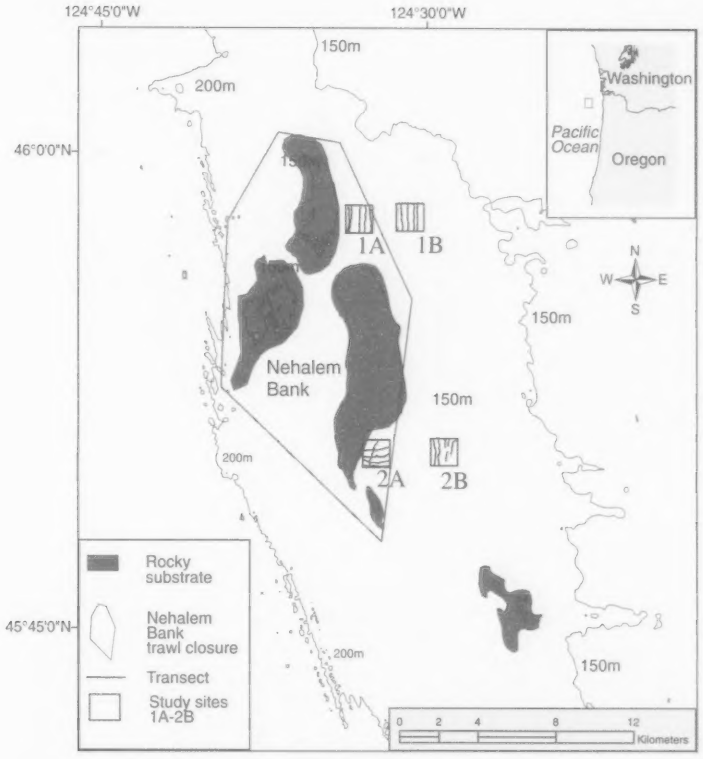


**Figure 1**

Map of the study area at Nehalem Bank, Oregon, showing the four study sites (1A, 1B, 2A, and 2B) where the effects of ocean shrimp (*Pandalus jordani*) trawling on macrobenthos and seafloor habitat were evaluated. The Nehalem Bank trawl closure is also outlined.

initial survey of the condition of two sites within this closed area to monitor changes over time (sites 1A and 2A, Fig. 1). We also surveyed two nearby sites that remain open to ocean shrimp trawling as control sites (sites 1B and 2B, Fig. 1).

In the absence of true control sites that have not been trawled, researchers studying trawl effects on habitat have resorted to comparing habitat condition across a gradient of trawling intensity (Thrush et al., 1998; Kaiser et al., 2000). The mud-habitat sites within the Nehalem Bank trawl closure area (sites 1A and 2A, Fig. 1) have not been as heavily trawled for ocean shrimp as have the two nearby mud seafloor sites that are closer to the center of the ocean shrimp trawl grounds (sites 1B and 2B, Fig. 1).

A second objective of this study was to compare the condition of the seafloor habitat and macrobenthos for the four sites to determine if current differences may be related to the amount of prior trawling. The nature of differences between these four sites, if related to trawling history, could be useful in developing hypotheses regarding expected changes within the closed areas over time.

## Materials and methods

### Study area and field surveys

Nehalem Bank is a 74.6 km$^2$ rocky outcrop composed of sandstone and siltstone located off northern Oregon, between the 150- and 200-m depth contours (Lanier, 2006). Our study sites comprised four square sections of mud habitat (1850 m wide) in the vicinity of Nehalem Bank, two within and two outside the area recently closed to trawling (Fig. 1). Our study design was chosen primarily to provide a detailed baseline survey of the limited areas of soft-bottom habitat that are enclosed within the Nehalem Bank trawl closure area (Fig. 1) so that the process of habitat recovery from physical trawl impacts can be examined in future studies. Accordingly, our design was much more spatially restricted than would be optimal for a study aimed primarily at quantifying the effects of trawling history on habitat and associated fauna. However, the contrast in trawling history between the eastern and western pairs of sites allowed for an analysis of how trawling may have impacted these sites.

We used trawl logbook data from the state of Oregon as one indicator of the history of trawling at the four study sites. Data for vessels that landed shrimp in other states were considered minimal and not included here because of a lack of availability of Washington and California ocean shrimp logbook data after 1992 (Hannah, 1999). The logbook information provides only haul start locations and not actual trawl paths; therefore it must be regarded as a crude index of the level of trawling at these sites. However, the pattern of the data that is available indicates that all four study sites have been predominantly impacted by ocean shrimp trawls. Ocean shrimp trawl start locations (starts) within these four sites from 1988 through 2007 averaged between 0.65 and 8.25 starts/yr (means for 5–year periods are shown in Fig. 2A), whereas groundfish trawl starts/yr averaged from 0.05 to 0.35 starts/yr. The dominance of ocean shrimp trawling at these sites is also understated by these averages because the available shrimp trawl logbook data are a subsample of the total ocean shrimp trawl effort (26–75% of total effort included; Hannah, 1995) whereas the groundfish trawl data represent a more complete census. The logbook data also show a large difference in ocean shrimp trawling history between each of the site pairs with similar latitude (between 1A and 1B, and between 2A and 2B in Fig. 2A). For the northern pair, the easternmost site (1B) has received on average, about seven times more ocean shrimp hauls than the western site (1A). The easternmost southern site (2B) has received an average of about six times more ocean shrimp hauls than the more western site (2A). Hereafter the two eastern sites will be referred to as heavily trawled (HT) and the western sites as lightly trawled (LT).

To conduct seafloor habitat surveys of the four sites, we chartered the 21-m shrimp fishing vessel *Miss Yvonne*, out of Newport, OR. Video surveys were conducted with a Phantom HD2+2 (Deep Ocean Engineering, San Leandro, CA) remotely operated vehicle (ROV) during 20–23 June 2007. Using this system, we gathered standard-resolution video and GPS location data along each of 21 transects (Fig. 1), which were viewed and recorded in real time. The transects were spaced systematically across each site; however, actual transect paths were dependent on the prevailing direction of vessel drift. Thus, they varied in orientation and in some instances were divided into segments because of unusable portions (Fig. 1). Lighting was provided by two 200W lights (Nuytco Research Limited Newtlite, North Vancouver, BC). This system is also equipped with two parallel forward-facing lasers (15 mW, red), situated 10 cm apart and aligned with the central axis of the primary camera (forward facing oblique), that can be used for scaling the field of view and objects viewed by the camera.

All four sites at Nehalem Bank had similar depth ranges (Table 1). The areas and linear distances surveyed were also similar, with the exception of site 2B, where an equipment malfunction resulted in a lack of ROV position data for a portion of two transects, reducing the linear distance surveyed to 7.11 km in comparison to about 9.30 km for each of the other sites.

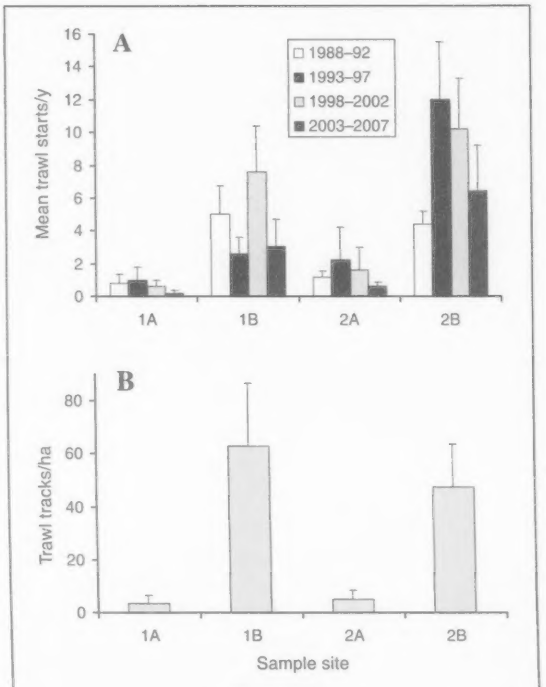


**Figure 2**

(**A**) Mean ocean shrimp (*Pandalus jordani*) trawl starts per year (±1 standard error [SE]) for four 5-year periods from subsampled fishery logbook data, and (**B**) the density of trawl tracks (tracks/ha, ±1 SE) observed with a remotely operated vehicle for four sites with different histories of ocean shrimp trawling at Nehalem Bank, Oregon (see Fig. 1).

### Video analysis

Processing of video data began with an initial review of the tapes to identify usable segments for quantitative analysis. Only short segments of video proved unusable, because of poor visibility, or because the ROV was either too far above the bottom, off the intended transect, or briefly pulled sideways by the research vessel. This initial review identified start and stop times of each usable segment for subsequent quantitative analysis (Table 1). Transects for which we report data are composites of these large segments of usable video data.

Organisms, and other features, including trawl tracks and biogenic features such as hagfish (*Eptatretus* spp.) burrows, were enumerated from the video only if they were in view at the vertical center of a standard video screen (50% line), where the lasers were also aligned. This approach avoided an unrealistic extension of the top of the camera's estimated field of view beyond the

**Table 1**

Depth range (m), number of transects surveyed, and area (ha) and linear distance (km) of transects surveyed with remotely operated vehicle at the four mud seafloor sampling sites at Nehalem Bank, Oregon (see Fig. 1), June 2007.

| Sampling site | Depth range (m) | Number of transects | Area surveyed (ha) | Distance surveyed (km) |
|---|---|---|---|---|
| 1A | 148.3–154.4 | 5 | 1.51 | 9.25 |
| 1B | 150.5–153.8 | 5 | 1.23 | 9.30 |
| 2A | 149.4–155.7 | 5 | 1.16 | 9.30 |
| 2B | 146.2–156.0 | 6 | 0.76 | 7.11 |

practical limits of visibility. As organisms crossed the 50% line, they were counted and visually identified to the lowest taxonomic level possible, with the exception of pandalid shrimp, which were very numerous but were not counted. Large white sea whips were all recorded as *Halipteris* spp.; however, some of the smaller specimens may actually have been *Stylatula* spp. Hagfish burrows were too numerous to count completely throughout the video footage and therefore were subsampled by randomly selecting three two-minute segments per videotape (26.2-min average duration) and counting all of the burrows in these subsamples.

We estimated the area of the belt transects surveyed by combining information on the change in position of the ROV over time and the width of the camera field of view at the 50% line. The on-ground width of the camera's field of view was calculated by measuring the distance between the two laser dots (mm) on a standard video screen every 30 seconds (based on the imprinted video time stamp) and applying an established relationship between the screen laser width and the on-ground width of view of the camera. Position data for the ROV were smoothed with a 9-point moving average before the distance covered in each 30-second interval was measured. A simple straight line "distance traveled" was calculated for each 30-second interval based on the smoothed position data at the start and end points of the interval. This distance was then multiplied by the average of the two estimates of the width of view at the start and end of each 30-second interval to approximate the total area surveyed. These areal estimates were then summed across all reviewed 30-second intervals to estimate the area in each belt transect.

To determine how ocean shrimp trawling may have affected the size distribution of sea whips, we measured the approximate size of all sea whips as they were enumerated at the 50% line. The measurement was taken when the base of the organism was at the 50% line, expressed as a multiple of the laser width separation (10 cm) in that video frame. Frequently, with the base of large sea whips positioned at the 50% line, only the bottom portion of the sea whip was visible. In these instances, the visible portion of the sea whip was measured and recorded as a minimum measurement, but was not excluded from the analysis.

### Statistical analysis

We compared the densities of invertebrates and physical bottom features, such as hagfish burrows and trawl tracks, between LT and HT sites (Fig. 1) using analysis of variance (ANOVA). Trawling history (LT or HT) and block (northern or southern station pair) were treated as main effects with interaction, and transects were treated as replicate samples. Although our primary interest was the effect of trawling on seabed structure and structure-forming invertebrates, we included in our statistical analysis all fish and invertebrate groups that were encountered in at least 50% of the transects, according to the approach of McConnaughey et al. (2000). Density data were transformed by using Box-Cox transformations with a displacement of 0.001 before ANOVA. The Box-Cox transformation employs a log-likelihood function to find a power transformation that best normalizes the data (Sokal and Rolf, 1981; McConnaughey et al., 2000). The residuals from each ANOVA were tested for normality with the Shapiro-Wilk goodness-of-fit test. Box-Cox transformations successfully normalized the density data for all of the taxa we compared statistically, with the exception of Dungeness crab (*Cancer magister*) and hagfish, as well as for the physical features we enumerated (trawl tracks and hagfish burrows). Sea whip length data were not adequately normalized by transformation ($P < 0.01$). For data that were not successfully normalized ($P > 0.05$), nonparametric Wilcoxon rank sum tests were applied to the northern and southern station pairs separately by using JMP® 6 statistical software (SAS Institute, Inc., Cary, NC). To compare the invertebrate species diversity between LT and HT sites, we calculated the Shannon-Wiener diversity index (Pielou, 1969) as well as species richness, defined as the number of species or taxonomic groups encountered at each site per unit of area sampled (Fig. 1).

## Results

Hagfish burrows were very abundant and were the dominant structural feature of the sediment surface at all four sites (Fig. 3A). These burrows were mounds in the seafloor, with cone-shaped depressions in the center, ranging in diameter from approximately 10 to 60 cm. We

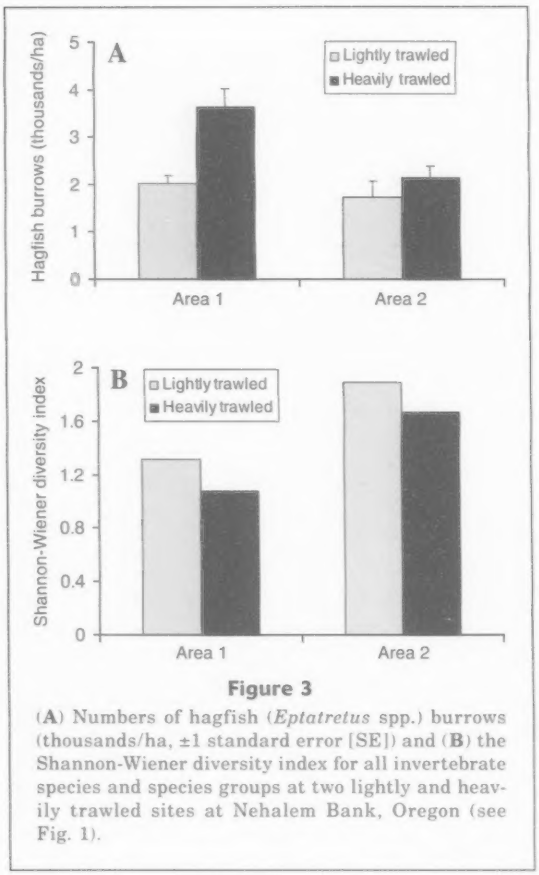


**Figure 3**

(**A**) Numbers of hagfish (*Eptatretus* spp.) burrows (thousands/ha, ±1 standard error [SE]) and (**B**) the Shannon-Wiener diversity index for all invertebrate species and species groups at two lightly and heavily trawled sites at Nehalem Bank, Oregon (see Fig. 1).

occasionally observed hagfish using the burrows. Counts of trawl door tracks, by site, corresponded generally with the average index of trawling history from logbook data (Fig. 2), however the trawl track data indicated more trawling at site 1B than at 2B and the logbook data indicated more trawling at 2B. The trawl door tracks that we observed were relatively large features in this very flat mud habitat, consisting of linear furrows about 0.2–0.5 m deep. The habitat at all four sites appeared very similar, but a few very small, low-relief, rocky outcrops were noted within site 1A. The most abundant benthic macroinvertebrates that we observed were sea whips and orange sea pens (*Ptilosarcus gurneyi*) at the two northern sites and sea whips and heart urchins (*Brisaster* spp.) at the two southern sites (Table 2). Unidentified flatfish, eelpouts (Zoarcidae), Pacific hake (*Merluccius productus*), and rockfishes (*Sebastes* spp.) were the most abundant fish species observed at the four sites (Table 2).

Analysis of variance showed substantial heterogeneity between the northern and southern site pairs, confirming the appropriateness of using the blocking variable. Sea whips and orange sea pens were more abundant at the northern sites (Table 2, blocking variable $P<0.001$), whereas heart urchins, squat lobsters (Galathoidea spp.), Pacific hake, eelpouts, juvenile rockfish, and skates (Rajidae) were more abundant at the southern sites (blocking variable $P<0.05$). The density of hagfish burrows was higher at the northern sites (Fig. 3A, blocking variable $P<0.001$). The density of trawl tracks was not significantly different between northern and southern site pairs (Fig. 3B, blocking variable $P>0.05$).

Statistically, trawling history (LT or HT) accounted for some of the heterogeneity between sites. The HT sites had more hagfish burrows (Fig. 3A, $P<0.05$) and trawl tracks (Fig. 2B, $P<0.01$) contributing to physical complexity, but had reduced densities of sea whips (Table 2, $P<0.01$). Densities of the orange sea pen were also lower at HT sites, but the difference was not statistically significant. The apparent influence of trawling history on the density of sea whips was much greater at the southern sites (interaction $P<0.01$), indicating that the effect of ocean shrimp trawling on sea whips could be variable between areas and possibly density dependent, having greater impacts at sites that are less favorable habitat for sea whips. It is also possible that this interaction indicates differences in sea whip abundance between sites that are unrelated to trawling history.

Several other benthic macroinvertebrates were observed at lower densities at the HT sites (Table 2) (indicating negative effects from chronic trawling) such as the flat mud star (*Luidia foliolata*, $P<0.001$), unidentified sea stars (Asteroidea, $P<0.05$), and squat lobsters (unidentified Galathoidea, $P<0.001$). The reduction in squat lobster density from trawling was greatest at the southern sites, where squat lobster densities were also the highest (interaction $P<0.05$), again indicating variability in how trawling influenced macroinvertebrate density between sites. Although their numbers were not tested statistically, sea cucumbers (unidentified Holothuroidea) and unidentified corals (Hydrocoralia) were observed at both LT sites (present in <50% of transects) but were not observed at either of the HT sites. Three taxonomic groups of fish were also observed at lower densities at HT sites, including juvenile rockfish ($P<0.01$), eelpouts ($P<0.01$), and skates ($P<0.05$).

Wilcoxon rank sum tests showed that for the southern sites, mean sea whip length was greater at the HT site ($P<0.001$) because of a relative lack of smaller individuals (Fig. 4). The difference in mean length between the northern HT and LT sites was not significant ($P>0.05$). Although not tested statistically, sea whips were much larger at the northern than at the southern sites where their densities were lower (Fig. 4).

Invertebrate diversity based on the Shannon-Wiener diversity index was higher at the LT sites (Fig. 3B) and generally higher at the southern sites because of reduced dominance of sea whips (Table 2). Species richness per unit of area surveyed was greatest at the two southern sites and was not consistently reduced at HT sites (13.8 and 17.1 taxonomic groups/ha at sites 2A and 2B, 9.3 and 10.6 taxonomic groups/ha at 1A and 1B, respectively). The absolute number of taxonomic groups was highest at the LT sites. Fourteen and 16 of the 17

**Table 2**

Mean densities (number/ha) and standard errors (SE) of epibenthic macroinvertebrates (pandalid shrimp excluded) and fish at four mud-habitat sites with different histories of ocean shrimp (*Pandalus jordani*) trawling off the northern Oregon coast (see Fig. 1). *P*-value shown is for the effect of trawling history (lightly or heavily trawled) on density in a two-factor analysis of variance on Box-Cox transformed data (ns=nonsignificant at $P>0.05$, nt=not tested, nm=not meaningful).

| | Taxon | | | | Density (number/ha) | | | | |
|---|---|---|---|---|---|---|---|---|---|
| | 1A | | 1B | | 2A | | 2B | | |
| | Mean | SE | Mean | SE | Mean | SE | Mean | SE | *P*-value |
| Invertebrates | | | | | | | | | |
| *Halipteris* spp. (sea whips) | 452.9 | 51.2 | 459.5 | 46.9 | 190.1 | 10.0 | 60.4 | 11.8 | 0.0025 |
| *Ptilosarcus gurneyi* (orange sea pen) | 141.8 | 48.6 | 100.8 | 9.2 | 26.9 | 9.7 | 14.5 | 4.1 | ns |
| *Stylasterias forreri* (fish-eating star) | 21.1 | 3.4 | 28.0 | 6.7 | 19.8 | 3.9 | 28.0 | 7.4 | ns |
| *Luidia foliolata* (flat mud star) | 28.8 | 4.1 | 9.7 | 1.9 | 27.2 | 3.5 | 7.8 | 2.8 | 0.0001 |
| Unidentified Asteroidea (sea stars) | 3.3 | 1.0 | 4.2 | 1.9 | 6.8 | 0.9 | 2.0 | 2.0 | 0.0236 |
| *Brisaster* spp. (heart urchins) | 103.6 | 42.9 | 44.8 | 7.1 | 92.6 | 14.1 | 96.4 | 14.9 | ns |
| *Cancer magister* (Dungeness crab) | 2.9 | 1.4 | 2.5 | 1.0 | 9.0 | 3.7 | 4.5 | 3.1 | ns[1] |
| Unidentified Ophiuroidea (basket stars) | 7.9 | 2.9 | 4.9 | 1.6 | 0.0 | nm | 0.0 | nm | nt |
| Unidentified Galatheoida (squat lobsters) | 2.0 | 0.9 | 0.8 | 0.8 | 92.0 | 10.9 | 4.5 | 3.1 | 0.0003 |
| *Rossia* spp. (bobtail squid) | 2.4 | 1.2 | 3.2 | 1.9 | 3.9 | 2.1 | 2.0 | 2.0 | nt |
| Unidentified Octopodidae | 0.0 | nm | 0.0 | nm | 0.0 | nm | 0.7 | 0.7 | nt |
| Unidentified anemone | 6.7 | 4.0 | 2.5 | 1.0 | 0.0 | nm | 0.0 | nm | nt |
| Unidentified corals (Hydrocoralia) | 1.4 | 1.4 | 0.0 | nm | 0.9 | 0.9 | 0.0 | nm | nt |
| Unidentified Echinoida (sea urchins) | 1.4 | 1.4 | 0.0 | nm | 23.6 | 13.2 | 2.0 | 2.0 | nt |
| Unidentified Holothuroidea (sea cucumbers) | 0.6 | 0.6 | 0.0 | nm | 11.9 | 2.0 | 0.0 | nm | nt |
| Unidentified invertebrates | 2.0 | 0.9 | 0.9 | 0.9 | 6.4 | 2.7 | 2.9 | 1.9 | nt |
| Fishes | | | | | | | | | |
| Unidentified flatfish | 359.1 | 44.4 | 315.7 | 24.8 | 322.3 | 22.2 | 458.7 | 34.4 | ns |
| *Merluccius productus* (Pacific hake) | 143.8 | 65.6 | 188.6 | 18.1 | 340.3 | 19.7 | 269.0 | 47.6 | ns |
| Zoarcidae (eelpouts) | 341.3 | 41.4 | 101.4 | 13.9 | 325.3 | 52.0 | 337.6 | 74.5 | 0.0051 |
| *Sebastes* spp. (rockfishes) | 55.7 | 9.0 | 20.9 | 7.8 | 94.1 | 16.7 | 62.2 | 7.9 | 0.0025 |
| *Eptatretus* spp. (hagfishes) | 1.4 | 0.9 | 3.9 | 1.8 | 7.2 | 2.3 | 10.2 | 3.5 | ns[1] |
| *Raja* spp. (skates) | 6.9 | 2.8 | 0.8 | 0.8 | 13.9 | 2.0 | 10.9 | 5.6 | 0.02 |
| Unidentified roundfish | 3.1 | 2.1 | 0.0 | nm | 19.2 | 18.2 | 6.1 | 2.3 | nt |
| *Anoplopoma fimbria* (sablefish) | 1.4 | 1.5 | 0.9 | 0.9 | 2.0 | 1.3 | 6.1 | 2.9 | nt |
| *Hippoglossus stenolepis* (Pacific halibut) | 0.0 | nm | 0.0 | nm | 2.7 | 1.7 | 0.0 | nm | nt |
| *Microstomus pacificus* (Dover sole) | 6.1 | 6.0 | 0.0 | nm | 9.4 | 5.8 | 3.1 | 2.1 | nt |
| *Hydrolagus colliei* (spotted ratfish) | 7.2 | 3.0 | 0.0 | nm | 62.1 | 15.3 | 0.7 | 0.7 | nt |
| *Sebastes elongatus* (greenstriped rockfish) | 1.3 | 0.8 | 0.0 | nm | 1.2 | 1.2 | 0.0 | nm | nt |
| Cottidae (sculpins) | 0.0 | nm | 1.6 | 1.0 | 0.0 | nm | 1.4 | 1.4 | nt |
| Agonidae (poachers) | 23.0 | 4.1 | 11.3 | 3.2 | 0.0 | nm | 0.0 | nm | nt |
| Unidentified fish | 0.0 | nm | 0.0 | nm | 0.0 | nm | 2.0 | 2.0 | nt |

[1] Not normalized by Box-Cox transformation, but ns in both Wilcoxon tests.

taxonomic groups identified in Table 2 were present at sites 1A and 2A, respectively, whereas only 13 of these groups were recorded for sites 1B and 2B.

## Discussion

The data presented here indicate that fishing with ocean shrimp trawls in the deepwater mud habitats near Nehalem Bank has reduced invertebrate diversity and negatively impacted the abundance of several common macroinvertebrate taxa, such as sea whips, sea cucumbers, flat mud stars, sea stars, and squat lobsters (Table 2). For sea cucumbers and squat lobsters, the negative effects on abundance are probably a result of both capture in ocean shrimp trawls and mortality from physical damage caused by trawl doors and groundlines. For the other taxa, the physical effects of trawl doors and groundlines are probably most important. The four Nehalem Bank sites studied here represent a small

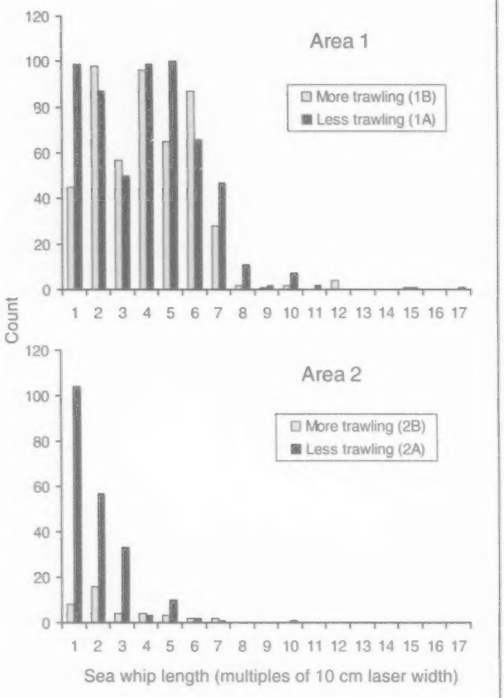


**Figure 4**

Length frequency of sea whips (*Halipteris* spp.) measured in multiples of the 10-cm interlaser width of a remotely operated vehicle at four sites with different histories of ocean shrimp trawling at Nehalem Bank, Oregon (see Fig. 1).

portion of the mud-seafloor habitat that receives some trawling annually for ocean shrimp, which in waters off Oregon can be more than 550,000 ha when ocean shrimp stock abundance is high (Hannah, 1995). Densities of many invertebrate taxa were very different at the northern and southern site pairs in this study, indicating a need for more spatially extensive research to understand the impacts of ocean shrimp trawling on habitat over a fishery scale (Thrush et al., 1998; Kaiser, 2003). The statistical significance of the interaction terms in the two-factor ANOVAs for sea whips and squat lobsters shows that the long-term fishery-scale effects of ocean shrimp trawling may depend on other habitat-specific influences on invertebrate density, in addition to fishery-related factors. More extensive sampling is needed to determine if other heavily trawled areas most closely resemble site 1B, site 2B, or something else entirely.

The changes we observed in HT sites at Nehalem Bank were less extreme than those attributed to groundfish trawling in other U.S. west coast studies (excluding Alaska). Engel and Kvitek (1998) studied HT and LT bottom trawl sites in more sandy habitats at slightly shallower depths in California, and found large reductions in most of the large epifaunal species or species groups at HT sites (50–90% reductions, Fig. 4 in Engel and Kvitek, 1998). Hixon and Tissot (2007) studied sites of mud habitat with different trawling histories off southern Oregon at deeper depths than those of our study. They found a large reduction in macroinvertebrate abundance on trawled seafloors, including an almost complete elimination of *Stylatula* spp., as well as a major shift in the dominant invertebrate taxa. Interpretation of their study however, is complicated by the fact that the sites they compared had nonoverlapping depth ranges (their "trawled" site was 274–361 m deep, "untrawled" site was 183–215 m deep), confounding depth and trawling-related effects on the biota. The diversity of macroinvertebrates was generally lower at HT than at LT Nehalem Bank sites in our study; however, most taxa were not as severely reduced as those in the studies by Engel and Kvitek (1998) and Hixon and Tissot (2007). Also, some species or groups that are considered vulnerable to trawl effects, like sea whips (Wilson et al., 2002) and orange sea pens, were found in both HT sites at Nehalem Bank and were abundant in HT site 1B (Table 2). Moreover, the invertebrate taxa found at all four Nehalem Bank sites were similar, except for the notable absence of sea cucumbers and unidentified corals at HT sites, a likely effect of the trawl fishery.

Smoothing of the sea bed and related physical reduction in habitat complexity noted in some other studies of bottom-fishing impacts (Auster et al., 1996; Collie et al., 1997; Engel and Kvitek, 1998) were not seen at the HT sites at Nehalem Bank. Instead, we found an increased roughness of surface topography resulting from more trawl tracks, similar to the findings of Tuck et al. (1998), along with more hagfish burrows, and increasing habitat complexity. However, our ROV video was mostly useful for detecting large topographic features like trawl tracks and hagfish burrows and therefore we may have missed changes in microtopography caused by trawling. Schwinghammer et al. (1996) and Kaiser et al. (2002) have argued that detecting the physical effects of trawling on habitat is highly dependent on the scale of measurement.

The moderate reductions in macroinvertebrates and lack of a reduction in physical habitat complexity from ocean shrimp trawling at Nehalem Bank could also be related to factors that are specific to the ocean shrimp fishery. The effect of trawling on seafloor habitats depends on local factors, such as gear, the spatial and temporal intensity of the fishery, the type of habitat, and the types of organisms normally found in that area (Jones, 1992; MacDonald et al., 1996). The semipelagic trawl gear used to fish for ocean shrimp has the potential for lower impacts on habitat and macroinvertebrate populations than typical bottom trawl gear because the net itself is not in contact with the seafloor and thus reduces capture efficiency for demersal fish and benthic macroinvertebrates (Hannah and Jones, 2003). The intensity of U.S. west coast ocean shrimp and bottom

trawl fisheries is also low in comparison to that of trawl fisheries in other areas, such as the Gulf of Mexico and New England (NRC, 2002). Effort in the ocean shrimp trawl fishery has also been reduced recently by a vessel buyback program that has reduced fleet size. Macroinvertebrate populations in the HT sites at Nehalem Bank may have recovered somewhat from the impacts of the heaviest trawling during earlier years (Fig. 2A). However, recovery is not likely to be a significant factor for *Halipteris* spp., which are believed to be very long-lived (Wilson et al., 2002). The deep mud habitats being trawled for ocean shrimp have low levels of natural disturbance and are considered some of the most vulnerable to the negative effects of physical disturbance and are expected to have long recovery times (Jones, 1992; Kaiser, 1998; Tuck et al., 1998; Kaiser et al,. 2002; Dernie et al., 2003). Over time, additional surveys of the Nehalem Bank sites should provide insight into both recovery time and the condition of fully recovered mud-seafloor habitats (recently closed sites 1A and 2A) as well as continued changes in areas that experience additional trawling (e.g., sites 1B and 2B).

Our data indicate that the effect of the ocean shrimp fishery on the complexity of mud-seafloor habitats near Nehalem Bank may be a mixture of physical and long-term ecological effects. The increased density of hagfish burrows at HT sites was unexpected. This finding conflicts with most other trawl-impacts studies that evaluated biogenic features in soft-bottom habitats (Auster et al., 1996; Simpson and Watling, 2005; Stone et al., 2005). One possible explanation for this difference is that through fishery removal of hagfish predators and competitors, or from supplementation of hagfish food resources with discards, the ocean shrimp fishery is creating conditions that favor the growth and survival of hagfish. This hypothesis is in general agreement with the findings from other studies that have shown benefits for scavenger populations as a result of trawling (Groenewold and Fonds, 2000; Rumohr and Kujawski, 2000), and is consistent with what little is known about hagfish food habits (Martini et al., 1997). It is unknown how increases in hagfish populations may have in turn influenced other aspects of the benthic ecology of the ocean shrimp grounds; however, it is possible that this ecological effect could generate changes that are equivalent to, or greater than, the direct physical effects of trawling. If fishery discards are stimulating hagfish population growth, it is possible that this effect will diminish over time because fish bycatch in the ocean shrimp fishery has been reduced roughly 66–86% (in terms of weight) by the requirement (since 2002) that vessels use approved bycatch reduction devices (Hannah and Jones, 2007).

To adequately understand and manage the ecosystem effects of trawl fisheries will require a great deal of information, well beyond basic information on removals and the physical effects of trawl footropes and doors. To prevent long-term detrimental effects from trawling, information on recovery times of macroinvertebrate populations is critical. The data developed here provide an opportunity for follow-up studies to better understand the recovery of macrobenthos and other changes in habitat after the cessation of trawl impacts at the Nehalem Bank closed area (Fig. 1). They also provide a starting point for understanding the effects of the ocean shrimp trawl fishery on the ecosystem.

## Acknowledgments

The skipper and crew of the FV *MissYvonne* provided critical expertise in successfully deploying the ROV from their vessel at Nehalem Bank. M. Schuiteman assisted with the ROV field work. This research was funded, in part, by National Oceanic and Atmospheric Administration award NA06NMF4070244 under the Interjurisdictional Fisheries Act.

## Literature cited

Auster, P. J., R. J. Malatesta, R. W. Langton, L. Watling, P. C. Valentine, C. L. S. Donaldson, E. W. Langton, A. N. Shephard, and I. G. Babb.
1996. The impacts of mobile fishing gear on seafloor habitats in the Gulf of Maine (Northwest Atlantic): implications for conservation of fish populations. Rev. Fish. Sci. 4:185–202.

Collie, J. S., G. A. Escanero, and P. C. Valentine.
1997. Effects of bottom fishing on the benthic megafauna of Georges Bank. Mar. Ecol. Progr. 155:159–172.

Dernie, K. M., M. J. Kaiser, and R. M. Warwick.
2003. Recovery rates of benthic communities following physical disturbance. J. Anim. Ecol. 72:1043–1056.

Engel, J., and R. Kvitek.
1998. Effects of otter trawling on a benthic community in Monterey Bay National Marine Sanctuary. Conserv. Biol.12:1204–1214.

Gibbs, P. J., A. J. Collins, and L. C. Collett.
1980. Effect of otter prawn trawling on the macrobenthos of a sandy substratum in a New South Wales estuary. Aust. J. Mar. Freshw. Res. 31:509–516.

Groenewold, S., and M. Fonds.
2000. Effects on benthic scavengers of discards and damaged benthos produced by the beam-trawl fishery in the southern North Sea. ICES J. of Mar. Sci. 57:1395–1406.

Hannah, R. W.
1995. Variation in geographic stock area, catchability and natural mortality of ocean shrimp (*Pandalus jordani*): some new evidence for a trophic interaction with Pacific hake (*Merluccius productus*). Can. J. Fish. Aquat. Sci. 52:1018–1029.
1999. A new method for indexing spawning stock and recruitment in ocean shrimp, *Pandalus jordani*, and preliminary evidence for a stock-recruitment relationship. Fish. Bull. 97:482–494.

Hannah, R. W., and S. A. Jones.
2000. Bycatch reduction in an ocean shrimp (*Pandalus jordani*) trawl from a simple modification to the trawl footrope. J. Northwest Atl. Fish. Sci. 27:227–234.
2003. Measuring the height of the fishing line and its effect on shrimp catch and bycatch in an ocean shrimp (*Pandalus jordani*) trawl. Fish. Res. 60:427–438.

2007. Effectiveness of bycatch reduction devices (BRDs) in the ocean shrimp (*Pandalus jordani*) trawl fishery. Fish. Res. 85:217–225.

Hixon, M. A., and B. N. Tissot.
2007. Comparison of trawled vs untrawled mud seafloor assemblages of fishes and macroinvertebrates at Coquille Bank, Oregon. J. Exp. Mar. Biol. Ecol. 344:23–34.

Jones, J. B.
1992. Environmental impact of trawling on the seabed: a review. N. Z. J. Mar. Freshw. Res. 26:59–67.

Kaiser, M. J.
1998. Significance of bottom-fishing disturbance. Conserv. Biol. 12:1230–1235.
2003. Detecting the effects of fishing on seabed community diversity: importance of scale and sample size. Conserv. Biol. 17:512–520.

Kaiser, M. J., J. S. Collie, S. J. Hall, S. Jennings, and I. R. Poiner.
2002. Modification of marine habitats by trawling activities: prognosis and solutions. Fish Fish. 3:114–136.

Kaiser, M. J., K. Ramsay, C. A. Richardson, F. E. Spence, and A. R. Brand.
2000. Chronic fishing disturbance has changed shelf sea benthic community structure. J. Anim. Ecol. 69:494–503.

Lanier, S.
2006. A comparison of seafloor sonar classification methods through the use of error matrices and 3 dimensional GIS visualization: a multibeam sonar investigation of Nehalem Bank, Oregon. M.S. thesis, 120 p. Oregon State Univ., Corvallis, OR.

Lindholm, J. B., P. J.Auster, and L. Kaufman.
1999. Habitat-mediated survivorship of juvenile (0-year) Atlantic cod *Gadus morhua*. Mar. Ecol. Progr. 180:247–255.

MacDonald, D. S., M. Little, N. C. Eno, and K. Hiscock.
1996. Disturbance of benthic species by fishing activities: a sensitivity index. Aquat. Cons.: Mar. Freshw. Ecosyst. 6:257–268.

Martini, F. H, M. P. Lesser, and J. B Heiser.
1997. Ecology of the hagfish, *Myxine glutinosa* L. in the Gulf of Maine: II. Potential impact on benthic communities and commercial fisheries. J. Exp. Mar. Biol. Ecol. 214:97–106.

McConnaughey, R. A., K. L. Mier, and C. B. Dew.
2000. An examination of chronic trawling effects on soft-bottom benthos of the eastern Bering Sea. ICES J. Mar. Sci. 57:1377–1388.

NRC (National Research Council).
2002. Effects of trawling and dredging on seafloor habitat, 126 p. National Academy Press, Washington, D.C.

Pielou, E. C.
1969. An introduction to mathematical ecology. Wiley, New York.

Rumohr, H., and T. Kujawski.
2000. The impact of trawl fishery on the epifauna of the southern North Sea. ICES J. Mar. Sci. 57:1389–1394.

Schwinghammer, P., J. Y. Guigné, and W. C Siu.
1996. Quantifying the impact of trawling on benthic habitat structure using high resolution acoustics and chaos theory. Can. J. Fish. and Aquat. Sci. 53:288–296.

Simpson, A. W., and L. Watling.
2005. Physical and biological effects of shrimp trawling on soft sediment habitats in the Gulf of Maine. Am. Fish. Soc. Symp. 41:602.

Sokal, R. R., and F. J. Rolf.
1981. Biometry. W. H. Freeman and Company, New York.

Stone, R. R, M. M. Masuda, and P. W. Malecha.
2005. Effects of bottom trawling on soft-sediment epibenthic communities in the Gulf of Alaska. Am. Fish. Soc. Symp. 41:461–475.

Thrush, S. F., J. E. Hewitt, V. J. Cummings, P. K. Dayton, S .J. Turner, G. A. Funnell, R. G. Budd, C. J. Milburn, and M. R. Wilkinson.
1998. Disturbance of the marine benthic habitat by commercial fishing: impacts at the scale of the fishery. Ecol. Appl. 8:866–879.

Tuck, I. D., S. J. Hall, M. R. Robertson, E. Armstrong, and D. J. Basford.
1998. Effects of physical trawling disturbance in a previously unfished sheltered Scottish sea loch. Mar. Ecol. Progr. 162:227–242.

Wilson, M. T., A. H. Andrews, A. L. Brown, and E. E. Cordes.
2002. Axial rod growth and age estimation of the sea pen, *Halipteris willemoesi* Kölliker. Hydrobiologia 471:133–142.

# Evaluation of the capture efficiency and size selectivity of four pot types in the prospective fishery for North Pacific giant octopus (*Enteroctopus dofleini*)

**Patrick D. Barry (contact author)**[1]
**Sherry L. Tamone**[1,2]
**David A. Tallmon**[1,2]

Email address for contact author: p.barry@uaf.edu

[1] School of Fisheries and Ocean Sciences
University of Alaska Fairbanks
17101 Point Lena Loop Rd.
Juneau, Alaska 99801

[2] University of Alaska Southeast
11120 Glacier Hwy.
Juneau, Alaska 99801

**Abstract**—Over 230 metric tons of octopus is harvested as bycatch annually in Alaskan trawl, long-line, and pot fisheries. An expanding market has fostered interest in the development of a directed fishery for North Pacific giant octopus (*Enteroctopus dofleini*). To investigate the potential for fishery development we examined the efficacy of four different pot types for capture of this species. During two surveys in Kachemak Bay, Alaska, strings of 16–20 sablefish, Korean hair crab, shrimp, and Kodiak wooden lair pots were set at depths ranging between 62 and 390 meters. Catch-per-unit-of-effort estimates were highest for sablefish and lair pots. Sablefish pots caught significantly heavier North Pacific giant octopuses but also produced the highest bycatch of commercially important species, such as halibut (*Hippoglossus stenolepis*), Pacific cod (*Gadus macrocephalus*), and Tanner crab (*Chionoecetes bairdi*).

Manuscript submitted 18 March 2009.
Manuscript accepted 15 October 2009.
Fish. Bull. 198:39–44 (2009).

The views and opinions expressed or implied in this article are those of the author (or authors) and do not necessarily reflect the position of the National Marine Fisheries Service, NOAA.

The North Pacific giant octopus (*Enteroctopus dofleini*) is a benthic cephalopod fished throughout its range from Baja California to the Aleutian Islands in Alaska and westward in the Pacific Ocean to Japan. Many artisanal fisheries use trailing hooks, longlines, handlines, and spears as means of harvest. Since the 1970s, increasing overseas food markets and local bait industries have triggered several attempts to develop a commercial fishery for the North Pacific giant octopus (hereafter referred to as "giant octopus" in this article) in Alaska (Paust, 1997), but little is known about the efficacy of different gear types for the capture of this species in Alaska.

Currently, the Alaska Department of Fish and Game allows commercial harvest of octopus within state waters only as incidental catch managed under state permits. Retention levels as bycatch vary from about 5% in the pot gear fishery for shrimp in southeast Alaska to about 20% in the state groundfish fisheries. Paust (1997) compared four lair pot designs and found that because of low construction costs, reduced space needed for storage, relative ease of handling, and a superior fishing performance over other lair pot designs, the wooden Kodiak pot would be the best choice for fishery development in Alaska. No baited pots were included in Paust's study design. Paust (1997) assumed new entrants into a directed fishery for giant octopus will most likely integrate directed fishing for the giant octopus as an off-season or secondary fishery. Such a developing fishery would have high start-up costs and no proven returns, limiting its participants to using fishing gear from other fisheries. Given the value of data on the effectiveness at capturing giant octopus with equipment already used in Alaska fisheries, we examined the efficiency and size selectivity of four pot types for their use in a directed fishery for this species.

## Materials and methods

Two surveys were completed (2–13 October 2006, and 25 November to 6 December 2006) in Kachemak Bay, Alaska (Fig. 1). Four types of pots were used during the course of the study: lair, Korean hair crab, sablefish, and shrimp pots (Fig. 2). Lair pots were constructed of wood, measured 60.96 cm × 30.48 cm × 30.48 cm with a 15.42 cm × 30.48 cm opening, and were left unbaited. Korean hair crab pots consisted of PVC piping and were 45 cm tall and had a 100-cm base diameter and a 26-cm plastic

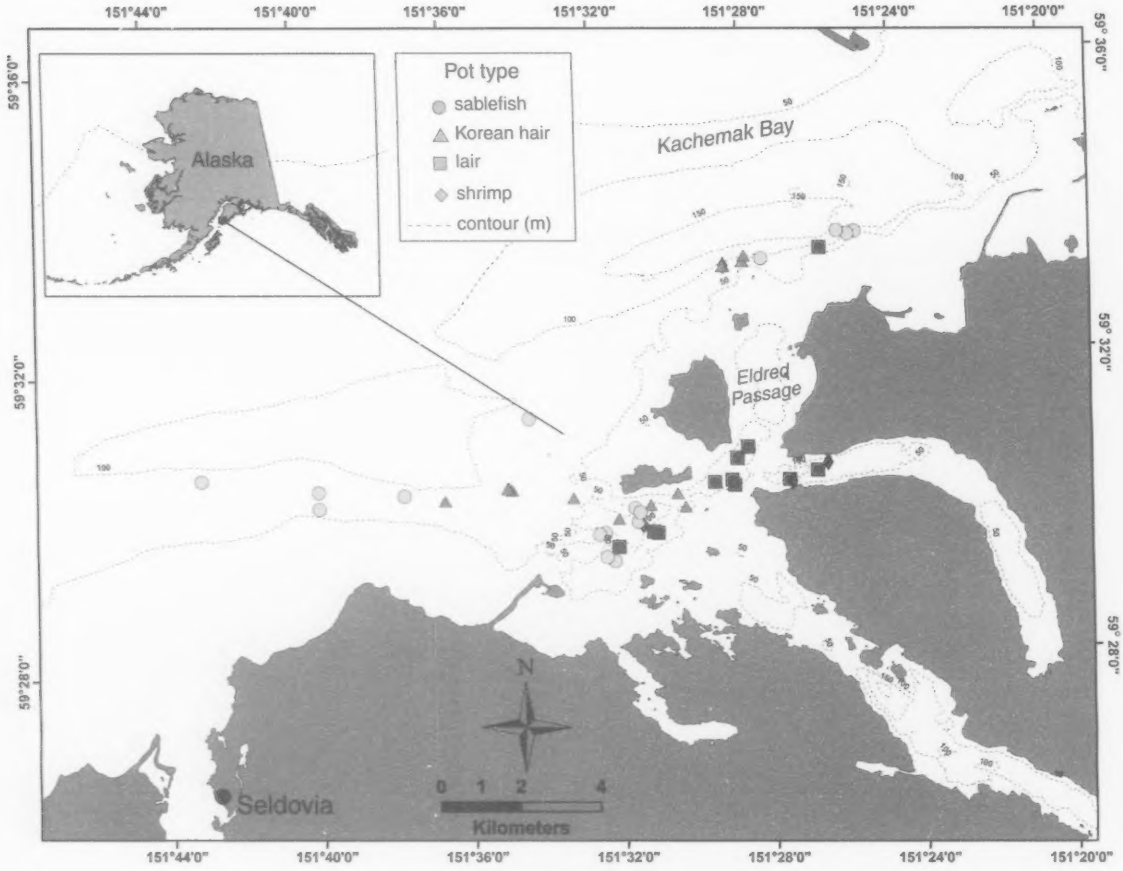


**Figure 1**

Map of Kachemak Bay, Alaska, and location of pots set to catch North Pacific giant octopus (*Enteroctopus dofleini*) to evaluate the efficiency of the pots for use in a directed North Pacific giant octopus fishery. Each marker represents the first marker buoy in a string of 16–20 pots, set during two surveys in 2006.

tunnel. Sablefish pots were made of 1.3-cm rebar and measured 147 cm tall and had a 122-cm bottom ring and a 71-cm top ring. The sock tunnel opening was 25 cm wide and located 76 cm from the bottom. The net used was 7-cm mesh black seine net. Korean hair crab and sablefish pots were baited with chopped herring. Both commercial and personal-use Ladner shrimp pots had three 7.62-cm tunnel openings and were baited with either herring or prawn pellets.

Each string of pots consisted of a single pot type to best replicate fishing practices and to make the process of setting and retrieving pots as safe as possible. Each string of pots consisted of 20 pots spaced nine meters apart and two marker buoys were attached to each end. Lair pot strings had only 16 pots. We removed the shrimp pots from the sampling design for the second survey because of their low catch per unit of effort (CPUE).

To facilitate handling, captured giant octopuses were placed in mesh bags and kept in individual (53 liters/ 60.7×40.4×31cm) Rubbermaid® containers. Containers were filled with seawater and the water was exchanged every five minutes by using a pump placed approximately one meter below the surface of the water. The sex of each animal was determined by the presence (male) or absence (female) of the hectocotylized right third arm. If the animal had lost the tip of its right third arm we could not determine sex. We recorded morphometric measurements including the interocular distance (IOD), mantle length (ML), and wet weight, as well as any identifying marks for each individual. Muscle tissue from the tip of the left third arm was clipped and preserved in 95% ethanol for future genetic analysis.

Descriptive summary statistics of individuals captured, capture rates of each pot type, and capture rates by survey were tabulated. A paired $t$-test was used to compare the weights of males ($n$=114) and females ($n$=128) captured. We could not determine sex for 8 individuals. They were omitted from all analyses of differences between the sexes. Size selectivity was as-

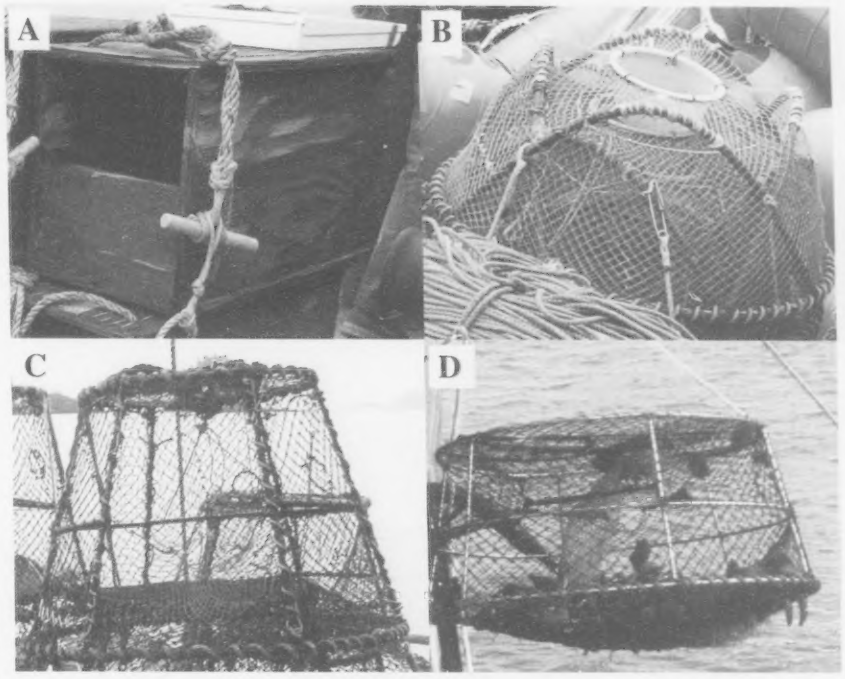


**Figure 2**

The four pot types we evaluated in Kachemak Bay, Alaska, in 2006 to determine their efficiency in capturing North Pacific giant octopus (*Enteroctopus dofleini*) for use in a directed fishery: (**A**) Lair pots; (**B**) Korean hair crab pots; (**C**) sablefish pots; and (**D**) shrimp pots.

sessed by comparing mean weight of octopuses caught in each pot type. Because of heteroscedasticity in the data we used a nonparametric Welch analysis of variance (ANOVA) to test for variation in the weight of octopuses by pot type, followed by Tukey's *post hoc* tests. In order to diminish the potential confounding effects of differences in depths at which pots were set, we reanalyzed weight by pot-type data using only giant octopuses caught within Eldred Passage where depth did not differ significantly by pot type, using an ANOVA and Fisher's least significant difference (LSD) test. Individual chi-square tests were used to determine whether there was a disproportionate number of males or females caught in any one trap type.

No standardized method exists to measure octopus CPUE. In octopus fisheries around the world CPUE is tailored to the type of fishery (Defeo and Castilla, 1998; Hernandez-Garcia et al., 1998; Sanchez et al., 2004). There are markets for both food and bait giant octopuses and in Alaska the fishery would not be size selective. In a full-time directed fishery where the ability to turn over gear is important, "the total catch in kilograms (kg) per days soaked" may be a most useful expression of effort. In contrast, kilograms per pot may be a more useful indicator of effort in a part-time fishery. The number of pots soaking may be more important if a vessel is employed to simultaneously take part in another fishery while its pots for giant octopus are soaking. Irrespective of the fishery structure, whether full-time or concurrent, both CPUE estimates provide valuable information for resource management. Both CPUE estimates were calculated for each individual survey and then averaged over surveys. No statistical tests were performed on CPUE data because the averages calculated over the two surveys are based on two estimates. Catch-per-unit-of-effort values for shrimp pots represent point estimates because shrimp pots were fished only in the first survey. We compared the average soak time of lair pots that caught giant octopuses to those that did not by using a *post hoc* *t*-test to investigate anecdotal evidence that would indicate that longer soak times increase the likelihood of capture.

## Results

We captured a combined total of 254 giant octopuses, four of which were dead and omitted from further analysis. The number of individuals captured was consistent

between surveys; 122 and 128 individuals captured in the first and second surveys, respectively. Of the total 250 individuals captured, the numbers caught among the pot types was as follows: 107 in lair pots, 35 in Korean hair pots, 102 in sablefish pots, and 6 in shrimp pots.

Sablefish pots captured significantly heavier individuals than all other pot types (Fig. 3), but the weight of these giant octopuses captured in the other three pot types did not differ significantly from one another (Welch ANOVA, df=3,32.241, $F$=28.115, $P$<0.001 Tukey HSD). The depth at which pots were set, however, was not determined at random. Larger giant octopuses may be found in deeper water resulting in biased estimates. Although a regression of weight by depth showed a very weak correlation (coefficient of correlation ($r^2$)=0.0019, $P$=0.49), in order to mitigate the potential confounding effects of depth, we re-analyzed weight by pot type using only giant octopuses caught within Eldred Passage where depth did not differ significantly by pot type. Giant octopuses caught in sablefish pots remained significantly heavier than those caught in both lair and shrimp pots, but there was not a significant difference in mean weight between sablefish and Korean hair crab pots (ANOVA, df=3, $F$=10.599, $P$<0.001 Fisher's LSD). Among the 112 males and 126 females captured, males were heavier than females ($t$-test, df=1, $F$=7.166, $P$=0.008). However, this finding did not seem to be driving the observed difference in weight by pot type because for each pot type both sexes were equally likely to be captured (lair: $\chi^2$=0.154, $P$=0.695, Korean hair crab: $\chi^2$=0.030, $P$=0.862, sablefish: $\chi^2$=0.853, $P$=0.356, and shrimp: $\chi^2$=0, $P$=1).

Capture efficiency varied both temporally and with the CPUE index (kg/days soaked vs. kg/pot set). Between the two surveys the efficiency of both lair and Korean hair crab pots increased and the efficiency of sablefish pots decreased. The average CPUE for all pot types between surveys ranged from 5.5 kg/pot (±1.7 SD [standard deviation]) for the lair pots to 0.4 kg/pot for shrimp pots, and 17.6 kg/days soaked (±2.7 SD) for the sablefish pots to 2.1 kg/days soaked for shrimp pots (Fig. 4). Lair pots that caught giant octopuses were not soaked longer than pots that did not capture octopuses ($t$-test df=1, $F$=0.214, $P$=0.644).

Both sablefish and Korean hair crab pots caught large numbers of commercially important crab and fish species as bycatch. Korean hair crab pots caught Tanner crabs (*Chionoecetes bairdi*) and Pacific cod (*Gadus macrocephalus*; sizes ranging from 26 to 100 cm total length). Sablefish pots caught *C. bairdi*, *G. macrocephalus*, and halibut (*Hippoglossus stenolepis*; sizes ranging from 29 to 112 cm total length). Lair and shrimp pots did not contain bycatch of commercially important species. Other bycatch species, caught in all four pot types were lyre crabs (*Hyas lyratus*), decorator crabs (*Oregonia gracilis*), sunflower sea stars (*Pycnopodia helianthoides*), and Oregon hairy tritons (*Fusitriton oregonensis*).

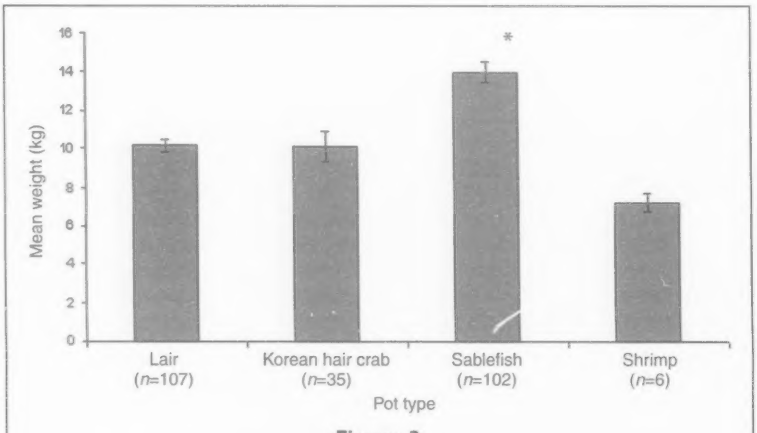


**Figure 3**

Mean weight (±standard error [SE]) in kilograms and numbers (in parentheses) of North Pacific giant octopus (*Enteroctopus dofleini*) caught in each of the four pot types, during two surveys in Kachemak Bay, Alaska, in 2006, evaluated for size selectivity for use in a directed North Pacific giant octopus fishery. The asterisk indicates a significant difference at $P$<0.001.

## Discussion

The internal volume of each pot may be a better indicator than the size of the pot entrance for the potential size of giant octopuses that will be caught. Although lair, Korean hair crab, and sablefish pots had similar size openings, the success of the sablefish pots may have been due to their volume being three times greater than that of the Korean hair crab pots and nearly twenty times that of the lair pots. The ability of giant octopuses to enter a trap is most likely determined by the size of its beak, the only hard part of its body.

Variation in the size of North Pacific giant octopuses caught by the different pot types may be influenced by differences in depth or substrate rather than by pot type alone. However, when pots laid at similar depths in Eldred Passage were analyzed, we observed similar trends in the data, indicating that sablefish pots have the potential to capture larger giant octopuses than the other pots.

Pot efficiency changed with different measurements of effort. Lair pots, because of their long soak times, may be more useful in a fishery where operators are fishing for giant octopus and another species concurrently. Anecdotal evidence from the use of lair pots indicates

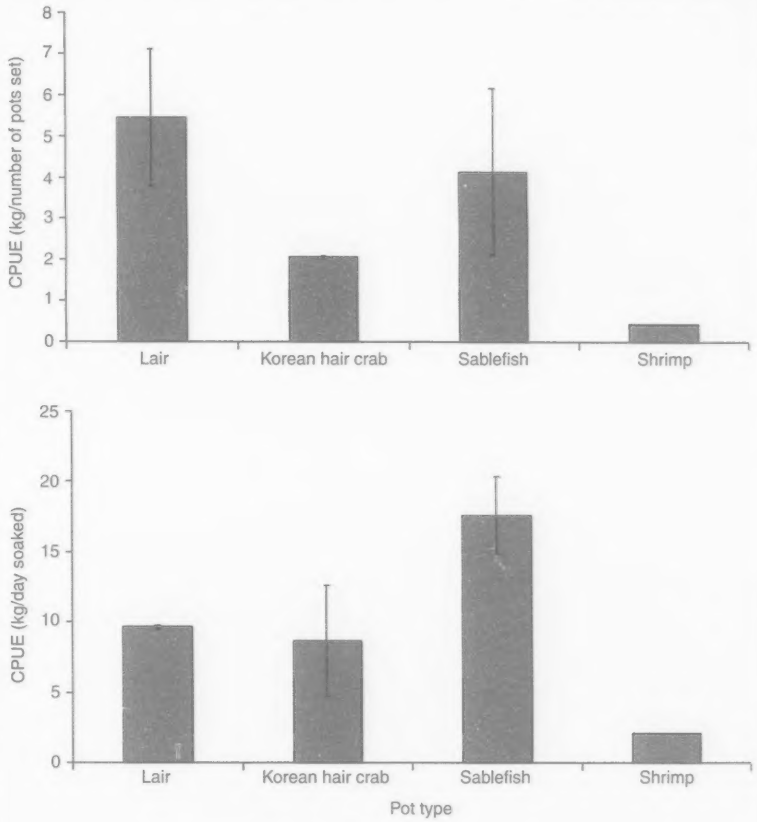


**Figure 4**

Mean catch per unit of effort (CPUE; ±standard deviation [SD]), measured as both kilograms per hours soaked and kilograms per number of pots set, for each of the four pot types evaluated for capture efficiency of North Pacific giant octopus (*Enteroctopus dofleini*) during two surveys in Kachemak Bay, Alaska, in 2006. Estimates of CPUE are based on a mean of two estimates; therefore no statistical tests were performed.

an optimal soak time of approximately seven days. These pots do not require baiting to be effective and therefore it is unlikely that prolonged soak times (longer than seven days) will decrease their effectiveness. We suspect that increasing the total volume of the pot and decreasing the size of the opening of lair pots may increase catch rates.

Sablefish pots proved to be the most efficient gear type tested in terms of kilograms per hours soaked, indicating that fewer pots could be fished with short soak times. Although their efficiency in terms of kg/pot may be lower than that of lair pots, shorter soak times allow for increased pot turnover. The capital investment for fishermen already using pots in the sablefish fishery would be minimal and the season could begin after the sablefish season closes in November. Shrimp pots captured relatively few octopuses and those caught generally were smaller in size, possibly because of the small diameter of the pot entrance. Korean hair crab pots caught only slightly larger individuals and had a similarly low CPUE, despite having a much larger entrance.

The high incidence of bycatch of commercially important species by the sablefish pots may limit their usefulness in a directed fishery for North Pacific giant octopus. Vessels targeting the giant octopus would not be allowed to target any other species and all bycatch would be limited to a small percentage of the total weight of the giant octopus onboard. Bycatch reducing devices have been successful in reducing the bycatch of sea turtles (Fratto et al., 2008), crabs (Furevik et al., 2008), and birds (Butler and Heinrich, 2007) in multiple pot fisheries while maintaining high catch rates of their target species. Depending on our ability

to minimize bycatch by sablefish pots, it may be a better strategy to use a pot type that is less efficient in terms of kilograms per hours soaked, but that has a lower bycatch rate.

Additional considerations to the season and type of pot used in a directed North Pacific giant octopus fishery must be made to ensure that fishermen are not disproportionately harvesting spawning giant octopuses. During two captures in which we manipulated females, they extruded spermatophores. Although females after spawning survive to care for eggs, males die within a month of copulation (Hartwick, 1983; Arnold et al., 1987) leading us to assume that the four octopuses captured dead were recently spawned males. Due to decomposition of the bodies we could not confirm sex; however, other observations of deteriorating body conditions of males during the second survey support this conclusion. Lair pots, to be efficient, rely on the giant octopuses using them as a den for short periods of time. During the breeding season, females may use these pots to lay and brood their eggs. If females do use lair pots for denning and giant octopuses exhibit a migration to inshore waters to reproduce (Hartwick, 1983), care must be taken to ensure a large enough escapement to prevent localized depletions and ensure sustainable harvest.

## Acknowledgments

We are grateful to those who helped in collecting data: D. Scheel, J. Grund, D. Veerhusen and the crew of the FV *Shady Lady*, G. Carroll and the crew of the FV *Centurion*, and J. Browning. We thank L. Kamin, S. Barry, and five anonymous reviewers for helpful comments on earlier versions of the manuscript, C. Hay-Jahans for statistical advice, and Q. Smith for assistance with GIS. This research was supported by a grant from the Alaska Fisheries Development Foundation, Inc.

## Literature cited

Arnold, J. M., K. Crawford, L. A. Jaffe, and W. C. Summers.
1987. Phylum Mollusca, class Cephalopoda, subclass Coleoidea. *In* Reproduction and development of marine invertebrates of the northern Pacific Coast (M. F. Strathman, ed.), p. 354–369. Univ. Washington Press, Seattle.

Butler, J. A., and G. L. Heinrich.
2007. The effectiveness of bycatch reduction devices on crab pots at reducing capture and mortality of diamondback terrapins (*Malaclemys terrapin*) in Florida. Estuaries Coasts 30:179–185.

Defeo, O., and J. C. Castilla.
1998. Harvesting and economic patterns in the artisanal *Octopus mimus* (Cephalopoda) fishery in a northern Chile cove. Fish. Res. 38:121–130.

Fratto, Z. W., V. A. Barko, P. R. Pitts, S. L. Sheriff, J. T. Briggler, K. P. Sullivan, B. L. McKeage, and T. R. Johnson.
2008. Evaluation of turtle exclusion and escapement devices for hoop-nets. J. Wild. Manag. 72:1628–1633.

Furevik, D. M., O. B. Humborstad, T. Jorgensen, and S. Lokkeborg.
2008. Floated fish pot eliminates bycatch of red king crab and maintains target catch of cod. Fish. Res. 92:23–27.

Hartwick, B.
1983. *Octopus dofleini*. *In* Cephalopod life cycles (P. R. Boyle, ed.), p. 277–291. Academic Press, London.

Hernandez-Garcia, V., J. L. Hernandez-Lopez, and J. J. Castro.
1998. The octopus (*Octopus vulgaris*) in the small-scale trap fishery off the Canary Islands (Central-East Atlantic). Fish. Res. 35:183–189.

Paust, B. C.
1997. *Octopus dofleini*: commercial fishery in Alaska. *In* Proceedings of the workshop on the fishery and market potential of octopus in California, p. 75–83. Smithsonian Institution, Washington, DC.

Sanchez, P., F. Maynou, and M. Demestre.
2004. Modelling catch, effort and price in a juvenile *Eledone cirrhosa* fishery over a 10-year period. Fish. Res. 68:319–327.

# Larval development of the spotfin tonguefish (*Symphurus oligomerus* Mahadeva and Munroe, 1990) (Pleuronectiformes: Cynoglossidae) from the Gulf of California, Mexico

**Ricardo J. Saldierna-Martínez (contact author)**[1]
**Gerardo Aceves-Medina**[1]
**Enrique A. González-Navarro**[2]

Email address for contact author: rsaldier@ipn.mx

[1] Departamento de Plancton y Ecología Marina
Centro Interdisciplinario de Ciencias Marinas
Av. Instituto Politécnico Nacional S/N
Colonia Playa Palo de Santa Rita
Apdo. Postal 592
La Paz, Baja California Sur 23000, Mexico

[2] Departamento de Biología Marina
Universidad Autónoma de Baja California Sur
Apdo. Postal 19-B
La Paz, Baja California Sur. 23080, Mexico

**Abstract**—Larval and early juvenile stages of *Symphurus oligomerus* are described from 24 specimens from the Gulf of California. Meristic features were 48–49 total vertebrae, 87–94 dorsal-fin rays, 73–77 anal-fin rays, 12 caudal-fin rays, and five hypural bones. Seven larvae and one juvenile were cleared and stained to obtain the pterygiophore formula (1-3-2-2-2) that confirmed the identification of *S. oligomerus*. The pigment pattern from preflexion to juvenile stage consists of three bands on the dorsal margin and two bands on the ventral margin formed by star-shaped melanophores on the left side of the body. The intestine in preflexion to postflexion larvae forms an abdominal projection that ends in a short conical appendix. The intestine is supported by three cartilaginous struts; larvae with these physical attributes are called exterilium larvae. Preflexion larvae have two elongated dorsal-fin rays, and in flexion to postflexion larvae the second to the fourth dorsal-fin rays are elongate. We found an apparent connection between the size at metamorphosis of the species of *Symphurus* and the depth distribution range of adults such that the fish species that metamorphose at a larger size have a deeper distribution as adults and exterilium larvae seem to correspond to species that have deeper distributions.

Manuscript submitted 15 October 2008.
Manuscript accepted 20 October 2009.
Fish. Bull. 108:45–55 (2010).

The views and opinions expressed or implied in this article are those of the author (or authors) and do not necessarily reflect the position of the National Marine Fisheries Service, NOAA.

The Cynoglossidae family in the eastern Pacific Ocean is represented by a single subfamily (Symphurinae) and a single genus (*Symphurus*; tonguefish). This genus has a world-wide distribution, including the eastern Pacific Ocean where it is represented by 18 species, inhabiting temperate and tropical waters on the continental shelf and slope (Munroe et al., 1995; Munroe and Robertson, 2005). Previous studies have demonstrated the diagnostic value of the pterygiophore interdigitation pattern (ID pattern) which, combined with other meristics, can be used to identify symphurine tonguefish all over the world (Munroe, 1992; Munroe et al., 1995). Species with the 1-3-2 and 1-3-3 ID patterns are found in both the Atlantic Ocean and in the tropical eastern Pacific Ocean from the Gulf of California to northern Peru. Species with the 1-3-4, 1-4-2, 1-4-3 and 1-5-3 ID patterns are found only in the New World. Currently, the early life history stages of seven species of symphurine tonguefishes occurring in the eastern Pacific can be distinguished from each other by their melanistic pigmentation patterns. *Symphurus callopterus* has an accumulation of pigment in the form of two oblique, incomplete and two complete bands on the caudal section of the body (Evseenko, 1990), whereas *S. williamsi* (Aceves et al., 1999), *S. elongatus* (Charter and Moser, 1996), *S. chabanaudi*, and *S. prolatinaris* (Evseenko and Shtaut, 2000) have blotches or spots or both on the dorsal and ventral margins of the body; and both *S. atricaudus* (Charter and Moser, 1996) and *S. atramentatus* (Saldierna-Martínez et al., 2005) have a series of dash-like spots on the dorsal and ventral margins of the body. Although *S. oligomerus* (spotfin tonguefish) is a species with wide distribution from the Gulf of California to Panama (Mahadeva and Munroe, 1990; Munroe et al., 1995), its larvae are still undescribed. This study provides the first description of the larval development of *S. oligomerus* from the preflexion to the juvenile stage.

## Materials and methods

Plankton samples were collected in November 2005 in the Gulf of California. Twenty-four oblique zooplankton tows were made with bongo nets with a mouth diameter of 60 cm and net mesh of 505 and 333 μm as detailed in Kramer et al. (1972). Three additional samples were obtained from multilevel oblique tows at 150–100, 100–50, and

**Table 1**

Sampling methods, locations, depths, and preservation methods for larval *Symphurus oligomerus* collected in the Gulf of California in 2005. B=bongo net, M=multilevel net, BL=body length.

| | Coordinates | | Number of specimens (BL, mm) | | |
|---|---|---|---|---|---|
| Net | N | W | Catch depth (m) | Ethyl alcohol | Formalin |
| B | 28°30′38″ | 113°6′39″ | 0–21 | 1 (18.0) | |
| B | 28°12′ | 112°17′ | 0–195 | 1 (15.8) | |
| B | 27°28′46″ | 112°16′27″ | 0–214 | | 1 (18.2) |
| B | 27°14′24″ | 111°14′24″ | 0–211 | 1 (14.6) | |
| B | 26°54′30″ | 111°46′16″ | 0–71 | | 2 (3.0–3.4) |
| B | 26°36′1.5″ | 110°32′1.5″ | 0–209 | 1 (8.8) | 3 (3.8–18.0) |
| B | 26°11′19″ | 111°18′31″ | 0–182 | | 3 (1.6–2.6) |
| B | 25°24′40″ | 109°16′28″ | 0–45 | 5 (6.8–10.4) | |
| B | 24°52′26″ | 109°48′19″ | 0–97 | 1 (12.0) | |
| M | 24°42′8″ | 110°17′28″ | 0–50 | | 1 (10.0) |
| M | 24°42′8″ | 110°17′28″ | 50–100 | | 2 (11.3–12.3) |
| M | 24°42′8″ | 110°17′28″ | 100–150 | | 2 (7.8–10.4) |

50–0 m with simple conical nets with a mouth diameter of 75 cm and net mesh of 333 μm (Table 1). Samples obtained with the 333-μm mesh bongo net and the multilevel tows were fixed in ethyl alcohol (96%), and samples from the 505-μm mesh bongo net were fixed with 10% formalin solution buffered with sodium borate.

Among the fish larvae taken in this collection, twenty-four specimens of larval and juvenile *Symphurus* (1.6–18.2 mm body length [BL]) were grouped because they shared the same meristic counts and pigmentation patterns. Comparison of this group of larvae with published descriptions of the early life stages of tonguefish from the eastern Pacific (Evseenko, 1990; Charter and Moser, 1996; Aceves et al., 1999; Evseenko and Shtaut, 2000; and Saldierna-Martínez et al., 2005) indicated that these specimens belonged to a species whose larval development had not been described. Seven larvae and one juvenile from this group of specimens were cleared and stained (Potthoff, 1984) and identified as *Symphurus oligomerus* on the basis of meristic characters (dorsal-fin rays, anal-fin rays, caudal-fin rays, total vertebrae, and hypural bones) and interdigitation of dorsal-fin pterygiophores and neural spines (ID pattern), which was 1-3-2-2-2 (Mahadeva and Munroe, 1990; Munroe, 1992; Munroe et al., 1995). Subsequently a developmental series of larvae was assembled by using similar pigmentation pattern (oblique band on the body) as well as meristic and morphometric features (total dorsal and anal-fin rays and conical appendix). Measurements to the nearest 0.1 mm were taken on the left side of the body as illustrated in Figure 1C and Table 2 by using a stereomicroscope (Stemi 2000-C, Zeiss) fitted with an ocular micrometer.

All larvae and juveniles were deposited in the Colección científica de huevos y larvas de peces del Pacífico Mexicano (ICTIOPLANCTON) registered with the Secretaría del Medio Ambiente y Recursos Naturales (B.C.S.-INV196-06-07) and located at the Departamento de Plancton y Ecología Marina, Centro Interdisciplinario de Ciencias Marinas-Instituto Politécnico Nacional (CICIMAR-IPN). Catalogue numbers for specimens of *S. oligomerus* deposited in this collection are L108–L126.

Illustrations of larval and juvenile stages of *S. oligomerus* were drawn with a camera lucida (Stereomicroscope Stemi SV8, Zeiss). Descriptions of larval and juvenile stages were based on 24 specimens from 1.6 to 18.2 mm BL. None of the specimens were in the yolksac stage, indicating that hatching takes place at sizes <1.6 mm notochord length (NL). Preflexion, flexion, postflexion, and juvenile stages accord with the larval fish developmental stages described by Ahlstrom (1976).

## Results

### Identification

Twenty-four specimens sharing similar morphometric and meristic characteristics were identified among the material examined. Seven larvae and one juvenile tonguefish from 7.8–18.2 mm BL were cleared and stained. These cleared specimens had the following ID patterns: 1-3-2-2-2 ($n$=7) and 2-3-2-2-2 ($n$=1). We observed differences in the number of hypural elements in the cleared and stained specimens; these differences were associated with the development stage, as well as with the degree of ossification of the hypural elements. Five hypural bones were observed in one postflexion larva and one juvenile (18.0 and 18.2 mm BL); four cartilaginous hypurals were present in four larvae (10.4 to 12.0 mm BL), and three cartilaginous hypurals were present in two larvae (7.8 and 10.0 mm BL). From these

**Table 2**

Abbreviations and definitions of terms used to describe the morphometric and meristic characters of *Symphurus oligomerus* larvae and juveniles.

| | |
|---|---|
| Body length (BL) | In preflexion and flexion stages, horizontal distance from snout tip to tip of notochord, referred to as notochord length (NL); in postflexion-stage larvae, from snout tip to posterior margin of hypural bones as standard length (SL) |
| Caudal region length (CRL) | Horizontal distance from posterior end of anus to tip of notochord in young larvae or to posterior margin of hypural bones in more developed larvae |
| Snout–anus length (SAL) | Horizontal distance through midline of body from snout tip to posterior margin of anus |
| Head length (HL) | Horizontal distance through midline of the head from snout tip to margin of cleithrum preceding pectoral fin base in small specimens, or to posterior margin of opercle in larger specimens |
| Eye diameter (ED) | Horizontal distance between anterior and posterior margins of left eye |
| Body depth at pelvic fin base (BD) | Vertical distance from dorsal to ventral margin of body, measured at pelvic fin base |
| Body depth at anus (BDA) | Vertical distance across body at anus prior to formation of dorsal fin pterygiophores (Moser, 1996) |
| Loop intestinal length (LIL) | Horizontal distance from cleithrum to tip of the conical appendix on the abdominal projection |
| Abdominal projection length (APL) | Horizontal distance from cleithrum to base of conical appendix on abdominal projection |
| Conical appendix length (CAL) | Horizontal distance from base to tip of conical appendix |
| Pterygiophore interdigitation pattern (ID pattern) | Number of proximal dorsal-fin pterygiophores in each of the five anterior interneural spaces (Munroe, 1992). |
| Internal cartilaginous struts (ICS) | Support internal of the intestinal sac, make-up for cartilaginous struts |

specimens and the remaining 14 larvae and two juveniles, we counted 48–49 vertebrae (more frequently 48), 87–94 dorsal-fin rays (more frequently 89–91), 73–77 anal-fin rays (more frequently 74–75), and 12 caudal-fin rays (Table 3). Of 18 species of *Symphurus* recognized in the eastern Pacific, only *S. gorgonae*, *S. oligomerus*, *S. microlepis*, and *S. diabolicus* have the 1-3-2-2-2 ID pattern. *Symphurus gorgonae* differs from the other species in having only four hypural bones, and *S. oligomerus*, *S. microlepis*, and *S. diabolicus* have five hypural bones (Munroe, 1992). *Symphurus diabolicus* and *S. microlepis* have more dorsal- (106–110 and 106, respectively) and anal- (89–96 and 92) fin rays and a higher number of vertebrae (57–59 and 57) than *S. oligomerus* (87–97 dorsal-fin rays, 72–83 anal-fin rays, and 48–52 total vertebrae). *Symphurus gorgonae* has fewer dorsal- (80–89) and anal- (63–74) fin rays than *S. oligomerus* (Munroe, 1992; Munroe and McCosker, 2001). Furthermore, *S. diabolicus*, is apparently endemic to the Galapagos Archipelago (Munroe and McCosker, 2001), whereas *S. microlepis* is collected off the coast of Panama in 530 m (Munroe et al., 1995; Munroe and McCosker, 2001). The combination of meristic features indicates that these larvae and juvenile specimens are *S. oligomerus*.

## Description of larval and juvenile stage of *Symphurus oligomerus*

**Morphological features** The early preflexion larvae (1.6 and 2.6 mm BL) have an elongate, slightly compressed body. The abdominal cavity with an intestinal loop extends beyond the lower contour of the body, forming a short and freely hanging abdominal projection. This projection is an elongate and relatively slender sac with transparent walls; the loop intestinal length ranges between 21% and 31% of the BL (Table 4). The end portion of the abdominal projection is a conical appendix whose length is 2.5–10% of the BL. During flexion until the juvenile stage (7.8–18.2 mm BL) the loop of the intestine is supported by three internal cartilaginous struts (ICS); two are located on either side of the intestinal sac (Figs. 1C and 2A) and the third is located near the pectoral fin base, supporting the lateral cartilages. The anus opens on the left side of the body. The head is small, 25% of BL (Table 4) and has a small and oblique snout. The posterior corner of the mouth never extends beyond the middle part of the left eye (Fig. 1A). In larvae between 3.4 mm BL and 3.8 mm BL, the swim bladder is located above the dorsal region of the intestinal sac

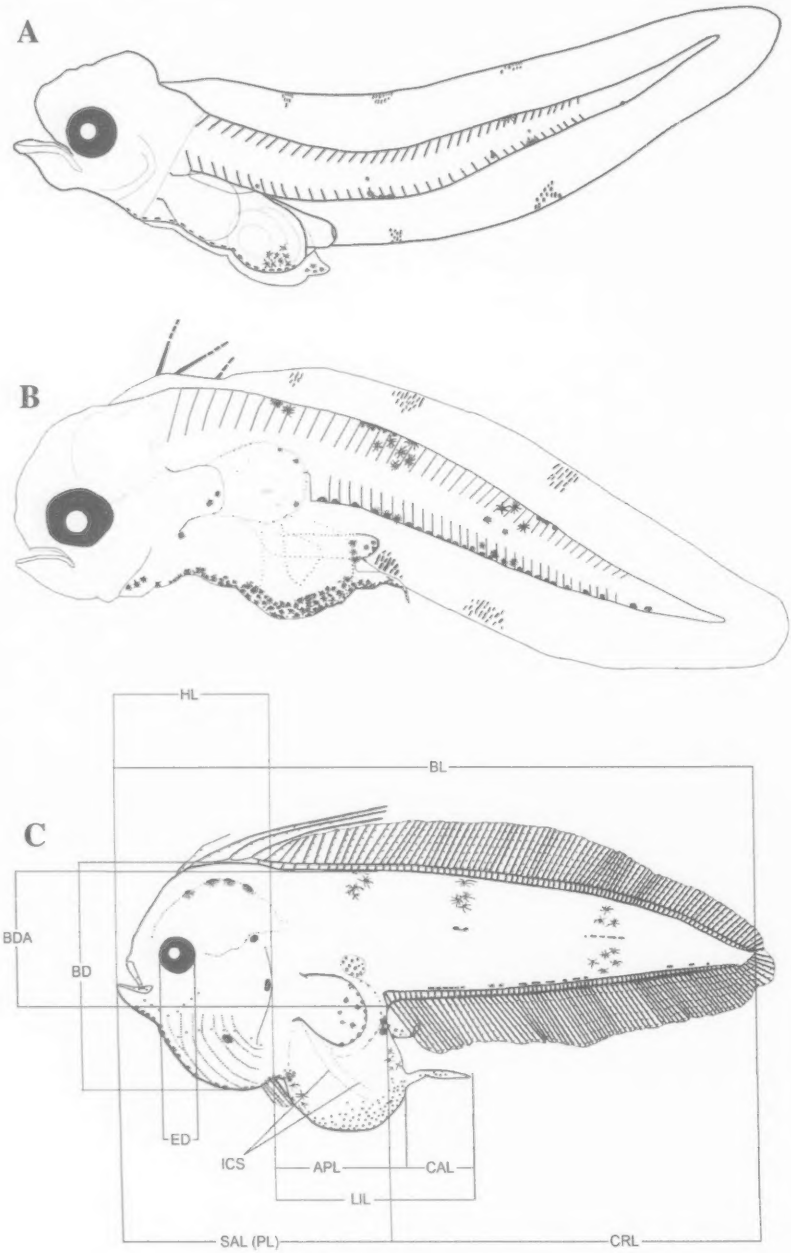


**Figure 1**

Spotfin tonguefish (*Symphurus oligomerus*): (**A**) preflexion larva (2.5 mm notochord length, NL); (**B**) preflexion larva (3.4 mm NL); and (**C**) flexion larva (7.8 mm body length) showing two internal cartilaginous struts (ICS). Morphometric measurements are HL=head length; BL=body length; CRL=caudal region length; SAL=snout–anus length; LIL=loop intestinal length; APL=abdominal projection length; CAL=conical appendix length; ED=eye diameter; BD=body depth at pelvic fin base; BDA=body depth at anus. Drawings by R. Saldierna.

**Table 3**

Larval and juvenile measurements (mm) for 24 specimens of spotfin tonguefish (*Symphurus oligomerus*) at various developmental stages: body length (BL), eye diameter (ED), head length (HL), snout–anus length (SAL), caudal region length (CRL), body depth at pelvic fin base (BD), body depth at anal fin (BDA), loop intestinal length (LIL), abdominal projection length (APL), conical appendix length (CAL), dorsal rays (DR), anal rays (AR), caudal rays (CR), total vertebrae (TV), hypural bones (H), and pterygiophore interdigitation pattern (ID). Not determined (nd) and incomplete dorsal-, anal-, and caudal-fin rays (+).

| | Measurement | | | | | | | | | | | | | | |
|---|---|---|---|---|---|---|---|---|---|---|---|---|---|---|---|
| Development stage | BL | ED | HL | SAL | CRL | BD | BDA | LIL | APL | CAL | DR | AR | CR | TV | H | ID |
| Start of preflexion | 1.6 | 0.10 | 0.3 | 0.8 | 0.8 | 0.3 | 0.1 | 0.49 | 0.5 | 0.04 | | | | | | |
| | 2.5 | 0.19 | 0.5 | 0.9 | 1.6 | 0.4 | 0.2 | 0.60 | 0.5 | 0.1 | | | | | | |
| | 2.6 | 0.19 | 0.6 | 1.0 | 1.7 | 0.5 | 0.2 | 0.71 | 0.6 | 0.1 | | | | | | |
| | 3.0 | 0.20 | 0.6 | 1.2 | 1.8 | 0.7 | 0.3 | 0.66 | 0.5 | 0.1 | | | | | | |
| | 3.4 | 0.27 | 0.8 | 1.3 | 2.1 | 0.8 | 0.4 | 1.01 | 0.7 | 0.3 | | | | | | |
| | 3.8 | 0.29 | 0.9 | 1.3 | 2.4 | 1.0 | 0.5 | 0.96 | 0.6 | 0.4 | | | | | | |
| | 6.8 | 0.32 | 1.7 | 2.6 | 4.2 | 2.0 | 1.3 | 1.60 | 1.1 | 0.5 | 80+ | 70+ | | | | |
| | 7.0 | 0.40 | 1.6 | 2.7 | 4.2 | 2.1 | 1.3 | 1.92 | 1.4 | 0.5 | 80+ | 70+ | 2+ | | | |
| Start of flexion | 7.1 | 0.36 | 1.2 | 2.7 | 4.4 | 2.3 | 1.4 | 1.62 | 1.0 | 0.6 | 84+ | 70+ | 6+ | | | |
| | 7.4 | 0.40 | 2.3 | 3.0 | 4.4 | 2.4 | 1.3 | nd | 1.4 | nd | 90 | 74 | 6+ | | | |
| | 7.8 | 0.40 | 2.2 | 3.1 | 4.7 | 2.7 | 1.4 | 2.26 | 1.5 | 0.8 | 91 | 75 | 6+ | 48 | 3 | 1-3-2-2-2 |
| | 8.8 | 0.40 | 2.1 | 3.0 | 5.8 | 2.1 | 1.8 | nd | nd | nd | nd | nd | 12 | | | |
| | 10.0 | 0.46 | 2.5 | 3.9 | 6.1 | 3.3 | 2.0 | 3.45 | 2.2 | 1.3 | 91 | 75 | 12 | 49 | 3 | 2-3-2-2-2 |
| | 10.4 | 0.46 | 2.8 | 4.1 | 6.2 | 3.3 | 2.0 | 3.45 | 2.3 | 1.2 | 87 | 74 | 12 | 48 | 4 | 1-3-2-2-2 |
| | 10.4 | 0.48 | 2.7 | 3.8 | 6.6 | 3.4 | 2.2 | 3.14 | 2.2 | 1.0 | 80+ | 74 | 12 | | | |
| | 10.6 | 0.46 | 2.8 | 4.1 | 6.4 | 3.3 | 2.2 | 2.99 | 1.8 | 1.2 | 91 | 74 | 12 | 49 | 4 | 1-3-2-2-2 |
| | 11.3 | 0.46 | 3.1 | 4.6 | 6.7 | 3.7 | 2.2 | 3.91 | 2.5 | 1.4 | 90 | 74 | 12 | 48 | 4 | 1-3-2-2-2 |
| | 12.0 | 0.46 | 3.0 | 4.6 | 7.4 | 3.5 | 2.3 | 3.44 | 2.6 | 0.9 | 88 | 73 | 12 | | | |
| | 12.3 | 0.46 | 3.0 | 4.6 | 7.7 | 4.0 | 2.8 | 2.99 | 1.8 | 1.2 | 89 | 75 | 12 | 49 | 4 | 1-3-2-2-2 |
| | 14.6 | 0.48 | 3.7 | 5.8 | 8.9 | 4.3 | 3.1 | 3.58 | 2.5 | 1.1 | 94 | 75 | 12 | | | |
| Start of postflexion | 18.0 | 0.58 | 4.5 | 6.3 | 11.7 | 4.9 | 3.3 | 4.37 | 3.5 | 0.9 | 89 | 75 | 12 | 48 | 5 | 1-3-2-2-2 |
| Start of juvenile | 15.8 | 0.60 | 3.5 | 5.2 | 10.6 | 3.8 | 3.2 | 2.51 | 1.8 | 0.7 | 89 | 77 | 12 | | | |
| | 18.0 | 0.58 | 3.5 | 4.9 | 13.1 | 4.0 | 3.7 | | | | 90 | 77 | 12 | | | |
| | 18.2 | 0.69 | 5.1 | 6.1 | 12.1 | 4.0 | 3.0 | | | | 88 | 76 | 12 | 48 | 5 | 1-3-2-2-2 |

**Table 4**

Morphometric proportions of larval and juvenile spotfin tonguefish (*Symphurus oligomerus*) by percentage of body length (BL, mm): eye diameter (ED), head length (HL), caudal region length (CRL), snout–anus length (SAL), body depth at pelvic fin base (BD), body depth at anal fin (BDA), loop intestinal length (LIL), abdominal projection length (APL), conical appendix length (CAL). nd = not determined.

| | | % of BL | | | | | | | |
|---|---|---|---|---|---|---|---|---|---|
| Development stage | BL(mm) | ED | HL | CRL | SAL | BD | BDA | LIL | APL | CAL |
| Start of preflexion | 1.6 | 6.09 | 21.79 | 51.15 | 48.72 | 18.27 | 7.31 | 31.67 | 29.23 | 2.44 |
| | 2.5 | 7.55 | 18.67 | 64.15 | 35.85 | 16.98 | 8.49 | 23.58 | 18.87 | 4.72 |
| | 2.6 | 7.28 | 21.84 | 63.22 | 36.78 | 17.24 | 8.39 | 27.36 | 21.84 | 5.52 |
| | 3.0 | 6.41 | 19.24 | 59.01 | 41.05 | 21.81 | 10.26 | 21.81 | 17.96 | 3.85 |
| | 3.4 | 8.04 | 22.86 | 61.43 | 38.57 | 22.86 | 11.43 | 30.00 | 20.00 | 10.00 |
| | 3.8 | 7.59 | 22.78 | 64.56 | 35.34 | 25.32 | 12.66 | 25.32 | 15.19 | 10.13 |
| | 6.8 | 4.71 | 24.71 | 62.35 | 38.82 | 29.41 | 18.82 | 23.53 | 16.47 | 7.06 |
| | 7.0 | 5.75 | 22.99 | 59.77 | 39.08 | 29.89 | 18.39 | 27.59 | 20.69 | 6.90 |
| Start of flexion | 7.1 | 5.04 | 16.53 | 62.18 | 37.82 | 32.77 | 20.17 | 22.69 | 14.29 | 8.40 |
| | 7.4 | 5.38 | 31.18 | 59.14 | 40.86 | 32.26 | 17.20 | nd | 19.35 | nd |
| | 7.8 | 5.10 | 27.55 | 60.20 | 39.80 | 34.69 | 18.37 | 28.78 | 18.98 | 9.80 |
| | 8.8 | 4.55 | 23.64 | 65.45 | 34.55 | 23.64 | 20.00 | nd | nd | nd |
| | 10.0 | 4.60 | 25.29 | 60.92 | 39.08 | 33.33 | 19.54 | 34.43 | 21.79 | 12.64 |
| | 10.4 | 4.44 | 26.67 | 60.00 | 40.00 | 32.22 | 19.44 | 33.33 | 22.22 | 11.11 |
| | 10.4 | 4.59 | 25.69 | 63.30 | 36.70 | 33.03 | 21.10 | 30.28 | 21.10 | 9.17 |
| | 10.6 | 4.35 | 26.09 | 60.87 | 39.13 | 31.52 | 20.65 | 28.26 | 17.39 | 10.87 |
| | 11.3 | 4.08 | 27.55 | 59.18 | 40.82 | 32.65 | 19.39 | 34.69 | 22.45 | 12.24 |
| | 12.0 | 3.85 | 25.00 | 61.54 | 38.46 | 28.85 | 19.23 | 28.76 | 21.40 | 7.36 |
| | 12.3 | 3.74 | 24.30 | 62.62 | 37.38 | 32.71 | 22.43 | 24.30 | 14.95 | 9.35 |
| | 14.6 | 3.29 | 25.20 | 60.66 | 39.37 | 29.13 | 21.26 | 24.53 | 17.32 | 7.21 |
| Start of postflexion | 18.0 | 3.19 | 24.88 | 65.06 | 35.08 | 27.43 | 18.50 | 24.24 | 19.13 | 5.10 |
| Start of juvenile | 15.8 | 3.81 | 21.90 | 67.15 | 32.85 | 24.09 | 20.44 | 15.93 | 11.68 | 4.25 |
| | 18.0 | 3.20 | 19.22 | 73.04 | 27.55 | 22.42 | 20.50 | | | |
| | 18.2 | 3.80 | 27.84 | 66.44 | 33.54 | 22.15 | 16.45 | | | |

(Fig. 1B). Notochord flexion begins in larvae larger than 7 mm BL and ends near 15 mm BL (Table 3). In the only postflexion larva collected (18 mm BL), the right eye had begun to migrate to the left side of the head (Fig. 2A). In the juvenile stage (15.8–18.2 mm BL) the protruding gut is incorporated within the ventral body profile and migration of the right eye is complete. Most of the body of the juvenile has very small ctenoid scales; each scale has a single denticle; the swim bladder, pectoral fins, and the conical appendix are no longer visible; and head length is 25% of the BL.

**Pigmentation** Preflexion larvae (1.6–3.0 mm BL) typically have three equidistant blotches on the distal margin of the dorsal fin fold, located approximately between myomeres 6–9, 16–19, and 28–33, and an additional blotch located on the dorsal margin of the body between myomeres 28 and 33. There are two blotches present on the distal margin of the anal fin fold and two blotches on the ventral margin of the body located at myomeres 16–19 and at myomeres 27–36. Several small star-shaped melanophores form a line along the ventral margin of the intestinal sac, nine similar melanophores are present on the left side of the gut, and three or four melanophores are present on the left side of the conical appendix (Fig. 1A).

Larvae 3.4–3.8 mm BL have a pigmentation pattern similar to that described above, but with slight changes in the numbers of myomeres forming the blotches (Fig. 1B); pigmentation is also more intense on the ventral area of the intestinal sac, where eight small star-shaped melanophores are located nearly at the distal margin of the left side of the anus. Small star-shaped melanophores are also present on the pectoral fins: three or more on the distal margin of the surrounding membrane of the pectoral fins, two or more on the distal region of the pectoral fin bud, and one on the pectoral fin base. Four similar melanophores are present on the swim bladder and several dot-like melanophores form a discontinuous line along the ventral margin of the axial musculature that does not reach the tip of the notochord (Fig. 1B).

Conspicuous at flexion stage are three vertical bands of star-shaped melanophores aligned perpendicular

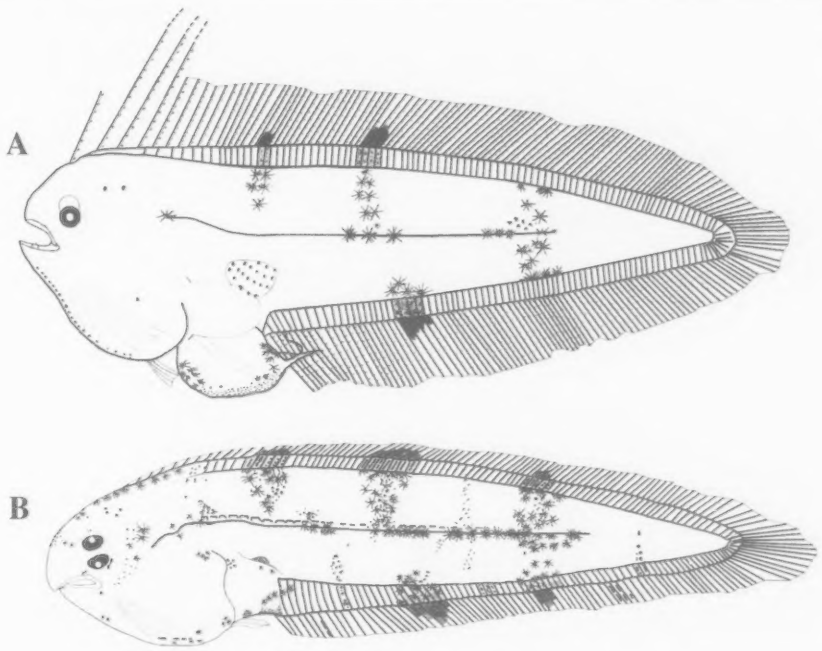


**Figure 2**

Spotfin tonguefish (*Symphurus oligomerus*): (**A**) postflexion larva (18.0 mm body length [BL]) showing two internal cartilaginous struts (ICS); and (**B**) juvenile (18.2 mm BL).

to the notochord (Fig. 1C). These bands begin on the dorsal and ventral margins of the body and extend toward the body midline (Fig. 1C). The pigment pattern consists of two incomplete and one complete band on the left side of the body, located approximately equidistant from each other. The most anterior band overlies the bases of dorsal-fin pterygiophores 11–19 and extends to midway between the dorsal margin and the body midline; the second incomplete band overlies the bases of dorsal-fin pterygiophores 29–35 and extends to the body midline; the third band is complete and overlies the bases of dorsal-fin pterygiophores 53–63. Two or three star-shaped melanophores overlie the notochord below the second dorsal band and three or four other similar melanophores overlie the notochord below the third dorsal band. The first ventral band is located on the bases of the anal-fin pterygiophores 19–27 and the second ventral band is located on the bases of the anal-fin pterygiophores 39–48. Two discontinuous series of dashed pigments are located on the anal fin; one lies over the bases of pterygiophores 9–70; the second series occurs on the bases of the anal-fin rays 1 to 45 and covers almost two-thirds the length of the postabdominal region (Fig. 1C).

Head pigment is first present in flexion-stage larvae. Two to four star-shaped melanophores are located on the dorsal margin of the brain; all are equidistant from each other and located between the first and fourth dorsal-fin rays (Fig. 1C). A comparison of specimens preserved in formalin and ethyl alcohol revealed that the first and fourth melanophores fade in specimens in the formalin solution. Two internal melanophores are present in the posterior head region; one is located in the middle of the cleithrum near the base of the pectoral bud and the second is located on the base of the brain near the cleithrum. The left side of the head also has three series of small star-shaped melanophores. The first series (visible in specimens preserved with formalin and ethyl alcohol) extends along the ventral head margin from the lower jaw tip to the pelvic fin base. The second series (visible only in specimens preserved with ethyl alcohol) forms 'V' located along the ventroposterior margin of the jaw to the ventroposterior margin of the eye. The third series (visible only in specimens preserved with ethyl alcohol) begins at the bases of the first branchiostegal rays and extends posteriorly to the cleithrum. One prominent pigment blotch is present between the fourth and fifth branchiostegal rays. Both upper and lower jaws have four to five star-shaped melanophores at the posterior region.

Several small, star-shaped melanophores are present on the pectoral fins of flexion larvae: two or more occur on the base, three or more on the external margin of the surrounding membrane, and two or more in the

middle of the pectoral-fin bud. Most of these pigments are lost in specimens preserved in formalin. Nine or more similar melanophores are also present on the swim bladder.

The pigmentation of postflexion larvae (Fig. 2A) is similar to that of flexion-stage larvae (Fig. 1C). The major difference in pigmentation between flexion and postflexion larvae is the increase in the extent of the dorsal and ventral bands of star-shaped melanophores which extend towards the midline of the body, as well as to the dorsal- and anal-fin rays. One solid dark line extends down the midline of the body over the notochord from the first vertebra towards the end of the third dorsal band. One star-shaped melanophore appears above the first vertebra (Fig. 2A).

The pigmentation pattern of the juvenile specimens is similar to those of late postflexion specimens (Fig. 2, A and B). In the juvenile stage, formation of the three bands on the dorsal margin and two bands on the ventral margin of the body reach their greatest extension in length and width. These pigment bands extend over the dorsal and anal fins, covering half to two-thirds of the fin rays (Fig. 2B).

One discontinuous dashed line of melanophores is present on the body midline over the notochord extending from the posterior region of the brain to the posterior third of the postabdominal region. A second solid dark line is observed down the midline of the body over the notochord from the posterior of the brain towards the end of the third dorsal band (Fig. 2B).

Clusters of small star-shaped melanophores are present near the anteriormost section of this series and another group between the first and second dorsal bands. Additionally, small star-shaped melanophores form an inverse 'Y' between the second and third dorsal bands; this group of pigments extends from the base of dorsal-fin rays 46 and 47 toward the first ventral band, where it forks near the midline of the body but never reaches the base of the anal fin.

The pigmentation in the cephalic region increases dramatically during the transformation to the juvenile stage especially on the dorsal margin of the head, around the eyes, and ventrally in the branchial and pelvic region (Fig. 2B). On the stomach, four groups of star-shaped melanophores are present on the anterodorsal section, the posterodorsal section, the posteroventral section and the near pelvic-fin base (Fig. 2B).

**Unpaired fin development** In early preflexion larvae, the dorsal, anal, and caudal fin folds are wide and distinct. The dorsal fin fold begins behind the brain area (Fig. 1A). In larger, preflexion larvae, the first three dorsal fin rays are inserted at the level of the posterior margin of the brain (Fig. 1B). In flexion larvae, the second, third, and fourth dorsal fin rays are elongate and almost all specimens have all the rays in dorsal and anal fins formed. The caudal fin is incomplete, with only three or four rays (Fig. 1C). In postflexion larvae by 18 mm BL, all unpaired fins are completely formed (Fig. 2A).

**Paired fin development** From the preflexion to postflexion stages, the pectoral fins are fanlike, and have a massive fin lobe and surrounding membrane. During the flexion stage, the pelvic fins become apparent, but are not well developed and contain only the rudiments of four rays. In postflexion larvae, the pelvic fin rays are completely formed (Fig. 2A). During the juvenile stage, the pectoral fins are absorbed (Fig. 2B).

## Discussion

Tonguefishes of the central-eastern Pacific are placed in a single genus (*Symphurus*) comprising 18 species. Previous studies have indicated the problems for identification of *Symphurus* species with overlapping meristic and morphometric characteristics and there have been few taxonomic studies of this genus. Insertion patterns of dorsal pterygiophores between dorsal neural spines (ID pattern) have proved to be useful in identifying members of this complex group if the ID pattern is combined with traditional meristic and morphometric characteristics (Munroe, 1992; Munroe et al., 1995).

The pigmentation pattern in early preflexion larvae of *S. oligomerus* is similar to that found in preflexion larvae (6.5 mm BL) of *S. atricaudus* (Charter and Moser, 1996) and *S. williamsi* (2.2 mm BL) by Aceves et al. (1999). However, *S. atricaudus* has up to four blotches on the dorsal and anal finfolds and *S. williamsi* has three melanophores along the dorsal margin of the body, two or three melanophores on the dorsal finfold, three melanophores along the ventral margin of the body, and one or two similar melanophores on the anal finfold. At this stage, it is not possible to distinguish the pigmentation patterns of early preflexion larvae of *S. callopterus* (Evseenko, 1990), *S. elongatus* (Charter and Moser, 1996), *S. chabanaudi* and *S. prolatinaris* (Evseenko and Shtaut, 2000), and *S. atramentatus* (Saldierna-Martínez et al., 2005) because the required diagnostic information is unavailable in the literature.

The pigmentation pattern in flexion larvae of *S. oligomerus* typically is composed of three oblique bands beginning in the dorsal margin of the body and running toward to the midline of the body. Only the third band reaches the mid line of the body. There is an oblique band on the ventral margin converging at the lateral midline with the third band of the dorsal margin and these two together have the appearance of a belt (Fig. 1C). This type of pigmentation is very similar to that described for flexion larvae of *S. callopterus* (7.5 mm SL), but *S. callopterus* has one more oblique band than *S. oligomerus*, which also has a larger abdominal projection (Evseenko, 1990).

All larvae *Symphurus* species from the eastern Pacific that have been described can be placed into three main groups based on pigmentation patterns (Saldierna-Martínez et al., 2005): 1) those with blotches on the dorsal and ventral margins of the body, such as *S. elongatus* (Charter and Moser, 1996), *S. williamsi* (Aceves et al., 1999), *S. chabanaudi*, and *S. prolatinaris* (Evseenko

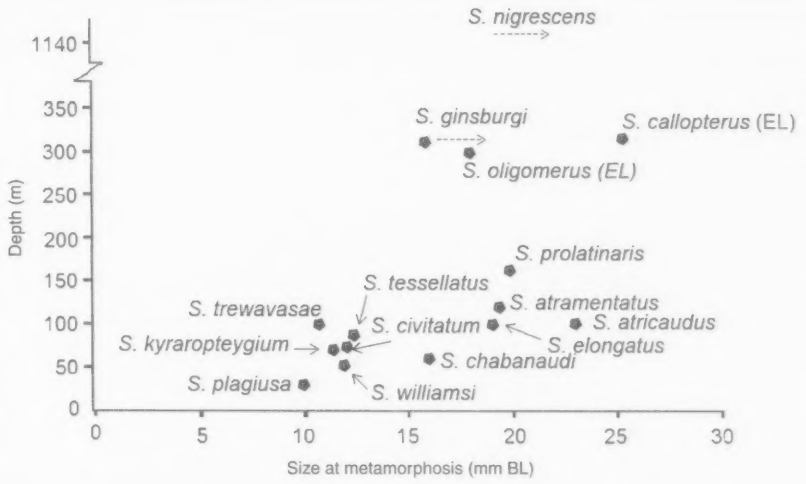


**Figure 3**

Size at metamorphosis recorded for species of *Symphurus* plotted against maximum depth distribution for adults of the same species. Arrows indicate that metamorphosis should occur at larger size because data in the graphic for these two species correspond to the largest postflexion larva described (source: Kyle, 1913; Evseenko, 1990; Schneider, 1990; Kurtz and Matsuura, 1994; Munroe et al., 1995; Munroe, 1998; Aceves et al., 1999; Evseenko and Shtaut, 2000; Saldierna-Martínez et al., 2005; Farooqi et al,. 2006; Fahay, 2007). EL=exterilium larvae.

and Shtaut, 2000); 2) those with a discontinuous series of dash-like melanophores on the dorsal and ventral margins of the body, such as *S. atricaudus* (Charter and Moser, 1996) and *S. atramentatus* (Saldierna-Martínez et al., 2005); and 3) those with heavily pigmented oblique bands extending from the dorsal to the ventral margins of the body, such as occurs in *S. callopterus* (Evseenko, 1990) and *S. oligomerus* (this study).

In addition to the three groups categorized by pigment patterns, Saldierna-Martínez et al. (2005) categorized *Symphurus* spp. larvae by the number of elongate dorsal-fin rays and the ID pattern as 1) those with 0–3 elongate dorsal-fin rays and the 1-5-3 ID pattern; 2) those with 5 elongate dorsal-fin rays and the 1-3-3 ID pattern; and 3) those with 7 elongate dorsal-fin rays and the 1-4-3 ID pattern. Saldierna-Martínez et al. (2005) suggested that the number of elongate dorsal-fin rays is a derived character, as was also suggested by Hensley and Ahlstrom (1984). Our study showed that the three elongate dorsal-fin rays in *S. oligomerus* are associated with the 1-3-2 ID pattern, which does not correspond to previously established findings and indicates a high variability for this characteristic, thus reducing its value for phylogenetic interpretation among cynoglossids.

Larvae of *S. oligomerus* have a slightly compressed and ribbonlike body. The intestine, similar to that of *S. callopterus*, is an elongate and relatively slender sac with transparent walls that form a short and freely hanging abdominal projection ending in a short conical appendix. The length of the intestinal sac is almost one-quarter of the body length and is shorter than that in *S. callopterus*, which is almost one-half to two-thirds of the body length. In both species, the intestinal sac is supported by three cartilages. Larvae with this kind of intestine have been called exterilium larvae (Fraser and Smith, 1974; Moser, 1981); they are found in *S. callopterus*, at 7.5–21 mm SL, (Evseenko, 1990), and in some ophidiiform larvae (Gordon et al., 1984) that have a well-developed coracoid process (Fahay and Nielsen, 2003; Okiyama and Yamaguchi, 2004). The length of the loop intestine and the exterilium support of the intestinal tract in *S. oligomerus* and *S. callopterus* are useful features for differentiateing them from other central-eastern Pacific species of *Symphurus*.

An ontogenetic relationship within this genus is the apparent connection between size at metamorphosis and the depth range of adults. Saldierna-Martínez et al. (2005) found that species inhabiting deep waters usually are larger at metamorphosis than species inhabiting shallow waters. This relationship has been observed in several groups of fishes (Moser, 1981). It appears that species of *Symphurus* are not an exception (Fig. 3). At metamorphosis, *S. oligomerus* is 18 mm BL and adults inhabit waters down to 300 m (Mahadeva and Munroe, 1990; Munroe et al., 1995). In the Atlantic Ocean, *S. nigrescens* has been collected over an extensive vertical range (47–1140 m) on the

continental shelf and upper continental slope (Munroe, 1990) and the largest described larva of *S. lactea* (=*S. nigrescens*) is 8 mm NL (Kyle, 1913), indicating that size at metamorphosis should be bigger than 18 mm. In general, all species of *Symphurus* that inhabit depths below 300 m have the conical appendix at the end of the abdominal projection and at least two of them have exterilium larvae (Fig. 3). Descriptions by *S. ginsburgi* (Kurtz and Matsuura, 1994) and *S. nigrescens* do not mention whether they have exterilium larvae, but the shape of the intestine and the conical process would indicate so.

Exterilium larvae are found in several phylogenetically unrelated taxa (Ahlstrom et al., 1984). Species with exterilium larvae are hypothesized to benefit in several ways: 1) an increase in the length and surface area of the gut greatly enhances digestion in oligotrophic environments (Moser 1981); 2) the exterilium projection protects against predators because pigment patterns and the physical structure of this feature mimic siphonophores or poisonous coelenterates (Fraser and Smith, 1974; Moser, 1981; Gordon et al., 1984); and 3) the free intestinal loop acts as a specialized structure that prolongs pelagic life (Moser, 1981).

## Acknowledgments

G.A.M. was supported by fellowships from Sistema Nacional de Investigadores and G.A.M. and R.S.M. by grants from Comisión de Operación y Fomento de Actividades Académicas and Estímulo al Desempeño de Investigación. The project was funded with grants from Centro Interdisciplinario de Ciencias Marinas-Instituto Politécnico Nacional, Secretaría de Investigación y Posgrado (SIP 20080918 and SIP 20090303), Consejo Nacional de Ciencia y Tecnología (FOSEMARNAT 2004-01-144 y SAGARPA 2007-117), y Comisión Nacional para el uso de la Biodiversidad (CONABIO-EC012). We thank Carlos Robinson and Instituto de Ciencias del Mar y Limnología at the Universidad Nacional Autónoma de México for their facilities to collect the zooplankton samples in the Gulf of California, as well as Thomas Munroe and all reviewers for their useful comments.

## Literature cited

Aceves M. G., E. González, and R. J. Saldierna.
1999. Larval development of *Symphurus williamsi* (Cynoglossidae: Pleuronectiformes) from the Gulf of California. Fish. Bull. 97:738–745.

Ahlstrom, E. H.
1976. Maintenance of quality in fish eggs and larval collected during plankton hauls. *In* Zooplankton fixation and preservation (H. F. Steedman, ed.), p. 313–318. UNESCO Press, Paris.

Ahlstrom, E. H., K. Amaoka, D. A. Hensley, H. G. Moser, and B. Y. Sumida.
1984. Pleuronectiformes: Development. *In* Ontogeny and systematics of fishes (H. G. Moser, W. J. Richards, D. M. Cohen, M. P. Fahay, A. W. Kendall, and S. L. Richardson, eds.), p. 640–670. Allen Press Inc., Lawrence, KS.

Charter, S. R., and H. G. Moser.
1996. Cynoglossidae: tonguefishes. *In* The early stages of fishes in the California Current region. CalCOFI Atlas 33 (H. G. Moser, ed.), p. 1408–1413. Allen Press, Inc., Lawrence, KS.

Evseenko, S. A.
1990. Unusual larvae of the marine tonguefish, *Symphurus* sp. (Cynoglossidae), from central waters of the eastern Pacific. J. Ichthyol. 30:148–154.

Evseenko, S. A., and M. I. Shtaut.
2000. Early stage of development of two species of tongue sole *Symphurus chabanaudi* and *Symphurus prolatinaris* (Cynoglossidae, Pleuronectiformes) from central eastern Pacific. J. Ichthyol. 40:751–761.

Fahay M. P.
2007. Early stage of fishes in the western North Atlantic Ocean (Davis Strait, Southern Greenland and Flemish Cap to Cape Hatteras). Vol. 2: Scorpaeniformes through Tetraodontiformes, p. 932–1696. Northwest Atl. Fish. Org., Nova Scotia.

Fahay, M. P., and J. G. Nielsen.
2003. Ontogenetic evidence supporting a relationship between *Brotulotaenia* and *Lamprogrammus* (Ophidiiformes: Ophidiidae) based on the morphology of exterilium and rubaniform larvae. Ichthyol Res. 50:209–220.

Farooqi T. W., R. F. Shaw, J. G. Ditty, and J. Lyczkowski-Shultz.
2006. Cynoglossidae: Tongue fishes, vol. II. *In* Early stages of Atlantic fishes: an identification guide for the western central North Atlantic (W. J. Richards, ed.), p. 2367–2379. CRC Press, Boca Raton, FL.

Fraser, T. H., and M. M. Smith.
1974. An exterilium larval fish from South Africa with comments on its classification. Copeia 1974:886–892.

Gordon, D. J., D. F. Markle, and J. E. Olney.
1984. Ophidiiformes: Development and relationships. *In* Ontogeny and systematics of fishes (H. G. Moser, W. J. Richards, D. M. Cohen, M. P., Fahay, A. W. Kendall Jr., and S. L. Richardson, eds.), p. 308–319. Allen Press, Inc., Lawrence, KS.

Hensley, D. A., and E. H. Ahlstrom.
1984. Pleuronectiformes: Relationships. *In* Ontogeny and systematics of fishes (H. G. Moser, W. J. Richards, D. M. Cohen, M. P., Fahay, A. W. Kendall Jr., and S. L. Richardson, eds.), p. 670–687. Allen Press, Inc., Lawrence, KS.

Kramer, D., M. J. Kalin, E. G. Stevens, J. R. Thrailkill, and J. R. Zweifel.
1972. Collecting and processing data from fish eggs and larvae in the California Current region. NOAA Tech. Rep. NMFS 370, 38 p.

Kurtz, F. W., and Y. Matsuura
1994. Early development of four tonguefishes of the genus *Symphurus* (Osteichthyes: Cynoglossidae) from the Southern Brazil. Japan. J. Ichthyol. 41(2):141–148.

Kyle, H. M.
1913. Flat-fish (Heterosomata). Rep. Dan. Oceanogr. Exped. Mediterr. 2(A):1–150.

Mahadeva N., and T. A. Munroe.
1990. Three new species of symphurine tonguefishes from tropical and warm temperate waters of the eastern Pacific (*Sumphurus*: Cynoglossidae: Pleuronectiformes). Proc. Biol. Soc. Wash. 103:931–954.

Moser, H. G.
1981. Morphological and functional aspects of marine fish larvae. *In* Marine fish larvae: morphology, ecology and relation to fisheries (R. Lasker, ed.), p. 89–131. Univ. Washington Press, Seattle.
1996. The early stages of fishes in the California Current region. CALCOFI Atlas 33, 1505 p. Allen Press, Inc., Lawrence, KS.
Munroe, T. A.
1990. Eastern Atlantic tonguefishes (*Symphurus*: Cynoglossidae, Pleuronectiformes), with descriptions of two new species. Bull. Mar. Sci. 47(2):464–515.
1992. Interdigitation pattern of dorsal-fin pterygiophores and neural spines, an important diagnostic character for symphurine tonguefishes (*Symphurus*: Cynoglossidae: Pleuronectiformes). Bull. Mar. Sci. 50:357–403.
1998. Systematics and ecology of tonguefishes of the genus *Symphurus* (Cynoglossidae: Pleuronectiformes) from the western Atlantic Ocean. Fish. Bull. 96:1–182.
Munroe, T. A., F. Krupp, and M. Schneider.
1995. Cynoglossidae. *In* Guia FAO para la identificación de especies para los fines de la pesca. Pacifico Centro-Oriental, vol. 2: Vertebrados-Parte 1 (W. Fischer, F. Krupp, W. Schneider, K. Carpenter, C. Summer, and V. Niem eds.), p. 1039–1059. FAO, Rome.
Munroe, T. A., and J. E. McCosker.
2001. Redescription of *Symphurus diabolicus*, a poorly-known, deep-sea tonguefish (Pleuronectiformes: Cynoglossidae) from the Galápagos Archipelago. Rev. Biol. Trop. 49(suppl. 1):187–198.
Munroe, T. A., and D. R. Robertson.
2005. *Symphurus ocellaris*, a new shallow-water symphurine tonguefish collected off Pacific Panama (Pleuronectiformes: Cynoglossidae). Proc. Biol. Soc. Wash. 118(3):576–581.
Okiyama, M., and M. Yamaguchi.
2004. A new type of exterilium larva referable to *Leptobrotula* (Ophidiiformes: Ophidiidae: Neobythitinae) from tropical Indo-West Pacific. Ichthyol. Res. 51:77–80.
Potthoff, T.
1984. Clearing and staining techniques. *In* Ontogeny and systematics of fishes (H. G. Moser, W. J. Richards, D. M. Cohen, M. P., Fahay, A. W. Kendall Jr., and S. L. Richardson, eds.), p. 35–37. Allen Press, Inc., Lawrence, KS.
Saldierna-Martínez, R. J., E. A. González-Navarro, and G. Aceves-Medina.
2005. Larval development of *Symphurus atramentatus* (Cynoglossidae: Pleuronectiformes) from the Gulf of California. Zootaxa 1016:1–14.
Schneider, W.
1990. FAO species identification sheets for fishery purposes. Field guide to the commercial marine resources of the Gulf of Guinea. FAO, Rome.

**Abstract**—Diet, gastric evacuation rates, daily ration, and population-level prey demand of bluefin tuna (*Thunnus thynnus*) were estimated in the continental shelf waters off North Carolina. Bluefin tuna stomachs were collected from commercial fishermen during the late fall and winter months of 2003–04, 2004–05, and 2005–06. Diel patterns in mean gut fullness values were used to estimate gastric evacuation rates. Daily ration determined from mean gut fullness values and gastric evacuation rates was used, along with bluefin tuna population size and residency times, to estimate population-level consumption by bluefin tuna on Atlantic menhaden (*Brevoortia tyrannus*). Bluefin tuna diet ($n$=448) was dominated by Atlantic menhaden; other teleosts, portunid crabs, and squid were of mostly minor importance. The time required to empty the stomach after peak gut fullness was estimated to be ~20 hours. Daily ration estimates were approximately 2% of body weight per day. At current western Atlantic population levels, bluefin tuna predation on Atlantic menhaden is minimal compared to predation by other known predators and the numbers taken in commercial harvest. Bluefin tuna appear to occupy coastal waters in North Carolina during winter to prey upon Atlantic menhaden. Thus, changes in the Atlantic menhaden stock status or distribution would alter the winter foraging locations of bluefin tuna.

Manuscript submitted 13 January 2009.
Manuscript accepted 21 October 2009.
Fish. Bull. 56–69 (2010).

The views and opinions expressed or implied in this article are those of the author (or authors) and do not necessarily reflect the position of the National Marine Fisheries Service, NOAA.

# Feeding ecology of Atlantic bluefin tuna (*Thunnus thynnus*) in North Carolina: diet, daily ration, and consumption of Atlantic menhaden (*Brevoortia tyrannus*)

**Christopher M. Butler (contact author)**
**Paul J. Rudershausen**
**Jeffrey A. Buckel**

Email address for contact author: c.m.butler@usm.edu

Department of Biology
Center for Marine Sciences and Technology
North Carolina State University
303 College Circle
Morehead City, North Carolina 28557

Present Address (for C. M. Butler): Center for Fisheries Research & Development
Gulf Coast Research Laboratory
The University of Southern Mississippi
703 East Beach Drive
Ocean Springs, Mississippi 39564

Ecosystem-based management of marine fisheries, as a complementary approach to single-species stock assessments, is now recommended (Latour et al., 2003). Ecosystem-based models incorporate ecological interactions to evaluate the potential flows of energy and biomass among interacting populations within an exploited ecosystem (Pauly et al., 2000). Some of these models allow comparisons between removals by natural predators and fisheries to help address tradeoffs (e.g., harvesting fewer prey to provide potential prey biomass for more predators) when fisheries for both predator and prey exist (Overholtz et al., 2008).

Atlantic menhaden (*Brevoortia tyrannus*) play a vital ecological role in estuarine and coastal habitats along the East Coast of the United States (Quinlan et al., 1999). From 2002 to 2006, Atlantic menhaden comprised between 27.0% to 30.5% of the total U.S. commercial landings in the Atlantic and represented one of the larger commercial fisheries in the United States (NOAA[1]). On the U.S. East Coast, there is much controversy over the Atlantic menhaden fishery and whether or not it should be reduced or shut down to prevent reductions in the availability of prey biomass. Atlantic menhaden are considered a primary forage species for several commercially and recreationally important predators including striped bass (*Morone saxatilis*), bluefish (*Pomatomus saltatrix*), and weakfish (*Cynoscion regalis*) (NEFSC[2]). In addition to these three predators, Kade (2000) found that Atlantic menhaden were a major component of Atlantic bluefin tuna (*Thunnus thynnus*, hereafter referred to as bluefin tuna) diet during one winter (1999) in North Carolina waters.

The bluefin tuna is a highly migratory pelagic species that is distributed throughout the North Atlantic Ocean. In western North Atlantic waters, bluefin tuna are found from Nova Scotia to Brazil (Block et al., 2001). Migrations are related to annual spawning and feeding events

[1] National Oceanic and Atmospheric Administration (NOAA). 2007. Annual Commercial Landing Statistics. [Available from http://www.st.nmfs.noaa.gov/st1/commercial/landings/annual_landings.html, accessed August 16, 2008.]

[2] NEFSC (Northeast Fisheries Science Center). 2006. 42nd northeast regional stock assessment workshop (42nd SAW) stock assessment report, part B: Expanded multispecies virtual population analysis (MSVPA-X) stock assessment model. U.S. Dep. Commer., Northeast Fish. Sci. Cent. Ref. Doc. 06-09b, 308 p.

(Rooker et al., 2007; Teo et al., 2007). Beginning in late November, bluefin tuna migrate into North Carolina coastal waters and feed upon local prey resources (Kade, 2000; Boustany, 2006). Atlantic menhaden aggregate off North Carolina to spawn during winter (Checkley et al., 1999) and may be the primary prey of bluefin tuna.

When compared to other teleosts, bluefin tuna have standard metabolic rates that are among the highest of any fish species (Dickson and Graham, 2004; Blank et al., 2007). These high metabolic demands require them to consume large amounts of prey. Thus, bluefin tuna have the potential to influence the abundance of other species within an ecosystem. Overholtz (2006) modeled predation demand of bluefin tuna on Atlantic herring (*Clupea harengus*) in the Northwest Atlantic during summer months. Consumption of Atlantic herring by bluefin tuna was highest in 1970, declined to a low in 1982, and increased through 2002. To our knowledge, the predatory impact of bluefin tuna on Atlantic menhaden during winter has not been examined.

Here, we describe the diets of bluefin tuna (>185 cm curved fork length) off North Carolina during winter. We also estimate field-derived gastric evacuation rates and daily ration; daily ration is used to estimate the population-level consumption of bluefin tuna on Atlantic menhaden. Lastly, we compare the population-level consumption of Atlantic menhaden by bluefin tuna with the predatory demand from other known Atlantic menhaden predators. The latter question was addressed at both current and rebuilt bluefin tuna populations to investigate predator and prey management implications.

## Materials and methods

### Study area

From 2003 to 2006, we sampled stomachs from commercially caught bluefin tuna landed in Beaufort and Morehead City, North Carolina. The fishery operated from November through January (length of season varied by year) within a 28-km radius (centered at approximately 34°26′N lat., 76°28′W long.) south of Cape Lookout shoals. Bluefin tuna were predominantly captured by trolling, where a dead-baited hook (with or without a lure) is pulled behind a moving vessel to imitate live prey. Generally, ballyhoo (*Hemiramphus brasiliensis*) was used as bait.

### Collection of samples

Bluefin tuna stomachs were collected during the winters of 2003–04 ($n$=42), 2004–05 ($n$=219), and 2005–06 ($n$=187) off the coast of North Carolina; during the first winter a pilot collection was undertaken and the results were included only in the overall diet analysis. For most bluefin tuna, stomachs and other viscera were removed at sea by the fishermen. Upon excision, all stomachs were stored on ice until they could be collected by researchers. In addition to the stomach, the fisherman was responsible for providing information on time and location of capture, curved fork length (*CFL*, cm), and dressed weight (*DW*, kg). Curved fork length was measured from the tip of the snout to the fork of the tail over the contour of the body. *DW* was obtained after the head, tail, and viscera had been removed. In instances where a *DW* was not recorded, one was estimated by using the allometric relationship of *CFL* to *DW* defined from the current study ($n$=379) as

$$DW = 7.625 \times 10^{-6} \cdot CFL^{3.088},\ r^2 = 0.871.$$

Dressed weights were converted to round weights (i.e., the total weight of a live fish; *RW*, kg) by using the regression equation ($n$=685) developed by Baglin (1980):

$$RW = -7.922 + 1.296 \cdot DW,\ r^2 = 0.874.$$

### Diet analysis

Individual stomach samples were opened and the contents placed in labeled plastic bags. Contents that could not be analyzed immediately were frozen for later analysis. All stomach contents were identified to the lowest possible taxon. Identifiable prey items were grouped by taxa and wet weight (g) was recorded. Teleosts or invertebrates that could not be identified were measured and recorded as unidentified species (e.g., "unidentified fish remains").

Diets were expressed by indices of percent frequency of occurrence (*%O*) and percent weight (*%W*) (Hyslop, 1980). Percent frequency of occurrence was calculated as the number of bluefin tuna that had ingested a specific prey item divided by the total number of bluefin tuna that contained prey. Percent weight was estimated as the total wet weight of a specific prey type divided by the total wet weight of all prey across the total number of stomachs samples.

Cumulative prey curves were constructed *a posteriori* by within-winter period (early December, late December, and January), year (2004–05 and 2005–06), and size class (large medium [individuals between 185.4 and 205.7 cm *CFL*] and giant [individuals >205.7 cm *CFL*]) to determine if the sample sizes were sufficient to describe bluefin tuna diets (Ferry and Cailliet, 1996). Prey species were grouped by family and the mean and standard deviation of the cumulative number of unique prey was calculated by randomly resampling the number of stomachs that contained prey 500 times (Bizzarro et al., 2007). The cumulative mean number of unique prey taxa calculated from randomized stomach samples was then plotted against the number of stomachs examined (Ferry and Cailliet, 1996). Sample size sufficiency for each prey curve was tested by the linear regression method (Bizzarro et al., 2007), where the slope from a regression of the mean number of unique prey items from the last four stomach samples was compared to a slope of zero (Student's $t$-test of the equality of two population regression coefficients; Zar, 1999). Sample

size sufficiency was reached if the difference between the slopes was not significantly different ($P>0.05$).

The effects of within-winter period, year, and size class on bluefin tuna diets were determined by using row×column ($R\times C$) tests of independence and using counts of stomachs with a particular prey species (Sokal and Rohlf, 1981). Prey species were grouped by family for $R\times C$ tests and degrees of freedom were calculated as (*rows*–1) (*columns*–1).

### Gastric evacuation rate and daily ration

Individual stomach fullness (kg prey/kg predator) values were highest in early afternoon and lowest during the early morning for both large medium and giant bluefin tuna. These high and low periods were used as beginning and ending points, respectively, to estimate gastric evacuation rates. Stomach fullness values were assigned to one-hour time periods (with the exception of the first and final hours when stomachs were at values before maximum and after minimum stomach fullness, respectively) to examine diel feeding patterns; data from 2004–05 ($n$=64) and 2005–06 ($n$=114) were pooled for this analysis to increase sample size. Gastric evacuation rates (*GER*) of bluefin tuna were estimated using an exponential decay model (Elliott and Persson, 1978),

$$S_t = S_0 \cdot e^{-GER \cdot t}, \quad (1)$$

where $S_t$ = the individual stomach fullness at time $t$;
$S_0$ = the stomach fullness at time $t$=0;
*GER* = the instantaneous rate of gastric evacuation (rate per hr); and
$t$ = the time in hours after peak gut fullness.

The number of fish used in this analysis was lower than the total collected because time of capture was not always provided by the fishing crew. Although other evacuation rate models have been used with tuna (e.g., linear, Olson and Boggs, 1986), we chose the exponential model because we could not test between multiple evacuation models given the gap in stomach contents data at night. Additionally, an exponential decline may better describe the evacuation rates of fish which require rapid digestion rates because of high metabolic demands (Bromley, 1994). The difference ($GER_{difference}$) between $GER_{large\ medium}$ and $GER_{giant}$ was estimated by using the nonlinear (NLIN) procedure of SAS (SAS, 1996). If the confidence interval of $GER_{difference}$ contained the value of zero then it was assumed that $GER_{large\ medium}$ and $GER_{giant}$ were not significantly different.

Daily ration (kg prey/kg predator/day) estimates of large medium, giant, and pooled bluefin tuna size classes were calculated by using the Eggers (1977) approach,

$$DR = 24 \cdot \bar{S} \cdot GER, \quad (2)$$

where $DR$ = the daily ration estimate; and
$\bar{S}$ = the mean stomach fullness of the hourly means.

For time points at which no stomachs were collected (1900–0300 Eastern Standard Time [EST]), stomach fullness values were estimated from the gastric evacuation model (described above).

### Population-level consumption

Annual population-level consumption of Atlantic menhaden by bluefin tuna during their residency in North Carolina ($C_{Pop}$) was estimated as

$$C_{Pop} = B_{BFT} \cdot P_{NC} \cdot DR \cdot W_{Mh} \cdot T_{NC}, \quad (3)$$

where $B_{BFT}$ = bluefin tuna biomass (kg);
$P_{NC}$ = proportion of the bluefin tuna population in North Carolina during the winter;
$DR$ = the estimate of bluefin tuna daily ration (kg prey/kg predator/day) in this study;
$W_{Mh}$ = the proportion by weight of Atlantic menhaden in bluefin tuna stomachs; and
$T_{NC}$ = the time (days) that bluefin tuna and Atlantic menhaden are both present in the coastal waters of North Carolina.

In order to determine the precision of $C_{Pop}$, a distribution of $C_{Pop}$ estimates was obtained by using simulation software (@RISK, vers. 5.0, Palisade Corp.). The Monte Carlo simulation approach is described in Overholtz (2006); briefly, a distribution was created for each variable in the $C_{Pop}$ equation above. Then, a random draw was made from each distribution and a new estimate of $C_{Pop}$ was made. This process was repeated 5000 times. The range of $C_{Pop}$ estimates was then compared to the range of consumption estimates previously published on other known Atlantic menhaden predators (e.g., bluefish, striped bass, weakfish, and the Atlantic Coast commercial harvest). The consumption estimates presented are annual and cover the entire U.S. East Coast. Given past bluefin tuna diet studies conducted on summer and fall feeding grounds (e.g., Chase 2002), we assume that Atlantic menhaden are not a major prey of bluefin tuna in other areas at other times of the year. Thus, our estimates off North Carolina during winter are likely indicative of the annual coastwide consumption of Atlantic menhaden by bluefin tuna.

Bluefin tuna captured in North Carolina were estimated to be predominantly age 6+ fish based on size-at-age regressions (Murray-Brown et al.[3]). The most recent (2005) population estimate was 94,836 age-6+ bluefin tuna (ICCAT, 2007). These values were coupled with individual mean weight-at-age[3] estimates to calculate the total biomass ($B_{BFT}$) of age 6+ bluefin tuna from the western Atlantic. A pert distribution of the mean, minimum, and maximum $B_{BFT}$ values was constructed by using one standard deviation below and above the

[3] Murray-Brown, M., S. McLaughlin, and C. Lopez. 2007. History of United States Atlantic bluefin tuna size class classification and changes. NOAA Fisheries Final Report, 14 p. U.S. Dep. Commerce, Silver Spring, MD.

calculated mean biomass; the assumed coefficient of variation was 30% (Overholtz, 2006).

It is unknown what proportion of the age-6+ bluefin tuna biomass occurs off North Carolina during winter. Therefore, we used data from a preliminary Ecopath model of the South Atlantic Bight which indicated that biomass levels ranged between 5% and 25% of the total age-6+ western Atlantic bluefin tuna population (Butler, 2007). A uniform distribution with this range of $P_{NC}$ values was used for the Monte Carlo simulation.

A pert distribution (Overholtz, 2006) was used to model the estimate of *DR* from the current study. Minimum and maximum estimates of *DR* were calculated as one standard deviation above and below the mean, respectively (Overholtz, 2006); the standard deviation of *DR* was calculated by the Delta method (Williams et al., 2002).

The proportion by weight of Atlantic menhaden in bluefin tuna diet ($W_{Mh}$) was modeled by a uniform distribution where the minimum and maximum values were the lowest and highest $W_{Mh}$ values observed annually in this and Kade's (2000) study. A uniform distribution was chosen because it allows an equal probability of occurrence for the estimated proportion by weight value (i.e., $W_{Mh}$) between the minimum and maximum observed values.

The maximum number of days ($T_{NC}$) that both Atlantic menhaden and bluefin tuna overlap in North Carolina is unknown. Adult Atlantic menhaden form large spawning congregations in the shelf waters off North Carolina from November through March (Checkley et al., 1999). Bluefin tuna are commercially harvested off North Carolina beginning in late November until the end of January. However, Boustany (2006) has shown that bluefin tuna fitted with pop-up satellite tags may extend their residency in these waters until late May. Thus, the maximum $T_{NC}$ was assumed to be 120 days (i.e., late November through late March) and a minimum was chosen arbitrarily at 30 days. A uniform distribution covering this range was used for the simulations.

To fully restore the western Atlantic bluefin tuna population, the International Commission for the Conservation of Atlantic Tunas (ICCAT) has recommended a targeted biomass level equivalent to that in 1975 (ICCAT, 2007). Thus, a new distribution of $C_{Pop}$ for a "restored" population was determined by using abundance-at-age data from 1975 for age-6+ bluefin tuna to calculate a new distribution of $B_{BFT}$. All other distributions for the "restored" analysis were identical to the distributions used for the current population model.

## Results

### Diet analysis

The stomach contents of 448 bluefin tuna were examined. Of these, 124 (100 nonempty) were large medium and 324 (252 nonempty) were giant tuna. Samples were further categorized by year and within-winter time period (i.e., 1–14 December, 15–31 December, and 1–31 January). The two December time periods were chosen because of good sample sizes throughout December and perceived changes in diets within that month. January was not split into two time periods because most January fish were caught within the first two weeks of the month during each year of the study.

Overall, stomachs of bluefin tuna contained fourteen families of teleosts, five species of portunid crabs, cephalopods (mainly *Loligo pealeii*), one species of elasmobranch (*Mustelus canis*), and unidentified algae. Atlantic menhaden (*Brevoortia tyrannus*) was the most common prey item by %*O* for both large medium (Table 1) and giant bluefin tuna (Table 2). By weight, Atlantic menhaden similarly dominated the diets of both size classes (Tables 1 and 2). Although Atlantic needlefish (*Strongylura marina*) were not important to large medium bluefin tuna, they were the second most identifiable prey item of giants (7.14% *O*, 3.16% *W*), mainly in one year (2005–06). Despite the occurrence of individual portunids and cephalopods in both size classes, they contributed little in terms of biomass. Other prey included several teleost species, elasmobranchs, bivalves, and algae that were rare items and that contributed little to the diet.

Sample sizes were adequate to describe the within-winter diet of giant bluefin tuna, as well as between winters for both size classes and size class comparisons. All within-winter periods for giant bluefin tuna, with the exception of January 2006, reached an asymptote (Table 3). Both large medium and giant size classes reached asymptotes when data were pooled by winter (Table 3). However, the within-winter analyses of large medium bluefin tuna were likely biased because of the low sample sizes. Randomized cumulative prey curves did not reach an asymptote for any of the within-winter periods for large medium bluefin tuna (Table 3). Given the difficulty in collecting large numbers of stomachs over short periods, the lack of a defined asymptote is not uncommon in diet studies of other apex species (Bethea et al., 2004).

Atlantic menhaden was the dominant prey of large medium bluefin tuna throughout the winter in both years (Fig. 1, A and B). Diets of large medium bluefin tuna were independent of within-winter time period (Table 4). Although Atlantic menhaden varied in importance, variability in other prey groups (e.g., portunids, teleosts) likely drove the within-winter effect of the giant size class (Fig. 2, A and B; Table 4). The diets of large medium bluefin tuna were dominated by Atlantic menhaden in both winters (Fig. 1C; Table 4). The diet of giant bluefin tuna did differ between years (Table 4) owing to the increased occurrence of Atlantic needlefish and cephalopods in 2005–06 (Fig. 2C). Overall, the two size classes differed in diets (Table 4). This result was likely driven by the higher occurrence of non-Atlantic menhaden prey types in giants than in large medium bluefin tuna (Figs. 1C and 2C).

**Table 1**

Stomach contents of large medium (185.4–205.7 cm curved fork length [CFL]) Atlantic bluefin tuna (*Thunnus thynnus*) caught off Cape Lookout, North Carolina, during Dec. 2003–Jan. 2004, Dec. 2004–Jan. 2005, and Dec. 2005–Jan. 2006. Diet is presented as percent frequency of occurrence (%*O*) and percent prey weight (%*W*).

| | Dec. 2003–Jan. 2004 | | Dec. 2004–Jan. 2005 | | Dec. 2005–Jan. 2006 | | Pooled years | |
|---|---|---|---|---|---|---|---|---|
| Prey item | %*O* | %*W* | %*O* | %*W* | %*O* | %*W* | %*O* | %*W* |
| Chordata | | | | | | | | |
| *Brevoortia tyrannus* | 76.92 | 89.41 | 96.88 | 98.97 | 82.61 | 96.43 | 91.00 | 98.42 |
| *Menticirrhus littoralis* | | | | | 4.35 | 1.45 | 1.00 | 0.24 |
| *Mugil cephalus* | | | 1.56 | 0.69 | | | 1.00 | 0.57 |
| *Pomatomus saltatrix* | | | 1.56 | 0.17 | | | 1.00 | 0.14 |
| *Strongylura marina* | | | | | 4.35 | 0.13 | 1.00 | 0.02 |
| Unidentified fish remains | 30.77 | 6.78 | 4.69 | 0.05 | 13.04 | 0.33 | 10.00 | 0.19 |
| Crustacea | | | | | | | | |
| *Ovalipes* sp. | | | | | 4.35 | 0.19 | 1.00 | 0.03 |
| *Portunus gibbesii* | | | 1.56 | 0.02 | | | 1.00 | 0.01 |
| *Portunus spinimanus* | | | 1.56 | 0.05 | 4.35 | 0.28 | 2.00 | 0.09 |
| *Portunus* spp. | | | | | 4.35 | 0.04 | 1.00 | 0.01 |
| Unidentified crab | 7.69 | 1.91 | 1.56 | 0.01 | 4.35 | 0.04 | 3.00 | 0.04 |
| Mollusca | | | | | | | | |
| *Loligo pealeii* | | | 1.56 | 0.04 | 8.70 | 1.11 | 1.00 | 0.03 |
| Unidentified squid | 7.69 | 0.02 | | | | | 3.00 | 0.18 |
| Protista | | | | | | | | |
| Unidentified algae | 15.38 | 1.87 | | | | | 2.00 | 0.03 |
| Total prey biomass (kg) | 1.45 | | 83.04 | | 16.37 | | 100.86 | |
| Total stomachs sampled | 14 | | 80 | | 30 | | 124 | |
| Stomachs with prey (%) | 13 (92.9) | | 64 (80.0) | | 23 (76.7) | | 100 (80.6) | |
| Empty stomachs (%) | 1 (7.1) | | 16 (20.0) | | 7 (23.3) | | 24 (19.4) | |
| Mean length of bluefin tuna (cm) | 198.57 | | 194.59 | | 197.18 | | 195.66 | |
| Standard error | 1.27 | | 0.62 | | 1.14 | | 0.52 | |
| Mean weight of bluefin tuna (kg) | 119.02 | | 108.66 | | 113.03 | | 110.89 | |
| Standard error | 2.89 | | 1.72 | | 3.03 | | 1.40 | |

When examined by %*W*, diets were almost always dominated by Atlantic menhaden (Fig. 1, D–F and Fig. 2, D–F). The only exception was the 1–14 December 2005 within-winter period when Atlantic needlefish accounted for approximately 60% of diet by weight for giant tuna. When pooled, diets varied little between winters (for either large medium or giant bluefin tuna) or between size classes (Figs. 1F and 2F).

### Gastric evacuation rates and daily ration

During winter in North Carolina, large medium and giant bluefin tuna appear to feed predominantly during diurnal time periods (Fig. 3, A and B). A small number of fish were caught on trolled baits several hours before sunrise, and those stomachs collected during presunrise hours were typically empty or contained food in the final stages of digestion (e.g., scales, bones, eye lenses, and pyloric stomachs of Atlantic menhaden), indicating that digestion occurred throughout the night and that feeding had not resumed until just before sunrise. Sample sizes for each size class were largest after sunrise (approximately 0700 EST) and remained high throughout the morning as gut fullness increased. Large medium bluefin tuna reached maximum gut fullness between 1200 and 1300 EST (time point zero on Fig. 3A). The estimate of *GER* (±standard error [SE]) for the large medium bluefin tuna size class was 0.13 ±0.05/hr. Giant bluefin tuna attained a maximum gut fullness between 1300 and 1400 EST (time point zero on Fig. 3B), and had a *GER* (±SE) of 0.12 ±0.04/hr. The confidence interval of $GER_{difference}$ contained the value of zero, and therefore there was no significant difference between $GER_{large\ medium}$ and $GER_{giant}$. Thus, a combined (large medium and giant) *GER* value (Fig. 3C) was used to estimate *DR*. The *GER* (±SE) was 0.12 ±0.03/hr for the combined analysis (Fig. 3C).

The mean (±SE) *DR* estimate of bluefin tuna in NC was 2.03% ±0.59. When multiplied by the mean weight of bluefin tuna collected during our study, the absolute daily consumption by an individual bluefin tuna in North Carolina during winter was 3.18 kg/day.

**Table 2**

Stomach contents of giant (>205.7 cm curve fork length [CFL]) Atlantic bluefin tuna (*Thunnus thynnus*) caught off Cape Lookout, North Carolina, during Dec. 2003–Jan. 2004, Dec. 2004–Jan. 2005, and Dec. 2005–Jan. 2006. Diet is presented as percent frequency of occurrence (%*O*) and percent prey weight (%*W*).

| | Dec. 2003–Jan. 2004 | | Dec. 2004–Jan. 2005 | | Dec. 2005–Jan. 2006 | | Pooled years | |
|---|---|---|---|---|---|---|---|---|
| Prey item | %*O* | %*W* | %*O* | %*W* | %*O* | %*W* | %*O* | %*W* |
| Chordata | | | | | | | | |
| *Ammodytes* sp. | | | 1.00 | 0.01 | | | 0.79 | <0.01 |
| *Anchoa hepsetus* | | | 1.00 | 0.01 | 0.73 | <0.01 | 0.79 | <0.01 |
| *Archosargus* sp. | | | 1.00 | 0.11 | 2.19 | 0.11 | 1.59 | 0.11 |
| *Brevoortia tyrannus* | 60.00 | 91.39 | 84.00 | 98.96 | 83.21 | 92.97 | 82.54 | 94.71 |
| *Chilomycterus* sp. | | | | | 1.46 | 0.07 | 0.79 | 0.04 |
| *Cynoscion regalis* | | | | | 1.46 | 0.46 | 0.79 | 0.31 |
| *Diapterus auratus* | 6.67 | 1.78 | | | | | 0.40 | 0.04 |
| Engraulidae | 6.67 | 0.16 | | | | | 0.40 | <0.01 |
| *Lagodon rhomboides* | | | | | 0.73 | 0.05 | 0.40 | 0.03 |
| *Micropogonias* sp. | | | | | 0.73 | 0.04 | 0.40 | 0.03 |
| *Mustelus canis* | | | | | 0.73 | 0.16 | 0.40 | 0.11 |
| *Orthopristis chrysoptera* | | | | | 2.19 | 0.04 | 1.19 | 0.03 |
| *Pomatomus saltatrix* | | | | | 0.73 | 0.01 | 0.40 | 0.01 |
| *Sphyraena borealis* | | | | | 0.73 | 0.04 | 0.40 | 0.02 |
| *Strongylura marina* | | | 1.00 | 0.01 | 12.41 | 4.61 | 7.14 | 3.16 |
| *Syngnathus louisianae* | | | 1.00 | 0.01 | | | 0.40 | <0.01 |
| *Syngnathus* sp. | | | | | 0.73 | <0.01 | 0.40 | <0.01 |
| Triglidae | 6.67 | 0.52 | | | | | 0.40 | 0.01 |
| Unidentified fish remains | 40.00 | 0.74 | 14.00 | 0.09 | 15.33 | 0.34 | 15.87 | 0.27 |
| Crustacea | | | | | | | | |
| *Callinectes sapidus* | 6.67 | 0.17 | | | | | 0.40 | <0.01 |
| *Ovalipes* sp. | 13.33 | 0.37 | 3.00 | 0.16 | 3.65 | 0.04 | 3.97 | 0.08 |
| Portunidae | 6.67 | 0.10 | 6.00 | 0.17 | 0.73 | <0.01 | 3.17 | 0.05 |
| *Portunus gibbesii* | 13.33 | 4.28 | 8.00 | 0.15 | 7.30 | 0.15 | 9.13 | 0.24 |
| *Portunus spinimanus* | 6.67 | 0.33 | 4.00 | 0.09 | 2.92 | 0.05 | 3.57 | 0.07 |
| *Portunus* spp. | | | 1.00 | 0.02 | 7.30 | 0.07 | 4.37 | 0.05 |
| Unidentified crab | 13.33 | 0.12 | 6.00 | 0.08 | 3.65 | 0.02 | 5.16 | 0.04 |
| Mollusca | | | | | | | | |
| *Loligo pealeii* | | | 2.00 | 0.07 | 2.19 | 0.48 | 1.98 | 0.35 |
| Unidentified squid | | | | | 8.03 | 0.30 | 4.37 | 0.20 |
| Unidentified clam | | | 1.00 | 0.06 | | | 0.40 | 0.02 |
| Protista | | | | | | | | |
| Unidentified algae | 6.67 | 0.03 | 1.00 | <0.01 | 0.73 | 0.01 | 1.19 | 0.01 |
| Total prey biomass (kg) | 7.54 | | 106.23 | | 245.43 | | 359.20 | |
| Total stomachs sampled | 28 | | 139 | | 157 | | 324 | |
| Stomachs with prey (%) | 15 (53.6) | | 100 (71.9) | | 137 (87.3) | | 252 (77.8) | |
| Empty stomachs (%) | 13 (46.4) | | 39 (28.1) | | 20 (12.7) | | 72 (22.2) | |
| Mean length of bluefin tuna (cm) | 217.56 | | 223.14 | | 225.92 | | 224.01 | |
| Standard Error | 1.89 | | 0.93 | | 1.12 | | 0.71 | |
| Mean weight of bluefin tuna (kg) | 155.12 | | 172.09 | | 179.17 | | 174.66 | |
| Standard Error | 5.25 | | 2.70 | | 3.37 | | 2.08 | |

### Population-level consumption

Using bluefin tuna abundance data from 2005, we estimated that $C_{Pop}$ ranged from 189 to 13,385 metric tons (t) (mean=3,021 t; Fig. 4A). For a completely restored bluefin tuna population, estimates ranged from 986 to 42,858 t (mean=10,020 t; Fig. 4B). At 2005 population levels, the maximum estimate of $C_{Pop}$ was below the majority of estimates of annual predatory demand by other predators of Atlantic menhaden; other predators were bluefish, striped bass, and weakfish (Fig. 5). However, the maximum estimate of $C_{Pop}$ by a fully restored

**Table 3**

Results from randomized cumulative prey curves for large medium and giant bluefin tuna (*Thunnus thynnus*) collected off Cape Lookout, North Carolina, during the 2004–05 and 2005–06 season. Values in bold indicate sufficient sample sizes to describe bluefin tuna diet at $\alpha$=0.05. Sample sizes ($n$), sampling statistics ($t$), and $P$-values are presented.

| Large medium | $n$ | $t$ | $P$-value | Giant | $n$ | $t$ | $P$-value |
|---|---|---|---|---|---|---|---|
| 2004–05 | | | | 2004–05 | | | |
| 1–14 Dec. | 20 | 56.003 | <0.001 | 1–14 Dec. | **16** | **2.152** | **0.164** |
| 15–31 Dec. | 40 | 5.061 | 0.037 | 15–31 Dec. | **57** | **4.042** | **0.056** |
| 1–31 Jan. | 4 | 5.590 | 0.031 | 1–31 Jan. | **27** | **3.839** | **0.062** |
| Pooled data | **64** | **0.965** | **0.435** | Pooled data | **100** | **2.541** | **0.126** |
| 2005–06 | | | | 2005–06 | | | |
| 1–14 Dec. | 8 | 8.914 | 0.012 | 1–14 Dec. | **24** | **3.891** | **0.060** |
| 15–31 Dec. | 10 | 20.350 | 0.002 | 15–31 Dec. | **87** | **2.460** | **0.133** |
| 1–31 Jan. | 5 | 6.699 | 0.022 | 1–31 Jan. | 26 | 10.298 | 0.009 |
| Pooled data | **23** | **3.888** | **0.060** | Pooled data | **137** | **–0.440** | **0.703** |

bluefin tuna population fell within the ranges of predatory demand of these other predators (Fig. 5). None of the consumption estimates of natural Atlantic menhaden predators approached the annual harvest from the commercial fishery.

**Table 4**

Chi-square values for comparisons of the effects of within-winter, year, and size class on dietary composition of Atlantic bluefin tuna (*Thunnus thynnus*) collected off Cape Lookout, North Carolina, during 2004–05 and 2005–06 as determined by $R \times C$ tests of independence (Sokal and Rohlf, 1981) of frequency (count) data. Degrees of freedom were calculated as (*rows*–1)(*columns*–1). Within-winter time periods (D1=1–14 December; D2=15–31 December; and J=1–31 January) and years were compared for each size class (large medium and giant tuna) from both years. The total number of nonempty stomachs analyzed for each comparison is given within parentheses.

| Groups compared | $\chi^2$ value | Degrees of freedom | $P$-value |
|---|---|---|---|
| Within-winter | | | |
| Large medium tuna | | | |
| D1 / D2 / J 2004–05 (64) | 10.864 | 10 | 0.210 |
| D1 / D2 / J 2005–06 (23) | 11.140 | 10 | 0.347 |
| Giant tuna | | | |
| D1 / D2 / J 2004–05 (100) | 16.182 | 14 | 0.303 |
| D1 / D2 / J 2005–06 (137) | 51.976 | 14 | <0.001 |
| Year | | | |
| Large medium tuna | | | |
| 2004–05 / 2005–06 (87) | 9.570 | 5 | 0.088 |
| Giant tuna | | | |
| 2004–05 / 2005–06 (237) | 19.736 | 8 | 0.011 |
| Size class | | | |
| Large medium /Giant (352) | 15.637 | 8 | 0.048 |

## Discussion

### Importance of Atlantic menhaden to bluefin tuna

Atlantic menhaden was the primary prey for both large medium and giant bluefin tuna during multiple winters in North Carolina; this focus on a single prey type is unusual for a marine apex predator. Although other prey were frequently present (e.g., portunid crabs), they contributed little in terms of biomass. With the exception of Kade (2000), Atlantic menhaden has not been considered a dominant prey of bluefin tuna along the U.S. East Coast (Chase, 2002). Kade's (2000) result for 1999 and now our results for subsequent years have confirmed that bluefin tuna are a consistent and potentially important predator of Atlantic menhaden during winter. Although these are the first quantitative studies to identify this predator-prey linkage, historic anecdotal information described bluefin tuna feeding on schools of Atlantic menhaden off New England in the 1800s (Goode, 1879).

The composition of bluefin tuna diet depends on prey availability and predator body size (Chase, 2002). In North Carolina, diets of large medium and giant bluefin tuna were dominated by Atlantic menhaden. Thus, there was no shift in diet with the increase in bluefin tuna length. Chase (2002) reviewed previous bluefin tuna diet studies and came to the conclusion that the diet of bluefin tuna from any particular study location is dominated by "a single, pelagic, schooling prey species." Atlantic menhaden appear to match this prey description during winter in North Carolina.

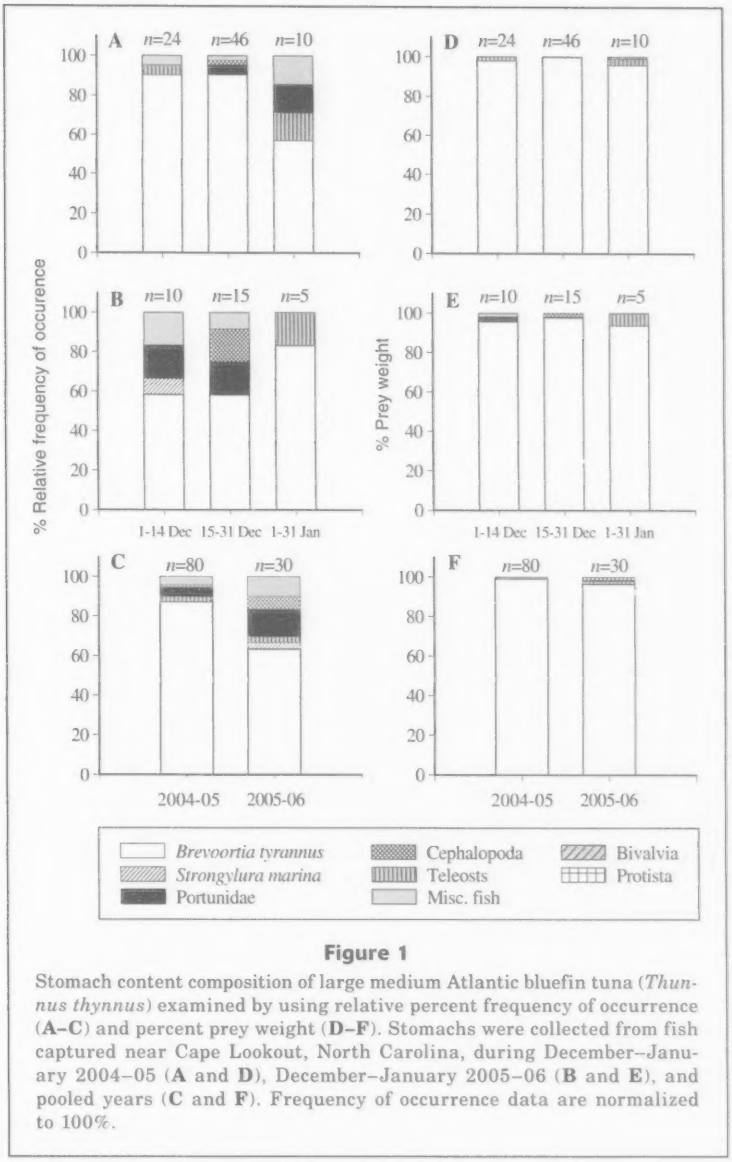


**Figure 1**

Stomach content composition of large medium Atlantic bluefin tuna (*Thunnus thynnus*) examined by using relative percent frequency of occurrence (**A–C**) and percent prey weight (**D–F**). Stomachs were collected from fish captured near Cape Lookout, North Carolina, during December–January 2004–05 (**A** and **D**), December–January 2005–06 (**B** and **E**), and pooled years (**C** and **F**). Frequency of occurrence data are normalized to 100%.

We regularly observed squid (*Loligo* spp.) and portunid crabs in bluefin tuna stomachs. Squid has been suggested as the second-most important prey item, behind teleosts, in several bluefin tuna diet studies (Dragovich, 1970; Eggleston and Bochenek, 1990; and Kade, 2000). Portunid crabs have previously been documented by Kade (2000), and authors such as Krumholz (1959), Dragovich (1970), and Chase (2002) have found minor amounts of crustaceans in the diet of bluefin tuna of various size classes and at various locations. The inclusion of cephalopods and crustaceans at certain times of the year may be a result of increases in their relative abundance. Juanes et al. (2001) found this to be the explanation for bluefish, a primary piscivore that included invertebrate prey in its diet when invertebrates were relatively abundant in the environment. No quantitative information exists on the distribution and abundance of potential prey. Thus, we were unable to make any conclusions about prey-type selectivity.

### Gastric evacuation and daily ration

Bluefin tuna in North Carolina were caught from approximately two hours before sunrise to late afternoon or evening. Time of catch could match bluefin tuna feeding periods or could be an artifact of fishing times.

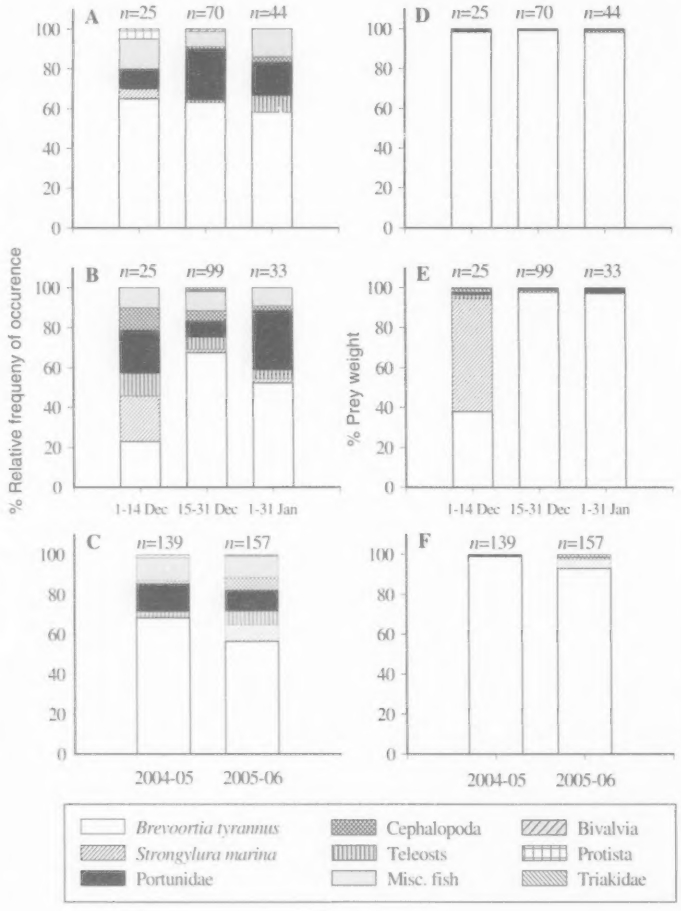


**Figure 2**

Stomach content composition of giant Atlantic bluefin tuna (*Thunnus thynnus*) examined using relative percent frequency of occurrence (**A–C**) and percent prey weight (**D–F**). Stomachs were collected from fish captured near Cape Lookout, North Carolina, during December–January 2004–05 (**A** and **D**), December–January 2005–06 (**B** and **E**), and pooled years (**C** and **F**). Frequency of occurrence data are normalized to 100%.

We suggest the former given that there has been little success at catching bluefin tuna at night during winter in North Carolina (G. Leone, personal commun.[4]). This finding is further corroborated by observed diurnal feeding patterns in other tuna species such as southern bluefin (*Thunnus maccoyii* [Young et al., 1997]), yellowfin (*Thunnus albacares* [Josse et al., 1998]), longtail (*Thunnus tonggol* [Griffiths et al., 2007]), blackfin (*Thunnus atlanticus* [Josse et al., 1998]), and skipjack (*Katsuwonus pelamis* [Magnuson, 1969]). Additionally, increased foraging activity has been observed during crepuscular hours in New England for Atlantic bluefin tuna (Lutcavage et al., 2000) and for Pacific bluefin tuna (*Thunnus orientalis*) in Alaska (Hobson, 1986). Given the feeding behavior of other tuna species, the absence of tuna catch at night, and the stage of digested items observed in presunrise stomach samples, we conclude that most feeding in North Carolina occurs during presunrise and diurnal hours.

To our knowledge, this is the first field estimate of *GER* for Atlantic bluefin tuna. Young et al. (1997) estimated an exponential *GER* for southern bluefin tuna as the greatest decline in gut fullness from one time point to the next (i.e., over a one-hour period). Given the way *GER* was calculated in their study, it is not comparable

[4] Leone, George. 2007. Morgan Harvest Inc., Morehead City, NC 28557.

to our estimate. The only other *GER* for a tuna species that we are aware of is that of Olson and Boggs (1986). Those authors found that under laboratory conditions, the *GER* of yellowfin tuna was best represented by a linear evacuation model and depended on the type, surface area, and digestibility of the prey consumed. Their results showed that mackerel, which contained the highest lipid level of the prey types they examined, were the most digestion-resistant and consequently took the longest (~18.5 hours) to evacuate. Because the diets of bluefin tuna in our study were dominated by Atlantic menhaden by weight, our *GER* estimates are representative of Atlantic menhaden prey and should be used with caution if applied to bluefin tuna that feed on other prey, particularly prey that may differ in digestibility (e.g., prey with an exoskeleton, and having differing lipid levels).

In the present study, several key assumptions were made to estimate *GER*. Because no fish were landed from 1900 to 0300 EST, we assumed that feeding was negligible at night. If bluefin tuna do feed throughout the night, then our *GER* and mean gut fullness values (estimated over a 24-hour period) could potentially be biased low (i.e., peak gut fullness would occur later in night with a shorter [and faster] time to digest prey). We also had to assume that stomachs were not completely emptied several hours before the first presunrise samples were collected. Given that many of the samples collected during presunrise hours contained prey in the final stages of digestion, this appears to be a valid assumption. If digestion was completed before the time of sunrise collections (shortening the time between peak and valley), then our current estimates of *GER* would be biased low (i.e., we would again be assuming a longer time to digest prey than what is actually true).

Estimates of digestion times in pen-held and wild Atlantic bluefin tuna corroborate our estimates of *GER*. Butler and Mason (1978) used stomach content analysis on pen-held giant bluefin tuna (>200 kg) that were fed a variety of "forage fish" species and determined that it took 18–20 hours to completely empty a full stomach (other than viscous liquid). Using acoustic telemetry, Stevens et al. (1978) fed mackerel to captive giant bluefin tuna (>200 kg) and identified gradual increases of stomach temperatures which lasted 14 to 20 hours following a feeding event. Similarly, Carey et al. (1984) used acoustic transmitters in pen-held fish to measure stomach contractions and temperature increases after bluefin tuna feeding events (prey=mackerel and herring) and concluded it took 18 to 21 hours before liquefied food was moved out of the stomach and into the intestine and pyloric caeca These studies indicate that complete evacuation time is not reached in less than 18 to 20 hours and support our estimated digestion time of ~20 hours (i.e., from peak gut fullness to gut fullness near zero).

The *DR* of giant bluefin tuna has been estimated in several studies by various methods. Palomares and Pauly (1989) estimated a *DR* of 1.08% body mass per day for maximum-size (e.g., $L_\infty$=332.0 cm) bluefin tuna, using

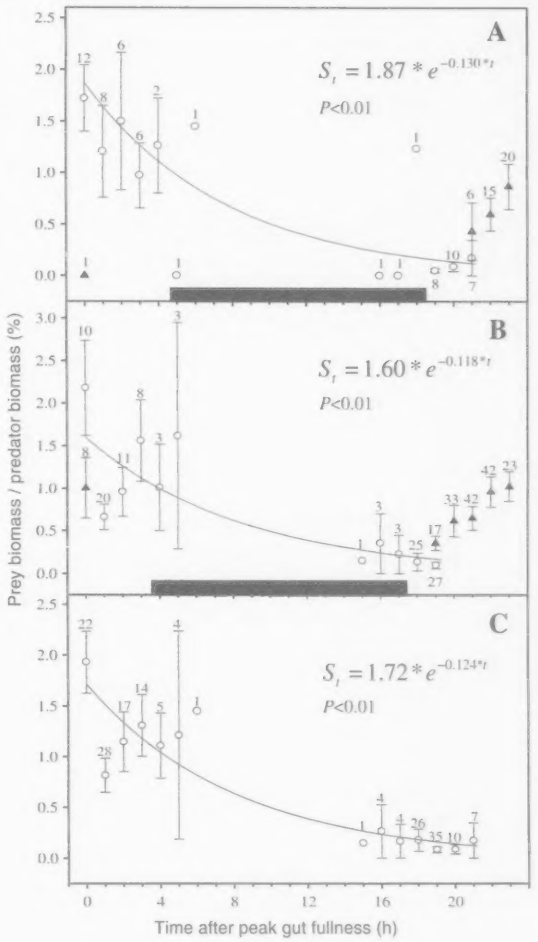


**Figure 3**

Diel patterns of mean gut fullness (kg prey/kg predator · 100%; ± standard error) for (**A**) large medium, (**B**) giant, and (**C**) pooled bluefin tuna (*Thunnus thynnus*) collected off Cape Lookout, North Carolina, during the winters of 2004–05 and 2005–06. Open circles represent values used to estimate gastric evacuation; filled triangles represent values that were not used during gastric evacuation estimates (see *Methods* section for description of data selection). The fit of the exponential gastric evacuation model ($S_t$=$S_0$·$e^{-GER \cdot t}$) is represented by the solid line, where $S_t$ is the individual stomach fullness (kg prey/kg predator) at time $t$; $S_0$ is the stomach fullness at time $t$=0; *GER* is the instantaneous rate of gastric evacuation (rate per hr); and $t$ is the time in hours after peak gut fullness. Samples sizes are listed above the mean gut fullness value. Time point 0=1200–1300 hours for (**A**) and 0=1300–1400 hours for (**B**); average time between sunset and sunrise is represented by solid horizontal bar.

a multiple regression model based on growth, mortality, and maximum length. Aguado-Giménez and García-García (2005) found that large (mean weight=237 kg) bluefin tuna held under fattening conditions consumed 1.56% body weight per day. Andreas Walli[5] estimated a *DR* of 1.1% [±0.3%] body mass per day based on heat incremented feeding of archival-tagged bluefin tuna tracked throughout the western Atlantic. Although the mean *DR* estimate (2.03% ±0.59%) from the current study is somewhat greater than that of previous studies, our estimate is potentially negatively biased for two reasons. First, we used the longest time between periods of peak stomach fullness and empty stomachs. Increasing the time required for gastric emptying effectively decreases the estimate of the amount of food consumed on a daily basis. Second, stomach fullness could be decreased by regurgitation during hook-and-line capture and digestion could be continued after death.

[5] Walli, Andreas. 2006. Unpubl. data. Stanford Univ., Stanford, CA 94305.

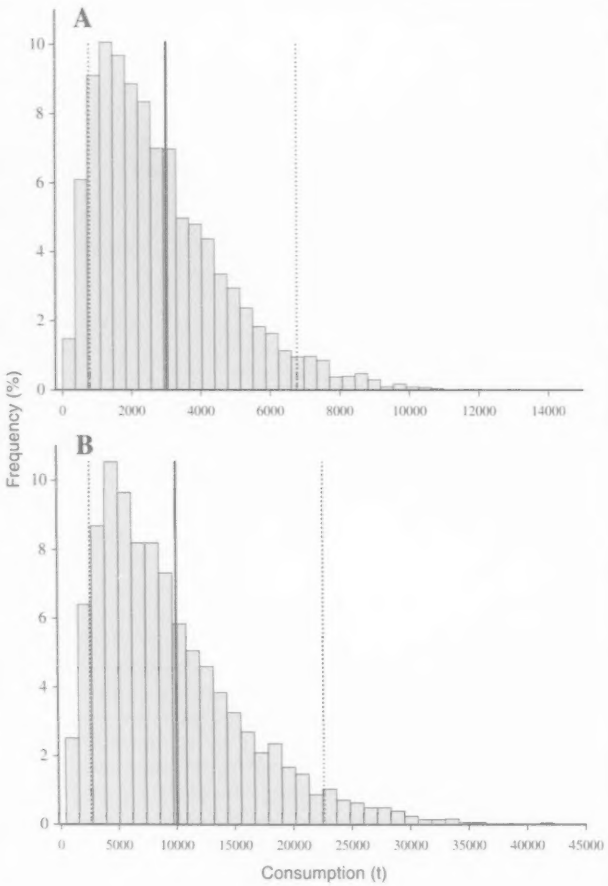


**Figure 4**

Frequency of Monte Carlo simulation results for consumption estimates (metric tons, t) of Atlantic menhaden (*Brevoortia tyrannus*) by (**A**) the current (2005) population of age-6+ western Atlantic bluefin tuna (*Thunnus thynnus*) and (**B**) a restored (to 1975 levels) western Atlantic bluefin tuna population of age-6+ fish. Mean (solid line) and 90% confidence intervals (dotted lines) are presented.

### Predatory impact

An understanding of predator-prey interactions is necessary for ecosystem-based assessment models. Bluefish, striped bass, weakfish, and fishermen are considered the dominant predators of Atlantic menhaden in current multispecies assessment models (NEFSC[2]). The assumption that bluefin tuna are not a dominant predator of Atlantic menhaden along the U.S. East Coast appears correct given the small amount of Atlantic menhaden consumed by bluefin tuna in relation to other Atlantic menhaden predators. However, the goal of ICCAT is to rebuild the biomass of western Atlantic bluefin tuna population to its 1975 level by 2018 (ICCAT, 2007). If the population is rebuilt, our estimates of consumption indicate that bluefin tuna should be considered in future multispecies modeling efforts where Atlantic menhaden are a focal prey. Similarly, Overholtz (2006) suggested that a recovery of the western bluefin tuna stock would make bluefin tuna a dominant predator of Atlantic herring in the Georges Bank region.

Similar to results for bluefish (Buckel et al., 1999; NEFSC[2]), striped bass (Hartman, 2003; Uphoff, 2003; NEFSC, 2006[2]), and weakfish (NEFSC[2]), our estimates of Atlantic menhaden consumption by bluefin tuna were lower than any of the annual coastwide estimates of Atlantic menhaden commercial harvests during the last 25 years[1]. However, with continued attempts at rebuilding populations of bluefin tuna, bluefish, striped bass, and weakfish stocks, predation mortality may become a more important component of the overall mortality rate of Atlantic menhaden. For future modeling efforts, it is important to note that sizes of Atlantic menhaden consumed by bluefin tuna were larger than previously reported sizes of Atlantic menhaden prey found in bluefish, striped bass, and weakfish (Butler, 2007). Additionally, competition for Atlantic menhaden resources during winter may be most important off of NC during winter, and future efforts to investigate this will require information on the spatial distribution of these predators during winter.

There were several sources of uncertainty in our analysis of predatory demand. First, our study was dependent on the commer-

cial bluefin tuna fishery which is limited to only those fish greater than 185 cm (*CFL*). Although infrequent, smaller bluefin are captured locally during the winter. If smaller size classes of bluefin tuna are consuming Atlantic menhaden during winter or at other times of the year, then they too should be considered in future consumption estimates. Currently, there is no evidence for this during non-winter months (Eggleston and Bochenek, 1990). Second, the stock assessment of western Atlantic bluefin tuna is uncertain given the debate regarding the influence of trans-Atlantic mixing. The most recent assessment (ICCAT, 2007) assumed a mixing rate of 1–2% between the east and west bluefin tuna stocks. Rooker et al. (2008) found that as many as 40% of the age 5+ bluefin tuna captured in the Mid-Atlantic bight were from the eastern stock. Bluefin tuna mixing rates for the U.S. South-Atlantic bight during the winter could be used to assign additional biomass from the eastern stock to the $B_{BFT}$ variable described above.

In summary, this study has filled a gap in the knowledge of the natural history of bluefin tuna and determined their potential impact on Atlantic menhaden. During the winter, the continental shelf of NC serves as a spawning ground for several estuarine-dependent species, including Atlantic menhaden. The diets of large medium and giant bluefin tuna have been dominated by Atlantic menhaden during recent winters (Kade, 2000; this study) and likely in earlier years. Therefore, the migrations to and residence times of bluefin tuna in NC will likely be dependent on the abundance of Atlantic menhaden. Within-winter shifts in bluefin tuna diets do occur. However, it is uncertain whether dietary changes are a result of the relative abundances of Atlantic menhaden compared to other prey. Quantitative data of prey type availability are lacking and should be considered in future studies.

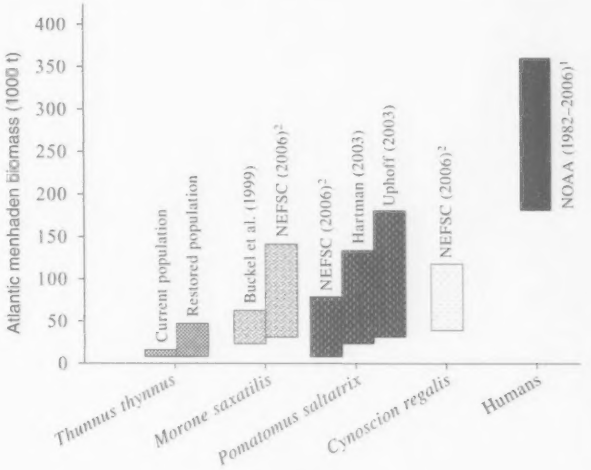


**Figure 5**

Estimated population-level consumption (metric tons, t) of Atlantic menhaden (*Brevoortia tyrannus*) by other important predators (see references provided on figure for further details from other studies); bottom and top of bars represent minimum and maximum estimated consumption (harvest) levels. Bluefin tuna (*Thunnus thynnus*) consumption estimates from this study are represented by the current (2005) abundance estimate for age-6+ western Atlantic bluefin tuna and a restored (to 1975 levels) age-6+ western Atlantic bluefin tuna population.

## Acknowledgments

This study was funded by a NC Sea Grant Fishery Resource Grant 04-EP-04. We would like to thank the commercial fishermen and tuna buyers who participated in the study, especially G. Leone, A. Ng, and J. Cox. We would like to give special thanks to J. Miller and J. Osborne for their assistance with data analyses and manuscript editing, D. Bethea and J. Bizzarro for their help with cumulative prey curve analysis, J. Morley for his assistance with prey identification, and J. Merrell for his help with data collection. We also thank J. Smith, N. McNeill, B. Block, A. Boustany, A. Walli, B. Chase, A. Bianchi, and E. Loew for providing either data or knowledge pertinent to the current research. The comments from three anonymous reviewers substantially improved this paper.

## Literature cited

Aguado-Giménez, F., and B. García-García.
2005. Growth, food intake and feed conversion rates in captive Atlantic bluefin tuna (*Thunnus thynnus* Linnaeus, 1758) under fattening conditions. Aquac. Res. 36:610–614.

Baglin, R. E., Jr.
1980. Length-weight relationships of western Atlantic bluefin tuna, *Thunnus thynnus*. Fish. Bull. 77:995–1000.

Bethea, D. M., J. A. Buckel, and J. K. Carlson.
2004. Foraging ecology of the early life stages of four sympatric shark species. Mar. Ecol. Prog. Ser. 268:245–264.

Bizzarro, J. J., H. J. Robinson, C. S. Rinewalt, and D. A. Ebert.
2007. Comparative feeding ecology of four sympatric skate species off central California. Environ. Biol. Fishes 80(2–3):197–200.

Blank, J. M., C. J. Farwell, J. M. Morrissette, R. J. Schallert, and B. A. Block.
2007. Influence of swimming speed on metabolic rates of juvenile pacific bluefin tuna and yellowfin tuna. Phys. Biochem. Zool. 80:167–177.

Block, B. A., H. Dewar, S. B. Blackwell, T. D. Williams, E. D. Prince, C. J. Farwell, A. Boustany, S. L. H. Teo, A. Seitz, A. Walli, and D. Fudge.
2001. Migratory movements, depth preferences, and thermal biology of Atlantic bluefin tuna. Science 293:1310–1314.

Boustany, A. M.
2006. An examination of population structure, movement patterns and environmental preferences in northern bluefin tuna. Ph.D. diss., 158 p. Stanford Univ., Stanford, CA.

Bromley, P. J.
1994. The role of gastric evacuation experiments in quantifying the feeding rates of predatory fish. Rev. Fish Biol. Fish. 4:33–66.

Buckel, J. A., M. J. Fogarty, and D. O. Conover.
1999. Mutual prey of fish and humans: a comparison of biomass consumed by bluefish, *Pomatomus saltatrix*, with that harvested by fisheries. Fish. Bull. 97:776–785.

Butler, C. M.
2007. Atlantic bluefin tuna (*Thunnus thynnus*) feeding ecology and potential ecosystem effects during winter in North Carolina. M.S. thesis, 106 p. North Carolina State Univ., Raleigh, NC.

Butler, M. J. A., and J. A. Mason.
1978. Behavioral studies on impounded bluefin tuna. Col. Vol. Sci. Pap. ICCAT, 7(2):379–382.

Carey, F. G., J. W. Kanwisher, and E. D. Stevens.
1984. Bluefin tuna warm their viscera during digestion. J. Exp. Biol. 109:1–20.

Chase, B. C.
2002. Differences in diet of Atlantic bluefin tuna (*Thunnus thynnus*) at five seasonal feeding grounds on the New England continental shelf. Fish. Bull. 100:168–180.

Checkley, D. M., Jr., P. B. Ortner, F. E. Werner, L. R. Settle, and S. R. Cummings.
1999. Spawning habitat of the Atlantic menhaden in Onslow Bay, North Carolina. Fish. Oceanogr. 8 (suppl. 2):22–36.

Dickson, K. A., and J. B Graham.
2004. Evolution and consequences of endothermy in fishes. Physiol. Biochem. Zool. 77:998–1018.

Dragovich, A.
1970. The food of bluefin tuna (*Thunnus thynnus*) in the western North Atlantic Ocean. Trans. Am. Fish. Soc. 99:726–731.

Eggers, D.M.
1977. Factors in interpreting data obtained by diel sampling of fish stomachs. J. Fish. Res. Board Can. 34:290–294.

Eggleston, D. B., and E. Bochenek.
1990. Stomach contents and parasite infestation of school bluefin tuna *Thunnus thynnus* collected from the Middle Atlantic Bight, Virginia. Fish. Bull. 88:389–395.

Elliott, J. M., and L. Persson.
1978. The estimation of daily rates of food consumption for fish. J. Anim. Ecol. 47:977–991.

Ferry, L. A., and G. M. Cailliet.
1996. Sample size and data: Are we characterizing and comparing diet properly? *In* Feeding ecology and nutrition in fish; proceedings of the symposium on feeding ecology and nutrition in fish; Int. Congress Biology of Fishes (D. Makinlay, and K. Shearer, eds.), p. 70–81. Am. Fish. Soc., San Francisco, CA.

Goode, G.B.
1879. The natural and economical history of the American menhaden. U.S. Comm. Fish and Fish., pt. 5, Rep. Comm. 1877 (append. A):1–529.

Griffiths, S. P., G. C. Fry, F. J. Manson, and R. D. Pillans.
2007. Feeding dynamics, consumption rates and daily ration of longtail tuna (*Thunnus tonggol*) in Australian waters, with emphasis on the consumption of commercially important prawns. Mar. Freshw. Res. 58:376–397.

Hartman, K. J.
2003. Population-level consumption by Atlantic coastal striped bass and the influence of population recovery upon prey communities. Fish. Manag. Ecol. 10:281–288.

Hobson, E. S.
1986. Predation on the Pacific sand lance, *Ammodytes hexapterus* (Pisces, Ammodytidae), during the transition between day and night in southeastern Alaska. Copeia 1986:223–226.

Hyslop, E. J.
1980. Stomach contents analysis – a review of methods and their application. J. Fish. Biol. 17:411–429.

ICCAT (International Commission for the Conservation of Atlantic Tunas).
2007. Report of the 2006 Atlantic bluefin tuna stock assessment session. Col. Vol. Sci. Pap. ICCAT, 60:652–880

Josse, E., P. Bach, and L. Dagorn.
1998. Simultaneous observations of tuna movements and their prey by sonic tracking and acoustic surveys. Hydrobiologia 371/372:61–69.

Juanes, F., J. A. Buckel, and F. S. Scharf.
2001. Predatory behavior and selectivity of a primary piscivore: comparing fish and non-fish prey. Mar. Ecol. Prog. Ser. 217:157–165.

Kade, T. C.
2000. The natural and social science implications of bluefin tuna migrations off the coast of North Carolina. M. S. thesis, 86 p. Duke Univ. Marine Laboratory, Beaufort, NC.

Krumholz, L. A.
1959. Stomach contents and organ weights of some bluefin tuna, *Thunnus thynnus* (Linnaeus), near Bimini, Bahamas. Zoologica 44:127–131.

Latour, R. J., M. J. Brush, and C. F. Bonzek.
2003. Toward ecosystem-based fisheries management: Strategies for multispecies modeling and associated data requirements. Fisheries 28:10–22.

Lutcavage, M. E., R. W. Brill, G. B. Skomal, B. C. Chase, J. L. Goldstein, and J. Tutein.
2000. Tracking adult North Atlantic bluefin tuna (*Thunnus thynnus*) in the northwestern Atlantic using ultrasonic telemetry. Mar. Biol. 137:347–358.

Magnuson, J. J.
1969. Digestion and food consumption by skipjack tuna (*Katsuwonus pelamis*). Trans. Am. Fish. Soc. 98:379–392.

Olson, R. J., and C. H. Boggs.
1986. Apex predation by yellowfin tuna (*Thunnus albacares*): Independent estimates from gastric evacuation and stomach contents, bioenergetics, and cesium concentrations. Can. J. Fish. Aquat. Sci. 43:1760–1775.

Overholtz, W. J.
2006. Estimates of consumption of Atlantic herring (*Clupea harengus*) by bluefin tuna (*Thunnus thynnus*) during 1970–2002: an approach incorporating uncertainty. J. Northw. Atl. Fish. Sci. 36:55–63.

Overholtz, W. J., L. D. Jacobson, and J. S. Link.
2008. An ecosystem approach for assessment advice and biological reference points for the Gulf of Maine-Georges Bank Atlantic herring complex. N. Am. J. Fish. Manag. 28:247–257.

Palomares, M. L., and D. Pauly.
1989. A multiple regression model for predicting the food consumption of marine fish populations. Aust. J. Mar. Freshw. Res. 40:259–273.
Pauly, D., V. Christensen, and C. J. Walters.
2000. Ecopath, Ecosim, and Ecospace as tools for evaluating ecosystem impact of fisheries. ICES J. Mar. Sci. 57:697–706.
Quinlan, J. A., B. O. Blanton, T. J. Miller, and F. E. Werner.
1999. From spawning grounds to the estuary: using linked individual-based and hydrodynamic models to interpret patterns and processes in the oceanic phase of Atlantic menhaden *Brevoortia tyrannus* life history. Fish. Oceanogr. 8:224–246.
Rooker, J. R., J. R. Alvarado Bremer, B. A. Block, H. Dewar, G. de Metrio, A. Corriero, R. T. Kraus, E. D. Prince, E. Rodríquez-Marín, and D. H. Secor.
2007. Life history and stock structure of Atlantic bluefin tuna (*Thunnus thynnus*). Rev. Fish. Sci. 15:265–310.
Rooker, J. R., D. H. Secor, G. DeMetrio, R. Schloesser, B. A. Block, and J. D. Neilson.
2008. Natal homing and connectivity in Atlantic bluefin tuna populations. Science 322:742–744.
SAS Institute.
1996. SAS/STAT user's guide, vers. 6, 4th ed., vol. 2. SAS Inst. Inc., Cary, NC.
Sokal, R. R., and F. J. Rohlf.
1981. Biometry: The principles and practice of statistics in biological research, 2nd ed., 880 p. W.H. Freeman, New York, NY.
Stevens, E. D., F. G. Carey, and J. Kanwisher.
1978. Changes in visceral temperature of Atlantic bluefin tuna. Col. Vol. Sci. Pap. ICCAT, 7(2):383–388.
Teo, S. L. H., A. Boustany, H. Dewar, M. J. W. Stokesbury, K. C. Weng, S. Beemer, A. C. Seitz, C. J. Farwell, E. D. Prince, and B. A. Block.
2007. Annual migrations, diving behavior, and thermal biology of Atlantic bluefin tuna, *Thunnus thynnus*, on their Gulf of Mexico breeding grounds. Mar. Biol. 238:1–18.
Uphoff, J. H., Jr.
2003. Predator-prey analysis of striped bass and Atlantic menhaden in upper Chesapeake Bay. Fish. Manag. Ecol. 10:313–322.
Williams, B. K., J. D. Nichols, and M. J. Conroy.
2002. Analysis and management of animal populations, 1040 p. Academic Press, San Diego, CA.
Young, J. W., T. D. Lamb, D. Le, R. W. Bradford, and A. W. Whitelaw.
1997. Feeding ecology and interannual variations in diet of southern bluefin tuna, *Thunnus maccoyii*, in relation to coastal and oceanic waters off eastern Tasmania, Australia. Environ. Biol. Fishes 50:275–291.
Zar, J. H.
1999. Biostatistical analysis, 4th ed., 929 p. Prentice-Hall, Upper Saddle River, NJ.

# Maturity and growth of female dusky rockfish (*Sebastes variabilis*) in the central Gulf of Alaska

**Elizabeth A. Chilton**

Email address: elizabeth.chilton@noaa.gov

National Oceanic and Atmospheric Association
National Marine Fisheries Service
Alaska Fisheries Science Center
Kodiak Laboratory
301 Research Court
Kodiak, Alaska 99615

**Abstract**—The dusky rockfish (*Sebastes variabilis*) has recently been resurrected as a distinct species in the genus *Sebastes*. Reproductive biology and growth were examined for this redescribed species in the central Gulf of Alaska. Age and length at 50% maturity were 9.2 years and 365 mm fork length, respectively, which are lower than previously reported. Fertilized ova and eyed embryos were observed in April and evidence of postparturition was not observed until May. The gonadosomatic index decreased with the onset of postparturition in May. Von Bertalanffy growth parameters for female dusky rockfish, estimated from the maturity samples, were significantly different from growth parameters derived from Gulf of Alaska fishery-independent survey data.

Manuscript submitted 6 August 2008.
Manuscript accepted 26 October 2009.
Fish. Bull. 108:70–78 (2010).

The views and opinions expressed or implied in this article are those of the author (or authors) and do not necessarily reflect the position of the National Marine Fisheries Service, NOAA.

One quarter of the 65 rockfish species distributed throughout the Northeast Pacific reside in the Gulf of Alaska (Love et al., 2002). Life history information is limited for these temperate rockfish species, such as the reproductive biology and growth rates of the female dusky rockfish (*Sebastes variabilis*) (Pallas, 1814), which is the predominant pelagic rockfish species on the central Gulf of Alaska shelf. Reproduction in rockfish species is viviparous; fertilization of oocytes is internal and adult females provide some nutritional support for the developing larvae until parturition (Boehlert and Yoklavich, 1984). Length at 50% maturity in female rockfish is variable, occurring at a larger size in more northerly species. Rockfish species in the Gulf of Alaska also have wide ranging growth rates, with pelagic shelf rockfish growing faster than their demersal shelf congeners (Haldorson and Love, 1991; Munk, 2001).

Dusky rockfish have recently been redescribed as a separate species (Orr and Blackburn, 2004). The light and dark color variations previously described for *S. ciliatus* (Tilesius, 1813) have been defined as two distinct species: *S. ciliatus* and *S. variabilis*. *Sebastes ciliatus* is the shallow water, dark variant that is now commonly called "dark rockfish," and *S. variabilis* is the deepwater, light variant which is now called "dusky rockfish." Dark rockfish are caught on shallow, nearshore rocky reefs and dusky rockfish are found less frequently in nearshore habitats and are often captured in large aggregations over the outer continental shelf (Orr and Blackburn, 2004). Dusky rockfish are patchily distributed; concentrated groups are found near the mouths of submarine gullies or canyons and along submerged banks (Reuter, 1999).

Before this study, estimates of dusky rockfish maturity for the Gulf of Alaska were based on visual observations of gonad maturity from a limited sample of this species in the Kodiak Island area. Previous work revealed the potential for incorrect identification of oocyte developmental stages with the macroscopic method in comparison to studies where the histological evaluation method has been used (McDermott, 1994; Zimmerman, 1997). Dusky rockfish growth parameters were derived from data sets collected before the redescription of dark and dusky rockfish.

The objective of this study was to provide improved life history data for the newly described dusky rockfish by 1) producing histologically derived estimates of the age and length at 50% maturity ($A_{0.5}$ and $L_{0.5}$); 2) describing the seasonal timing of ovary development in female dusky rockfish; and 3) comparing growth rates and weight-length relationships derived from the maturity-estimate samples to a larger data set collected in the central Gulf of Alaska for both male and female dusky rockfish.

In the Gulf of Alaska, management of the dusky rockfish resource is aided by the annual pelagic shelf rockfish stock assessment and fisheries evaluation process, with the use of a fishery-independent age-based

**Table 1**

Summary of seasonal data and collection method for central Gulf of Alaska female dusky rockfish (*Sebastes variabilis*) samples used to estimate reproductive maturity, gonadosomatic index, and growth parameters. Sample collections: trawl = bottom trawl; hook-and-line.

| Port sample collections | Chartered vessel collections | Trawl survey collections |
|---|---|---|
| February 2000<br>$n$=4 | March 2000<br>$n$=9 (trawl)<br>$n$=8 (hook-and-line) | July 2000<br>$n$=1 |
| January 2001<br>$n$=15 | April 2000<br>$n$=3 (hook-and-line) | January 2001<br>$n$=27 |
| February 2001<br>$n$=3 | November 2000<br>$n$=36 (trawl) | May 2001<br>$n$=18 |
| March 2001<br>$n$=20 | April 2001<br>$n$=14 (trawl)<br>$n$=30 (hook-and-line) | June 2001<br>$n$=5 |

assessment model to determine the fishing quota for this rockfish species. Maturity estimates and growth parameters derived from this study could improve the estimation of spawning stock biomass and the stock recruitment relationship of future dusky rockfish stock assessments.

## Materials and methods

Samples for the maturity estimates were randomly collected from three sources: 1) port sampling of commercial jig and trawl fisheries around Kodiak Island, Alaska; 2) hook-and-line and bottom trawl samples from chartered vessels around Kodiak Island; and 3) bottom trawl sampling during the Gulf of Alaska groundfish trawl survey conducted by the National Marine Fisheries Service (NMFS) in 2001. Samples were collected from February through April, June, and November of 2000, and from January through June of 2001 (Table 1). The majority of the samples were collected locally from nearshore waters on the southeast side of Kodiak Island. Specific catch locations were not available for many of the samples because of the confidential nature of the catch reporting system; however, Alaska Department of Fish and Game statistical areas were reported with each collection and are used here to show generalized collection locations (Fig. 1).

Sagittal otoliths and ovaries were collected from each individual female rockfish, as well as fork length (FL) to the nearest mm, total body weight (W) to the nearest gram, and individual ovary weight to the nearest gram. Otoliths were aged according to standard break and burn procedures (Chilton and Beamish, 1982). Tissue samples used for histological maturity examination were taken from the middle of the right ovary and fixed in a 10% neutral buffered formalin solution. Tissue was taken from the left ovary if the right ovary was torn because it has been determined in previous histological studies of rockfish maturity that there is no difference in oocyte development between the left and right ovary (Shaw, 1999). These tissue samples taken at all macroscopic stages, except stage 5 (eyed larvae), were embedded in paraffin, thin sectioned to 7 $\mu$m with a rotary microtome, mounted on slides, and stained with standard hematoxylin and eosin (Sheehan and Hrapchak, 1980). Ovary samples with eyed larvae were fragile and not amenable to the paraffin and sectioning process.

A compound microscope and ocular micrometer were used to measure the diameter of the oocytes. The diameter of the fifth largest oocyte on a randomly selected transect along the histological cross section of the gonad was used as the decisive factor for evaluating the most advanced nonatretic oocyte and to determine the developmental stage of the ovary (West, 1990). This method eliminated the possibility of a single and largest oocyte misrepresenting the development stage of the ovary. These ovary stages were evaluated on the basis of seven maturity stages and corresponding oocyte development previously described for northern rockfish (*S. polyspinis*) (Chilton, 2006) (Table 2). Ovaries with vitellogenic oocytes developed to the migratory nucleus stage or the presence of postovulatory follicles were used as evidence of a mature ovary sample. Nichol and Pikitch (1994) found darkblotched rockfish (*S. crameri*) oocytes in the early vitellogenic stage (described as secondary yolk formation) with high levels of atresia (resorption of the unfertilized oocyte) and classified females with ovaries developed to this stage as functionally immature.

Age and length at 50% maturity ($A_{0.5}$ and $L_{0.5}$) were determined by fitting a logistic function to the maturity data as a function of age or length with generalized linear modeling generated by S-plus statistical software, and then evaluating the fitted model at a maturity proportion of 0.50 (S-plus, vers. 6.2; Insightful Corp., Seattle, WA). The variance of $A_{0.5}$ and $L_{0.5}$, as well as 95% confidence intervals (CI), were estimated by bootstrapping methods (Efron and Tibshirani, 1993).

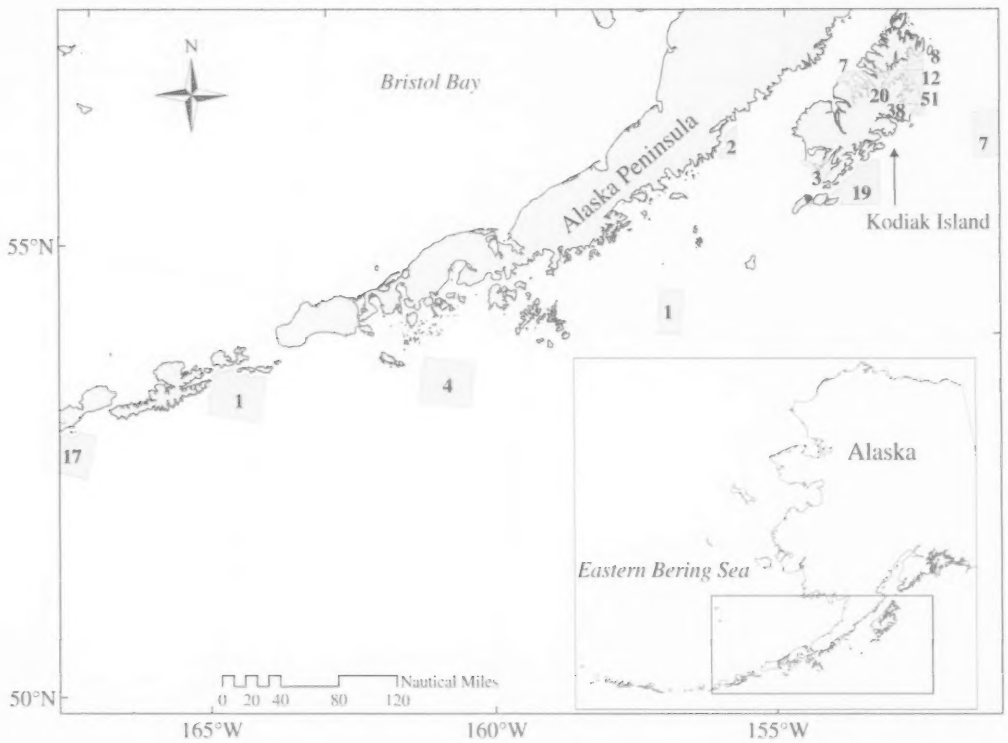


**Figure 1**

Locations in the central Gulf of Alaska where female dusky rockfish (*Sebastes variabilis*) samples were collected in 2000 and 2001 for the growth and maturity study. Number of samples collected within each Alaska Department of Fish and Game statistical area, delineated by shaded blocks, are reported in each block.

A gonadosomatic index ($I_G$) was calculated with the formula

$$\left[IG = 100(\textit{gonad weight}\ (g)/\textit{total body weight}\ (g))\right], \quad (1)$$

to show seasonal changes in development of the ovary with respect to the total body weight. Gonad weights were not collected in May of 2001.

Growth parameters for the female dusky rockfish collected in the Gulf of Alaska for the maturity estimates were calculated by using nonlinear least squares to fit the von Bertalanffy growth equation to age-length data. The von Bertalanffy equation can be expressed as

$$L_t = L_\infty\left(1 - e^{(-k^*(t-t_0))}\right), \quad (2)$$

where $L_t$ = the predicted length (mm FL) at age $t$ (years);
$L_\infty$ = the mean asymptotic length (mm) at maximum age;
$k$ = the growth constant (per year); and
$t_0$ = the age (years) at which the fish would have been zero length.

Von Bertalanffy growth parameters for dusky rockfish in the central Gulf of Alaska were compared to the growth parameters derived from data collected for the maturity study (above). A larger set of age-length data, randomly collected from the 1996 to 2003 NMFS Gulf of Alaska groundfish surveys (GOAS), was used for male and female dusky rockfish separately and for combined sexes if no difference was found. A growth function was fitted to the data to test for significant differences in growth rate between the males and females and the combined-sex age-length data. Differences between sexes in the von Bertalanffy growth parameters were tested with a likelihood ratio test (Kimura, 1980; Haddon, 2001). This test was also used to determine whether growth parameters of female dusky rockfish caught in the NMFS GOAS were different from those values calculated from the maturity study collection.

An allometric weight-length function expressed as $W = aL^b$, where $W$ is weight in grams, and $L$ is length in millimeters, was fitted to the weight and length data from the maturity samples collected in 2000–01, and the NMFS GOAS data from 1996 to 2003. Values for constants a and b were estimated by linear regression of logarithmically transformed weight-length data

**Table 2**

Maturity criteria for staging gonads of female dusky rockfish (*Sebastes variabilis*) based on macroscopic and microscopic observations. Adapted from Chilton (2006).

| Maturity stage | Macroscopic description | Histological description | Oocyte stages |
|---|---|---|---|
| 1 Immature | Thin and thready ovaries, pink or light red in color; oocytes are not visible | Oogonial nests and unyolked oocytes, oocyte diameter is between 80 and 150 $\mu$m | Oogonia organized into nests (ON) with some oocytes at early perinucleus (EP) and late perinucleus (LP) development |
| 2 Maturing or intermediate | Ovaries cream to light yellow in color with thin ovarian wall; oocytes visible | Initial yolk accumulation in oocytes with yolk globules very small, oocyte diameter 160 to 320 $\mu$m | LP and stage-1 through stage-2 yolk accumulation in oocytes, ON and EP stage oocytes are also present |
| 3 Vitellogenesis | Individual eggs are visible, bright yellow in color; ovarian wall thickening and darkly pigmented | Yolk globules and oil vesicles present, oocyte diameter 400 to 600 $\mu$m | Tertiary yolk stage and initial oil vacuoles coalescing in oocytes |
| 4 Fertilized | Large translucent eggs with pink to yellow tint, ovaries enlarged to accommodate large hydrated eggs | Embryo diameter is 600 to as large as 950 $\mu$m | Stage-8 migratory nucleus through early embryonic development |
| 5 Eyed larvae | Ovary enlarged with eyed larvae, ovarian wall thin and transparent, easily torn or broken open | Embryos with dark pigmented eyes | Eyed larvae |
| 6 Postparturition | Ovary flaccid and dark red in color, some eyed larvae are visible | Postovulatory follicles (POF) and atretic oocytes, residual larvae are present | Evidence of parturition based on POF, atretic oocytes and residual embryos |
| 7 Resting | Ovary pink to reddish grey in color, eggs are small and opaque | Oogonial nests and resorption of POF as well as atretic oocytes | ON through EP stage oocytes, POF and atretic oocytes present |

in the weight-length relationship. The residuals of the log-transformed weight-length data were approximately normally distributed and no transformations were made (Gerritsen and McGrath, 2007). Student's $t$-test was used to test for a significant difference in the weight-length relationship from the maturity-estimate samples compared to female dusky rockfish from the NMFS GOAS samples (Snedecor and Cochran, 1989).

## Results

A total of 193 ovaries with corresponding otoliths and fish lengths were collected to estimate $A_{0.5}$ and $L_{0.5}$ of female dusky rockfish. Three otoliths were unreadable, resulting in 190 samples used for the age at 50% maturity estimate analysis of which 166 samples were collected along the east and south side of Kodiak Island and 24 were collected during May and June 2001 from the NMFS GOAS along the Alaska Peninsula. The ages of female dusky rockfish ranged from 3 to 50 years and lengths ranged from 190 mm to 500 mm FL. The age at 50% maturity was estimated at 9.2 years (95% CI=8.2–10.2; Fig. 2A) and the length at 50% maturity was estimated at 365 mm FL (95% CI=354–378; Fig. 2B and Table 3).

Histological methods used to evaluate ovary development in this study resulted in observations of vitellogenic oocytes present in all seven months sampled; January through June, and November. Stage-4 fertilized ova, and stage-5 eyed embryos were observed only in April, and stage-6 postparturition was not observed until May, although a small number of ovaries were at stage 7 in April (Fig. 3). These results indicate that the peak of dusky rockfish fertilization in the central GOA occurred in April followed by parturition in May when postovulatory follicles (POFs) were present. The ovaries exhibiting POFs and extrusion of larvae, stage 7, in April were from females ranging in size from 300 to 360 mm (7 to 9 years of age) and could be an example of delayed oocyte development due to their smaller size.

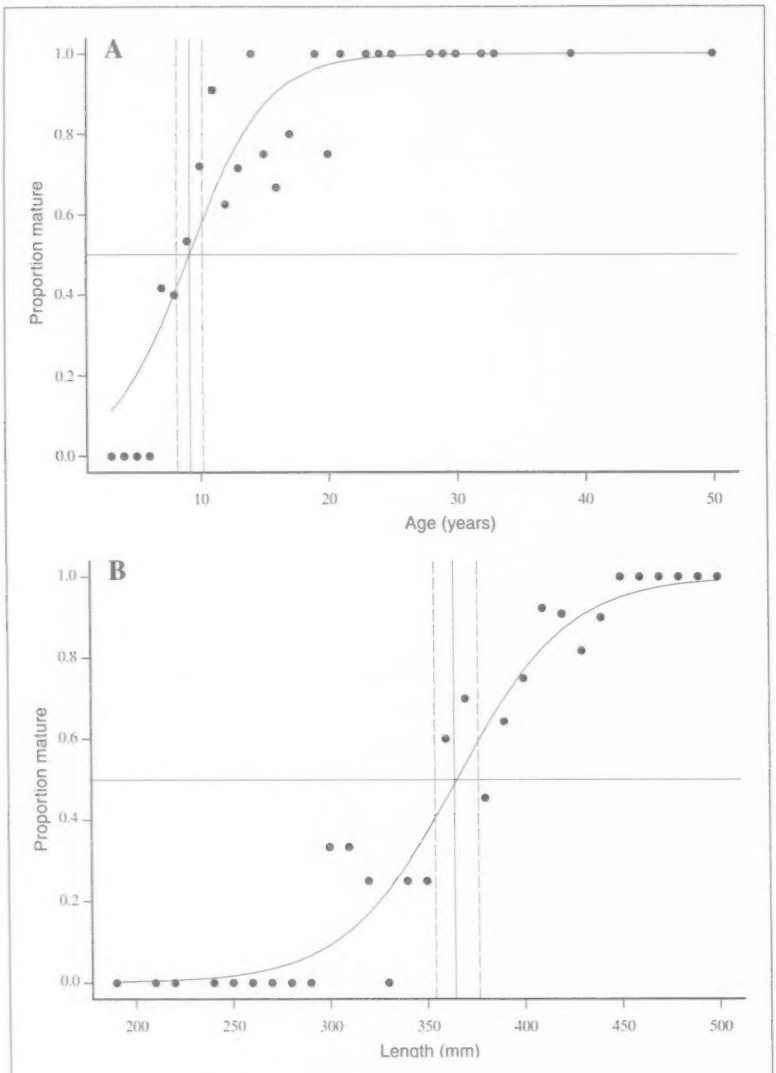


**Figure 2**

(**A**) Age ($A_{0.5}$), and (**B**) length ($L_{0.5}$) at 50% maturity (horizontal line) for female dusky rockfish (*Sebastes variabilis*) captured in the central Gulf of Alaska ($n$=190). Each circle represents one data point and the vertical dashed lines denote 95% confidence intervals for $A_{0.5}$ and $L_{0.5}$.

The gonadosomatic index ($I_G$) began increasing in November and January, reaching a maximum in March, followed by a decrease in April. The lowest value observed was from one sample collected in June and qualitatively appeared to follow the decreasing trend (Fig. 4). This increase in $I_G$ from late winter to spring shows an increase in the ratio of ovary weight to total body weight with the development of fertilized ova in April. The lowest $I_G$ value in June corresponded with low ovary weight due to postparturition. The seasonal trend of decreasing $I_G$, coupled with the monthly ovary development results of this study, indicates May as the peak month of parturition for dusky rockfish in the central Gulf of Alaska.

Von Bertalanffy growth parameters for female dusky rockfish from the maturity estimate sample were $L_\infty$=449 mm, $k$=0.219, and $t_0$=0.855 in contrast to values of $L_\infty$=480 mm, $k$=0.211, and $t_0$=1.106 for females from the NMFS GOAS. The female dusky rockfish from the NMFS GOAS were slower growing than females collected for the maturity estimate as reflected by the different mean asymptotic length and growth coefficients

(Fig. 5A). The likelihood ratio test showed a significant difference in growth parameters between the female dusky rockfish caught in the maturity study and females from the NMFS GOAS ($\chi^2$=158.8, df =3, $P$<0.001) (Table 4).

Von Bertalanffy growth parameters for male dusky rockfish from the NMFS GOAS were $L_\infty$=461 mm, $k$=0.243, and $t_0$=1.232 compared to values of $L_\infty$=480 mm, $k$=0.211, and $t_0$=1.106 for females; these results indicate that female dusky rockfish have a slower growth rate but a larger mean asymptotic length than males (Fig. 5B). The likelihood ratio test showed a significant difference between male and female dusky rockfish ($\chi^2$=61.5, df=3, $P$<0.001) from the NMFS GOAS (Table 4).

There was a significant difference detected in the slopes of the log-transformed weight-length data derived from the female dusky rockfish maturity sample when compared to female dusky rockfish caught in the NMFS GOAS according to the Student's $t$-test ($t$=4.94, $P$<0.005) (Table 5). Although the slope of the weight-length data from the maturity study was significantly different from the NMFS GOAS, both data sets had comparable length ranges with 190 to 500 mm FL for the maturity study and 170 to 530 mm FL for the NMFS GOAS. Consequently, this difference is not likely due to trawl gear selectivity in the NMFS GOAS.

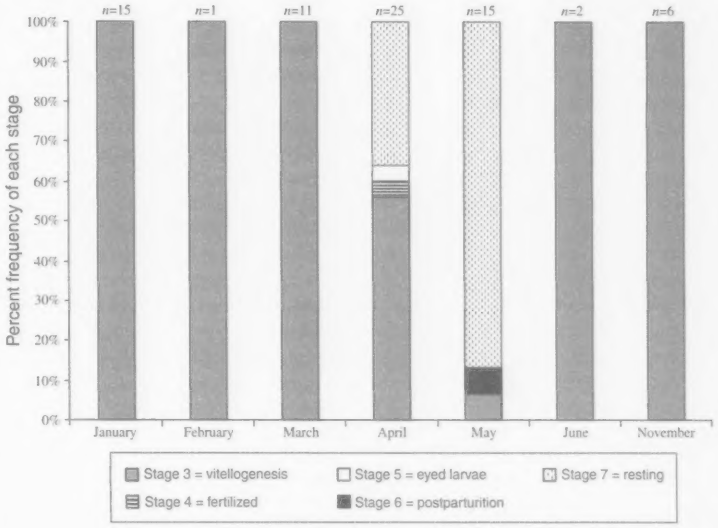


**Figure 3**

Percent frequency of the most advanced oocyte stage present in female dusky rockfish (*Sebastes variabilis*) for each month that this species was sampled in the central Gulf of Alaska in 2000 and 2001 to determine growth and maturity. Sample sizes are shown above each column.

**Table 3**

Maturity parameters and variances for female dusky rockfish (*Sebastes variabilis*) in the central Gulf of Alaska estimated by fitting a logistic function to the maturity data as a function of age or length with generalized linear modeling. a=scaling constant; b=allometric growth parameter.

| | Value | Variance |
|---|---|---|
| $L_{0.5}$ | 365 mm | 38.055 |
| a | –12.728 | 3.581 |
| b | 0.035 | 2.408 |
| $A_{0.5}$ | 9.2 years | 0.254 |
| a | –3.047 | 0.528 |
| b | 0.332 | 0.007 |

## Discussion

The maturity parameters presented in this study are not consistent with previously reported estimates of size and age at 50% maturity for female dusky rockfish of 11.3 years and 428 mm (Love et al., 2001), which are higher and larger than the results from the present study. The differences could be due to the timing, sample size, and method of determining the previous maturity estimates, where ovary development was evaluated at a macroscopic level from a small number of samples. The results of this study are based on a larger sample, collected over multiple months during a two-year period, and on an improved method to evaluate ovary development and may therefore represent a better estimate of maturity.

The seasonal timing of parturition in dusky rockfish is comparable to that of other Gulf of Alaska rockfish species, in April and May (Love et al., 2001; Chilton, 2006). Parturition begins to occur in female northern rockfish from the central Gulf of Alaska in April and higher numbers of POFs are found in May and June (Chilton, 2006). The small number of samples collected for this study in June prevented an estimation of the extent of parturition in dusky rockfish beyond the month of May. The smaller mature dusky rockfish exhibiting stage-7 ovaries in April were most likely fertilized in the previous reproductive season which could have occurred as late as July in the previous year. Nichol and Pikitch (1994) found that oocytes of smaller mature female darkblotched rockfish developed later in the season than oocytes from larger mature females.

The corresponding increase in female dusky rockfish ovary weight compared to total body weight, or gonadosomatic index ($I_G$), is a result of the advancement of

**Table 4**

Von Bertalanffy growth parameters for dusky rockfish (*Sebastes variabilis*) calculated from National Marine Fisheries Service, Gulf of Alaska groundfish survey data and the central Gulf of Alaska maturity study data. $L_\infty$=mean asymptotic length at maximum age; $k$=growth constant; $t_0$=age of fish at zero length; $n$=number of samples.

| | $L_\infty$ (mm) | $k$ | $t_0$ | $n$ |
|---|---|---|---|---|
| Gulf of Alaska groundfish survey (1996–2003) | | | | |
| Females | 480 | 0.211 | 1.106 | 752 |
| Males | 461 | 0.243 | 1.232 | 698 |
| Sexes combined | 472 | 0.223 | 1.117 | 1450 |
| Gulf of Alaska maturity study (2000–01) | | | | |
| Females | 449 | 0.219 | 0.855 | 190 |

**Table 5**

Estimated weight-length parameters for dusky rockfish (*Sebastes variabilis*) captured in the National Marine Fisheries Service, Gulf of Alaska groundfish surveys and the central Gulf of Alaska maturity study. a=scaling constant; b=allometric growth parameter; $n$=number of samples.

| Weight-length constants | a | b | $n$ |
|---|---|---|---|
| Gulf of Alaska combined sex from NMFS groundfish surveys (1996–2003) | 0.0088 | 3.11 | 1581 |
| Gulf of Alaska females (1996–2003) | 0.0100 | 3.09 | 817 |
| Maturity study females (2000–01) | 0.0131 | 3.04 | 176 |

oocyte development in March, followed by a decrease in the $I_G$ with the onset of parturition occurring from April through June. This pattern of increasing $I_G$ until release of the developed larvae at parturition occurs in other rockfish species. The highest $I_G$ values for *S. thompsoni* were recorded in March and a corresponding increase in the frequency of gestation (fertilized ova). Subsequently lower $I_G$ values occurred in April and May because of an increased frequency of parturition during those months (Lee et al., 1998).

Previous research on dusky rockfish growth in the Gulf of Alaska (GOA) has revealed no differences between sexes or management regions. Reuter (1999) estimated growth parameters of dusky rockfish from the combined 1990–96 NMFS GOAS and commercial fisheries data and found no differences in growth between the three management regions, eastern GOA, central GOS, and western GOA, and no difference in growth between sexes with values of $L_\infty$=457 mm, $k$=0.22, $t_0$=0.74 for males, and females of $L_\infty$=461 mm, $k$=0.25, $t_0$=1.24. However, the results of the present study indicate significant differences between male and female growth parameters estimated from the fishery-independent data collected on the NMFS GOAS.

It is not unusual for female rockfish to grow larger than males but at a slower rate, because of the tradeoff between somatic growth and growth for reproduction (Helser et al., 2007). The differences in growth parameters between previous research and this study could be due to the combination of dark and dusky rockfish species in the commercial fishing data or due to the NMFS GOAS data, which were collected before 1996. Before 1996, the light and dark color variant of dusky rockfish caught on the NMFS GOAS were combined into a single species group as dusky rockfish and this treatment prevents comparison of dusky rockfish growth parameters before 1996. Differences in von Bertalanffy growth parameters and the weight-length relationship between the NMFS GOAS and the maturity-estimate collection in this study could be due to the timing of the sample collection. The NMFS GOAS occurs in the months of June and July whereas samples

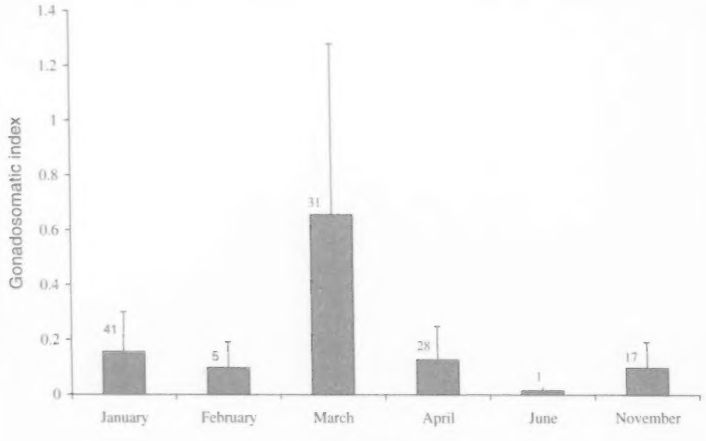


**Figure 4**

Mean monthly gonadosomatic indices for female dusky rockfish (*Sebastes variabilis*) captured in the central Gulf of Alaska ($n$=124). Sample sizes are shown above each column; bars indicate 5% confidence intervals.

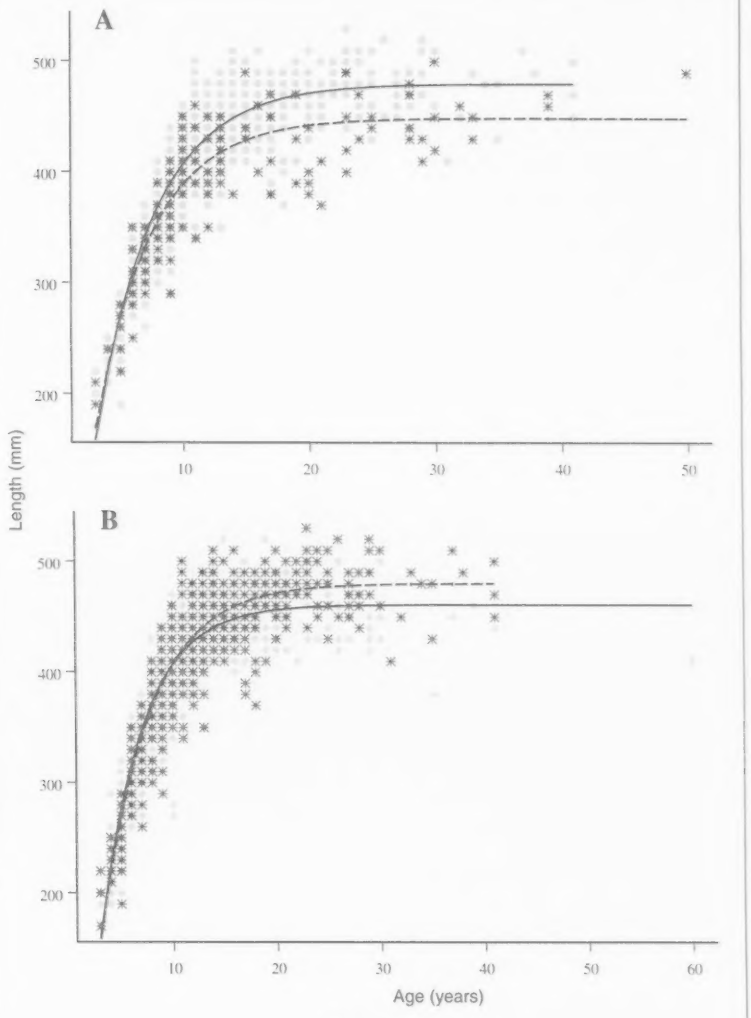


**Figure 5**

Growth curves for (**A**) female dusky rockfish (*Sebastes variabilis*) determined from 1996–2003 National Marine Fisheries Service (NMFS) Gulf of Alaska groundfish survey (GOAS) samples (gray circles) and the 2000–2001 central Gulf of Alaska maturity samples (asterisks) ($n$=940); and (**B**) NMFS GOAS male (gray diamonds) and female (asterisks) dusky rockfish ($n$=1450). Solid line (NMFS GOAS females) and dashed line (maturity sample females) in (A) illustrate the predicted relationship as do the solid (males) and dashed (females) lines in (B). Overlapping symbols in (A) and (B) represent two data points with the same value.

for the maturity estimate were collected throughout the year.

Future studies focusing on the reproductive maturity of rockfish would benefit from the collection of samples throughout the year. In this study, the seasonal timing of ovary collections for the maturity estimate was crucial for the histological evaluation of the most advanced oocytes within developing ovaries, as well as for highlighting the possibility of delayed development of small mature females within a year. In previous studies, where a histological method has been used to evaluate rockfish reproduction, the need for seasonal sampling has been emphasized (Nichol and Pikitch, 1994; Shaw, 1999; Chilton, 2006). The differences in growth

parameters and weight-length relationships between the maturity-estimate collection and the NMFS GOAS are an indication that sampling throughout the year, in months additional to those of the summer survey, could improve those estimates and could prove beneficial to the assessment of dusky rockfish and management of the pelagic shelf rockfish fisheries.

## Acknowledgments

The author sincerely thanks the Alaska Department of Fish and Game Kodiak staff for access to dock-side sample collections; the Alaska Fisheries Science Center Age and Growth Program staff for aging rockfish otoliths; D. Somerton for analysis and manuscript guidance; D. Nichol, M. Wilkins, R. Foy, and A. Moles for comments on the manuscript, and three anonymous reviewers.

## Literature cited

Boehlert, G. W., and M. M. Yoklavich.
1984. Reproduction, embryonic energetics, and the maternal-fetal relationship in the viviparous genus *Sebastes* (Pisces: Scorpaenidae). Biol. Bull. 167:354–370.

Chilton, E. A.
2006. Maturity and growth of northern rockfish (*Sebastes polyspinis)* in the central Gulf of Alaska. Alaska Fish. Res. Bull. 12:263–268.

Chilton, D. E., and R. J. Beamish.
1982. Age determination methods for fishes study by the groundfish program at the Pacific Biological Station. Can. Spec. Publ. Fish. Aquat. Sci. 60:1–102.

Efron, B., and R. Tibshirani.
1993. An introduction to the bootstrap, 436 p. Chapman and Hall, New York.

Gerritsen, H. D., and D. McGrath.
2007. Significant differences in the length-weight relationship of neighboring stocks can result in biased biomass estimate: Examples of haddock (*Melanogrammus aeglefinus*, L.) and whiting (*Merlangius merlangus*, L.). Fish. Res. 85:106–111.

Haddon, M.
2001. Modeling and quantitative methods in fisheries, 406 p. Chapman and Hall/CRC, Boca Raton, FL.

Haldorson, L., and M. Love.
1991. Maturity and fecundity in the rockfish, *Sebastes* spp., a review. Mar. Fish. Rev. 53:25–31.

Helser, T. E., I. J. Stewart, and H. L. Lai.
2007. A Bayesian hierarchical meta-analysis of growth for the genus *Sebastes* in the eastern Pacific Ocean. Can. J. Fish. Aquat. Sci. 64:470–485.

Kimura, D. K.
1980. Likelihood methods for the von Bertalanffy growth curve. Fish. Bull. 77:765–776.

Lee, J. S., C. M. An, and S. H. Huh.
1998. Reproductive cycle of the goldeye rockfish, *Sebastes thompsoni* (Teleostei: Scorpaenidae). J. Korean Fish. Soc. 31:8–16.

Love, M., M. Yoklavich, and L. Thorsteinson.
2002. The rockfishes of the northeast Pacific, 405 p. Univ. California Press, Los Angeles, CA.

McDermott, S. F.
1994. Reproductive biology of rougheye and shortraker rockfish, *Sebastes aleutianus* and *Sebastes borealis*. M.S. thesis, 89 p. Univ. Washington, Seattle.

Munk, K. M.
2001. Maximum ages of groundfishes in waters off Alaska and British Columbia and considerations of age determination. Alaska Fish. Res. Bull. 8:12–2.

Nichol, D. G., and E. K. Pikitch.
1994. Reproduction of darkblotched rockfish off the Oregon Coast. Trans. Am. Fish. Soc. 123:469–481.

Orr, J. W., and J. E. Blackburn.
2004. The dusky rockfishes (Teleostei: Scorpaeniformes) of the North Pacific Ocean: resurrection of *Sebastes variabilis* (Pallas, 1814) and a redescription of *Sebastes ciliatus* (Telesis, 1813). Fish. Bull. 102: 328–348.

Reuter, R. F.
1999. Describing dusky rockfish (*Sebastes ciliatus*) habitat in the Gulf of Alaska using historical data. Masters thesis, 83 p. California State Univ., Hayward.

Shaw, F. R.
1999. Life history traits of four species of rockfish (Genus *Sebastes*). M.S. thesis, 178 p. Univ. Washington, Seattle.

Sheehan, D. C., and B. B. Hrapchak.
1980. Theory and practice of histotechnology, 2nd ed., 481 p. Battelle Press, Columbus, OH.

Snedecor, G. W., and W. G. Cochran.
1980. Statistical methods, 8th ed., 503 p. Iowa State Univ. Press, Ames.

West, G.
1990. Methods of assessing ovarian development in fishes: A review. Aust. J. Mar. Freshw. Res. 41:199–222.

Zimmermann, M.
1997. Maturity and fecundity of arrowtooth flounder, *Atheresthes stomias*, from the Gulf of Alaska. Fish. Bull. 95:598–611.

# Environmental characterization of seasonal trends and foraging habitat of bottlenose dolphins (*Tursiops truncatus*) in northern Gulf of Mexico bays

**Cara E. Miller (contact author)**

**Donald M. Baltz**

Email address for contact author: cara.miller@flinders.edu.au

Department of Oceanography and Coastal Sciences
Louisiana State University
Baton Rouge, Louisiana 70803
Present address: School of Biological Sciences
Flinders University
G.P.O. Box 2100
Adelaide 5001 South Australia, Australia

**Abstract**—A description of the foraging habitat of a cetacean species is critical for conservation and effective management. We used a fine-scale microhabitat approach to examine patterns in bottlenose dolphin (*Tursiops truncatus*) foraging distribution in relation to dissolved oxygen, turbidity, salinity, water depth, water temperature, and distance from shore measurements in a highly turbid estuary on the northern Gulf of Mexico. In general, environmental variation in the Barataria Basin marine environment comprises three primary axes of variability (i.e., factors: temperature and dissolved oxygen, salinity and turbidity, and distance and depth) that represent seasonal, spatial-seasonal, and spatial scales, respectively. Foraging sites were differentiated from nonforaging sites by significant differences among group size, temperature, turbidity, and season. Habitat selection analysis on individual variables indicated that foraging was more frequently observed in waters 4–6 m deep, 200–500 m from shore, and at salinity values of around 20 psu. This fine-scale and multivariate approach represents a useful method of exploring the complexity, gradation, and detail of the relationships between environmental variables and the foraging distribution patterns of bottlenose dolphin.

Manuscript submitted 20 October 2008.
Manuscript accepted 29 October 2009.
Fish. Bull. 108:79–86 (2009).

The views and opinions expressed or implied in this article are those of the author (or authors) and do not necessarily reflect the position of the National Marine Fisheries Service, NOAA.

Identifying bottlenose dolphin (*Tursiops truncatus*) foraging habitat is critical for effective species conservation. However, simply describing foraging habitat as a geographic location or habitat type may be inadequate and incomplete given the heterogenous and variable nature of marine environments (Miller and Cribb, 2009). Therefore, measuring and quantifying the environmental variables that characterize bottlenose dolphin foraging habitat provides a more powerful and flexible tool for implementing management strategies.

For the well-studied bottlenose dolphin (*Tursiops* spp.), investigations into foraging habitat have been undertaken with a range of approaches in a wide variety of locations. In some instances, general habitat type and oceanographic features have been related to congregations of bottlenose dolphin prey by observations of increased rates of feeding, notably in estuarine areas (Ballance, 1992) and at interfaces between open ocean and protected estuaries, seagrass beds, and mangrove shorelines (Grigg and Markowitz, 1997; Harzen, 1998). Gregory and Rowden (2001) have observed feeding activity in association with tidal movement. Hastie et al. (2004) correlated surface feeding behavior with submarine habitat characteristics, and Bailey and Thompson (2006) used modeling techniques to further quantify and investigate these relationships. Others have investigated the frequency of feeding behavior in relation to group size (Shane et al., 1986; Gregory and Rowden, 2001) and Campbell et al. (2002) suggested that larger groups are more effective and efficient in searching for food by using cooperative feeding tactics. Numerous other studies have noted similar relationships between seasonal environmental patterns and the frequency of bottlenose dolphin sightings (Wilson et al., 1997; Stockin et al., 2006), but environmental variables relating to this seasonality have not always been quantified.

The objective of our research was to investigate the differences in environmental habitat between foraging and nonforaging locations of bottlenose dolphins within an inshore bay of the Northern Gulf of Mexico (Waring et al., 2007). In addition, the marine environment of the study site was characterized on a seasonal basis. The fine-scale approach we employed measured a suite of environmental variables and allowed us to discern more spatially explicit patterns of habitat use by bottlenose dolphins.

## Methods

### Study area

This study was conducted in Barataria Basin, an estuary along the northern

Gulf of Mexico on the Louisiana coast directly west of the Mississippi River. The region is both humid and subtropical and is dominated by saltmarsh vegetation (Day et al., 1989). Barataria and Caminada bays lie in the lower saline portion of Barataria Basin,; they are turbid bays of less than 2 m in depth (on average), have limited tidal amplitude (less than 0.32 m), and are separated from the Gulf of Mexico by a series of barrier islands (Baltz et al., 1993).

### Survey method

Monthly surveys were initiated in Barataria Basin in June 1999 and continued until May 2002. Two or more independent observers used a small 3.5-m (17-ft) motorboat to survey six designated strata in random order and sequence (Miller, 2003). When a bottlenose dolphin group was sighted, standard photo-identification techniques were used to document individuals (Würsig and Würsig, 1977). Microhabitat data were also collected. More specifically, an onboard Hydrolab (Environmental Data Systems, model CR2-SU, Austin, TX) was used to record sea-surface temperature (°C), salinity (psu), and dissolved oxygen (mg/L). Furthermore, a weighted line measured shallow depths (m), and nautical charts and mapping software were used for deeper water measurements and to determine distance to the nearest shore (m). Lastly, water samples were collected for laboratory assessment of turbidity (nephelometric turbidity units [NTU]) using a Hach 2100N Turbidimeter (Loveland, CO). Bottlenose dolphin group size and composition were recorded, as well as the presence of juveniles and calves (Miller, 2003). Behaviors were categorized as foraging, social, rest, and travel behaviors (Allen and Read, 2000). However, for this article only foraging activity defined by one or more of the following behaviors was used: fish in mouth, numerous steep dives in rapid succession, quick circling behavior at the water surface, or direct pursuit of a prey item (Allen et al., 2001). All sightings were made during daylight hours in Beaufort Sea state conditions of 3 or less.

### Statistical methods

Environmental variables were assessed for univariate and bivariate normality and when necessary were transformed to meet normality requirements. Seasonal (Fall: September–November, Winter: December–February, Spring: March–May, and Summer: June–August) differences among dissolved oxygen, turbidity, salinity, water depth, water temperature, and distance from shore were assessed by using a multivariate analysis of variance (MANOVA) approach and pair-wise comparisons. Least-square means with Tukey's adjustment were performed on variables and produced a significant Shapiro-Wilks result.

A factor analysis (FA) of dissolved oxygen, turbidity, salinity, water depth, water temperature, and distance from shore was employed to examine the pattern of habitat use by bottlenose dolphins and also to highlight relationships among individual variables. The number of orthogonal components retained for interpretation was chosen after examining the scree plot for Eigen values >1, and interpretation was aided by a varimax rotation.

A logistic regression and habitat suitability curves (Saucier and Baltz, 1993) were used to investigate whether particular environmental variables were useful in describing foraging activity. The forward stepwise logistic regression with maximum likelihood estimation (with a Wald chi-square statistic) was used to select variables that were most strongly related to the observed activity. Variables investigated in this analysis were dissolved oxygen, turbidity, salinity, water depth, water temperature, distance from shore, time of day, season, and the minimum number of individuals present in a group. Variable multicollinearity was checked before the analysis by using variance inflation factor (VIF) values and the final model was evaluated by a Hosmer and Lemeshow test. Least-square means (with associated standard errors) of foraging and nonforaging observations were computed for all significant variables. To describe seasonal foraging activity, seasons in which the highest proportion of foraging and nonforaging observations took place were used for modeling.

Habitat suitability curves (Baltz et al., 1993) were constructed to characterize the patterns of dissolved oxygen, turbidity, salinity, water depth, water temperature, distance from shore, and group size at sites where foraging was observed. For this approach, we considered the proportional frequency of foraging and nonforaging activity at defined intervals for each environmental variable along its range. Specifically, a foraging habitat suitability value was calculated by dividing the probability of observing foraging in each interval by the total number of observations in each. Habitat suitability values were normalized to a scale of 0 (nonforaging) to 1 (high probability of foraging) by dividing each habitat suitability interval value by the highest habitat suitability interval value of each environmental variable.

## Results

Number of survey days and frequency of bottlenose dolphin groups sighted were relatively even across seasons as was the proportion of observations during which foraging activity was observed. Nevertheless there was some variability in the number of individuals seen throughout the year (Table 1). Variability in the environmental characteristics of the study area was also evident. Significant seasonal differences in dissolved oxygen, turbidity, salinity, and water temperature were detected by a MANOVA. Posterior pair-wise comparisons were used on significant variables (Table 2). Water temperatures were significantly different across all four seasons and, as expected, were lowest in winter and highest in summer. Minimum observed dissolved oxygen levels were found

**Table 1**

Seasonal frequency of number of sightings, number of individuals seen (based on minimum group size), and number of sightings during which foraging behavior was observed for bottlenose dolphins (*Tursiops truncatus*) in northern Gulf of Mexico bays from June 1999 until May 2002.

| | Winter | Spring | Summer | Fall | Total |
|---|---|---|---|---|---|
| Number of observations | 68 | 60 | 71 | 70 | 269 |
| Minimum number of individuals | 327 | 422 | 595 | 550 | 1894 |
| Number of foraging observations | 18 | 24 | 21 | 25 | 88 |

**Table 2**

Overall and seasonal means for environmental conditions used by bottlenose dolphins (*Tursiops truncatus*) in the Barataria Bay study area measured from June 1999 to May 2002. Significant seasonal differences ($P<0.025$) in least-square means (±1 standard error [SE]) are indicated by different superscripted letters reading across each row.

| Variable | Winter | Spring | Summer | Fall | Overall mean |
|---|---|---|---|---|---|
| Temperature (°C) | 13.96 ±0.45$^{a}$ | 23.00 ±0.47$^{b}$ | 30.12 ±0.44$^{c}$ | 25.99 ±0.44$^{d}$ | 23.37 ±0.43 |
| Dissolved oxygen (mg/L) | 11.58 ±0.28$^{a}$ | 9.07 ±0.27$^{b}$ | 6.99 ±0.30$^{c}$ | 7.90 ±0.29$^{c}$ | 8.98 ±0.19 |
| Salinity (psu) | 24.15 ±0.51$^{a}$ | 21.99 ±0.54$^{b}$ | 20.84 ±0.50$^{b}$ | 24.06 ±0.50$^{a}$ | 22.77 ±0.27 |
| Turbidity (NTU) | 14.15 ±0.87$^{a}$ | 13.50 ±0.92$^{a}$ | 11.19 ±0.85$^{ab}$ | 9.76 ±0.85$^{b}$ | 12.08 ±0.45 |
| Distance from shore (m) | 69.04 ±12.78 | 111.42 ±13.61 | 91.73 ±12.51 | 70.14 ±12.60 | 84.77 ±6.47 |
| Depth (m) | 2.82 ±0.23 | 2.54 ±0.25 | 2.33 ±0.23 | 2.72 ±0.23 | 2.60 ±0.12 |

in summer and fall and increased significantly in spring and again in winter. Mean salinity values fell into two general groupings; fall-winter salinities were higher than those for summer-spring. Turbidity levels were less distinct seasonally. Although the highest turbidity levels seen in winter and spring were significantly different from those seen in fall, levels seen in summer were not significantly different from either. The MANOVA did not reveal any seasonal differences in distance from shore or water depth.

Spatial and seasonal environmental variation in the study area was considerable, and many of the variables were strongly correlated. The FA included all survey observations and resolved the six environmental variables into three orthogonal factors that explained 71% of the variation in the data (Table 3). Each of the six environmental variables loaded heavily on at least one factor. Factor 1 accounted for 30% of the variation and loaded heavily on temperature and dissolved oxygen. The signs of these loadings were opposite and represented an inverse seasonal relationship. Factors 2 and 3 each accounted for an approximate additional 20% of the variation. Factor 2 loaded strongly and positively on both salinity and turbidity and did not reflect the negative relationship expected over larger salinity gradients. Strong positive loadings for the two spatial variables of distance from shore and depth were evident

**Table 3**

Rotated factor loadings of environmental variables measured at observation sites of bottlenose dolphins (*Tursiops truncatus*) in lower Barataria and Caminada bays, Louisiana, from June 1999 until May 2002. Magnitude and signs of factor loadings indicate strength and direction of the influence of each variable on a factor. Figures in bold indicate the most important variable for the given factor. The variances explained by the Eigen value for each factor are expressed as absolute, proportional, and cumulative values.

| | Factors | | |
|---|---|---|---|
| Environmental variable | 1 | 2 | 3 |
| Temperature (°C) | **−0.88** | −0.36 | −0.01 |
| Dissolved oxygen (mg/L) | **0.94** | −0.16 | −0.04 |
| Salinity (psu) | 0.02 | **0.82** | 0.16 |
| Turbidity (NTU) | 0.06 | **0.67** | −0.19 |
| Distance from shore (m) | −0.23 | −0.05 | **0.70** |
| Depth (m) | 0.21 | 0.01 | **0.81** |
| Variance explained | 1.85 | 1.20 | 1.18 |
| Proportion | 0.31 | 0.20 | 0.20 |
| Cumulative proportion | 0.31 | 0.51 | 0.71 |

**Table 4**

A forward stepwise logistic regression characterizing variables important in describing bottlenose dolphin (*Tursiops truncatus*) foraging sites in Barataria Basin, Louisiana, during from June 1999 to May 2002. Individual variables were entered and kept in the model with an $\alpha$-level of 0.20. Variables are listed below from highest to lowest Wald $\chi^2$ statistic. Order of variable entry into the model is also indicated. Foraging and nonforaging least-square means (±1 standard error [SE]) were calculated for significant continuous variables, and highest and lowest proportions of foraging activity were given for season.

| Order | Effect | Wald $\chi^2$ | Pr > $\chi^2$ | Foraging (Mean ±1 SE) | Nonforaging (Mean ±1 SE) |
|---|---|---|---|---|---|
| 3 | Temperature | 6.78 | <0.01 | 24.28 ±0.75 | 22.82 ±0.54 |
| 1 | Minimum group size | 5.54 | 0.02 | 9.27 ±0.72 | 5.92 ±0.52 |
| 2 | Turbidity | 4.79 | 0.03 | 13.22 ±0.78 | 11.65 ±0.56 |
| 4 | Season | 2.30 | 0.13 | Spring (39.3%) | Winter (73.5%) |

in factor 3. Distance from shore was greatest in open waters areas north of barrier islands where wetland areas were more sparsely distributed and also in some of the channels and passes opening into the Gulf of Mexico. These channels and passes were also typically the deepest parts of the study area.

Minimum group size followed by turbidity, temperature, and season were found to be the most important variables describing foraging sites according to a forward stepwise logistic regression (Table 4). The selected model was a reasonable fit (Hosmer and Lemeshow criterion, $\chi^2_8$=5.79, $P$=0.67). Minimum group size, turbidity and temperature were all higher during foraging observations, and the incidence of foraging was highest in spring (39.3%) and lowest in winter (26.5%). Overall, foraging behavior was observed during 88 of the 269 sightings.

Specific ranges and levels of turbidity, water depth, water temperature, distance from shore, and minimum group size were found to have higher probabilities of foraging activity according to habitat suitability curves. Foraging suitability was calculated to be greatest between temperatures of 20° and 24°C (Fig. 1). Foraging was more commonly observed when dissolved oxygen content was around 6 mg/L and declined as values increased (Fig. 1). Foraging was also more often observed in salinity values around 20 psu, turbidity values between 20 and 28 NTU, distances between 200 and 500 m from shore, and water depths between 4 and 6 m (Figs. 1 and 2). A positive relationship between increased number of foraging observations and minimum group size was also evident (Fig. 2).

## Discussion

### Variables related to foraging

Our research into bottlenose dolphin foraging habitat in the northern Gulf of Mexico revealed that water temperature may be a more informative indicator of distribution and foraging activity than season. This assertion is consistent with documented correlations between water temperature fluctuations (associated with La Niña events) and short-beaked common dolphin (*Delphinus delphis*) distribution (Neumann, 2001) and distributional range limits for some Delphinidae species determined by water temperature (Gaskin, 1968). Furthermore, Tershy et al. (1990) found seasonal patterns that correlated with the presence of fin (*Balaenoptera physalus*) and Bryde's (*Balaenoptera edeni*) whales within the Gulf of California and that were negatively correlated with increasing water temperature.

However, the importance of other variables (i.e., dissolved oxygen, turbidity, and salinity) is noteworthy. These variables also showed significant seasonal differences (Table 2). Salinity and temperature are known to be major determinants of coastal and estuarine community structure, in part because of salt tolerances and adaptations of associated flora and fauna (Day et al., 1989). Estuaries are often considered nurseries for juvenile fish and invertebrate species and it is likely that increased prey densities are related to the noted associations between cetaceans and estuarine areas (Ballance, 1992; Grigg and Markowitz, 1997; Harzen, 1998). Selzer and Payne (1988) also documented a seasonal correlation between sea surface temperatures and salinities with Atlantic white-sided (*Lagenorhynchus acutus*) and short-beaked common dolphin (*Delphinus delphis*) distributions and hypothesized that the interactions of salinity and temperature with sea floor topography and associated upwelling may be related to prey aggregations. Studies documenting turbidity and dissolved oxygen have been less common. Brager et al. (2003) assessed Hector's dolphin (*Cephalorhynchus hectori*) habitat in relation to sea surface temperature, water depth, and water clarity and, although relationships varied by region and season, they found significant relationships between all three variables, for both individual variables and variables in combination. We also demonstrated that proportionally more foraging occurred in turbid waters, possibly indicating that higher levels of suspended sediments allow bottlenose dolphins to forage more effectively on prey that rely on visual

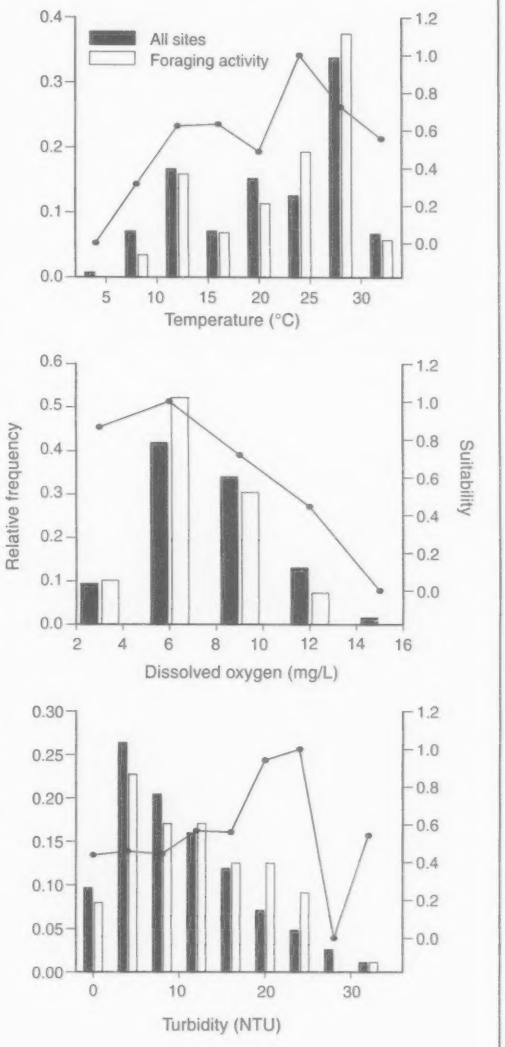


**Figure 1**

Foraging suitability curves for bottlenose dolphins (*Tursiops truncatus*) observed in northern Gulf of Mexico bays from June 1999 to May 2002 for temperature, dissolved oxygen, and turbidity (in nephelometric turbidity units [NTU]). Vertical bars indicate frequency of overall observations (black) and foraging activity (white) for each given interval. Black lines indicate the relative suitability of variable values for foraging activity.

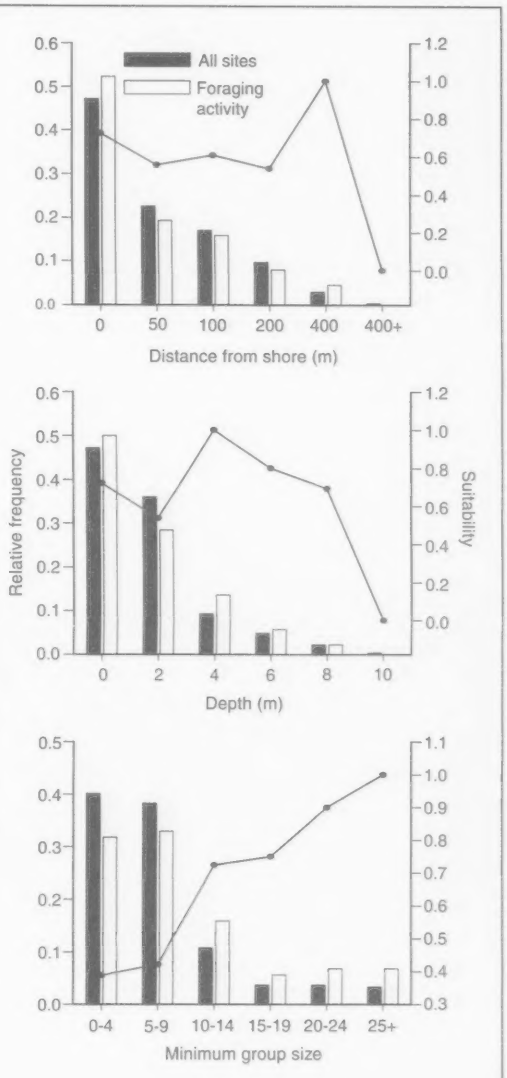


**Figure 2**

Foraging suitability curves for bottlenose dolphins (*Tursiops truncatus*) observed in northern Gulf of Mexico bays from June 1999 to May 2002 for distance to shore, depth, and minimum group size. Vertical bars indicate frequency of overall observations (black) and foraging activity (white) for each given interval. Black lines indicate the relative suitability of variable values for foraging activity.

detection of predators. However, it should be noted that on an overall basis most of the foraging occurred in less turbid waters.

It is logical that the movement and distribution of prey are important features for characterizing dolphin foraging habitat. Larger group sizes were identified as an important factor in differentiating sightings based on foraging activity (Table 4, Fig. 2). Nevertheless, it is difficult to know whether increased group sizes are formed in response to favorable environmental conditions for prey congregation or whether individuals gather together as part of a strategy to increase

foraging success and efficiency. Group sizes of pantropical spotted (*Stenella attenuata*), spinner (*Stenella longirostris*), and short-beaked common dolphins in the eastern Pacific Ocean have been observed to mirror the diurnal group-size fluctuations of yellowfin tuna (*Thunnus albacares*), one of their common prey (Scott and Cattanach, 1998). Cockroft and Peddemors (1990) noted the synchrony of pilchard (*Sardinops ocellatus*) movements with the migration of common dolphins during winter months up the eastern coast of South Africa. Both Corkeron (1990) and Grigg and Markowitz (1997) identified food patchiness and interspecific interactions as important influences on Tursiops spp. group size.

### Applications of a microhabitat approach

The ability to describe cetacean habitat hinges on the capacity to measure the suite of important and appropriate environmental variables at the correct scale for which they exert influence (Ingram and Rogan, 2002; Redfern et al., 2006). This task is not trivial and noted issues with describing and researching cetacean habitat include the following: it is often unknown which variables (and how many) are the most pertinent to study; it is difficult to obtain measurements for some variables (even when they might be considered important); the scale at which the variable may influence cetacean distribution may be masked or uncertain; and the relationship between cetacean distribution and the given environmental variable may be correlated with and confounded by additional variables or factors. Our investigations into dolphin foraging habitat addressed some of these difficulties. Specifically, foraging habitat was measured on the same scale and with variables similar to those that have been used for habitat characterization studies of potential prey items in the same study area (Baltz et al., 1993; Baltz et al., 1998). Such a basis created a strong premise for asserting that foraging habitat could be characterized in the same manner. In addition, the collection of a suite of variables was instructive for investigating variables that might be synergistic or correlated.

A description of the characteristics of cetacean foraging habitat is also contingent on accurately assessing and identifying feeding behavior and possibly accounting for variations in feeding strategies, both of which are particularly pertinent for bottlenose dolphins given that they are both flexible and opportunistic in their feeding activity (Shane et al., 1986). Observations of feeding in association with shrimp boats have been documented in Texas waters (Brager, 1993) and feeding on mudbanks by partial beaching has been observed in some salt-marsh areas (Hoese, 1971). In Shark Bay, Western Australia, a number of individuals have been observed carrying sponges on their rostra in what is hypothesized to be a foraging aid (Smolker et al., 1997). Furthermore, in different habitats bottlenose dolphins have been observed to forage on different prey items (Gannon and Waples, 2004), while individuals of some cetacean species have been documented using distinctive foraging patterns while in close proximity to one another (Hoelzel et al., 1989). These considerations emphasize the need to understand the complexity of foraging behavior for a given species and may also support the need to analyze different foraging techniques separately.

Our findings provide a useful approach to identifying variables that are important in describing bottlenose dolphin foraging habitat; however, other unquantified variables such as boat activity (Lusseau, 2005), presence of competitors and predators such as sharks (Heithaus and Dill, 2006), El Niño events (Bearzi, 2005), seabed gradients (Ingram and Rogan, 2002), and weather and climate front patterns (Mendes et al., 2002) may have confounded these observations.

## Conclusions

Long-term site fidelity and residency of many bottlenose dolphin populations indicate that individual populations likely have unique relationships with the given bay, estuary, or coastline that they inhabit. Characterizing foraging habitat for the bottlenose dolphin population in Barataria Basin is therefore a useful exercise because this small population (Miller, 2003) is presently managed as a distinct estuarine stock within the northern Gulf of Mexico (Waring et al., 2007).

## Acknowledgments

The authors would like to acknowledge the many volunteers who participated in field and laboratory work for this project, particularly H. Holwager. In addition, the first author is grateful for financial assistance from the Louisiana Board of Regents Fellowship program and for support from the Department of Oceanography and Coastal Sciences at Louisiana State University during her dissertation research. This article was improved by comments from three anonymous reviewers. Research was undertaken through a NMFS permit granted to the authors.

## Literature cited

Allen, M. C., and A. J. Read.
2000. Habitat selection of foraging bottlenose dolphins in relation to boat density near Clearwater, Florida. Mar. Mamm. Sci. 16:815–824.

Allen, M. C., A. J. Read, J. Gaudet, and L. S. Sayigh.
2001. Fine-scale habitat selection of foraging bottlenose dolphins *Tursiops truncatus* near Clearwater, Florida. Mar. Ecol. Progr. Ser. 222:253–264.

Bailey, H., and P. Thompson.
2006. Quantitative analysis of bottlenose dolphin movement patterns and their relationship with foraging. J. Anim. Ecol. 75:456–465.

Ballance, L. T.
1992. Habitat use patterns and ranges of the bottlenose dolphin in the Gulf of California, Mexico. Mar. Mamm. Sci. 8:262–274.
Baltz, D. M., J. W. Fleeger, C. F. Rakocinski, and J. N. McCall.
1998. Food, density, and microhabitat: factors affecting growth and recruitment potential of juvenile saltmarsh fishes. Environ. Biol. Fish. 53:89–103.
Baltz, D. M., C. Rakocinski, and J. W. Fleeger.
1993. Microhabitat use by marsh-edge fishes in a Louisiana estuary. Environ. Biol. Fish. 36:109–126.
Bearzi, M.
2005. Aspects of the ecology and behaviour of bottlenose dolphins (*Tursiops truncatus*) in Santa Monica Bay, California. J. Cetacean Res. Manag. 7:75–83.
Brager, S.
1993. Diurnal and seasonal behavior patterns of bottlenose dolphins (*Tursiops truncatus*). Mar. Mamm. Sci. 9:434–438.
Brager, S., J. A. Harraway, and B. F. J. Manly.
2003. Habitat selection in a coastal dolphin species (*Cephalorhynchus hectori*). Mar. Biol. 143:233–244.
Campbell, G. S., B. A. Bilgre, and R. H. Defran.
2002. Bottlenose dolphins (*Tursiops truncatus*) in Turneffe Atoll, Belize: occurrence, site fidelity, group size and abundance. Aquat. Mamm. 28:170–180.
Cockroft, V. G., and V. M. Peddemors.
1990. Seasonal distribution and density of common dolphins *Delphinus delphis* off the south-east coast of Southern Africa. S. Afr. J. Mar. Sci. 9:371–377.
Corkeron, P. J.
1990. Aspects of the behavioral ecology of inshore dolphins *Tursiops truncatus* and *Sousa chinensis* in Moreton Bay, Australia. *In* The bottlenose dolphin (S. Leatherwood and R. R. Reeves, eds.), p. 285–294. Academic Press, New York.
Day, Jr. J. W., C. A. S. Hall, W. M. Kemp, and A. Yáñez-Arancibia.
1989. Estuarine ecology, 576 p. Wiley Interscience, New York.
Gannon, D. P., and D. M. Waples.
2004. Diets of coastal bottlenose dolphins from the U.S. Mid-Atlantic coast differ by habitat. Mar. Mamm. Sci. 20:527–545.
Gaskin, D. E.
1968. Distribution of Delphinidae (Cetacea) in relation to sea-surface temperatures off eastern and southern New Zealand. N. Z. J. Mar. Freshw. Res. 2:527–534.
Gregory, P. R., and A. A. Rowden.
2001. Behaviour patterns of bottlenose dolphins (*Tursiops truncatus*) relative to tidal state, time-of-day, and boat traffic in Cardigan Bay, West Wales. Aquat. Mamm. 27:105–113.
Grigg, E., and H. Markowitz.
1997. Habitat use by bottlenose dolphins (*Tursiops truncatus*) at Turneffe Atoll, Belize. Aquat. Mamm. 23:163–170.
Harzen, S.
1998. Habitat use by the bottlenose dolphin (*Tursiops truncatus*) in the Sado Estuary, Portugal. Aquat. Mamm. 24:117–128.
Hastie, G. D., B. Wilson, L. J. Wilson, K. M. Parsons, and P. M. Thompson.
2004. Functional mechanisms underlying cetacean distribution patterns: hotspots for bottlenose dolphins are linked to foraging. Mar. Biol. 144:397–403.
Heithaus, M. R., and L. M. Dill.
2006. Does tiger shark predation risk influence foraging habitat use by bottlenose dolphins at multiple spatial scales? Oikos 114:257–264.
Hoese, H. D.
1971. Dolphin feeding out of water in a salt marsh. J. Mammal. 52:222–223.
Hoelzel, A. R., E. M. Dorsey, and S. J. Stern.
1989. The foraging specializations of individual minke whales. Anim. Behav. 45:581–591.
Ingram, S. N., and E. Rogan.
2002. Identifying critical areas and habitat preferences of bottlenose dolphins *Tursiops truncatus*. Mar. Ecol. Progr. Ser. 244:247–255.
Lusseau, D.
2005. Residency pattern of bottlenose dolphins *Tursiops* spp. in Milford Sound, New Zealand, is related to boat traffic. Mar. Ecol. Progr. Ser. 295:265–272.
Mendes, S., W. Turrell, T. Lütkebohle, and P. Thompson.
2002. Influence of the tidal cycle and a tidal intrusion front on the spatio-temporal distribution of coastal bottlenose dolphins. Mar. Ecol. Progr. Ser. 239:221–229.
Miller, C.
2003. Abundance trends and environmental habitat usage patterns of bottlenose dolphins (*Tursiops truncatus*) in lower Barataria and Caminada bays, Louisiana. Ph.D. diss., 125 p. Louisiana State Univ., Baton Rouge.
Miller, C., and N. Cribb.
2009. Describing cetacean habitat in Australian waters. La Mer 46:77–84.
Neumann, D. R.
2001. Seasonal movements of short-beaked common dolphins (*Delphinus delphis*) in the north-western Bay of Plenty, New Zealand: influence of sea-surface temperature and El Nino/La Nina. New Zeal. J. Mar. Freshw. Res. 35:371–374.
Redfern, J. V., M. C. Ferguson, E. A. Becker, K. D. Hyrenbach, C. Good, J. Barlow, K. Kaschner, M. F. Baumgartner, K. A. Forney, L. T. Ballance, P. Fauchald, P. Halpin, T. Hamazaki, A. J. Pershing, S. S. Qian, A. Read, S. B. Reilly, L. Torres, and F. Werner.
2006. Techniques for cetacean-habitat modelling. Mar. Ecol. Progr. Ser. 310:271–295.
Saucier, M. H., and D. M. Baltz.
1993. Spawning site selection by spotted seatrout (*Cynoscion nebulosus*) and black drum (*Pogonias cromis*) in Louisiana. Environ. Biol. Fish. 36:257–272.
Scott, M. D., and K. L. Cattanach.
1998. Diel patterns in aggregations of pelagic dolphins and tunas in the eastern Pacific. Mar. Mamm. Sci. 14:401–428.
Selzer, L. A., and P. M. Payne.
1988. The distribution of white-sided (*Lagenorhynchus acutus*) and common dolphins (*Delphinus delphis*) vs. environmental features of the continental shelf of the northeastern United States. Mar. Mamm. Sci. 4:141–153.
Shane, S., R. S. Wells, and B. Würsig.
1986. Ecology, behavior, and social organization of the bottlenose dolphin: a review. Mar. Mamm. Sci. 2:34–63.

Smolker, R., A. Richards, R. Connor, J. Mann, and P. Berggren.
1997. Sponge carrying by dolphins (Delphinidae, *Tursiops* sp.): A foraging specialization involving tool use? Ethology 103:454–465.

Stockin, K. A., C. R. Weir, and G. J. Pierce.
2006. Examining the importance of Aberdeenshire (UK) coastal waters for North Sea bottlenose dolphins (*Tursiops truncatus*). J. Mar. Biol. Assoc. U.K. 86:201–207.

Tershy, B. R., D. Breese, and C. S. Strong.
1990. Abundance, seasonal distribution and population composition of balaenopterid whales in the Canal de Ballenas, Gulf of California, Mexico. Rep. Int. Whal. Comm. Spec. Issue 12:369–375.

Waring, G. T., E. Josephson, C. P. Fairfield-Walsh, and K. Maze-Foley (eds.).
2007. US Atlantic and Gulf of Mexico marine mammal stock assessments—2007, 415 p. NOAA Tech. Memo. NMFS-NE-205 Woods Hole, MA.

Wilson, B., P. M. Thompson, and P. S. Hammond.
1997. Habitat use by bottlenose dolphins: seasonal distribution and stratified movement patterns in the Moray Firth, Scotland. J. Appl. Ecol. 34:1365–1374.

Würsig, B., and M. Würsig.
1977. The photographic determination of group size, composition, and stability of coastal porpoises (*Tursiops truncatus*). Science 198:755–756.

# A molecular genetic investigation of the population structure of Atlantic menhaden (*Brevoortia tyrannus*)

**Abigail J. Lynch**
**Jan R. McDowell (contact author)**
**John E. Graves**

Email address for contact author: McDowell@vims.edu

Virginia Institute of Marine Science
School of Marine Science
College of William and Mary
Rt. 1208 Greate Rd.
Gloucester Point, Virginia 23062

**Abstract**—Atlantic menhaden (*Brevoortia tyrannus*), through landings, support one of the largest commercial fisheries in the United States. Recent consolidation of the once coast-wide reduction fishery to waters within and around Chesapeake Bay has raised concerns over the possibility of the loss of unique genetic variation resulting from concentrated fishing pressure. To address this question, we surveyed variation at the mitochondrial cytochrome *c* oxidase subunit I (COI) gene region and seven nuclear microsatellite loci to evaluate stock structure of Atlantic menhaden. Samples were collected from up to three cohorts of Atlantic menhaden at four geographic locations along the U.S. Atlantic coast in 2006 and 2007, and from the closely related Gulf menhaden (*B. patronus*) in the Gulf of Mexico. Genetic divergence between Atlantic menhaden and Gulf menhaden, based on the COI gene region sequences and microsatellite loci, was more characteristic of conspecific populations than separate species. Hierarchical analyses of molecular variance indicated a homogeneous distribution of genetic variation within Atlantic menhaden. No significant variation was found between young-of-the-year menhaden (YOY) collected early and late in the season within Chesapeake Bay, between young-of-the-year and yearling menhaden collected in the Chesapeake Bay during the same year, between YOY and yearling menhaden taken in Chesapeake Bay in successive years, or among combined YOY and yearling Atlantic menhaden collected in both years from the four geographic locations. The genetic connectivity between the regional collections indicates that the concentration of fishing pressure in and around Chesapeake Bay will not result in a significant loss of unique genetic variation.

Manuscript submitted 23 January 2009.
Manuscript accepted 3 November 2009.
Fish. Bull. 108:87–97 (2010).

The views and opinions expressed or implied in this article are those of the author (or authors) and do not necessarily reflect the position of the National Marine Fisheries Service, NOAA.

Atlantic menhaden (*Brevoortia tyrannus*) is an ecologically and economically important species along the U.S. East Coast. As a filter-feeder and key prey fish, it provides a critical link between primary production and larger piscivorous predators, such as striped bass (*Morone saxatilis*), bluefish (*Pomatomus saltatrix*), and weakfish (*Cynoscion regalis*). The commercial fishery for Atlantic menhaden consists of a small bait fishery and a larger reduction fishery. Of the 20 menhaden reduction plants (where menhaden are "reduced" to meal and oil) that were once operating along the U.S. Atlantic coast, only the Reedville, Virginia, facility is currently active. The concentration of fishing effort for Atlantic menhaden in and around Chesapeake Bay has raised concerns among many environmentalists and sport fishermen about the possibility of "localized depletion" of Atlantic menhaden in the area. A potential consequence of localized depletion could be the loss of unique genetic variation within Atlantic menhaden, if there is spatial partitioning of genetic variation (stock structure) within the species.

Results of previous analyses of the stock structure of Atlantic menhaden have been discordant. Two populations of Atlantic menhaden, one north and the other south of Long Island, New York, were suggested on the basis of vertebral counts and transferrin allele frequencies (Sutherland, 1963; Epperly, 1989). Two populations, one north and one south of Cape Hatteras, North Carolina, have also been proposed. This division was based on the presence of small, sexually mature fish before the arrival of the larger, migrating fish in North Carolina waters and the presence of spawning fish off northern Florida in late winter and early spring (June and Nicholson, 1964). One coast-wide population has been indicated by tag recovery studies (Nicholson, 1978), which have shown that Atlantic menhaden of differing ages and sizes share the overwintering grounds off Cape Hatteras and undergo seasonal migrations and that larger fish travel farther north. The Atlantic States Marine Fisheries Commission currently assesses Atlantic menhaden as a single coast-wide stock.

In addition to the uncertainty regarding the stock structure of Atlantic menhaden, the relationship between Atlantic menhaden and Gulf menhaden (*B. patronus*) is not well understood. The mean values of several of the morphometric and meristic characters are significantly different between the two putative species, although the ranges of variation are coincident (Dahlberg, 1970). Similarly, preliminary genetic analyses indicate limited divergence between the putative species, and therefore the use of larger sample sizes and additional genetic characters have been recommended (Avise et al., 1989; Anderson, 2007).

**Table 1**

Collection location, date of collection, and number of Atlantic menhaden (*Brevoortia tyrannus*) and Gulf menhaden (*B. patronus*) analyzed in this study and range of sample fork lengths. For all collections outside the Chesapeake Bay, young-of-the-year (YOY) and yearling samples are pooled.

| Collection | Location | Date | *n* | Fork length (mm) |
|---|---|---|---|---|
| New England 2006 | Gloucester, MA | Aug. 2006 | 25 | 43–58 |
| New England 2007 | Gloucester, MA | Aug. 2007 | 25 | 34–64 |
| Mid-Atlantic 2006 | Pennsville, NJ | Aug. 2006 | 27 | 61–110 |
| Mid-Atlantic 2007 | Oakwood Beach, NJ | June 2007 | 25 | 77–190 |
| Chesapeake Bay YOY 2006 | Gloucester Point, VA | May 2006 | 25 | 27–67 |
| Chesapeake Bay yearling 2006 | Gloucester Point, VA | Aug. 2006 | 18 | 120–200 |
| Chesapeake Bay YOY (early) 2007 | Gloucester Point, VA | May 2007 | 25 | 34–84 |
| Chesapeake Bay YOY (late) 2007 | Gloucester Point, VA | Aug. 2007 | 31 | 35–99 |
| Chesapeake Bay yearling 2007 | Gloucester Point, VA | June 2007 | 18 | 114–184 |
| U.S. South Atlantic 2006 | Beaufort, SC | Aug. 2006 | 28 | 41–113 |
| U.S. South Atlantic 2007 | Beaufort, SC | April 2007 | 41 | 28–181 |
| Gulf menhaden 2006 | Galveston, TX | Oct. 2006 | 25 | not recorded |
| Gulf menhaden 2007 | Cameron, LA | Oct. 2007 | 25 | 52–91 |

In this study, analyses of sequence data from the mitochondrial cytochrome *c* oxidase subunit I (COI) gene region and allele frequencies of seven nuclear microsatellite loci were used to investigate the genetic relationships of Atlantic and Gulf menhaden, the stock structure of Atlantic menhaden, and to evaluate the potential for loss of unique genetic variation resulting from "localized depletion" of Atlantic menhaden within the Chesapeake Bay region.

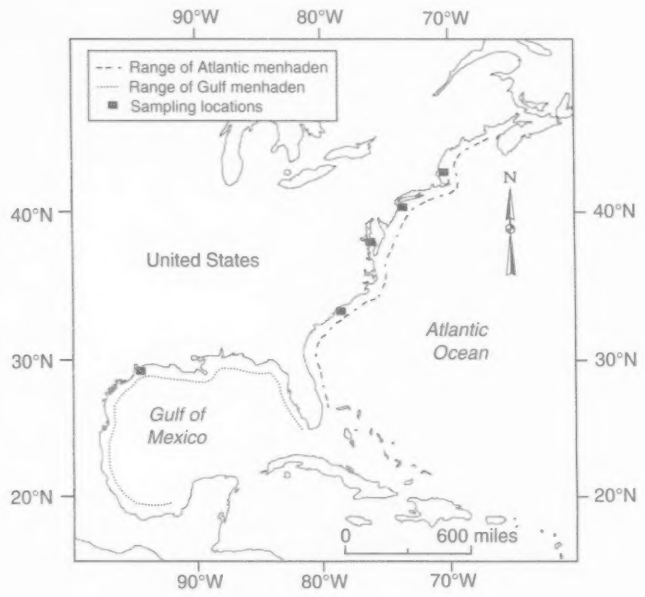


**Figure 1**

Map of ranges of Atlantic menhaden (*Brevoortia tyrannus*) and Gulf menhaden (*B. patronus*) and the approximate location of sites sampled in 2006–2007 for the analysis of stock structure in Atlantic menhaden.

## Materials and methods

### Sample collection

Young-of-the-year (YOY) and yearling Atlantic menhaden were sampled from New England (MA), the U.S. mid-Atlantic (NJ), Chesapeake Bay (VA), and the U.S. South Atlantic (SC) in 2006 and 2007, and YOY Gulf menhaden were sampled from the Gulf of Mexico in 2006 and 2007 (Table 1; Fig. 1). For all collections outside the Chesapeake Bay, samples of YOY and yearling Atlantic menhaden were pooled. For Chesapeake Bay collections, scales were aged from a subsample of 20% of individuals taken in 2007 and length was used as a surrogate for the remaining samples (where fish less than 100 mm fork length were considered YOY and fish greater than 100 mm fork length were considered yearling). The younger cohorts were sampled because they are less likely to have migrated far from where they were spawned. Local experts identified menhaden on the basis of morphological characters and capture location. Muscle tissue samples were taken from each individual and either frozen or stored in DMSO buffer (Seutin et al., 1991) at room temperature. Voucher specimens were retained from all U.S. Atlantic

coast regions in 2007 to corroborate field identifications. Some of the identifications were retroactively verified with sequences from a portion of the mtDNA control region, namely haplotypes were compared to those of Anderson (2007).

Total genomic DNA was extracted from each tissue sample by using a Qiagen DNeasy® Tissue Kit (Qiagen, Valencia, CA) and following the manufacturer's protocol. A 459 base-pair (bp) fragment of the mitochondrial cytochrome *c* oxidase subunit I (COI) gene region (F: 5′CTTTCGGCTACATGGGAATG3′ and R: 5′AGCCCTAGGAAGTGTTGTGG5′, GenBank accession number DQ867533), a 535-bp fragment of the mitochondrial control region (Pro-F: 5′ CTA CCY CYA ACT CCC AAA GC 3′, [Gray et al., 2008] and Phe-R: 5′ GTA AAG TCA CGA CCA AAC C 3′, [Brendtro et al., 2008], and eight microsatellite loci *Asa*2, *Asa*4, *Asa*16, [Brown et al., 2000]; *Aa*16, [Faria et al., 2004]; *Asa*B020, *Asa*C334, *Asa*D055, [Julian and Bartron, 2007]; *Sar*BH04, [Pereyra et al., 2004]), were amplified in either 5-μL (microsatellites) or 10-μL (COI) reaction volumes using the polymerase chain reaction (PCR) with the conditions outlined in Lynch (2008).

Mitochondrial PCR products were purified for sequencing by using column filtration with a QIAquick® PCR purification kit (Qiagen) following the manufacturer's protocol, and the concentration was measured with a BioMate™ 3 series UV Sspectrophotometer (Thermo Spectronic, Madison, WI). PCR products were prepared for sequencing with the ABI PRISM® BigDye™ Terminator, vers 3.1 cycle sequencing kit (Applied Biosystems, Foster City, CA) at a 1:8 dilution and sequenced on an 80-cm capillary ABI PRISM® 3130*xl* genetic analyzer (Applied Biosystems). Samples were sequenced in the forward and reverse direction.

The chromatographic curves for each 80-cm capillary sequence were analyzed using Sequencing Analysis Software, vers. 5.2 (Applied Biosystems). All mitochondrial sequences were edited with Sequencher 4.7.2 (Gene Codes Corp., Ann Arbor, MI), variable positions were confirmed visually, and sequences were aligned by using the ClustalW algorithm (Thompson et al., 1994) for multiple alignments in MacVector 9.0.1 (MacVector Inc., Cary, NC).

Microsatellite loci were amplified by PCR by using locus-specific fluorescent labels with the conditions outlined in Lynch (2008). Following amplification, 1 μL of PCR product for each locus was combined with PCR products from three other unique locus and fluorescent label combinations (4 μL total), 6 μL HiDi formamide (Applied Biosystems), and 0.3 μL 500 Liz Gene Scan Size standard (Applied Biosystems). The reaction mixture was denatured at 95°C for 10 minutes before being separated on a 36-cm capillary ABI PRISM® 3130*xl* Genetic Analyzer (Applied Biosystems) according to the manufacturer's protocol. The chromatic peaks for each microsatellite locus were scored by GeneMarker AFLP/Genotyping Software, vers. 1.60 (SoftGenetics, State College, PA). Once scored, MicroChecker 2.2.3 (Van Oosterhout et al., 2004) was used to check for the presence of null alleles and evidence of scoring errors. To ensure consistency, 20% of the samples were re-analyzed from the point of DNA extraction through allele scoring.

### Genetic analyses

Once aligned, the mitochondrial sequences were characterized in Arlequin 3.11 (Excoffier et al., 2005) to determine the number of haplotypes ($N_h$), number of polymorphic sites ($S$), and variable base-pair (bp) locations within a sequence set. Diversity indices, including haplotype diversity ($h$), nucleotide sequence diversity ($\pi$), and mean number of pairwise differences ($k$) within each collection were also estimated in Arlequin 3.11 (Excoffier et al., 2005). To visualize genetic relationships among mitochondrial sequences, median-joining networks were drawn in Network 4.2.0.1 (Bandelt et al., 1999).

For the microsatellite data, Genepop 3.4 (Raymond and Rousset, 1995) was used to determine observed heterozygosity ($H_O$) and expected heterozygosity ($H_E$) and to perform exact tests for deviations of genotypic distributions from the expectations of Hardy-Weinberg equilibrium for each locus at each collection location (10,000 iterations; Guo and Thompson, 1992). Significance levels were adjusted for multiple testing by using a Bonferroni correction (Rice, 1989). Arlequin 3.11 (Excoffier et al., 2005) was used to determine the number of alleles ($a$), and Microsatellite Analyzer (MSA) (Dieringer and Schlötterer, 2003) was used to determine the allele size range ($as$). Allelic richness ($R_s$) was estimated in FSTAT 2.9.3.2 (Goudet, 1995).

Using both mitochondrial COI sequence data ($\Phi_{ST}$) and nuclear microsatellite data ($F_{ST}/R_{ST}$), we performed a hierarchical analysis of molecular variance (AMOVA) to test for partitioning of variation among defined groups. The groups tested were the following: temporal collections within an age class at a location (e.g., 2007 YOY in Chesapeake Bay sampled early [May] and late [August] in the season), between collections of an age class taken at the same location in different years (e.g., the 2006 year class sampled in Chesapeake Bay as YOY in 2006 and yearling in 2007), between age classes within a region (e.g., YOY and yearling menhaden in Chesapeake Bay in 2007), among Atlantic coast regions both including and excluding the Gulf of Mexico (e.g., New England, mid-Atlantic, Chesapeake Bay, U.S. South Atlantic, and Gulf of Mexico), among COI clades (e.g., "Atlantic only," "ubiquitous," and "anomalous" samples), and between Atlantic and Gulf menhaden. AMOVA calculations based on microsatellite data were analyzed by using both $F_{ST}$ (Weir and Cockerham, 1984) and $R_{ST}$ (Slatkin, 1995) distance methods. Estimates of population pairwise $\Phi_{ST}$ and $F_{ST}/R_{ST}$ were calculated in Arlequin 3.11 (Excoffier et al., 2005) and adjusted for multiple testing with a Bonferroni correction (Rice, 1989).

To assess the statistical power for detecting population differentiation with the applied set of microsatellite markers and sample sizes, a simulation was implemented with POWSIM (Ryman and Palm, 2006), which

**Table 2**

Sequence statistics of Atlantic menhaden (*Brevoortia tyrannus*) and Gulf menhaden (*B. patronus*) based on cytochorme *c* oxidase subunit I (COI) gene region by location, clade, and across all locations: number of individuals ($n$), number of haplotypes ($N_h$), number of polymorphic sites ($S$), number of transitions ($Ts$), number of transversions ($Tv$), haplotype diversity ($h$), mean nucleotide sequence diversity ($\pi$), and mean number of pairwise differences ($k$) and standard error (SE).

| Collection | $n$ | $N_h$ | $S$ | $Ts$ | $Tv$ | $h$ ±SE | $\pi$ ±SE | $k$ ±SE |
|---|---|---|---|---|---|---|---|---|
| New England | 50 | 29 | 47 | 47 | 4 | 0.940 ±0.0206 | 0.0258 ±0.0132 | 11.8 ±5.45 |
| mid-Atlantic | 52 | 32 | 66 | 67 | 5 | 0.956 ±0.0163 | 0.0286 ±0.0145 | 13.1 ±6.01 |
| Chesapeake Bay | 117 | 50 | 62 | 63 | 3 | 0.932 ±0.0147 | 0.0267 ±0.0135 | 12.3 ±5.58 |
| U.S. South Atlantic | 69 | 44 | 66 | 67 | 2 | 0.954 ±0.0166 | 0.0295 ±0.0149 | 13.5 ±6.16 |
| Atlantic menhaden | 288 | 109 | 97 | 99 | 6 | 0.941 ±0.0084 | 0.0274 ±0.0137 | 12.6 ±5.69 |
| Gulf menhaden | 50 | 25 | 34 | 33 | 5 | 0.879 ±0.0419 | 0.0071 ±0.0041 | 3.23 ±1.70 |
| Atlantic + Gulf menhaden | 338 | 124 | 99 | 101 | 7 | 0.940 ±0.0079 | 0.0258 ±0.0129 | 11.8 ±5.37 |
| ubiquitous clade | 235 | 98 | 76 | 76 | 7 | 0.924 ±0.0138 | 0.0081 ±0.0045 | 3.71 ±1.88 |
| Atlantic only clade | 100 | 23 | 22 | 22 | 1 | 0.732 ±0.0456 | 0.0036 ±0.0024 | 1.65 ±0.98 |

estimates statistical power by testing different combinations of number of samples, sample sizes, number of loci, number of alleles, and allele frequencies for any hypothetical degree of differentiation ($F_{ST}$). To match the number of collection locations and magnitude of $F_{ST}$ estimates in this study, five hundred replicates were performed on five populations by using Fischer's method with the following combinations of effective population size ($N_e$) and generations of drift before sampling ($t$): 10,000: 50, 5000: 25, 1000: 5 ($F_{ST}$=0.0025); 10,000: 201, 5000: 100.5, 1000: 20.1 ($F_{ST}$=0.01); 10,000: 1025.8, 5000: 512.9, 1000: 102.6 ($F_{ST}$=0.05). The hypothetical sample sizes were set to the average across all loci for each sampling location. An additional simulation was performed with $t$=0, to assess $\alpha$ (type-I) error. The estimate of power was reported as the proportion of significant outcomes ($P$<0.05).

## Results

The COI fragment was sequenced for 289 Atlantic menhaden and 50 Gulf menhaden. Overall, the fragment contained 99 polymorphic sites (97 in Atlantic menhaden): 5 first codon positions, 1 second codon position, and 91 third codon positions; 101 transitions (99 in Atlantic menhaden), 7 transversions (6 in Atlantic menhaden); and produced 124 haplotypes (109 in Atlantic menhaden) (Table 2). All substitutions were synonymous, resulting in identical amino acid sequences. Haplotype diversity ($h$) estimates for the Atlantic and Gulf menhaden sampling locations ranged from 0.879 in Gulf menhaden to 0.956 in the U.S. mid-Atlantic, with an overall (pooled) estimate of 0.940 (0.941 for Atlantic menhaden). Mean nucleotide sequence diversity ($\pi$) estimates for Atlantic and Gulf menhaden sampling locations ranged from 0.0071 in Gulf menhaden to 0.030 in the U.S. South Atlantic, with an overall (pooled) estimate of 0.026 (0.027 for Atlantic menhaden). The mean number of pairwise differences ($k$) ranged from 3.2 in Gulf menhaden to 13.5 in the U.S. South Atlantic, with an overall (pooled) estimate of 12.6 for Atlantic menhaden and 11.8 for Atlantic and Gulf menhaden combined.

The median-joining network for the 109 COI Atlantic menhaden haplotypes showed two extensive clusters (clades) separated by 17 substitutions and one minor grouping of three individuals separated by 24 substitutions (Fig. 2). In order to discriminate between the alternate possibilities that either the three individuals were one of the other North American *Brevoortia* species that had been misidentified in the field as Atlantic menhaden, or that there is incomplete lineage sorting at the COI locus, the more rapidly evolving mitochondrial control region was sequenced and compared to those generated by Anderson (2007) for the four species of North American menhaden (GenBank accession numbers EF119342-EF119454). The control region sequences for the three individuals unambiguously clustered with the "ubiquitous large-scaled" menhadens in an unweighted pair group method with arithmetic mean (UPGMA) tree with these sequences, indicating that the field identifications were correct and that the result was likely attributable to incomplete lineage sorting at the COI locus. Examination of the microsatellite genotypes of these three individuals supported this conclusion.

The distribution of the two major COI clades differed among Atlantic and Gulf menhaden. Clade I, the "ubiquitous" clade, comprised all Gulf menhaden samples and 64% of Atlantic menhaden samples. Clade II, the "Atlantic-only" clade, comprised 35% of Atlantic menhaden samples and was not detected in Gulf menhaden (Table 2). A contingency table of the four Atlantic menhaden sampling locations indicated that clades I and II were homogeneously distributed among the U.S. Atlantic Coast sampling locations ($\chi^2$=0.478; $\chi^2_{0.05,3}$; $P$>0.05).

Eight microsatellite loci, *Aa*16, *Asa*2, *Asa*4, *Asa*16, *Asa*B020, *Asa*D055, *Asa*C334, and *Sar*BH04, were amplified for the Atlantic menhaden and Gulf menhaden

samples. The genotypic distributions of all loci in all samples conformed to the expectations of Hardy-Weinberg equilibrium with the exception of locus *Asa*16 (Table 3). Both the exact test in Genepop and the MicroChecker analysis revealed a significant or nearly significant deficiency of *Asa*16 heterozygotes in all samples, indicating the presence of a null allele. Consequently, this locus was not included in any of the population structure analyses.

For the seven remaining loci, the number of alleles ($a$) across all Atlantic menhaden samples ranged from 8 at *Aa*16 and *Asa*C334 to 22 at *Asa*B020, and the allelic richness ($R_s$) ranged from 7.98 at *Aa*16 to 21.8 at *Asa*B020. Allele size ranges were similar for Atlantic menhaden and Gulf menhaden across all seven loci. However, average $a$ and $R_s$ values across all loci were lower in Gulf menhaden as compared to Atlantic menhaden (Table 3).

AMOVAs of the COI haplotype data and microsatellite genotype data were performed to evaluate the temporal and spatial partitioning of genetic variation within Atlantic menhaden (Table 4). No significant differences were detected between early (May) and late (August) collections of YOY Atlantic menhaden in Chesapeake Bay in 2007. Likewise, no differences were detected among year classes of Atlantic menhaden in the Chesapeake Bay based on a comparison of YOY and yearling menhaden collected in Chesapeake Bay in 2006 or a comparison of YOY and yearling menhaden collected in Chesapeake Bay in 2007. Following the same cohort in the same location across years, a comparison of YOY menhaden collected in 2006 with yearling menhaden collected in 2007 in the Chesapeake Bay, did not result in a significant difference based on either the mitochondrial ($\Phi_{ST}$) or the microsatellite ($R_{ST}$). However, the microsatellite ($F_{ST}$) AMOVA produced a significant result, where 1.80% ($P$=0.02) of the variance was attributed to differences within the same cohort in Chesapeake Bay in successive years.

Samples of YOY and yearling menhaden (combined) from four geographic regions along the U.S. Atlantic Coast (New England, mid-Atlantic, Chesapeake Bay, and U.S. South Atlantic) were compared to test for evidence of spatial partitioning of genetic variation. Only the AMOVA based on the microsatellite $F_{ST}$ was significant, attributing 0.58% ($P$<0.001) of variation to sampling location. No pairwise comparisons of $\Phi_{ST}$, $F_{ST}$ or $R_{ST}$ revealed statistically significant variation between any two sampling regions of Atlantic menhaden after a Bonferroni correction (Table 5).

All pairwise comparisons between Atlantic menhaden and Gulf menhaden collections revealed statistically significant variation. The mitochondrial ($\Phi_{ST}$) AMOVA between Atlantic and Gulf menhaden attributed 18.2% ($P$<0.001) of the variance to differences between putative species. Likewise, in the microsatellite comparison, the $F_{ST}$ and $R_{ST}$ AMOVAs attributed 11.5% ($P$<0.001) and 38.75% ($P$<0.001) of variance to variation between Gulf and Atlantic menhaden samples.

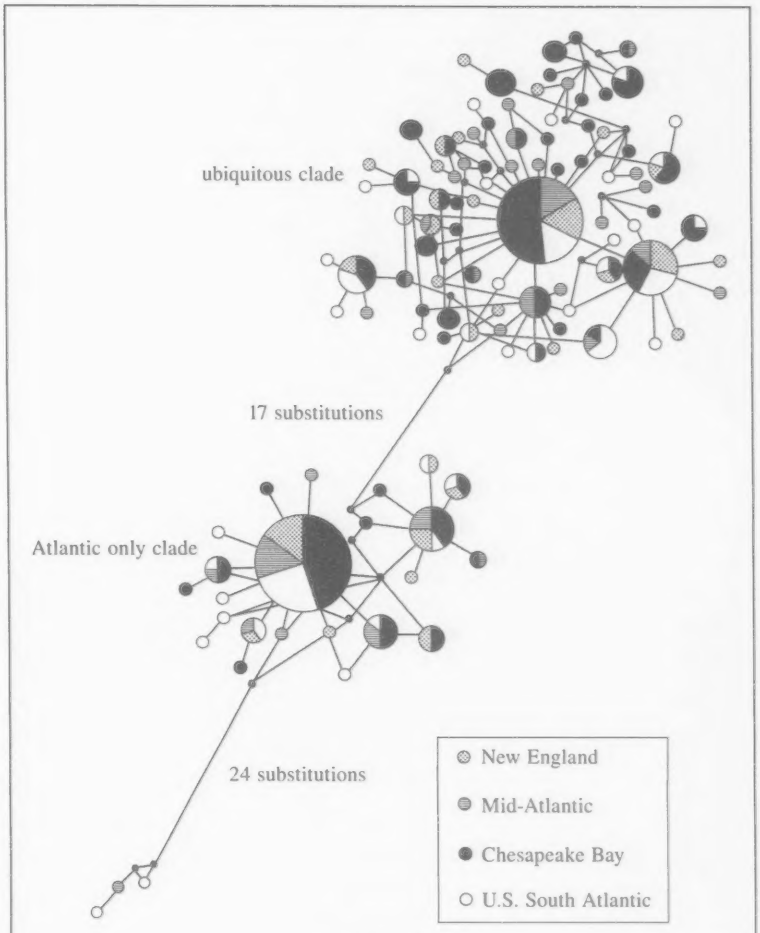


**Figure 2**

Median-joining network of 109 Atlantic menhaden (*Brevoortia tyrannus*, $n$=289) cytochrome $c$ oxidase subunit I (COI) haplotypes. The observed haplotypes are sized according to frequency and coded by area. Sample sizes: New England ($n$=50), mid-Atlantic ($n$=53), Chesapeake Bay ($n$=117), U.S. South Atlantic, ($n$=69). The hypothesized intermediate haplotypes are denoted by the smallest circles shaded dark gray.

**Table 3**

Summary statistics for Atlantic menhaden (*Brevoortia tyrannus*) and Gulf menhaden (*B. patronus*) collections by locus. Number of individuals (*n*), number of alleles (*a*), allele size range (*as*), allelic richness ($R_s$), observed heterozygosity ($H_O$), expected heterozygosity ($H_E$), and probability of conformance with Hardy-Weinberg Expectations (HWE). ** indicates significant deviation from the expectations of HWE after correction for multiple tests (initial $\alpha$=0.05, $k$=8).

| | Locus | | | | | | | | |
|---|---|---|---|---|---|---|---|---|---|
| Sample | *Aa*16 | *Asa*2 | *Asa*4 | *Asa*16 | *Asa*B020 | *Asa*C334 | *Asa*D055 | *Sar*BH04 | Average across loci |
| New England | | | | | | | | | |
| *n* | 47 | 44 | 44 | 45 | 47 | 49 | 44 | 40 | 45 |
| *a* | 7 | 6 | 9 | 16 | 13 | 8 | 15 | 12 | 10.75 |
| *as* | 139–155 | 210–237 | 168–204 | 247–292 | 142–184 | 118–146 | 254–314 | 179–221 | |
| *Rs* | 4.98 | 5.64 | 8.42 | 13.2 | 12.64 | 7.14 | 14.24 | 11.47 | 9.72 |
| *Ho* | 0.638 | 0.614 | 0.75 | 0.66 | 0.787 | 0.531 | 0.75 | 0.675 | 0.68 |
| *HE* | 0.709 | 0.6 | 0.722 | 0.809 | 0.894 | 0.593 | 0.907 | 0.72 | 0.74 |
| *HWE* | | | | ** | | | | | |
| mid-Atlantic | | | | | | | | | |
| *n* | 51 | 50 | 47 | 50 | 49 | 51 | 36 | 49 | 47.88 |
| *a* | 5 | 8 | 12 | 17 | 19 | 5 | 14 | 12 | 11.5 |
| *as* | 139–155 | 213–234 | 162–222 | 223–286 | 130–193 | 122–138 | 254–326 | 179–221 | |
| *Rs* | 4.07 | 7.15 | 11.0 | 14.4 | 17.75 | 4.41 | 14 | 10.8 | 10.45 |
| *HO* | 0.588 | 0.54 | 0.809 | 0.808 | 0.898 | 0.431 | 0.917 | 0.694 | 0.71 |
| *HE* | 0.625 | 0.659 | 0.839 | 0.877 | 0.902 | 0.436 | 0.917 | 0.759 | 0.75 |
| *HWE* | | | | | | | | | |
| Chesapeake Bay | | | | | | | | | |
| *n* | 116 | 113 | 101 | 110 | 115 | 113 | 112 | 110 | 111.25 |
| *a* | 7 | 9 | 12 | 21 | 20 | 7 | 18 | 13 | 13.38 |
| *as* | 139–155 | 210–237 | 162–198 | 223–298 | 130–196 | 122–146 | 238–334 | 179–221 | |
| *Rs* | 4.4 | 6.89 | 9.58 | 21 | 15.8 | 5.75 | 15.4 | 9.14 | 11 |
| *HO* | 0.586 | 0.584 | 0.752 | 0.773 | 0.904 | 0.593 | 0.893 | 0.627 | 0.71 |
| *HE* | 0.629 | 0.649 | 0.825 | 0.917 | 0.888 | 0.638 | 0.912 | 0.738 | 0.77 |
| *HWE* | | | | ** | | | | | |
| U.S. South Atlantic | | | | | | | | | |
| *n* | 53 | 68 | 53 | 69 | 66 | 63 | 63 | 56 | 61.38 |
| *a* | 7 | 7 | 12 | 18 | 19 | 6 | 17 | 12 | 12.25 |
| *as* | 139–157 | 216–237 | 165–201 | 223–289 | 130–187 | 118–138 | 238–326 | 179–221 | |
| *Rs* | 4.7 | 6.89 | 10.51 | 12.8 | 15.94 | 5.07 | 15.96 | 11.16 | 10.38 |
| *HO* | 0.691 | 0.662 | 0.698 | 0.797 | 0.833 | 0.556 | 0.905 | 0.625 | 0.72 |
| *HE* | 0.712 | 0.657 | 0.802 | 0.9 | 0.887 | 0.57 | 0.923 | 0.802 | 0.78 |
| *HWE* | | | | | | | | | |
| All Atlantic | | | | | | | | | |
| *n* | 268 | 276 | 246 | 274 | 278 | 277 | 256 | 256 | 266.38 |
| *a* | 8 | 10 | 18 | 23 | 22 | 8 | 20 | 15 | 15.5 |
| *as* | 139–157 | 210–237 | 162–222 | 223–298 | 130–196 | 118–146 | 238–334 | 179–221 | |
| *Rs* | 7.98 | 9.93 | 17.8 | 23 | 21.8 | 7.99 | 20 | 15 | 15.44 |
| *HO* | 0.621 | 0.6 | 0.751 | 0.785 | 0.867 | 0.543 | 0.875 | 0.647 | 0.71 |
| *HE* | 0.664 | 0.643 | 0.81 | 0.911 | 0.893 | 0.583 | 0.915 | 0.76 | 0.77 |
| *HWE* | | | | ** | | | | | |
| Gulf menhaden | | | | | | | | | |
| *n* | 49 | 49 | 44 | 45 | 49 | 49 | 45 | 44 | 46.75 |
| *a* | 9 | 10 | 10 | 15 | 19 | 9 | 18 | 12 | 12.75 |
| *as* | 135–161 | 210–237 | 165–198 | 223–298 | 130–196 | 118–154 | 258–330 | 169–215 | |
| *Rs* | 4.69 | 8.65 | 9.27 | 12.8 | 17.88 | 8.73 | 16.9 | 10.87 | 11.22 |
| *HO* | 0.449 | 0.653 | 0.682 | 0.7 | 0.896 | 0.898 | 0.864 | 0.4 | 0.69 |
| *HE* | 0.448 | 0.641 | 0.79 | 0.812 | 0.939 | 0.855 | 0.912 | 0.442 | 0.73 |
| *HWE* | | | | | | | | | |

**Table 4**

Analysis of molecular variance (AMOVA) among Atlantic menhaden (*Brevoortia tyrannus*) and Gulf menhaden (*B. patronus*) based on cytochorme *c* oxidase subunit I (COI) sequence data and seven microsatellite loci (*Aa*16, *Asa*2, *Asa*4, *Asa*B020, *Asa*D055, *Asa*C334, *Sar*BH04) grouped by collection time for Chesapeake Bay samples; by age class (following the 2006 year class) for Chesapeake Bay samples; by age class for Chesapeake Bay in 2006 and 2007; by region for all Atlantic coast samples (New England, mid-Atlantic, Chesapeake Bay, and U.S. South Atlantic); by region for large-scale samples (New England, mid-Atlantic, Chesapeake Bay, U.S. South Atlantic, and Gulf menhaden); by cytochrome *c* oxidase subunit I clade for large-scale samples ("Atlantic only" clade, "ubiquitous" clade, anomalous samples); and by putative species (Atlantic and Gulf menhaden). The distance methods used were pairwise differences ($\Phi_{ST}$), number of different alleles ($F_{ST}$), and sum of squared allele size differences ($R_{ST}$); all with 10,000 permutations. Bolded *P*-values indicate significance ($P<0.05$) after Bonferroni correction (initial $\alpha=0.05/2=0.025$).

| | $\Phi$-statistics | *P* | $F_{ST}$ | *P* | $R_{ST}$ | *P* |
|---|---|---|---|---|---|---|
| Grouped by collection time | | | | | | |
| between collection times | −0.0195 | 0.587 | 0.00096 | 0.398 | 0.0155 | 0.171 |
| Grouped by age class (in successive years) | | | | | | |
| between years | −0.0364 | 0.88 | 0.0294 | 0.047 | −0.00103 | 0.436 |
| Grouped by age class (within 2006) | | | | | | |
| between age classes | −0.0203 | 0.552 | −0.007 | 0.732 | −0.0087 | 0.52 |
| Grouped by age class (within 2007) | | | | | | |
| between age classes | −0.0033 | 0.382 | 0.0099 | 0.066 | 0.0233 | 0.114 |
| Grouped by region (Atlantic coast only) | | | | | | |
| among regions | −0.0089 | 0.920 | 0.0037 | 0.041 | −0.0053 | 0.902 |
| Grouped by region (large-scaled menhaden combined) | | | | | | |
| among regions | 0.0605 | <0.0001 | 0.0489 | <0.0001 | 0.0403 | <0.0001 |
| Grouped by COI clade | | | | | | |
| among clades | 0.8659 | <0.0001 | 0.00379 | 0.068 | 0.0059 | 0.148 |
| Grouped by putative species (Atlantic and Gulf menhaden) | | | | | | |
| between species | 0.176 | <0.0001 | 0.128 | <0.0001 | 0.102 | <0.0001 |
| among regions within a species | −0.00822 | 1 | 0.0043 | 0.0205 | −0.00511 | 0.872 |

**Table 5**

Estimates of pairwise $\Phi_{ST}$, above diagonal (*), and pairwise $F_{ST}$ (and $R_{ST}$), below diagonal, between regional collections of Atlantic menhaden (*Brevoortia tyrannus*) and Gulf menhaden (*B. patronus*) based on cytochorme *c* oxidase subunit I (COI) sequence data and seven microsatellite loci, respectively. Bolded values indicate significance after correction for multiple tests ($\alpha=0.05$, $k=3$ for comparisons within Atlantic menhaden).

| Collection | New England | mid-Atlantic | Chesapeake Bay | U.S. South Atlantic | Gulf |
|---|---|---|---|---|---|
| New England | * | −0.006 | −0.004 | −0.005 | **0.032** |
| mid-Atlantic | 0.004 (0.000) | * | −0.001 | −0.004 | **0.027** |
| Chesapeake Bay | 0.004 (−0.011) | 0.009 (−0.000) | * | −0.000 | **0.048** |
| U.S. South Atlantic | −0.006 (−0.012) | 0.010 (0.001) | 0.003 (−0.005) | * | **0.029** |
| Gulf menhaden | **0.106 (0.080)** | **0.157 (0.091)** | **0.130 (0.100)** | **0.106 (0.073)** | * |

The POWSIM analysis showed that 94.2%, 93.8%, and 92.6% of the tests where the $N_e$:$t$ combination led to $F_{ST}=0.0025$ (10,000: 50, 5000: 25, 1000: 5, respectively), 100% of the tests where the $N_e$:$t$ combination led to $F_{ST}=0.01$ (10,000: 201, 5000: 100.5, 1000: 20.1), and 100% of the tests where the $N_e$:$t$ combination led to $F_{ST}=0.05$ (10,000: 1025.8, 5000: 512.9, 1000: 102.6) were statistically significant, indicating that there was sufficient statistical power to detect population differences with the set of microsatellite markers and sample sizes used in this study.

## Discussion

The mitochondrial and nuclear markers employed in this analysis revealed considerable variation within Atlantic menhaden. The seven microsatellite loci surveyed were highly variable and the number of alleles per locus and average heterozygosities ($a=5–21$, $H_{exp}=0.435–0.924$) were within the range of variation reported for other clupeids ($a=1–56$, $H_{exp}=0.066–0.98$, Brown et al., 2000; McPherson et al., 2001; Olsen et al., 2002; Faria et al., 2004; Anderson and McDonald, 2007; Volk et al., 2007).

Typically, one would not consider using the mitochondrial COI gene region for an analysis of stock structure because this locus tends to be highly conserved in most organisms, exhibiting low levels of intraspecific variation (Meyer, 1993). However, previous studies have documented very high levels of variation throughout the Atlantic menhaden mitochondrial genome (Avise et al., 1989; Bowen and Avise, 1990; Anderson, 2007), and in a preliminary analysis of various menhaden mitochondrial gene regions, we found COI to be sufficiently variable for an analysis of stock structure. The COI genetic diversity in Atlantic menhaden ($\pi$=2.74%) is an order of magnitude higher than the average within-species divergence reported for other fishes. For example, Ward et al. (2005) reported an average $\pi$ of 0.39% for Australian marine fishes, and Hubert et al. (2008) reported a $\pi$ of 0.302% for Canadian freshwater fishes.

There were significant differences in the distribution of COI haploytpes and microsatellite allele frequencies between Atlantic and Gulf menhaden, although both classes of markers indicate the two species are very closely related ($F_{ST}$=0.104). These results are consistent with those of Anderson (2007) who surveyed variation at four microsatellite loci, estimating an $F_{ST}$ of 0.110 between Atlantic and Gulf menhaden. These $F_{ST}$ values are more typical of differences between populations than species. For comparison, $F_{ST}$ values between genetically distinct stocks of clupeid fishes based on microsatellites range from 0.002 to 0.226 (Shaw et al., 1999; Sugaya et al., 2008), and are approximately one-fourth of the $F_{ST}$ values between other pairs of North American menhadens (0.355–0.488; Anderson, 2007).

A low level of genetic divergence between Atlantic and Gulf menhaden was also noted for the mitochondrial COI gene region ($\Phi_{ST}$=0.178)—a result consistent with a previous restriction fragment length polymorphism (RFLP) analysis of the mitochondrial genome (Avise et al., 1989) and sequence analysis of the control region (Anderson, 2007) of these two species. In the present study, we did not find a single COI nucleotide position that distinguished Atlantic from Gulf menhaden. In a survey of 207 fishes, including several congeners, Ward et al. (2005) reported that all had different COI sequences. Furthermore, mean nucleotide differences between closely related species were 25 times higher (on average) than differences within species. In the present study, however, the nucleotide sequence diversity for Atlantic and Gulf menhaden combined ($\pi$=0.0258) was less than that for Atlantic menhaden alone ($\pi$=0.0274).

When compared with Gulf menhaden, Atlantic menhaden are generally larger, have a less convex body shape, and have a higher number of predorsal scales, vertebrae, and ventral scutes (Bigelow et al., 1963). Although the mean values of some of the morphometric and meristic characters are significantly different between the two species, the ranges of variation are coincident (Dahlberg, 1970). Although Atlantic menhaden and Gulf menhaden are morphologically similar, their geographic ranges are not believed to overlap (Bigelow et al., 1963). Thus, the species are typically distinguished by capture location. The high level of genetic and morphological similarity of Atlantic and Gulf menhaden raises concern over the validity of the two species. A thorough morphological and genetic analysis of the same individuals will be required to resolve this problem.

In the present analysis of Atlantic and Gulf menhaden mitochondrial COI gene region sequences, two distinct mitochondrial clades were noted, one of which was found only in Atlantic menhaden, and the other in both Atlantic and Gulf menhaden. These results are similar to those found in a previous RFLP analysis of the whole mitochondrial genome (Avise et al., 1989) and in a sequence analysis of the control region (Anderson, 2007). Avise (1992) hypothesized that the separation of two mitochondrial clades between the Atlantic Ocean and the Gulf of Mexico was a result of historical isolation of Atlantic and Gulf menhaden by the Florida peninsula during times of cooler water temperatures and subsequent unidirectional gene flow during geologically recent times. Anderson (2007) postulated that the distribution of these two clades in Atlantic menhaden supported very recent gene flow between Atlantic and Gulf menhaden because the highest frequency of "Atlantic-only" haplotypes occurred in the northernmost Atlantic menhaden sampling location. However, the purported geographic cline in the distribution of the "Atlantic-only" clade haplotypes was only qualitatively addressed and was based on a small sample size ($n$=37) of Atlantic menhaden. In the present study, the more extensive sampling regime for Atlantic menhaden along the U.S. Atlantic coast ($n$=289) refutes Anderson's (2007) hypothesis, because a chi-square analysis of the presence of the two clades among Atlantic coast sampling locations did not indicate a heterogeneous distribution.

### Population structure

Stock structure analyses of Atlantic menhaden along the U.S. Atlantic coast have indicated as few as one and as many as three different stocks based on spawning time, spawning location, and migration tracks (Sutherland, 1963; June and Nicholson, 1964; Nicholson, 1978; Epperly, 1989). We analyzed the distribution of allelic variation of rapidly evolving molecular characters to evaluate population structure of Atlantic menhaden. The resulting AMOVAs did not reveal any significant portion of molecular variance was due to variation between the following group comparisons: YOY menhaden collected in Chesapeake Bay early and late in the season during the same year; YOY and yearling menhaden collected in Chesapeake Bay in successive years (following the 2006 year class); YOY and yearling menhaden collected in Chesapeake Bay in the same year (comparing 2005–2006, 2006–2007 year classes); and YOY and yearling menhaden (combined) from the four geographic regions along the U.S. Atlantic coast (New England, mid-Atlantic, Chesapeake Bay, and U.S. South Atlantic). The POWSIM analysis indicates that the sample sizes and

suite of microsatellite markers used in this study were sufficient for detecting even weak levels of differentiation ($F_{ST} \geq 0.0025$).

Although none of the five COI $\Phi_{ST}$ AMOVAs or five microsatellite $R_{ST}$ AMOVAs were significant, two of the five microsatellite $F_{ST}$ AMOVAs showed a small but statistically significant partitioning of genetic variation between YOY and yearling menhaden collected in Chesapeake Bay in successive years (following the 2006 year class, 1.80%, $P=0.0176$) and YOY and yearling menhaden (combined) from the four geographic regions along the U.S. Atlantic coast (0.575%, $P=0.0000$).

The pairwise comparisons between sample locations corroborate the $\Phi_{ST}$ and $R_{ST}$ AMOVA results. No pairwise comparison revealed a statistically significant difference between any two of the four geographic regions of Atlantic menhaden after Bonferroni correction. These findings support the hypothesis that the significant results from the $F_{ST}$ AMOVAs were a result of random processes and not biologically meaningful (for a discussion see Waples, 1998). The collective results indicate no significant partitioning of genetic variation between the sampling regions of Atlantic menhaden, and the null hypothesis that Atlantic menhaden comprise a single stock along the U.S. Atlantic coast cannot be rejected.

The lack of statistically significant genetic differences among Atlantic menhaden sampling regions is consistent with the life history traits of the species. Of all the North American *Brevoortia*, Atlantic menhaden undertake the longest coastal migrations and have the most temporally and geographically protracted spawning season (Whitehead, 1985). Atlantic menhaden are batch spawners, spawning multiple times during a year. Additionally, Atlantic menhaden larvae are found in waters from Maine to Mexico and are the most widely distributed larvae of any clupeoid in the western North Atlantic; (Kendall and Reintjes, 1975). The larvae can take up to 90 days to cross the continental shelf and are affected by along-shore transport, coastal storms, freshwater discharge from estuaries, and wind-forcing (Checkley et al., 1988). Menhaden also undergo an ontogenetic shift in migration, where larger fish migrate farthest north (Dryfoos et al., 1973). These characteristics appear to keep Atlantic menhaden—and their gene pool—well mixed.

Population structure has not been found in genetic analyses of other clupeids including Atlantic herring (*Clupea harengus*) (Grant, 1984), twaite shad (*Alosa fallax*) (Volk et al., 2007), and European pilchard (*Sardina pilchardus*) (Gonzalez and Zardoya, 2007). In contrast, some clupeid species exhibit significant stock structure, often attributed to the presence of geographic barriers or temporal reproductive isolation. These include Pacific herring (*Clupea pallasi*) stocks in the eastern North Pacific and Bering Sea (Grant and Utter, 1984), in the Bering Sea and Gulf of Alaska separated by the Alaska Peninsula (O'Connell et al., 1998), and from Honshu and Hokkaido Islands (Sugaya et al., 2008). Shaw et al. (1999) also found significant genetic structuring between Icelandic summer-spawners, Norwegian spring-spawners, and Norwegian fjord stocks of Atlantic herring.

### Implications for management

Loss of unique genetic variation due to fishing pressure, habitat degradation, and hatchery stocking has been reported for Pacific cod (*Gadus macrocephalus*), leopard darter (*Percina panterina*), Japanese flounder (*Paralichthys olivaceus*), and American shad (*Alosa sapidissima*) (Grant and Stahl, 1988; Echelle et al., 1999; Brown et al., 2000; Sekino et al., 2003), and there is concern that a concentration of fishing effort in and around Chesapeake Bay could result in the loss of unique genetic variation in Atlantic menhaden. In this study we have demonstrated high genetic variability and a homogeneous distribution of genetic variation within Atlantic menhaden from four sampling locations along the U.S. Atlantic coast—a result consistent with the current management practice that recognizes a single stock of Atlantic menhaden. The apparent genetic connectivity between New England, mid-Atlantic, Chesapeake Bay, and U.S. South Atlantic samples indicates that loss of unique genetic variation due to the consolidation of fishing pressure in Chesapeake Bay is not likely. Our analysis of mitochondrial and nuclear loci revealed significant allele frequency differences between Atlantic and Gulf menhaden, supporting independent management of these resources. However, the small magnitude of these differences found in this and previous studies would indicate that a re-evaluation of the specific status of the two putative species, based on analyses of morphological and genetic characters, is warranted.

## Acknowledgments

This project was funded by the Virginia Marine Resources Commission (RF-07-06). We thank J. Anderson, J. Archambault, H. Corbett, B. Dailey, P. Lynch, G. Nelson, and T. Tuckey for providing menhaden samples. This is Virginia Institute of Marine Science contribution no. 3049.

## Literature cited

Anderson, J. D.
2007. Systematics of the North American menhadens: molecular evolutionary reconstructions in the genus *Brevoortia* (Clupeiformes: Clupeidae). Fish. Bull. 205:368–378.

Anderson, J. D., and D. L. McDonald.
2007. Morphological and genetic investigations of two western Gulf of Mexico menhadens (*Brevoortia* spp.). J. Fish Biol. 70: 139–147.

Avise, J. C.
1992. Molecular population structure and biogeographic history of a regional fauna: a case history with lessons for conservation biology. Oikos 63:62–76.

Avise, J. C., B. W. Bowen, and T. Lamb.
1989. DNA fingerprints from hypervariable mitochondrial genotypes. Mol. Biol. Evol. 6:258–269.

Bandelt, H., P. Forster, and A. Röhl.
1999. Median-joining networks for inferring intraspecific phylogenies. Mol. Biol. Evol. 16:37–48.

Bigelow, H. B., M. G. Bradbury, J. R. Dymond, J. R. Greeley, S. F. Hildebrand, G. W. Mead, R. R. Miller, L. R. Rivas, W. C. Schroeder, R. D. Suttkus, and V. D. Vladykov.
1963. Genus *Brevoortia* Gill 1861: Menhaden. *In* Fishes of the western North Atlantic (H. B. Bigelow, ed.), p. 343–380. Sears Foundation Mar. Res., Yale Univ., New Haven, CT.

Bowen, B. W., and J. C. Avise.
1990. Genetic structure of Atlantic and Gulf of Mexico populations of sea bass, menhaden, and sturgeon: influence of zoogeographic factors and life-history patterns. Mar. Biol. 107:371–381.

Brendtro K. S., J. R. McDowell, and J. E. Graves.
2008. Population genetic structure of escolar (*Lepidocybium flavobrunneum*). Mar. Biol. 155:11–22.

Brown, B. L., T. P. Gunter, J. M. Waters, and J. M. Epifanio.
2000. Evaluating genetic diversity associated with propagation-assisted restoration of American shad. Conserv. Biol. 14:294–303.

Checkley, D. M., S. Raman, G. L. Mailet, and K. M. Mason.
1988. Winter storm effects on the spawning and larval drift of a pelagic fish. Nature 335:346–348.

Dahlberg, M. D.
1970. Atlantic and Gulf of Mexico menhadens, Genus *Brevoortia* (Pisces: Clupeidae). Bull. Fla. Mus. Nat. Hist. Biol. Sci.15:91–162.

Dieringer, D., and C. Schlötterer.
2003. Microsatellite analyzer (MSA): a platform independent analysis tool for large microsatellite data sets. Mol. Ecol. Notes 3:167–169.

Dryfoos, R. L., R. P. Cheek, and R. L. Kroger.
1973. Preliminary analyses of Atlantic menhaden, *Brevoortia tyrannus*, migrations, population structure, survival and exploitation rates, and availability as indicated from tag returns. Fish. Bull. 71:719–734.

Echelle, A. F., A. A. Echelle, L. R. Williams, C. S. Toepfer, and W. L. Fischer.
1999. Allozyme perspective on genetic variation in a threatened percid fish, the leopard darter (*Percina pantherina*). Am. Midl. Nat. 142:393–400.

Epperly, S. P.
1989. A meristic, morphometric and biochemical investigation of Atlantic menhaden, *Brevoortia tryannus* (Latrobe). J. Fish Biol. 35:139–152.

Excoffier, L., G. Laval, and S. Schneider.
2005. Arlequin (vers. 3.0): an integrated software package for population genetics data analysis. Evol. Bioinformatics Online 1:47–50.

Faria R., S. Wallner, S. Weiss, and P. Alexandrino.
2004. Isolation and characterization of eight dinucleotide microsatellite loci from two closely related clupeid species (*Alosa alosa* and *A. fallax*). Mol. Ecol. Notes 4:586–588.

Gonzalez E. G., and R. Zardoya.
2007. Isolation and characterization of polymorphic microsatellites for the sardine *Sardina pilchardus* (Clupeiformes: Clupeidae). Mol. Ecol. Notes 7:519–921.

Goudet, J.
1995. FSTAT (vers. 1.2): A computer program to calculate F-statistics. J. Hered. 86:485–486.

Grant W. S.
1984. Biochemical population genetics of Atlantic herring, *Clupea harengus*. Copeia 1984:357–364.

Grant W. S., and G. Stahl.
1988. Description of electrophoretic loci in Atlantic cod, *Gadus morhua*, and comparison with Pacific cod, *Gadus macrocephalus*. Hereditas 108:27–36.

Grant W. S., F. M. Utter.
1984. Biochemical population genetics of Pacific herring (*Clupea pallasi*). Can. J. Fish. Aquat. Sci. 41:856–864.

Gray, K. N., J. R. McDowell, B. B. Collette, and J. E. Graves.
2008. An investigation of the global stock structure of the marlinsucker (*Remora osteochir*) inferred from mitochondrial control region sequence data. Bull. Mar. Sci. 84:25–42.

Guo, S. W., and E. A. Thompson.
1992. Performing the exact test for Hardy-Weinberg proportion for multiple alleles. Biometrics 48:361–372.

Hubert, N., R. Hanner, E. Holm, N. E. Mandrak, E. Taylor, M. Burridge, D. Watkinson, A. Curry, P. Bentzen, J. Zhang, J. April, and L. Bernatchez.
2008. Identifying Canadian freshwater fishes through DNA barcodes. PLoSONE 3(6):e2490.

Julian, S. E., and M. L. Bartron.
2007. Microsatellite DNA markers for American shad (*Alosa sapidissima*) and cross-species amplification within the family Clupeidae. Mol. Ecol. Notes 1:1–3.

June, F. C., and W. R. Nicholson.
1964. Age and size composition of the menhaden catch along the Atlantic coast of the United States, 1958. U.S. Fish Wildl. Serv. Spec. Sci. Rep. Fish. 446:1–25.

Kendall, A. W., Jr., and J. W. Reintjes.
1975. Geographic and hydrographic distribution of Atlantic menhaden eggs and larvae along the middle Atlantic coast from *RV* Dolphin Cruises, 1965–66. Fish. Bull. 73:317–330.

Lynch, A. J.
2008. A molecular analysis of Atlantic menhaden (*Brevoortia tyrannus*) stock structure. M.S. thesis, 120 p. Virginia Inst. Mar. Sci., College of William and Mary, Gloucester Point, VA.

McPherson, A. A., P. T. O'Reilly, T. L. McParland, W. M. Jones, and P. Bentzen.
2001. Isolation of nine novel tetranucleotide microsatellites in Atlantic herring (*Clupea harengus*). Mol. Ecol. Notes 1:31–32.

Meyer, A.
1993. Evolution of mitochondrial DNA in fishes. *In* Biochem. Mol. Biol. Fishes, vol. 2 (P. W. Hochachka, and T. P. Mommsen, eds.), p. 1–38. Elsevier Sci., Amsterdam, Netherlands.

Nicholson, W. R.
1978. Movements and population structure of Atlantic menhaden indicated by tag returns. Estuaries 1:141–150.

O'Connell M., M. C. Dillon, and J. M. Wright.
1998. Development of primers for polymorthic microsatellite loci in Pacific herring (*Clupea harengus pallasi*). Mol. Ecol. 7:357–363.

Olsen, J. B., C. J. Lewis, E. J. Kretschmer, S. L. Wilson, and J. E. Seeb.
2002. Characterization of 14 tetranucleotide microsatellite loci derived from Pacific herring. Mol. Ecol. Notes 2:101–103.

Pereyra, R. T., E. Saillant, C. L. Pruett, Rexroad III, C. E., and A. Rocha-Olivares.
2004. Characterization of polymorphic microsatellites in the Pacific sardine *Sardinops sagax sagax* (Clupeidae). Mol. Ecol. Notes 4:739–741.

Raymond, M., and F. Rousset.
1995. GENEPOP (vers. 1.2): population genetics software for exact test and ecumenicism. J. Hered. 86:248–249.

Rice, W. R.
1989. Analyzing tables of statistical tests. Evolution 43:223–225.

Ryman, N., and S. Palm.
2006. POWSIM: a computer program for assessing statistical power when testing for genetic differentiation. Mol. Ecol. Notes. 6:600–602.

Sekino, M., K. Saitoh, T. Yamada, A. Kumagai, M. Hara, and Y. Yamashita.
2003. Microsatellite-based pedigree tracing in a Japanese flounder *Paralichthys olivaceus* hatchery strain: implications for hatchery management related to stock enhancement program. Aquaculture 221:255–263.

Seutin, G., B. N. White, and P. T. Boag.
1991. Preservation of avian blood and tissue samples for DNA analyses. Can. J. Zool. 69:82–90.

Shaw, P. W., C. Turan, J. M. Wright, M. O'Connell, and G. R. Carvalho.
1999. Microsatellite DNA analysis of population structure in Atlantic herring (*Clupea harengus*), with direct comparison to allozyme and mtDNA RFLP analyses. Heredity 83:490–499.

Slatkin, M.
1995. A measure of population subdivision based on microsatellite allele frequencies. Genetics 139:457–462.

Sugaya T., M. Sato, E. Yokoyama, Y. Nemoto, T. Fujita, H. Okouchi, K. Hamasaki, and S. Kitada.
2008. Population genetic structure and variability of Pacific herring *Clupea pallasii* in the stocking area along the Pacific coast of northern Japan. Fish. Sci. 74:579–588.

Sutherland, D. F.
1963. Variation in vertebral numbers of juvenile Atlantic menhaden. U.S. Fish. Wildl. Serv. Spec. Sci. Rep. Fish. 435:1–8.

Thompson, J. D., D. G. Higgins, and T. J. Gibson.
1994. CLUSTALW: improving the sensitivity of progressive multiple sequence alignment through sequence weighting positions-specific gap penalties and weight matrix choice. Nucleic Acids Res. 22:4673–4680.

Van Oosterhout C., B. Hutchinson, D. Wills, and P. Shipley.
2004. Micro-Checker (vers. 2.23): microsatellite data checking software. Mol. Ecol. Notes 4:535–538.

Volk, J. D., Bekkevold, and V. Loeschcke.
2007. Weak population differentiation in northern European populations of the endangered anadromous clupeid *Alosa fallax*. J. Fish Biol. 71:461–469.

Waples, R. S.
1998. Separating the wheat from the chaff: patterns of genetic differentiation in high gene flow species. J. Hered. 89:438–450.

Ward, R. D., T. S. Zemlak, B. H. Innes, P. R. Last, and P. D. N. Herbert.
2005. DNA barcoding Australia's fish species. Philos. Trans. R. Soc. Lond., Ser. B: Biol. Sci. 360:1847–1857.

Weir, B. S., and C. C. Cockerham.
1984. Estimating *F*-Statistics for the analysis of population structure. Evolution 38:1358–1370.

Whitehead, P. J. P.
1985. Clupeoid fishes of the world (Suborder Clupeoidei): an annotated and illustrated catalogue of the herrings, sardines, pilchards, sprats, shads, anchovies, and wolf-herrings: part 1—Chirocentridae, Clupeidae and Pristigasteridae. FAO Fish. Synop. 7:210–217.

# Variation in the isotopic signatures of juvenile gray snapper (*Lutjanus griseus*) from five southern Florida regions

**Trika Gerard (contact author)**

**Barbara Muhling**

Email address for contact author: trika.gerard@noaa.gov

National Oceanic and Atmospheric Administration
National Marine Fisheries Service
Southeast Fisheries Science Center
75 Virginia Beach Dr.
Miami, Florida 33149

**Abstract**—Measurements of $^{18}O/^{16}O$ and $^{13}C/^{12}C$ ratios in the carbonate of juvenile gray snapper (*Lutjanus griseus*) sagittal otoliths collected during 2001–2005 from different southern Florida regions indicated significant variations in the ratios between Florida Bay and surrounding areas. Annual differences in isotopic composition were also observed. Classification accuracy of individual otoliths to a region averaged 80% (63% to 96%), thereby enabling the probability of assigning an unknown individual to the appropriate juvenile nursery habitat. Identification of isotopic signatures in the otoliths of gray snapper from Florida Bay and adjacent ecosystems may be important for distinguishing specific portions of the bay that are crucial nursery grounds for juveniles. Separation of gray snapper between geographic regions and nursery sites is possible and has the potential to establish a link between adult gray snapper present on offshore reefs and larvae and juveniles at nursery habitats in Florida Bay or adjacent areas.

Manuscript submitted 4 December 2008.
Manuscript accepted 6 November 2009.
Fish. Bull. 104:98–105 (2010).

The views and opinions expressed or implied in this article are those of the author (or authors) and do not necessarily reflect the position of the National Marine Fisheries Service, NOAA.

Identification of nursery habitats is important for effective management of coral reef fishes. Many reef fish are commercially, recreationally, and ecologically important and are believed to migrate to reefs from juvenile nursery areas such as seagrass and mangrove habitats. Little is known about the nature of these nursery areas or the migration corridors that exist between nursery areas and coral reefs. Otolith microchemistry is a proven method for determining the early stage habitats of juvenile fishes, particularly if tagging studies are not feasible (Gao et al., 2004). Trace elements and stable isotopes obtained from the otoliths of teleost fish have been well documented as useful tools for providing a wealth of information on environmental variations and stock structure of fish throughout their life history (Stephenson et al., 2001). New research has shown that the stable isotopic composition of otoliths provides a way of identifying fish that have inhabited different water masses, therefore serving as a tracer for distinguishing various nursery habitats of fish populations (Ashford and Jones, 2006).

The application of the stable isotopic composition of otoliths as a natural chemical tag can help in the evaluation of the significance of estuaries as nursery grounds for coral reef fish, and determine which habitats, such as seagrass beds, mangrove islands, and mangrove shorelines, within an estuary are most important as nursery areas for producing adult coral reef fish. Each of these habitats supplies juvenile reef fish with nutrition and shelter from predators. Gray snapper (*Lutjanus griseus*) juveniles are often present in a variety of estuarine ecosystems with soft and hard bottom habitats and with a wide range of temperatures and salinities (Bortone and Williams[1]).

Gray snapper are an economically important Florida reef fish. They make up a large proportion of the commercial and recreational finfish landings for the state and are the most popular game fish, with the highest recreational landings in Florida Bay (Starck and Schroeder, 1971; Lara et al., 2008). After spawning, larvae spend approximately 20–35 days as pelagic plankton at sizes ranging from 10–20 mm standard length (SL). They then settle as early juveniles in seagrass beds at sizes of approximately 40–50 mm SL (Richards et al., 2005) and migrate to coral reef habitats as adults.

The goal of this study was to analyze and assess the spatial and temporal variation of stable isotopic carbon and oxygen composition in the otoliths of juvenile gray snapper from southern Florida. This analysis will help determine the importance of Florida Bay as a nursery ground

[1] Bortone, S., and J. Williams. 1986. Species profiles: Life histories and environmental requirements of coastal fishes and invertebrates (South Florida)—gray, lane, mutton, and yellowtail snappers. U. S. Fish and Wildlife Service Biol. Rep. 82(11.52), 18 p.

before juvenile gray snapper make an ontogenetic shift to the nearby Florida reef tract. We examined variation in the otolith stable isotopic chemistry ($\delta^{13}C$ and $\delta^{18}O$) of juvenile gray snapper among various regions of southern Florida, and among sites within these regions, over four years. Differences in isotopic composition of the otoliths for regions and sites were used to determine if, and at what spatial scale, specific nursery grounds for juvenile gray snapper exist.

## Materials and methods

### Sample collection

A total of 317 juvenile gray snapper were collected between 2001 and 2005 from 27 sites within five geographical regions of Southern Florida: Ten Thousand Islands, Biscayne Bay, Florida Bay, Lower Florida Keys, and Dry Tortugas (Fig. 1). Eight to ten fish per site collected in 2002 and 2003 were used for an analysis of spatial variation and ten each from two sites collected in 2001, 2002, 2004, and 2005 were used for an analysis of temporal variation. The fish sampled ranged from 50 to 210 mm SL. For consistency, only gray snapper measuring 100 mm SL or larger, collected between May and September, were used in statistical analyses. Habitats at the sites varied from seagrass beds to mangrove islands and mangrove-lined coastlines. All samples were obtained by using traditional hook-and-line gear, baited with fresh shrimp, except for the collection of gray snapper from the Ten Thousand Islands region that was obtained from bycatch of crab traps. Juvenile gray snapper were collected between March and November. Samples remained frozen until dissection for removal of otoliths.

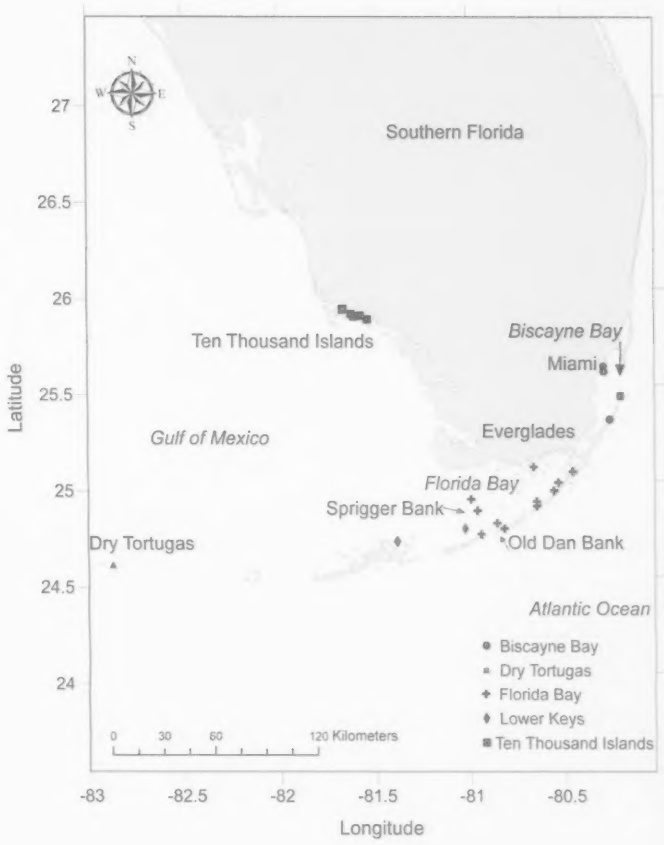


**Figure 1**

Collection sites for juvenile gray snapper (*Lutjanus griseus*) from five southern Florida regions: Ten Thousand Islands, Florida Bay, Biscayne Bay, Lower Keys, and Dry Tortugas. Gray snapper were collected in the summer of 2002 and 2003 for analysis of otolith microchemistry in order to identify individuals to specific nursery sites.

### Sample analysis

According to Campana (1999), there is no significant difference in the chemical composition between the left or right otolith of a fish; therefore either otolith was randomly chosen. All dissection, cleaning, and drying of otoliths were conducted in a class-100 laminar flow clean hood by using acid-washed glass knives and probes. After the removal of all extraneous tissue, the otoliths were rinsed with milli-Q water.

Otoliths are composed of 96% calcium carbonate in the form of aragonite, 3% protein, and 1% inorganics (Arslan and Paulson, 2003); therefore, deproteination procedures were conducted on all otoliths. During deproteination, the mass of the whole otolith was obtained; then whole otoliths were crushed to a fine powder with an agate mortar and pestle and transferred to a 15 ml plastic centrifuge tube. For otoliths larger than 17 mg, only one half or one quarter of the crushed whole otolith powder was used. Depending on the otolith mass, various volumes of 10% sodium hypochlorite were added to the crushed otolith and the mixture was allowed to sit for 48 hours. Samples were rinsed with milli-Q water and centrifuged for 1.5 minutes between rinses before being dried in an oven at 60°C for six hours (Gaughan et al.[2]). Stable isotope analyses were carried out at the University of Miami Stable Isotope Laboratory, Miami,

[2] Gaughan, D. J., G. A. Baudains, R. W. D. Mitchell, and T. I. Leary. 2001. Pilchard *(Sardinops sagax)* nursery areas and recruitment process assessment between different regions in southern Western Australia. Fish. Res. Rep. Dep. of Fish 131:1–44. Government of Western Australia, Dep. Fisheries, Fisheries Research Division, WA Marine Research Laboratories, PO Box 20 North Beach, Western Australia 6920.

Florida, by using a ThermoQuest Finnigan Delta Plus mass spectrometer (Thermo Fisher Scientific, Inc., Bremen, Germany) with a Kiel III device. Standard mass spectrometric techniques were applied after the carbonate was decomposed to $CO_2$ with 100% phosphoric acid. ISODAT software (Thermo Fisher Scientific, Inc., Waltham, MA) indicated all isotopic values, which are reported with standard delta notation (‰):

$$\delta^{18}O = \left[\left(\left(^{18}O/^{16}O\right)_x / \left(^{18}O/^{16}O\right)_s\right) - 1\right] \times 1000,$$

where $X$ = sample; and
$S$ = the marine carbonate standard Vienna Peedee belemnite, VPDB (Gao et al. 2001).

### Statistical analysis

To account for any effect of fish size on $\delta^{13}C$ and $\delta^{18}O$ isotope ratios, the relationship between each isotope and otolith mass (which is considered to be proportional to fish age) was examined within each regional group. Where a significant linear relationship was found, isotopic ratios were corrected by using the following formula:

$$R_{corr} = R - (B \times Mass),$$

where $R$ = isotopic ratio;
$B$ = slope; and
$Mass$ = otolith mass.

Permutational multivariate analysis of variance (PERMANOVA) was used to test for differences in isotopic signatures among years, regions, and sites within regions. PERMANOVA is a "semiparametric," multivariate version of a univariate one-way ANOVA (Anderson, 2001), producing a pseudo $F$-statistic, and a $P$-value. Canonical analysis of principal coordinates (CAP), with the "leave-one-out" method of cross-validation was used to assess whether juvenile snapper from South Florida marine ecosystems could be accurately classified to one of the five regions. Sample collection between years, regions, and times of year was not consistent, and therefore only data from "summer" (May to September) were included. The four larger regions (Biscayne Bay, Florida Bay, Lower Keys, and Ten Thousand Islands) were sampled at least once in 2002 and 2003 only. Therefore, only data from these two years were used to assess spatial variation in isotope signatures. Old Dan Bank and Sprigger Bank in Florida Bay were sampled in late May–June in 2001, 2002, 2004, and 2005; thus, temporal variation was also investigated. Age-length estimates for juvenile gray snapper from Florida were used to ensure that the otolith samples reflected juvenile isotopic signatures within the year of collection (Allman and Grimes, 2002; Gerard, 2007). Isotope data were normalized before analysis, and all multivariate analyses were completed in Primer-6, (Plymouth Marine Laboratory, Ivybridge, U.K.) with PERMANOVA add-on.

## Results

### Spatial variation

An initial PERMANOVA between years and regions (except the Dry Tortugas) for 2002 and 2003 data combined showed significant differences between regions (pseudo-$F$=358.3, $P$<0.001) and years (pseudo-$F$=41.8, $P$<0.001). Because this analysis showed that data from the two years could not be pooled, further analyses were performed on each year separately. Across both years, the Dry Tortugas and Florida Bay regions had the highest stable isotopic carbon ratios, and Ten Thousand Island had the lowest (Fig. 2). Stable oxygen isotopic ratios were lowest at the Ten Thousand Islands and highest in Florida Bay. Pairwise PERMANOVA on 2002 and 2003 data that were treated separately showed significant differences between all regions in both years at $P$<0.05.

More than one site was sampled within the same region and in the same month on only three occasions: in Florida Bay in June 2002 and September 2003, and in the Ten Thousand Islands in September 2002. PERMANOVA indicated that isotope signatures from fish collected at different sites within these regions were significantly different (Florida Bay June 2002: pseudo-$F$=8.90, $P$<0.001; Florida Bay September 2003: pseudo-$F$=7.60, $P$=0.003; Ten Thousand Islands September 2002: pseudo-$F$=10.66, $P$<0.001. Pairwise PERMANOVA tests between sites within a region showed that the strength of differences in isotope signatures among sites was variable (Table 1). Differences between the same sites within Florida Bay in June 2002 tended to be stronger than in September 2003.

Leave-one-out cross validation analysis for 2002 data only yielded an average classification accuracy of 79.7%. Classification success rates were 68.0% (Florida Bay), 50.0% (Biscayne Bay), 100.0% (Ten Thousand Islands), 83.3% (lower Florida Keys), and 90.0% (Dry Tortugas). The same analysis on 2003 data returned much lower classification successes, with 63.5% overall (Florida Bay [69.4%], Biscayne Bay [60.0%], Ten Thousand Islands [90.0%], lower Florida Keys [38.9%]). This result was largely due to the absence of samples from the Dry Tortugas in 2003 (which were strongly distinct from other regions in 2002) and to the lower classification success in the Lower Keys in 2003 than in 2002. Classification success rates for Biscayne Bay, Florida Bay, and the Ten Thousand Islands were similar between years.

### Temporal variation

Samples were taken at both Old Dan Bank and Sprigger Bank in late May or June of 2001, 2002, 2004, and 2005. Scatter plots showed significant overlap between samples from different years (Figs. 3 and 4). PERMANOVA revealed significant differences between samples from 2004 and 2002, and 2004 and 2005 at both sites (Table 2). At Old Dan Bank, results for 2001 were also significantly different from those for 2004,

and at Sprigger Bank, results for 2002 were also distinct from those for 2005. Where interannual differences were present, they were usually most discernible with respect to carbon, and less so for oxygen (Figs. 3 and 4). The annual mean SL of fish used in this analysis ranged from 135 mm (±2.6 mm standard error [SE]) in 2002 to 169 mm (±3.4 mm SE) in 2001 at Old Dan Bank, and from 156 mm (±13.5 mm SE) in 2001 to 160 mm (±16.1 mm SE) in 2005 at Sprigger Bank. However, the linear correlation between fish standard length and carbon isotope signature for samples included in temporal analyses was very weak, and only marginally significant (correlation coefficient $r^2$=0.03, $P$=0.04).

## Discussion

Otoliths can be used to separate fish by region on the basis of isotopic composition. This study revealed spatial separation for carbon and oxygen isotopes between five geographical regions in southern Florida. In any marine ecosystem, temperature and salinity interact to influence the concentrations of oxygen isotopes. Carbon and oxygen isotopic concentrations typically increase with salinity and decrease with increasing temperature (Elsdon and Gillanders, 2002).

Oxygen isotopes in the otolith are deposited in equilibrium with the carbon isotopic composition of the ambient water in which the fish resides (Campana, 1999). Carbon isotopes in the otolith, however, are deposited in disequilibrium to ambient carbon isotopic composition of the water mass. This disequilibrium is explained as an effect of metabolism and therefore provides information on the position of a fish in the food chain and on changes in metabolic rate over the life of a fish (Gauldie, 1996; Dufour et al., 2005; Huxham et al., 2007). The regional variation in the otolith isotopic composition of gray snapper indicates the regional differences in the environmental conditions and nutrient sources available to these fish throughout their early life. Regional isotopic differences provide a unique chemical signature that can be used to identify where individual adult gray snapper spend their time as juveniles.

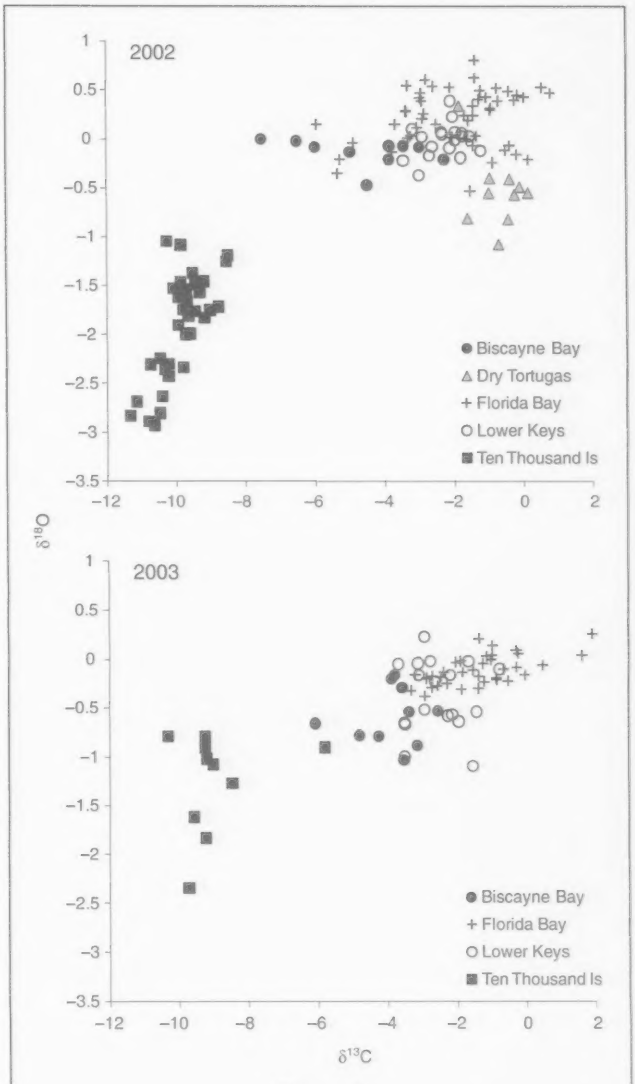


**Figure 2**

Scatter plot depicting spatial separation of juvenile gray snapper (*Lutjanus griseus*) stable isotope otolith signatures ($\delta^{18}O$ and $\delta^{13}C$) collected in 2002 and 2003 among five southern Florida regions: Ten Thousand Islands, Florida Bay, Biscayne Bay, Lower Keys and Dry Tortugas.

Results show spatial separation of stable oxygen and carbon isotopic ratios among **collection** sites within a region. Significant differences in carbon and oxygen isotopic composition among sites (approximately 10 km apart) indicate high site fidelity and a high classification accuracy for specific sites at this scale. Classification success with the leave-one-out cross validation procedure for a single observation in a region was approximately 80%, thereby allowing for the possibility classifying an unknown fish with reasonable certainty to a region. The spatial stable isotopic variation, coupled with a successful cross validation result, provides a means of substantiating the hypothesis that juvenile gray snapper exhibit strong site fidelity, and provides a specific isotopic tag to determine whether Florida Bay is a significant source of adults on the reef.

Elemental composition of otoliths has been shown to be valuable for identifying the relative contribution of juveniles from different nursery habitats to adult

**Table 1**

Results of pairwise permutational multivariate analysis of variance (PERMANOVA) of juvenile gray snapper (*Lutjanus griseus*) otolith stable isotope signatures among sampling sites, within sampled region, for Florida Bay (June 2002 and September 2003), and the Ten Thousand Islands (September 2002).

| Region and month | Sites compared | Test statistic (pseudo-*F*) | *P*-value | Number of permutations |
|---|---|---|---|---|
| Florida Bay | | | | |
| June 2002 | Black Betsy Key, Old Dan Bank | 3.69 | 0.002 | 997 |
| | Black Betsy Key, Sprigger Bank | 4.07 | 0.001 | 993 |
| | Black Betsy Key, Schooner Bank | 0.38 | 0.864 | 991 |
| | Old Dan Bank, Sprigger Bank | 2.57 | 0.008 | 990 |
| | Old Dan Bank, Schooner Bank | 2.97 | 0.001 | 991 |
| | Sprigger Bank, Schooner Bank | 3.07 | 0.002 | 993 |
| Sept 2003 | Old Dan Bank, Sprigger Bank | 4.04 | 0.001 | 995 |
| | Old Dan Bank, Schooner Bank | 1.79 | 0.083 | 994 |
| | Sprigger Bank, Schooner Bank | 1.86 | 0.073 | 991 |
| Ten Thousand Is. (west coast) | | | | |
| Sept 2002 | Blackwater Bay, Faka Bay | 4.34 | 0.003 | 637 |
| | Blackwater Bay, Palm Bay | 1.29 | 0.252 | 35 |
| | Blackwater Bay, Pumpkin Bay | 1.70 | 0.132 | 441 |
| | Faka Bay, Palm Bay | 3.03 | 0.015 | 275 |
| | Faka Bay, Pumpkin Bay | 3.74 | 0.004 | 986 |
| | Palm Bay, Pumpkin Bay | 0.56 | 0.625 | 165 |

populations (Martin and Wuenschel, 2006). Lara et al. (2008), using trace elemental analysis, found an overall cross validation success rate of 82% for classifying randomly selected samples to a juvenile nursery habitat signature in one of five regions: Biscayne Bay, Florida Bay, lower Florida Keys, Ten Thousand Islands, and Dry Tortugas. However, that study had a lower percentage for successfully classifying unknown samples to two regions, Dry Tortugas (50%) and Ten Thousand Islands (52%). In the current study, isotopes allowed us to distinguish between sites that the elemental ratios in the Lara et al. study were unable to separate and provided a clearer successful classification for all regions. The Dry Tortugas and Ten Thousand Islands regions showed the highest percentage for successful classification, 90% and 100%, respectively, compared to other regions analyzed. These two regions are geographically the farthest separated, Dry Tortugas has the most oceanic influence, and Ten Thousand Islands has the most freshwater influence from Taylor Slough and Shark River Slough through the Florida Everglades. There was also some interannual variability in classification success in the Lower Keys.

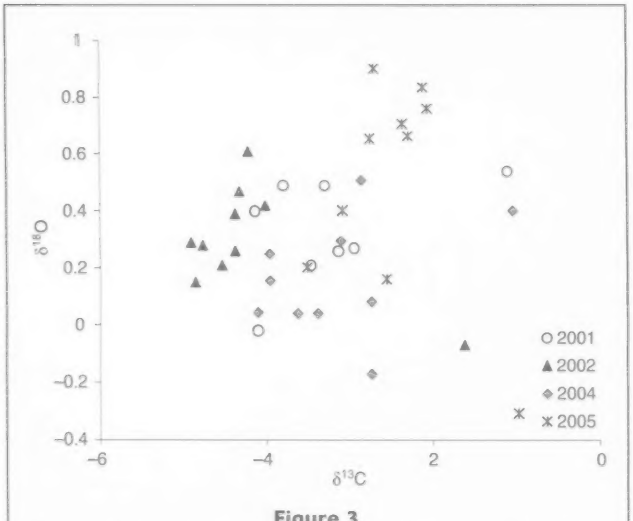


**Figure 3**

Scatter plot depicting variation in juvenile gray snapper (*Lutjanus griseus*) stable isotope otolith signatures ($\delta^{18}O$ and $\delta^{13}C$) from the summer of 2001, 2002, 2004, and 2005 from Sprigger Bank, Florida Bay.

Temporal variation of stable isotopic ratios of carbon and oxygen in the otoliths of gray snapper has not been previously studied in southern Florida. This study indicates that temporal variation in carbon and oxygen isotopic ratios was expressed in otolith samples collected from years 2001 through 2005. Swearer et al. (2003) tested temporal variation of three species (topsmelt [*Atherinops affinis*], arrow goby [*Clevelandia ios*], and California halibut [*Paralichthys californicus*]), collected in spring and autumn of 1996 from Carpinteria Marsh in southern

**Table 2**

Results of pairwise permutational multivariate analysis of variance (PERMANOVA) of juvenile gray snapper (*Lutjanus griseus*) otolith stable isotope signatures among sampled years, for sampling sites Old Dan Bank, and Sprigger Bank, Florida Bay.

| | Years compared | Test statistic (pseudo-*F*) | *P*-value | Number of permutations |
|---|---|---|---|---|
| Old Dan Bank | 2001, 2002 | 1.53 | 0.09 | 995 |
| | 2001, 2004 | 1.84 | 0.05 | 993 |
| | 2001, 2005 | 1.11 | 0.30 | 992 |
| | 2002, 2004 | 2.76 | <0.001 | 992 |
| | 2002, 2005 | 1.50 | 0.10 | 981 |
| | 2004, 2005 | 2.13 | 0.01 | 979 |
| Sprigger Bank | 2001, 2002 | 1.65 | 0.07 | 990 |
| | 2001, 2004 | 1.27 | 0.23 | 984 |
| | 2001, 2005 | 1.52 | 0.11 | 979 |
| | 2002, 2004 | 2.26 | 0.01 | 989 |
| | 2002, 2005 | 2.86 | <0.001 | 989 |
| | 2004, 2005 | 2.26 | 0.02 | 988 |

California. Their results showed a substantial degree of temporal variation in chemical signatures between collection periods. Assessing the temporal variation of isotopic signatures is useful for potential determination of environmental change or lack of site fidelity in fishes within Florida Bay. Preliminary results from acoustic telemetry on juvenile gray snapper in a Florida coastal Atlantic marine estuary, Loxahatchee, and otolith chemical signature analysis of juvenile gray snapper in Florida Bay indicate high site fidelity (Lara et al., 2008). Based on these results, it is probable that the variations shown during annual sampling of the same sites in Florida Bay are a result of differences in environmental conditions such as temperature and salinity, possibly resulting from changes in water management practices or weather events.

Significant differences between both oxygen and carbon isotopic signatures in otoliths were present between sampled years. However, differences with respect to carbon were more pronounced than differences in respect to oxygen. Otolith carbon isotopic signatures can be affected by water temperature and salinity (Elsdon and Gillanders, 2002), and by the trophic position and diet of the fish (Shiao et al., 2009).

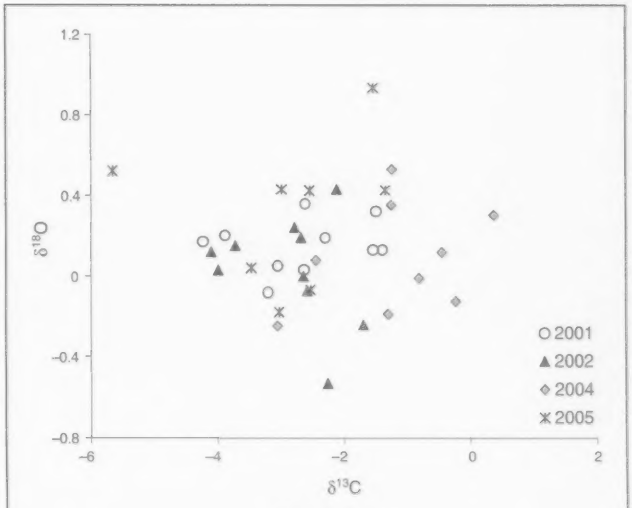


**Figure 4**

Scatter plot depicting variation in juvenile gray snapper (*Lutjanus griseus*) stable isotope otolith signatures ($\delta^{18}O$ and $\delta^{13}C$) from the summer of 2001, 2002, 2004, and 2005 from Old Dan Bank, Florida Bay.

Historically, Florida Bay has experienced dramatic changes in salinity levels as a result of changes in water management practices and land use upstream. The impact of salinity changes on juvenile fish habitats, such as seagrass beds and mangroves, and on fishes is still unknown. The positive relationship between oxygen isotopic ratios and salinity makes it possible to look closer at salinity levels of portions of Florida Bay from 2000 to 2005. Kelble et al. (2007) examined mean annual Florida Bay salinity from 1998 through 2004 using flow-through system data from survey cruises. Results showed low salinity levels in the summer of 2002 (29–34‰), and much higher salinity levels in the summer of 2004 (37–42‰). Otolith carbon isotopic signatures from both Sprigger Bank and Old Dan Bank were significantly lower in 2002 than in 2004—a result that may have reflected the lower salinity conditions in 2002. Oxygen isotopic signatures, however, were similar between these two years at both sites.

The formation of otolith carbonate is an inorganic reaction where calcium carbonate is precipitated from

the endolymphatic fluid. The carbon isotopic ratios in the otolith, in addition to pure kinetic effects, are controlled by only those metabolic pathways that modify the $\delta^{13}C$ of the endolymphatic fluid (Radtke, 1996). Diet has a pronounced and significant effect on carbon isotopic ratios in the otoliths. The markedly different mean salinity values for summer 2002 and summer 2004 indicate differences in freshwater inflow to Florida Bay. These differing regimes would likely have influenced primary productivity in the bay, in terms of chlorophyll biomass and food-web structure, which could ultimately be recorded as differences in carbon isotopic ratios in juvenile fishes. Autotrophs, mangrove detritus, seagrass, and particulate organic matter play a pivotal role as important sources of nutrition for juvenile gray snapper (Melville and Connolly, 2003). Different plant groups display different carbon isotopic ratios in their organic material depending on the photosynthetic pathway used, and carbon isotopic ratios for the otoliths of prey organisms act as labels that can be measured through to higher trophic level consumers. Recorded variations of carbon isotopic ratios for the otoliths may therefore constitute a record of the food that these gray snapper consumed and show potential for assessing the health of the Florida Bay ecosystem.

Mulcahy (1979) found that stable carbon isotopic ratios for the otoliths of a benthopelagic fish increased with fish age. This increase with maturity of the fish was attributed to a decrease in the metabolic production rate of dissolved inorganic carbon. Because we examined only juvenile and small adult fish of a relatively narrow size range, it is unlikely that the observed differences in carbon isotopic ratios were due to differences in age-dependent metabolism.

Spatial separation of regions and collection sites as shown in this study by using isotopic analysis of otoliths has the potential for establishing habitat linkages between adult gray snapper on offshore reefs to those in nursery habitats in Florida Bay and other surrounding areas. Results indicate that fishery managers should address the whole ecosystem and connectivity between habitats of a known species rather than site-specific management. Managing and protecting a particular species requires spatially explicit characterization of all habitats and processes encountered during the life history of a species for the design of marine protected areas in coastal regions (Thorrold et al., 2001). Connectivity must be taken into consideration when assessing management effectiveness of economically important reef fish species that use multiple habitats throughout their life.

## Acknowledgments

We thank all within NOAA Southeast Fisheries Science Center, Early Life History Unit for their assistance collecting samples and P. Swart and A. Saied of the University of Miami, Rosenstiel School for Marine and Atmospheric Studies, for their assistance with stable isotope analysis. I especially thank D. Jones for doing the initial statistical analysis and M. Lara for improving this project. The constructive comments of J. Bohnsack, J. Lamkin, and W. Richards were helpful in revising this manuscript. This study was funded in part by the South Florida Science Program, NOAA Coral Reef Conservation Program, and NOAA Educational Partnership Program.

## Literature cited

Allman, R.J. and C.B. Grimes.
2002. Temporal and spatial dynamics of spawning, settlement, and growth of Gray snapper (*Lutjanus griseus*) from the West Florida shelf as determined from otolith microstructures. Fish. Bull. 100:391–403.

Anderson, M. J.
2001. A new method for non-parametric multivariate analysis of variance. Austral. Ecol. 26:32–46.

Arslan, Z., and A. J. Paulson.
2003. Solid phase extraction for analysis of biogenic carbonates by electrothermal vaporization inductively coupled plasma mass spectrometry (ETV-ICP-MS): an investigation of rare earth element signatures in otolith microchemistry. Anal. Chim. Acta 476:1–13.

Ashford, J., and C. Jones.
2006. Oxygen and carbon stable isotopes in otoliths record spatial isolation of Patagonian toothfish (*Dissostichus eleginoides*). Geochim. Cosmochim. Acta 71:87–94.

Campana, S.
1999. Chemistry and composition of fish otoliths: pathways, mechanisms and applications. Mar. Ecol. Progr. Ser. 188:263–297.

Dufour, E., W. P. Patterson, T. Höök, and E. S. Rutherford.
2005. Early life history of Lake Michigan alewives (*Alosa pseudoharengus*) inferred from intra-otolith stable isotope ratios. Can. J. Fish. Aquat. Sci. 62:2362–2370.

Elsdon, T. S., and B. M. Gillanders.
2002. Interactive effects of temperature and salinity on otolith chemistry: challenges for determining environmental histories of fish. Can. J. Fish. Aquat. Sci. 59:1796–1808.

Gao Y., S. Joner, R. Svec., and K. Weinberg.
2004. Stable isotopic comparison in otoliths of juvenile sablefish, *Anoplopoma fimbria*, from waters off the Washington and Oregon coast. Fish. Res. 68(1–3): 351–360.

Gauldie, R. W.
1996. Biological factors controlling the carbon isotope record in fish otoliths: principles and evidence. Comp. Biochem. Physiol. 115B(2):201–208.

Gerard, T.
2007. The use of otolith microchemistry to monitor and evaluate the movement of coral reef fish in Southern Florida waters. Ph.D. diss., 74 p. A&M Univ., Tallahassee, FL.

Huxham, M., E. Kimani, J. Newton, and J. Augley.
2007. Stable isotope records from otoliths as tracers of fish migration in a mangrove system. J. Fish Biol. 70:1554–1567.

Kelble, C. R., E. M. Johns, W. K. Nuttle, T. N. Lee, R. H. Smith, and P. B. Ortner.
2007. Salinity patterns of Florida Bay. Estuar. Coast. Shelf Sci. 71:318–334.

Lara, M., D. Jones, J. Lamkin, C. Jones, and L. Chen.
2008. Spatial variation of otolith elemental signatures among juvenile gray snapper nursery regions within South Florida's marine ecosystems. Mar. Biol. 153:235–248.

Martin, G. B., and M. J. Wuenschel.
2006. Effect of temperature and salinity on otolith element incorporation in juvenile gray snapper *Lutjanus griseus*. Mar. Ecol. Progr. Ser. 324:229–239.

Melville, A. J., and R. M. Connolly.
2003. Spatial analysis of stable isotope data to determine primary sources of nutrition for fish. Oecologia 136:499–507.

Mulcahy, S. A.
1979. Isotopic composition of otoliths from a benthopelagic fish *Coryphaenoides acrolepis*, Macrouridae: Gadiformes. Oceanol. Acta. 2:423–427.

Radtke, R.L.
1996. Environmental information stored in otoliths: insights from stable isotopes. Mar. Biol. 127:161–170.

Richards, W. J., K. C. Lindeman, J. Lyczkowski-Shultz, D. M. Drass, C. B. Paris, J. M. Leis, M. Lara, and B. H. Comyns.
2005. Lutjanidae: Snappers. *In* Early stages of Atlantic fishes, vol. 2 (W. J. Richards, ed.), p. 1549–1586. CRC Press, Boca Raton, FL.

Shiao, J. C., T. F. Yui, H. Hoie, U. Ninnemann, and S. K. Chang.
2009. Otolith O and C stable isotope composition of southern bluefin tuna *Thunnus maccoyii* (Pisces: Scombridae) as possible environmental and physiological indicators. Zool. Stud. 48:71–82.

Starck, W. A., and R. E. Schroeder.
1971. Investigations on the gray snapper *Lutjanus griseus*. Studies in tropical oceanography 10, 24 p. Univ. Miami Press, Coral Gables, FL.

Stephenson, P. C., J. S. Edmonds, M. J. Moran, and N. Caputi.
2001. Analysis of stable isotope ratios to investigate stock structure of red emperor and rankin cod in North Western Australia. J. Fish. Biol. 58:126–144.

Swearer, S. E., G. E. Forrester, M. A. Steele, A. J. Brooks, and D.W. Lea.
2003. Spatio-temporal and interspecific variation in otolith trace elemental fingerprints in a temperate estuarine fish assemblage. Estuar. Coast. Shelf Sci. 56(5–6):1111–1123.

Thorrold, S., C. Latkoczy, P. K. Swart, and C. M. Jones.
2001. Natal homing in a marine fish metapopulation. Science 29:297–299.

# Assessing trends in the density of Atlantic croaker (*Micropogonias undulatus*): a comparison of passive acoustic and trawl methods

**Damon P. Gannon (contact author)**[1]

**Janet G. Gannon**[2]

Email address for contact author: dgannon@bowdoin.edu

[1] Bowdoin Scientific Station
c/o Biology Department
Bowdoin College
6500 College Station
Brunswick, Maine 04011

[2] Biology Department
Bowdoin College
6500 College Station
Brunswick, Maine 04011

**Abstract**—Using data collected simultaneously from a trawl and a hydrophone, we found that temporal and spatial trends in densities of juvenile Atlantic croaker (*Micropogonias undulatus*) in the Neuse River estuary in North Carolina can be identified by monitoring their sound production. Multivariate analysis of covariance (MANCOVA) revealed that catch per unit of effort (CPUE) of Atlantic croaker had a significant relationship with the dependent variables of sound level and peak frequency of Atlantic croaker calls. Tests of between-subject correspondence failed to detect relationships between CPUE and either of the call parameters, but statistical power was low. Williamson's index of spatial overlap indicated that call detection rate (expressed by a 0–3 calling index) was correlated in time and space with Atlantic croaker CPUE. The correspondence between acoustic parameters and trawl catch rates varied by month and by habitat. In general, the calling index had a higher degree of overlap with this species' density than did the received sound level of their calls. Classification and regression tree analysis identified calling index as the strongest correlate of CPUE. Passive acoustics has the potential to be an inexpensive means of identifying spatial and temporal trends in abundance for soniferous fish species.

Manuscript submitted 8 February 2009.
Manuscript accepted 13 November 2009.
Fish. Bull. 108:106–116 (2009).

The views and opinions expressed or implied in this article are those of the author (or authors) and do not necessarily reflect the position of the National Marine Fisheries Service, NOAA.

Many fish species communicate acoustically, producing sounds under a variety of conditions, such as when engaging in reproductive activities, defending territory, competing for food, or responding to threats (Ladich, 1997, 2004; Myrberg, 1997). Fishery scientists can take advantage of sounds produced by fishes to study certain aspects of fish biology. Passive acoustic techniques (i.e., the use of hydrophones to receive and record sounds made by fishes) have been used by fishery scientists primarily to characterize temporal and spatial patterns in spawning activity (reviewed by Gannon, 2008). For example, some investigators have coupled passive acoustic surveys with collection of adult fish or newly fertilized oocytes to help confirm the species identifications of the callers and to correlate certain behaviors (i.e., spawning) with specific sound types (e.g., Saucier and Baltz, 1993). However, the objective of many fishery assessments is to obtain some measure of fish abundance. Passive acoustics may provide data that would allow indices of abundance to be calculated. But to our knowledge, passive acoustic methods have not yet been used in this fashion and no studies have formally evaluated their potential for assessing relative abundance.

Atlantic croaker (Sciaenidae: *Micropogonias undulatus*) are an abundant, estuary-dependent sciaenid found in the coastal waters of the mid-Atlantic and southern United States. Off North Carolina, Atlantic croaker spawn in the ocean from September to February, and juveniles are found in mesohaline estuaries throughout summer (see Eby, 2001). Sciaenids, including Atlantic croaker, are well known for their noise-making abilities. Members of the family produce sound by the movement of bilaterally paired muscles that surround the swim bladder, which cause the swim bladder to vibrate (reviewed by Ramcharitar et al., 2006). In Atlantic croaker, both males and females possess well-developed sonic muscles. Their sonic muscles develop when they are approximately 45 mm standard length (long before sexual maturation commences), and their sonic muscles do not undergo atrophy after spawning to the extent seen in other sciaenids (Hill et al., 1987; Vance et al., 2002). Atlantic croaker produce three types of acoustic calls: reproductive calls, disturbance calls, and "knock calls" (Connaughton et al., 2003; Fine et al., 2004; Gannon, 2007). Knock calls consist of 1–6 brief pulses (88–106 msec), or "knocks," with a mode of 2 pulses and repetition rate of 16.1 pulses per second (Gannon, 2007). Knock calls are broadband with dominant frequencies varying inversely with fish size, ranging from approxi-

mately 600 to 1,600 Hz (Gannon, 2007). Juvenile and mature Atlantic croaker are known to produce knock calls in the estuarine waters of North Carolina from June to November (Gannon, 2007). Knock calling occurs throughout the day and night, but production of knock calls by Atlantic croaker stocked in a research pond peaked at night at an average rate of 1.0 calls per fish per minute (Gannon, 2007). Their extensive calls make Atlantic croaker ideal for a study by passive acoustic means.

We conducted trawl surveys concurrently with passive acoustic surveys for young-of-the-year Atlantic croaker in the Neuse River estuary in North Carolina to assess the utility of passive acoustics to quantify temporal and spatial trends in the density, habitat selection, and associations with environmental variables of this species. We used multivariate analysis of covariance (MANCOVA) to investigate the relationships among call parameters, fish density, and environmental variables; Williamson's index to measure the degree of spatial overlap between Atlantic croaker catches and the occurrence of their calls; and classification and regression tree analysis (CART) to identify the best set of acoustic and environmental variables for predicting Atlantic croaker distribution.

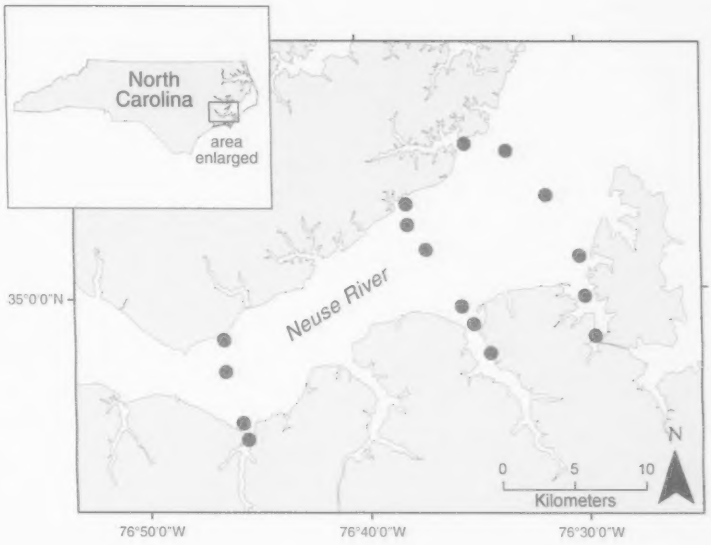


**Figure 1**

Neuse River study area showing stations (●) where concurrent otter trawl and passive acoustic sampling for Atlantic croaker (*Micropogonias undulatus*) took place from June to October of 2000.

## Materials and methods

### Field sampling

From June through October of 2000, we performed paired trawl and passive acoustic surveys from a 7-m outboard-powered vessel. Estimates of Atlantic croaker density derived from the trawl data were used as a benchmark against which acoustically derived estimates could be compared. The study area was a 300-km$^2$ region of the Neuse River estuary, centered at 35.0°N, 76.6°W. The survey design consisted of 16 sampling stations arranged along three transects (Fig. 1). In an effort to sample the full range of depths and habitat types within the study area, we distributed the transects along the length of the estuary, and each transect completely crossed the river.

Because sound propagation is affected by environmental conditions, each sampling station was characterized with regard to its habitat type. The three habitat types considered were 1) the tributary creeks and bays ("creeks"); 2) the main stem of the Neuse River >3.5 m in depth ("mid-river"); and 3) the main stem of the Neuse River <3.5 m in depth ("river edge"). These categories were used because the Neuse River estuary has relatively low habitat diversity: there is little submerged vegetation; oyster reefs are sparse (Lenihan and Peterson, 1998); and bottom substrate consists of sand, silt, and clay. Therefore, habitat diversity depends primarily on depth and sediment grain size (which is negatively correlated with depth).

Knock calling by Atlantic croaker peaks at night, but the fish produce sound throughout the day (Gannon, 2007). Pilot studies in the Neuse River estuary showed that the diversity of fish species producing calls was highest at night, making it difficult to quantify calling activity of any one species. Therefore, we sampled during daylight hours (from two hours after sunrise to two hours before sunset) to minimize any potential biases associated with diel variation in sound production or in vulnerability to our sampling net. Because few other species in the area call during the day, Atlantic croaker sounds dominated the sound field during the day.

At each sampling station, an acoustic recording was made before each trawl, thus each acoustic recording was paired with a trawl sample. The recording location was at the geographical midpoint of the trawl path so that the acoustic recording and trawling would sample fish from the same geographic area. The recording site was approached on a heading that was perpendicular to the trawl path to minimize any potential disturbance to the fish. Upon arrival at the recording site, the engine of the boat was turned off. Recording commenced approximately two minutes after the boat arrived on station and then a two-minute recording was made. Choice of recording length followed the reasoning and methods of Mok and Gilmore (1983) and Luczkovich et al. (1999). The recording system consisted of an HTI 96 hydrophone (High Tech, Inc., Gulfport, MS),

a TCD-D8 digital audio tape (DAT) recorder (Sony Corp., Tokyo, Japan), and a personal computer. The hydrophone was omnidirectional and had a frequency range of 2 Hz to 30 kHz and a sensitivity of –164 dB re 1V/μPa (μPa=micropascal). The DAT recorder operated at a sampling rate of 44.1 kHz, with a frequency range of 20 Hz to 22 kHz (±1 dB). Data from the DAT recorder were downloaded to a personal computer running CoolEdit 2000 (Syntrillium Software, Inc., Scottsdale, AZ). The recording levels for the DAT recorder and computer were standardized for all recordings. The entire recording system (hydrophone, DAT recorder, and computer) was calibrated by recording a series of reference tones and using linear regression to determine how relative root mean squared (RMS) levels related to absolute RMS levels ($r^2$=0.99; Gannon et al., 2005).

To minimize movement of the hydrophone through the water (thus minimizing hydrodynamic noise), the hydrophone was suspended approximately halfway between the surface and seafloor from a 4-kg mushroom anchor that was suspended 50 cm below a 30-cm diameter buoy by an elastic shock cord. Immediately after making each two-minute recording, we deployed the trawl net. We used a 3.4-meter otter trawl with 3.8-cm mesh and a 3-mm mesh liner in the codend. We trawled in a straight line, parallel to the bottom contour, for four minutes at a speed of 1.3 m/sec, which resulted in trawl distances of approximately 300 m. The locations of each recording site and of the beginning and ending of each trawl were recorded with a Garmin GPS120 and a Garmin GBR21 differential beacon receiver (Garmin, George Town, Cayman Islands). The exact length of each trawl was calculated from the beginning and ending positions of the trawls.

Three hundred meters was chosen as the trawl length based on estimates of the maximum range over which we would likely be able to detect calling Atlantic croaker (~150 m). Maximum detection range depends upon the source level of the sound, the level of background noise at the same frequency, and characteristics of the transmitting medium (Pierce, 1989; Richardson et al., 1995). We lacked information on these parameters; therefore we used the theoretical range at which a signal would be diminished by 30 dB re 1 μPa because of spreading loss as an estimate of the range over which a sound could be detected (Gannon, 2003).

All fish and invertebrates captured were identified, counted, and measured (standard length). Catch per unit of effort (CPUE) was calculated as the number of Atlantic croaker >45 mm standard length that were caught per 100 meters of linear trawling distance. CPUE was calculated for Atlantic croaker >45 mm because this is the size at which they develop sonic muscles and thus become capable of producing sound (Hill et al., 1987; Gannon, 2007). At each sampling site we also recorded temperature, salinity, and dissolved oxygen concentration at 0.2 m above the bottom, using a Minisonde multiprobe and Surveyor 4 data logger (Hydrolab, Hach Environmental, Loveland, TX).

### Acoustical analyses

Acoustical analyses were performed with CoolEdit 2000 and Raven 1.1 (Cornell Univ., Ithaca, NY). We discriminated Atlantic croaker sounds from other sounds in our field recordings by the methods outlined in Gannon (2007). Briefly, we compared spectrographs from our field recordings to spectrographs of recordings from Atlantic croaker made in captivity. We also compared our field recordings to published descriptions of calls of all other known soniferous species encountered in the estuary (e.g., Fish and Mowbray, 1970; Mok and Gilmore, 1983; Sprague and Luczkovich, 2001). We excluded recordings containing sounds of boats or rain, those in which the Beaufort sea state was ≥3, and those made when bottlenose dolphins (*Tursiops truncatus*) were present, because these factors may have affected rates of sound production by Atlantic croaker (see Luczkovich et al., 2000) or our ability to detect sounds.

We investigated how trawl CPUE and environmental conditions related to three acoustic parameters: 1) received sound level (in dB re 1 μPa), 2) rate of detection of Atlantic croaker calls by our hydrophone (expressed as a calling index), and 3) peak acoustic frequency of Atlantic croaker calls (the loudest frequency recorded). We hypothesized that received sound level and calling index should be influenced by the number of fish calling. Environmental factors were included in the analysis because of their potential to also affect the acoustic parameters. For example, temperature is known to affect the frequency characteristics of sciaenid calls (Connaughton et al., 2000), and the characteristics of the transmission medium can cause different frequency components of a call to differ in their propagation efficiencies (Richardson et al., 1995, p. 27–30).

The Atlantic croaker sounds that we recorded exhibited energy peaks between 600 and 1200 Hz (Gannon, 2007). Besides Atlantic croaker calls, there were few background sounds in this frequency range. But background noise was common at other frequencies. Therefore, we calculated the received sound level attributable to Atlantic croaker as the level within the 600 to 1200 Hz band, using an FFT (Fast Fourier Transform) size of 2048. The received sound level was calculated over the entire two-minute recording period from each sampling station.

Calling rate reached a saturation point at approximately 100 calls/min, above which the exact number of fish calls per minute could not be determined. Therefore, we used a calling index to quantify the occurrence of Atlantic croaker calls, following Heyer et al. (1994), Luczkovich et al. (1999), and Gannon (2007). The calling index was on a scale from zero to three (0=no calls, 1=1–10 calls/min, 2=10–100 calls/min, and 3=greater than 100 calls/min).

### Statistical analyses

Before we performed statistical analyses, we transformed CPUE values by $\ln(x+1)$, which gave a better fit to a

normal distribution in a Q-Q plot than did the raw data. To investigate whether acoustic variables were related to local densities of Atlantic croaker or other environmental variables, we performed a MANCOVA with the two continuous acoustic parameters (received sound level and peak frequency) as dependent variables, with habitat and month as factors, and with CPUE, dissolved oxygen, and temperature as covariates. MANCOVA was run in SPSS vers. 16 (SPSS, Inc., Chicago, IL).

We used Williamson's index of spatial overlap (Williamson, 1993) to characterize the extent to which Atlantic croaker calling was spatially correlated with Atlantic croaker density. Williamson's index is customarily used to measure spatial overlap of the distribution of two species, such as that between a predator and its prey (Williamson, 1993; Garrison, 2000; Garrison et al., 2002; Link and Garrison, 2002). Here we used it to compare two independent measures of distribution for the same species. The index ($O_{ij}$) is calculated as follows:

$$O_{ij} = \frac{\sum_{z=1}^{m}(N_{jz}n_{iz})m}{\sum_{z=1}^{m}(N_{jz})\cdot\sum_{z=1}^{m}(n_{iz})}, \quad (1)$$

where $m$ = the number of samples;
$z$ = a discrete sampling location;
$N_j$ = the relative abundance of Atlantic croaker as determined by trawl CPUE; and
$n_i$ = the relative abundance of Atlantic croaker as determined by passive acoustic methods (either calling index or relative received amplitude of calls).

Index values >1 indicate spatial overlap greater than would be expected by chance, and values <1 reflect less spatial overlap than expected.

We applied Williamson's index to compare 1) CPUE to calling index and 2) CPUE to received sound level. We determined the significance of $O_{ij}$ using a randomization procedure developed by Garrison (2000). The test statistic $O_{ij}$ was compared to a random distribution of overlap values in which each value of $N_j$ was randomly paired with a value for $n_i$ to calculate a randomized $O_{ij}$. This was done 4999 times, and the observed test statistic $O_{ij}$ (the 5000$^{th}$ instance) was then compared to the generated distribution. Significance of the value was judged by the proportion of randomized $O_{ij}$ values that were greater than the observed $O_{ij}$ (a value was judged to be significant if fewer than 5% of the randomized values were greater than $O_{ij}$).

Classification and regression tree (CART) analysis was used to explore relationships between the dependent variable CPUE and eight independent variables (day of year, dissolved oxygen concentration, temperature, salinity, depth, calling index, received sound level, and distance to nearest creek). The CART method tests the global null hypothesis of independence between the dependent variable and each of the independent variables and identifies critical threshold values for the significant independent variables (Urban, 2002). Our study area was spatially structured with regard to habitat type (i.e., the mid-river habitat was a contiguous region at the center of the study area, the creeks were at the outer edges of the study area, and the mid-river habitat was a contiguous ring separating the mid-river from the creeks). Thus, the three habitat types were spatially correlated. To avoid multicollinearity in our analyses, we used a single variable ("distance to creek") to represent the position of each sampling station in relation to each of the three habitats (i.e., any station close to the creeks was necessarily far from the mid-river and vice-versa). ArcGIS vers. 9.2 (Environmental Systems Research Institute, Redlands, CA) was used to calculate the distance from each sampling location to the creek habitat. We ran the CART analysis using the "Party" library in the R software environment (vers. 2.6.1, R Development Core Team; Hothorn et al., 2006). *P*-values were calculated by using a quadratic test statistic.

## Results

From June to October of 2000, we performed 14 simultaneous trawl and passive acoustic surveys, for a total of 224 paired samples. Sixty four samples were excluded from analysis because of a high sea state (Beaufort scale), rain, boat noise, or the presence of dolphins. Noise from rough sea conditions, rain, and passing boats may not have affected the calling behavior of Atlantic croaker, but these noise sources masked the croakers' calls, making it difficult to reliably measure their acoustic characteristics. Recordings made in the presence of bottlenose dolphins appeared to have long periods of silence punctuated by short, sporadic outbursts of croaker calls. Therefore we excluded these samples because there appeared to be a change in Atlantic croaker calling behavior when dolphins were present. Exclusion of these 64 samples left a total sample size of 160; 70 in the tributary creeks, 53 along the river edge, and 37 in middle of the river (rough sea conditions and boat noise were most prevalent in the mid-river habitat). All Atlantic croaker caught in the study were young of the year.

CPUEs were highest in all habitats during June (Fig. 2A) and the general trend was for declining densities throughout the five-month study, likely the result of a large pulse of recruitment in spring, followed by mortality or emigration throughout summer and fall. Atlantic croaker densities were lowest in the mid-river habitat during July and August, coinciding with the occurrence of hypoxic conditions. Atlantic croaker recolonized the mid-river habitat when dissolved oxygen conditions improved in September and October. Standard lengths of croaker increased throughout the period from June to October in all habitats but were consistently lower in the mid-river habitat than in the other habitats (Fig 2B). Calling indices, representing

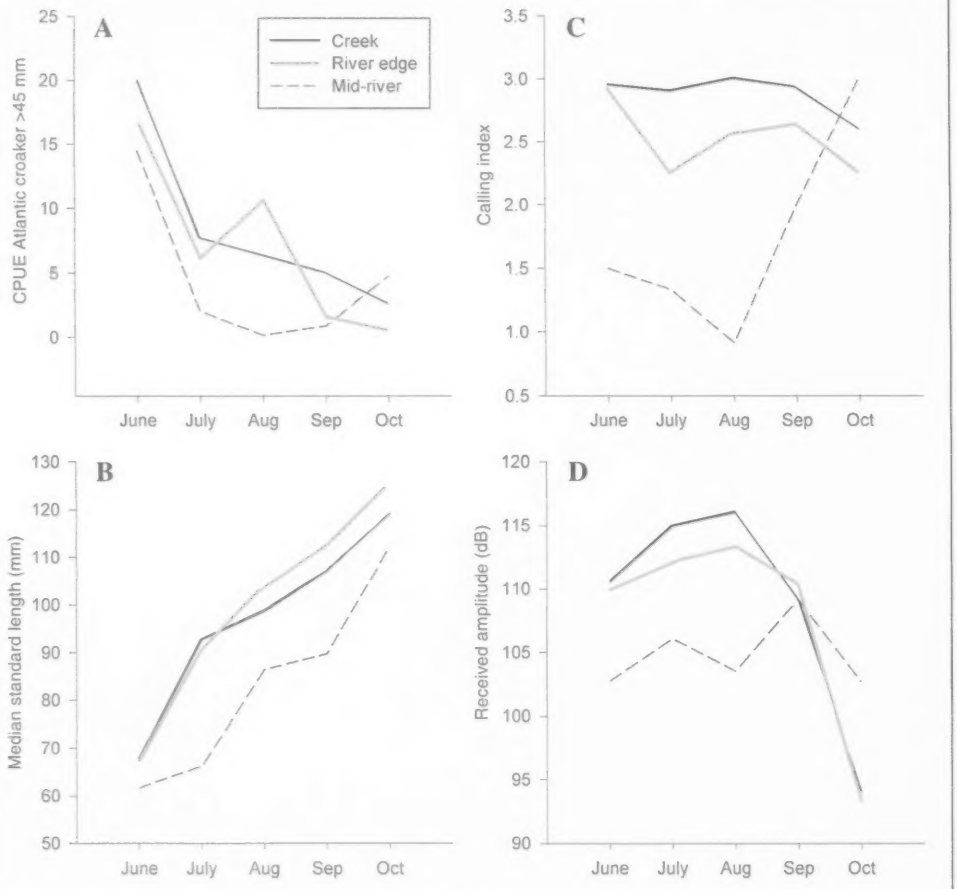


**Figure 2**

Monthly mean values for the creek, river edge, and mid-river habitats of the Neuse River estuary from June to October of 2000 for (**A**) trawl catch per unit of effort for Atlantic croaker greater than 45 mm standard length, (**B**) median standard length of Atlantic croaker in each trawl, (**C**) Atlantic croaker calling index, (**D**) sound level of Atlantic croaker calls received at the hydrophone, (**E**) peak acoustic frequency of Atlantic croaker calls, (**F**) temperature, (**G**) dissolved oxygen concentration, and (**H**) salinity. Dashed line at 2.3 mg/L in G represents the hypoxia avoidance threshold for Atlantic croaker (Eby and Crowder, 2002).

the rate at which Atlantic croaker knock calls were detected, were high and relatively consistent in the creek and river edge habitats throughout the study period (Fig. 2C). In contrast, the mean calling index in the mid-river fell to a minimum of 0.91 in August and then increased sharply to its maximum value of 3.0 in October. Received sound levels peaked during August in the creek and river edge habitats (116 and 113 dB, respectively), and then fell sharply (Fig. 2D). Received levels in the mid-river peaked in September (109 dB). Overall, there was a declining trend in peak acoustic frequency of the calls throughout the five-month study period (Fig 2E), after an initial increase in July in the mid-river and river edge habitats. The creek habitat was the warmest habitat in June and the coolest in October (Fig. 2F). The mid-river was the coolest habitat in June and the warmest in October. Dissolved oxygen concentration at the bottom of the water column was lowest during summer and was always lower in the mid-river habitat (the deepest portion of the study area) and highest in the river edge habitat (Fig 2G). During August, the mean dissolved oxygen concentration in the mid-river was 1.1 (standard deviation=1.6) mg/L, which was well below the 2.3 mg/L avoidance threshold that Eby and Crowder (2002) found for Atlantic croaker in the Neuse River. Salinity was highest in July and August and was higher in the mid-river habitat than in the other two habitats (Fig. 2H).

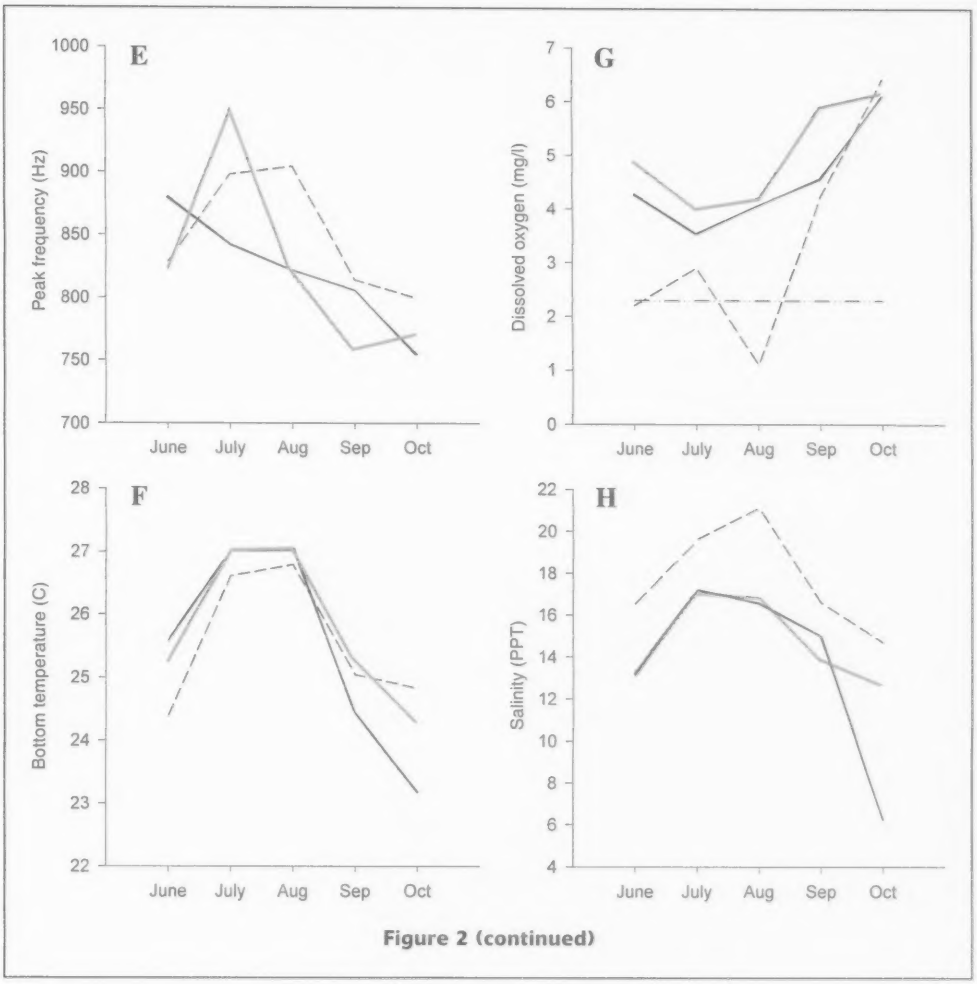


**Figure 2 (continued)**

CPUE ($F_{2,125}$=3.130, $P$=0.047), dissolved oxygen ($F_{2,125}$=4.21, $P$=0.017), and temperature ($F_{2,125}$=7.63, $P$=0.001) had significant overall effects in the MANCOVA (Table 1). Between-subject tests that provided separate results for each dependent variable showed that dissolved oxygen concentration ($F_1$=7.69, $P$=0.006), temperature ($F_1$=6.3, $P$=0.013), and habitat ($F_2$=4.55, $P$=0.012) were significantly associated with received sound level, and partial correlations indicated that each of these parameters accounted for 5–7% of the variance in sound level (Table 2). The interaction of month×habitat was associated with peak frequency of Atlantic croaker calls ($F_6$=2.31, $P$=0.038). For every 1-mg/L increase in dissolved oxygen concentration, the sound level of Atlantic croaker calls increased by 0.87 dB, and for every 1-degree increase in temperature there was an increase in sound level of 1.01 dB (Table 3). Although CPUE had significant overall effects in the MANCOVA (Table 1), the between-subject analysis did not detect significant relationships with either of the two dependent variables (Tables 2 and 3). This finding may have been due to the low statistical power associated with CPUE.

Williamson's indices demonstrated significant spatial overlap in the distributions of Atlantic croaker derived independently from acoustic and trawl data. Williamson's indices were between 0.959 and 1.488 for all combinations of month and habitat (Table 4). Calling indices corresponded better with CPUE than did received sound levels of Atlantic croaker calls. Spatial overlap between calling index and the actual density of Atlantic croaker (CPUE) was higher in July and August than in June, September, or October, and correspondence was stronger in the mid-river and river edge habitats than in the creeks.

With CART analysis we identified calling index as the predictor variable with the strongest correlation with CPUE (Fig. 3). Calling indices of 0 and 1 were associated with significantly lower densities of Atlantic croaker than were calling indices >1. Day of year and

**Table 1**

Multivariate analysis of covariance (MANCOVA) of the relationships among the dependent variables, received sound level and peak acoustic frequency of Atlantic croaker (*Micropogonias undulatus*) calls; the covariates dissolved oxygen concentration (DO), temperature (Temp), and trawl catch per unit of effort for Atlantic croaker (CPUE); and fixed factors of month and habitat and their interaction in North Carolina's Neuse River estuary (test statistic=Hotelling's trace statistic).

| Effect | Test statistic | $F$ | Hypothesis df | Error df | $P$ | Partial $\eta^2$ [1] | Power |
|---|---|---|---|---|---|---|---|
| Intercept | 0.812 | 50.75 | 2 | 125 | 0.000 | 0.45 | 1.00 |
| DO | 0.067 | 4.21 | 2 | 125 | 0.017 | 0.06 | 0.73 |
| Temp | 0.122 | 7.63 | 2 | 125 | 0.001 | 0.11 | 0.94 |
| CPUE | 0.05 | 3.13 | 2 | 125 | 0.047 | 0.05 | 0.59 |
| Month | 0.078 | 1.62 | 6 | 248 | 0.142 | 0.04 | 0.62 |
| Habitat | 0.072 | 2.25 | 4 | 248 | 0.065 | 0.04 | 0.65 |
| Month × Habitat | 0.155 | 1.60 | 12 | 248 | 0.092 | 0.07 | 0.83 |

[1] Partial $\eta^2$ is a standard measure of effect size (the proportion of variance in the dependent variable that is attributable to the independent variable, after partialling out the other independent variables). It varies between 0 and 1, and its meaning is similar to that of an $R^2$ in multiple regression or multiple correlation (Zar, 1999, p. 319).

**Table 2**

Between-subject effects from a multivariate analysis of covariance (MANCOVA) to investigate the relationships among the dependent variables received sound level (Level) and peak acoustic frequency (Frequency) of Atlantic croaker (*Micropogonias undulatus*) calls; the covariates dissolved oxygen concentration (DO), temperature (Temp), and trawl catch per unit of effort of Atlantic croaker (CPUE); and fixed factors of month and habitat, and their interaction in North Carolina's Neuse River estuary.

| Source | Dependent variable | df | $F$ | $P$ | Partial $\eta^2$ [1] | Power |
|---|---|---|---|---|---|---|
| Corrected model | Level[2] | 14 | 4.97 | 0.000 | 0.36 | 1.00 |
| | Frequency[3] | 14 | 2.74 | 0.001 | 0.23 | 0.99 |
| Intercept | Level | 1 | 56.29 | 0.000 | 0.31 | 1.00 |
| | Frequency | 1 | 12.33 | 0.001 | 0.09 | 0.94 |
| DO | Level | 1 | 7.69 | 0.006 | 0.06 | 0.79 |
| | Frequency | 1 | 3.44 | 0.066 | 0.03 | 0.45 |
| Temp | Level | 1 | 6.30 | 0.013 | 0.05 | 0.70 |
| | Frequency | 1 | 3.48 | 0.064 | 0.03 | 0.46 |
| CPUE | Level | 1 | 2.55 | 0.113 | 0.02 | 0.35 |
| | Frequency | 1 | 1.46 | 0.229 | 0.01 | 0.22 |
| Month | Level | 3 | 1.54 | 0.208 | 0.04 | 0.40 |
| | Frequency | 3 | 1.60 | 0.193 | 0.04 | 0.41 |
| Habitat | Level | 2 | 4.55 | 0.012 | 0.07 | 0.77 |
| | Frequency | 2 | 0.67 | 0.513 | 0.01 | 0.16 |
| Month × Habitat | Level | 6 | 1.08 | 0.377 | 0.05 | 0.41 |
| | Frequency | 6 | 2.31 | 0.038 | 0.10 | 0.78 |

[1] Partial $\eta^2$ is a standard measure of effect size (the proportion of variance in the dependent variable that is attributable to the independent variable, after partialling out the other independent variables). It varies between 0 and 1, and its meaning is similar to that of an $R^2$ in multiple regression or multiple correlation (Zar, 1999, p. 319).

[2] Type-III sum of squares: $R^2$=0.356 (adjusted $R^2$=0.284)

[3] Type-III sum of squares: $R^2$=0.233 (adjusted $R^2$=0.148)

distance to creek were also significantly correlated with Atlantic croaker density (Fig. 3). Catch rates of Atlantic croaker were significantly higher before June 11 (day 161) than were those later in the summer or fall, and catch rates were significantly higher within 525 m of the creeks than they were beyond this distance.

## Discussion

The global MANCOVA test found trawl CPUE to be a significant factor (Table 1). But the MANCOVA test of between-subject correspondence failed to detect any significant relationship between CPUE and received sound

**Table 3**

Covariate parameter estimates from a multivariate analysis of covariance (MANCOVA) to investigate the relationships among the dependent variables received sound level (Level) and peak acoustic frequency (Frequency) of Atlantic croaker (*Micropogonias undulatus*) calls; the covariates dissolved oxygen concentration (DO), temperature (Temp), and trawl catch per unit effort of Atlantic croaker (CPUE); and fixed factors of month and habitat, and their interaction in North Carolina's Neuse River estuary.

| | | | | | | 95% Confidence interval for B | |
|---|---|---|---|---|---|---|---|
| Dependent variable | Covariate | *B* | Standard error of *B* | *t* | *P* | Lower bound | Upper bound |
| Level | Intercept | 79.94 | 10.33 | 7.74 | <0.001 | 59.49 | 100.39 |
| | DO | 0.87 | 0.31 | 2.77 | 0.006 | 0.25 | 1.49 |
| | Temp | 1.01 | 0.40 | 2.51 | 0.013 | 0.21 | 1.80 |
| | CPUE | 0.94 | 0.59 | 1.60 | 0.113 | −0.23 | 2.10 |
| Frequency | Intercept | 561.36 | 157.92 | 3.56 | 0.001 | 248.85 | 873.87 |
| | DO | −8.88 | 4.79 | −1.86 | 0.066 | −18.36 | 0.59 |
| | Temp | 11.41 | 6.12 | 1.87 | 0.064 | −0.69 | 23.52 |
| | CPUE | 10.83 | 8.96 | 1.21 | 0.229 | −6.90 | 28.57 |

level for Atlantic croaker calls, which may have been due to low statistical power (power=0.35; Table 2). There was a high degree of spatial overlap between measures of Atlantic croaker density derived from trawl CPUEs and calling index, especially in the mid-river habitat during August. With CART analysis we identified a significant relationship between calling index and CPUE (Fig. 3). Taken together, these data indicate that passive acoustic techniques have the potential to be a means of assessing trends in abundance and habitat selection for soniferous fishes. However, the relationships between data derived from passive acoustics and those from traditional capture methods are not simple. Further development of analytical methods may clarify these relationships. Use of a calling index with a resolution greater than four levels; the ability to quantify the Atlantic croakers' contribution to ambient noise levels with greater precision; and a better understanding of how the acoustic source levels of individual fish are affected by dissolved oxygen concentration, temperature, and body size may result in an improved ability to estimate Atlantic croaker density based on passive acoustic data.

An important result of this study is the demonstration that environmental factors (e.g., dissolved oxygen, temperature, and habitat) appear to influence the relationship between acoustically derived indices of Atlantic croaker density and trawl CPUE. Many factors can influence calling behavior, spectral qualities of calls, and distance over which calls transmit. For example, Connaughton et al. (2000) showed that the sound pressure level, pulse repetition rate, and dominant frequency of disturbance calls made by weakfish (*Cynoscion regalis*) increased with increasing temperature and that dominant frequency varied inversely with fish size. Thus, temporal trends in peak frequency of Atlantic croaker calls likely resulted from changes in temperature and growth of the juvenile fish (Fig 2, A and E). Changes in dissolved oxygen concentration may have also affected calling behavior, but this topic has not been well studied in sciaenids.

**Table 4**

Williamson's index of spatial overlap between trawl catch per unit of effort of Atlantic croaker (CPUE) and two passive acoustic measures of Atlantic croaker (*Micropogonias undulatus*) density, calling index (CI) and received sound level of calls (RL), in the Neuse River estuary from June to October of 2000 (* indicates $P<0.01$).

| | CI and CPUE | RL and CPUE |
|---|---|---|
| Jun–Oct | 1.150* | 1.002 |
| Jun | 1.083 | 1.036 |
| Aug | 1.264* | 0.959 |
| Oct | 1.092 | 1.012 |
| Creeks | 1.019 | 1.018 |
| River edge | 1.132* | 0.989 |
| Mid-river | 1.478* | 1.061 |

Propagation of sound is affected by absorption, spreading loss, and scattering (reflection and refraction) (Richardson et al., 1995, p. 27–30); therefore, factors such as water depth, temperature gradients, density gradients, turbulence, suspended particles, bottom topography, and substrate type affect how sound travels and how efficiently sound is detected. That the highest spatial overlap values between CPUE and calling index (up to 1.48) occurred during August in the mid-river habitat likely reflects the high degree of patchiness in Atlantic croaker distribution related to the patchiness of hypoxia in this habitat. Also, the mid-river habitat was deeper and had smoother bathymetry than the other habitats, which may have resulted in a more uniform transmis-

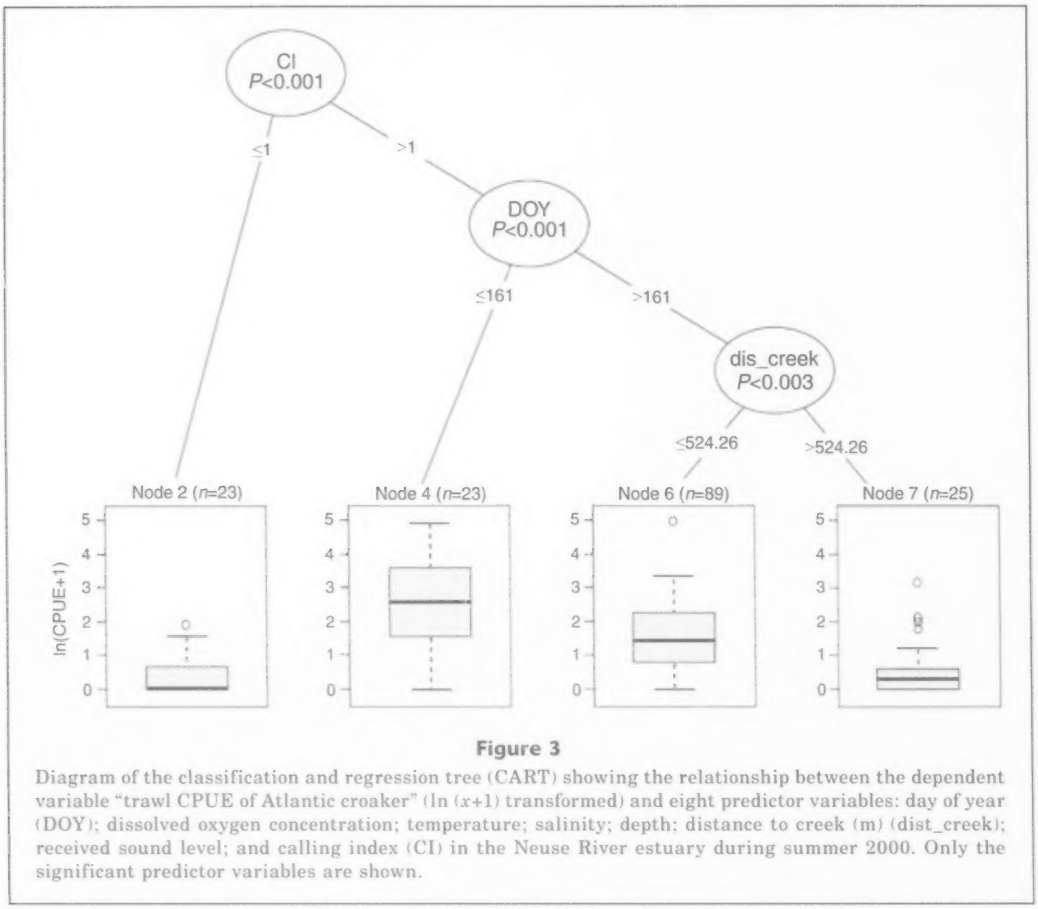


**Figure 3**

Diagram of the classification and regression tree (CART) showing the relationship between the dependent variable "trawl CPUE of Atlantic croaker" (ln ($x$+1) transformed) and eight predictor variables: day of year (DOY); dissolved oxygen concentration; temperature; salinity; depth; distance to creek (m) (dist_creek); received sound level; and calling index (CI) in the Neuse River estuary during summer 2000. Only the significant predictor variables are shown.

sion environment. This study illustrates the importance of planning passive acoustic surveys carefully to control for the confounding effects of environmental variables.

One major assumption used in this article is that the trawl data reflect actual Atlantic croaker densities in a consistent manner over time and across habitats. All fish sampling techniques have biases. For example, the catch efficiency of our trawl gear may have varied among the three habitats, by fish size, or between calling and noncalling fish. Therefore, some of the variation in the relationship between catch rates and sound production may have been due to variation in the catch efficiency of our trawl net, as well as in the variation in acoustic parameters. Because trawling is the most common method for assessing the abundance of demersal marine fishes, it is important to investigate the relationship between passive acoustic measures of abundance and those obtained from trawling.

Either the physical presence of, or the sound produced by, our boat could have caused a temporary disturbance of Atlantic croaker. For example, it may have caused the fish to flee from the immediate area or to change their acoustic behavior, which could have biased our results. Any disturbance would likely have been more pronounced in shallow water. We did not specifically investigate whether our boat may have affected our results. But there are a few points to consider. First, playback experiments of boat sounds in tanks elicited no significant change in swimming speed, turning rate, or depth in the water column of Atlantic croaker (D. Gannon, unpubl. data). Second, field recordings from the Neuse River that included the sounds of passing boats did not indicate an acoustic response from Atlantic croaker. The croaker sounds seemed to continue uninterrupted as boats passed by (but these boat sounds often masked the croaker sounds, and therefore such recordings were eliminated from our analysis). Third, the Neuse River estuary is highly turbid. Secchi depths during the summer are usually less than 1 m, which would limit visual detection of the boat. Finally, calling indices, received sound levels, and trawl catches were generally higher at shallow sampling stations (creek and river edge) than at deep ones (mid-river). In future studies an investigation of potential biases caused by disturbance from the sampling vessel would be worthwhile.

Although they tend to yield coarse data, there are some potential advantages to passive acoustic methods (see reviews by Rountree et al., 2006; Gannon, 2008; and Luczkovich et al., 2008.). In comparison with traditional fishery survey techniques (e.g., trawl surveys), passive acoustic surveys can be accomplished more quickly and cheaply with small vessels, few personnel, and low-cost equipment. Simple recording systems, such as the one used here, cost just a few hundred dollars and, in most cases, passive acoustic systems can be deployed with ease by one or two people in a small boat. Acoustic data loggers and telemetered sensors also allow remote data collection over long periods of time. Passive acoustic methods can allow the sampling of soniferous species that live on the bottom, within protective structures, or at great depths, and therefore, may be more appropriate than traditional sampling nets or active acoustic methods in some cases. Because of its relatively low cost, the ease with which it can be used, and its ability to collect data remotely from several sites simultaneously, passive acoustics allows larger areas to be monitored at higher sampling intensities than would be possible with a traditional survey method. Finally, passive acoustic methods are noninvasive and do not damage the habitat. Traditional fishery sampling techniques often cause high mortality rates of captured species and damage benthic habitat. Also, there has been much concern recently regarding anthropogenic noise in the sea (e.g., Popper et al., 2005, 2007); therefore passive acoustics can be more desirable than active acoustics in some situations.

Passive acoustics holds promise as a supplement to capture-based methods for assessing trends in relative abundance and for describing spatiotemporal patterns in distributions of soniferous fishes. To our knowledge, this is the first published attempt to compare passive acoustic data with data on the relative abundance of a soniferous fish species derived from traditional fisheries sampling techniques. Future research effort in fish passive acoustics should 1) help us to develop methods of quantifying calling rates with greater precision; 2) improve measurements of the contribution of the target species' calls to the ambient sound; and 3) provide a better understanding of how the source levels of the calls of individual fish are affected by dissolved oxygen concentration, temperature, and body size.

## Acknowledgments

We thank E. Horn, D. Waples, and many volunteers who assisted in the field. The U.S. Environmental Protection Agency (grant no. R261000-01-0 to L. Crowder and A. Read), Taylor Foundation, and Oak Fund provided funding. This research was conducted under a collecting permit issued by the North Carolina Division of Marine Fisheries to the Duke University Marine Laboratory, and in compliance with the U.S. Animal Welfare Act under a protocol issued by Duke University's Institutional Animal Care and Use Committee (protocol nos. A343-98-8, A418-99-08-2, A418-99-08-3, and A212-01-08). This article is contribution number 206 from the Bowdoin Scientific Station.

## Literature cited

Connaughton, M. A., M. L. Fine, and M. H. Taylor.
2000. Effects of fish size and temperature on weakfish disturbance calls: implications for the mechanism of sound generation. J. Exp. Biol. 203:1503–1512.

Connaughton, M. A., M. L. Lunn, M. L. Fine, and M. H. Taylor.
2003. Characterization of sounds and their use in two sciaenid species: weakfish and Atlantic croaker. *In* Listening to fish: passive acoustic applications in marine fisheries (R. Rountree, C. Goudey, and T. Hawkins, eds.), p. 21–25. Mass. Inst. Tech. Sea Grant College Program, Publication no. MITSG 03-2, Cambridge, MA.

Eby, L. A.
2001. Response of a fish community to frequent and infrequent disturbances in an estuarine ecosystem. Ph. D. diss., 276 p. Duke Univ., Durham, NC.

Eby, L. A. and L. B. Crowder.
2002. Hypoxia-based habitat compression in the Neuse River Estuary: context-dependent shifts in behavioral avoidance thresholds. Can. J. Fish. Aquat. Sci. 59:952–965.

Fine, M. L., J. Shrinel, and T. M. Cameron.
2004. The effect of loading on disturbance sounds of the Atlantic croaker *Micropogonias undulatus*: air versus water. J. Acoust. Soc. Am. 116:1271–1275.

Fish, M. P. and W. H. Mowbray.
1970. Sounds of western North Atlantic fishes: a reference file of biological underwater sounds. Johns Hopkins Press, Baltimore, MD.

Gannon, D. P.
2003. Behavioral ecology of an acoustically mediated predator-prey system: bottlenose dolphins and sciaenid fishes. Ph.D. diss., 244 p. Duke Univ., Durham, NC.
2007. Acoustic behavior of Atlantic croaker, *Micropogonias undulatus* (Sciaenidae). Copeia 2007:186–192.
2008. Passive acoustic techniques in fisheries science: a review and prospectus. Trans. Am. Fish. Soc. 137:638–656.

Gannon, D. P., N. B. Barros, D. P. Nowacek, A. J. Read, D. M. Waples, and R. S. Wells.
2005. Prey detection by bottlenose dolphins (*Tursiops truncatus*): an experimental test of the passive listening hypothesis. Anim. Behav. 69:709–720.

Garrison, L. P.
2000. Spatial and dietary overlap in the Georges Bank groundfish community. Can. J. Fish. Aquat. Sci. 57:1679–1691.

Garrison, L. P., W. Michaels, J. S. Link, and M. J. Fogarty.
2002. Spatial distribution and overlap between ichthyoplankton and pelagic fish and squids on the southern flank of Georges Bank. Fish. Oceanog. 11:267–285.

Heyer, W. R., M. A. Donnelly, R. W. McDiarmid, L. C. Hayek, and M. S. Foster.
1994. Measuring and monitoring biological diversity: standard methods for amphibians. Smithsonian Institution Press, Washington, DC.

Hill, G. L., M. L. Fine, and J. A. Musick.
1987. Ontogeny of the sexually dimorphic sonic muscle in three Sciaenid species. Copeia 1987:708–713.

Hothorn T., K. Hornik, and A. Zeileis.
2006. Unbiased recursive partitioning: a conditional inference framework. J. Computat. Graphic. Stats. 15:651–674.

Ladich, F.
1997. Agonistic behaviour and significance of sounds in vocalizing fish. Mar. Behav. Physiol. 29:87–108.
2004. Sound production and acoustic communication. *In* The senses of fishes: adaptations for the reception of natural stimuli (G. van der Emde, J. Modgands, and B. G. Kapoor, eds.), p. 210–230. Narosa Publ. House, New Delhi.

Lenihan, H. S. and C. H. Peterson.
1998. How habitat degradation through fishery disturbance enhances impacts of hypoxia on oyster reefs. Ecol. Appl. 8:128–140.

Link, J. S. and L. P. Garrison.
2002. Trophic ecology of Atlantic cod *Gadus morhua* on the northeast US continental shelf. Mar. Ecol. Progr. Ser. 227:109–123.

Luczkovich, J. J., H. J. Daniel, M. Hutchinson, T. Jenkins, S. E. Johnson, R. C. Pullinger, and M. W. Sprague.
2000. Sounds of sex and death in the sea: bottlenose dolphin whistles suppress mating choruses of silver perch. Bioacoustics 10:323–334.

Luczkovich, J. J., D. A. Mann and R. A. Rountree.
2008. Passive acoustics as a tool in fisheries science. Trans. Am. Fish. Soc. 137:533–541.

Luczkovich, J. J., M.W. Sprague, S. E. Johnson, and R. C. Pullinger.
1999. Delimiting spawning areas of weakfish *Cynoscion regalis* (family Sciaenidae) in Pamlico Sound, North Carolina using passive hydroacoustic surveys. Bioacoustics 10:143–160.

Mok, H. K. and R. G. Gilmore.
1983. Analysis of sound production in estuarine fish aggregations of *Pogonias cromis, Bairdiella chrysoura*, and *Cynoscion neubulosus* (Sciaenidae). Bull. Inst. Zool. Acad. Sinica 22:157–186.

Myrberg, A. A.
1997. Underwater sound: its relevance to behavioral functions among fishes and marine mammals. Mar. Freshw. Behav. Physiol. 29:3–21.

Pierce, A. D.
1989. Acoustics: an introduction to its physical principals and applications. Acoustical Soc. America, Woodbury, NY.

Popper, A. N., M. B. Halvorsen, E. Kane, D. D. Miller, M. E. Smith, P. Stein, and L. E. Wysocki.
2007. The effects of high-intensity, low-frequency active sonar on rainbow trout. J. Acoust. Soc. Am. 122:623–635.

Popper, A. N., M. E. Smith, P. A. Cott, B. W. Hanna, A. O. MacGillivray, M. E. Austin, and D. A. Mann.
2005. Effects of exposure to seismic airgun use on hearing of three fish species. J. Acoust. Soc. Am. 117:3958–3971.

Ramcharitar, J., D. P. Gannon, and A. N. Popper.
2006. Bioacoustics of fishes of the family Sciaenidae (croakers and drumfishes). Trans. Am. Fish. Soc. 135:1409–1431.

Richardson, W. J., C. R. Greene, C. I. Malme, and D. H. Thomson.
1995. Marine mammals and noise, 576 p. Academic Press, San Diego, CA.

Rountree, R. A., R. G. Gilmore, C. A. Goudey, A. D. Hawkins, J. Luczkovich, and D. A. Mann.
2006. Listening to fish: Applications of passive acoustics to fisheries science. Fisheries 31:433–446.

Saucier, M. H. and D. M. Baltz.
1993. Spawning site selection by spotted seatrout, *Cynoscion nebulosus*, and black drum, *Pogonias cromis*, in Louisiana. Environ. Biol. Fishes 36:257–272.

Sprague, M. W. and J. J. Luczkovich.
2001. Do striped cusk-eels *Ophidion marginatum* (Ophidiidae) produce the "chatter" sound attributed to weakfish *Cynoscion regalis* (Sciaenidae)? Copeia 2001:854–859.

Urban, D., S. Goslee, K. Pierce, and T. Lookingbill.
2002. Extending community ecology to landscapes. Ecoscience 9:200–212.

Vance, T. L., J. M. Hewson, S. Modla, and M. A. Connaughton.
2002. Variability in sonic muscle size and innervation among three sciaenids: spot, Atlantic croaker, and weakfish. Copeia 2002:1137–1143.

Williamson, C. E.
1993. Linking predation risk models with behavioral mechanisms: identifying population bottlenecks. Ecology 75:320–331.

Zar, J. H.
1999. Biostatistical analysis, 4th ed., 663 p. + append. Prentice Hall, Inc., Upper Saddle River, NJ.

# Fishery Bulletin

## Guidelines for authors

### Manuscript Preparation

Contributions published in *Fishery Bulletin* describe original research in marine fishery science, fishery engineering and economics, as well as the areas of marine environmental and ecological sciences (including modeling). Preference will be given to manuscripts that examine processes and underlying patterns. Descriptive reports, surveys, and observational papers may occasionally be published but should appeal to an audience outside the locale in which the study was conducted. Although all contributions are subject to peer review, responsibility for the contents of papers rests upon the authors and not on the editor or publisher. *Submission of an article implies that the article is original and is not being considered for publication elsewhere.* **Articles** may range from relatively short contributions (10–15 typed, double-spaced pages, tables and figures not included) to extensive contributions (20–30 typed pages). Manuscripts must be written in English; authors whose native language is not English are strongly advised to have their manuscripts checked by English-speaking colleagues before submission.

**Title page** should include authors' full names and mailing addresses and the senior author's telephone, fax number, and e-mail address, and a list of key words to describe the contents of the manuscript. **Abstract** should be limited to 200 words (one-half typed page), state the main scope of the research, and emphasize the author's conclusions and relevant findings. Do not review the methods of the study or list the contents of the paper. Because abstracts are circulated by abstracting agencies, it is important that they represent the research clearly and concisely. **Text** must be typed in 12 point Times New Roman font throughout. A brief introduction should convey the broad significance of the paper; the remainder of the paper should be divided into the following sections: **Materials and methods, Results, Discussion** (or **Conclusions**), and **Acknowledgments**. Headings within each section must be short, reflect a logical sequence, and follow the rules of multiple subdivision (i.e., there can be no subdivision without at least two items). The entire text should be intelligible to interdisciplinary readers; therefore, all acronyms, abbreviations, and technical terms should be written out in full the first time they are mentioned. Include FAO common names for species in the list of keywords and in the introduction. Regional common names may be used throughout the rest of the text if they are different from FAO common names which can be found at http://www.fishbase.org/search.html. Follow the U.S. Government Printing Office Style Manual (2000 ed.) and Scientific Style and Format: the CSE Manual for Authors, Editors, and Publishers (7th ed.) for editorial style; for fish nomenclature follow the most current issue of the American Fisheries Society's Common and Scientific Names of Fishes from the United States, Canada, and Mexico, 6th ed. Dates should be written as follows: 11 November 2000. Measurements should be expressed in metric units, e.g., 58 metric tons (t); if other units of measurement are used, please make this fact explicit to the reader. Write out the numbers zero through nine unless they form part of measurement units (e.g., nine fish but 9 mm). Refrain from using the shorthand slash (/), an ambiguous symbol, in the general text

**Literature cited** comprises published works and those accepted for publication in peer-reviewed literature (in press). Follow the name and year system for citation format in the "Literature cited" section (that is say, citations should be listed alphabetically by the authors' last names, and then by year if there is more than one citation with the same authorship). If there is a sequence of citations in the text, list chronologically: (Smith, 1932; Green, 1947; Smith and Jones, 1985). Abbreviations of serials should conform to abbreviations given in the Serial Sources for the BIOSIS Previews Database. Authors are responsible for the accuracy and completeness of all citations. Literature citation format: Author (last name, followed by first-name initials). Year. Title of report or manuscript. Abbreviated title of the series to which it belongs. Always include number of pages. Cite all software and special equipment or chemical solutions used in the study, not in a footnote but within parentheses in the text (e.g., SAS, vers. 6.03, SAS Inst., Inc., Cary, NC).

**Tables** are often overused in scientific papers; it is seldom necessary or even desirable to present all the data associated with a study. Tables should not be excessive in size and must be cited in numerical order in the text. Headings should be short but ample enough to allow the table to be intelligible on its own. All unusual symbols must be explained in the table legend. Other incidental comments may be footnoted with italic numeral footnote markers. Use asterisks to indicate probability in statistical data. Do not type table legends on a separate page; place them above the table data. *Do not submit tables in photo mode.*

- Zeros should precede all decimal points for values less than one.
- Sample size, $n$, should be italicized.
- Capitalize the first letter of the first word in all labels within figures.
- Do not use overly large font sizes in maps and for units of measurements along axes in figures.
- Do not use bold fonts or bold lines in figures.
- Do not place outline rules around graphs.
- Do not use horizontal lines through graphs to indicate measurement units.

- Use a comma in numbers of five digits or more (e.g. 13,000 but 3000).
- Maps require a North arrow and degrees latitude-longitude (e.g., 170°E).

**Figures** include line illustrations, photographs (or slides), and computer-generated graphs and must be cited in numerical order in the text. Graphics should aid in the comprehension of the text, but they should be limited to presenting patterns rather than raw data. Figures should not exceed one figure for every four pages of text. Figures must be labeled with author's name and number of the figure. Avoid placing labels vertically (except of y axis). Figure legends should explain all symbols and abbreviations and should be double-spaced on a separate page at the end of the manuscript. Please note that we do not print graphs in color.

**Failure to follow these guidelines and failure to correspond with editors in a timely manner will delay publication of a manuscript.**

**Copyright law** does not apply to *Fishery Bulletin*, which falls within the public domain. However, if an author reproduces any part of an article from *Fishery Bulletin* in his or her work, reference to source is considered correct form (e.g., Source: Fish. Bull 97:105).

## Submission

The Scientific Editorial Office encourages authors to submit their manuscripts as a *single* PDF (preferred) or Word (zipped) document by e-mail to Fishery.Bulletin@noaa.gov. Please use the subject heading, "Fishery Bulletin manuscript submission". *Do not* send encrypted files. Please provide names and contact information for 3–4 suggested reviewers. Commerce Department personnel should submit papers under a completed NOAA Form 25-700. Or you may send your manuscript on a compact disc in one of the above formats. For further details on electronic submission, please contact the Scientific Editorial Office directly (see address below).

Richard D. Brodeur, Ph.D.
Scientific Editor, *Fishery Bulletin*
Northwest Fisheries Science Center
2030 S. Marine Science Dr.
Newport, Oregon 97365-5296

Once the manuscript has been accepted for publication, you will be asked to submit a final electronic copy of your manuscript. When requested, the text and tables should be submitted in Word or Word Rich Text Format. Figures should be sent as PDF files, Windows metafiles, tiff files, or EPS files. Send a copy of figures in the original software if conversion to any of these formats yields a degraded version.

**Questions?** If you have questions regarding these guidelines, please contact the Managing Editor, Sharyn Matriotti, at

Sharyn.Matriotti@noaa.gov

Questions regarding manuscripts under review should be addressed to Richard Brodeur, Scientific Editor, at Rick.Brodeur@noaa.gov.

# *Fishery Bulletin*

## Subscription form

Superintendent of Documents **Publications** Order Form

*5178

☐ YES, please send me the following publications:

____ Subscriptions to *Fishery Bulletin*
for $36.00 per year ($50.40 foreign)

The total cost of my order is $ _____ . Prices include regular domestic postage and handling and are subject to change.

_____
(Company or Personal Name) (Please type or print)

_____
(Additional address/attention line)

_____
(Street address)

_____
(City, State, ZIP Code)

_____
(Daytime phone including area code)

_____
(Purchase Order No.)

Charge your order.
IT'S EASY!

VISA

MasterCard

**Please Choose Method of Payment:**

☐ Check Payable to the Superintendent of Documents

☐ GPO Deposit Account ☐☐☐☐☐☐–☐

☐ VISA or MasterCard Account

☐☐☐☐☐☐☐☐☐☐☐☐☐☐☐☐

☐☐☐☐ (Credit card expiration date)

**To fax your orders (202) 512-2250**

_____
(Authorizing Signature)

Mail To: Superintendent of Documents
P.O. Box 371954, Pittsburgh, PA 15250-7954

***Thank you for your order!***
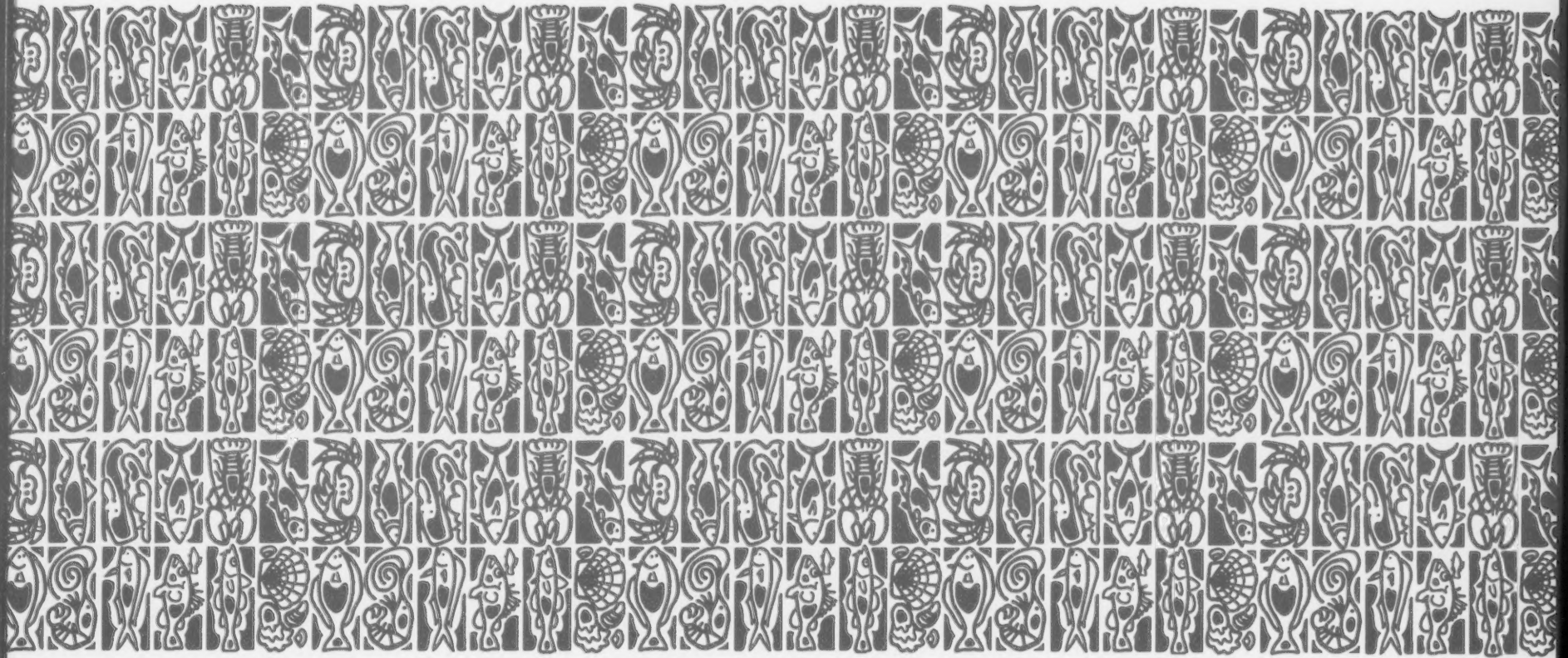
Also available online at http://bookstore.gpo.gov/collections/fishery-bulletin